

Revista **ALCONPAT**

Latin American Journal of Quality Control, Pathology and Construction Recovery

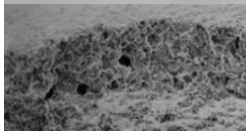
DOI: <http://dx.doi.org/10.21041/ra.v8i3>
editorial.revista.alconpat@gmail.com

eISSN: 2007-6835

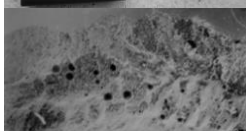
Volume 8

September - December 2018

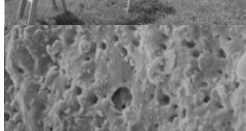
Issue 3



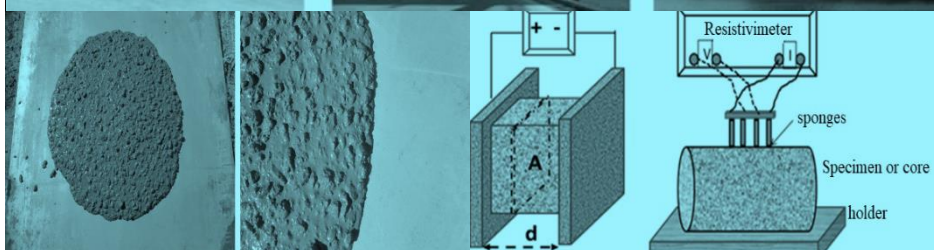
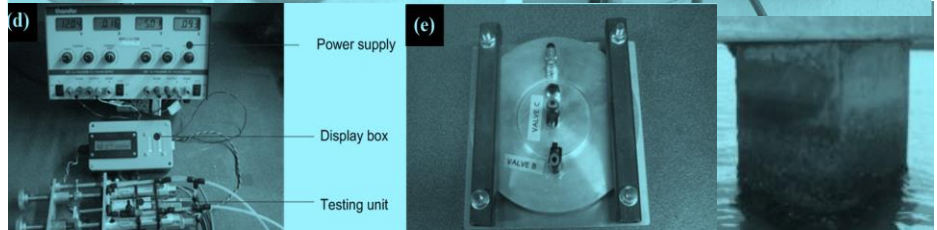
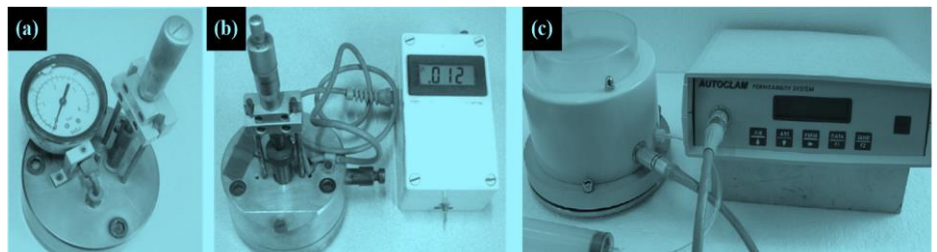
PRIMER 2
(a) 100 μm



PRIMER 4
100 μm



PRIMER 6
10 μm



Latin American Journal of Quality Control, Pathology and Construction Recovery

<http://www.revistaalconpat.org>



ALCONPAT International

Founders members:

Liana Arrieta de Bustillos – **Venezuela**
Antonio Carmona Filho - **Brazil**
Dante Domene – **Argentina**
Manuel Fernández Cánovas – **Spain**
José Calavera Ruiz – **Spain**
Paulo Helene, **Brazil**

Board of Directors International:

President of Honor

Angélica Ayala Piola, **Paraguay**

President

Carmen Andrade Perdriz, **Spain**

General Director

Pedro Castro Borges, **Mexico**

Executive Secretary

José Iván Escalante García, **Mexico**

Technical Vice President

Enio Pazini Figueiredo, **Brazil**

Administrative Vice President

Luis Álvarez Valencia, **Guatemala**

Manager

Paulo Helene, **Brazil**

Revista ALCONPAT

Editor in Chief:

Dr. Pedro Castro Borges
Centro de Investigación y de Estudios Avanzados del Instituto
Politécnico Nacional, Unidad Mérida (CINVESTAV IPN –
Mérida)
Merida, Yucatan, **Mexico**

Co-Editor in Chief:

Arch. Margita Kliewer
Universidad Católica “Nuestra Señora de la Asunción”
Asuncion, **Paraguay**

Executive Editor:

Dr. José Manuel Mendoza Rangel
Universidad Autónoma de Nuevo León, Facultad de Ingeniería
Civil
Monterrey, Nuevo Leon, **Mexico**

Associate Editors:

Dr. Manuel Fernandez Canovas Universidad
Politécnica de Madrid. Madrid, **Spain**

Ing. Raúl Husni

Facultad de Ingeniería Universidad de Buenos Aires. Buenos
Aires, **Argentina**

Dr. Paulo Roberto do Lago Helene

Universidade de São Paulo.

São Paulo, **Brazil**

Dr. José Iván Escalante García

Centro de Investigación y de Estudios Avanzados del
Instituto Politécnico Nacional (Unidad Saltillo) Saltillo,
Coahuila, **Mexico**.

Dr. Mauricio López.

Departamento de Ingeniería y Gestión de la Construcción,
Escuela de Ingeniería,
Pontificia Universidad Católica de Chile
Santiago de Chile, **Chile**

Dra. Oladis Troconis de Rincón Centro de Estudios de

Corrosión Universidad de Zulia

Maracaibo, **Venezuela**

Dr. Fernando Branco Universidad

Técnica de Lisboa

Lisboa, **Portugal**

Dr. Pedro Garcés Terradillos

Universidad de Alicante

San Vicente, **Spain**

Dr. Andrés Antonio Torres Acosta

Instituto Mexicano del Transporte / Universidad Marista de
Querétaro

Querétaro, **Mexico**

Dr. Luiz Fernández Luco

Universidad de Buenos Aires – Facultad de Ingeniería –
INTECIN

Buenos Aires, **Argentina**

**JOURNAL OF THE LATIN AMERICAN
ASSOCIATION OF QUALITY CONTROL,
PATHOLOGY AND RECOVERY OF
CONSTRUCTION**

<http://www.revistaalconpat.org>

With great satisfaction, we present the third issue of the 8th year of the Revista ALCONPAT (RA).

The aim of the journal is to publish case studies, quotable production (basic and applied research, reviews) and documentary research, related to the themes of our association, namely quality control, pathology and recovery of constructions.

In 2017 a workshop on service life prediction of reinforced concrete in the CONPAT 2017, to honor Carmen Andrade because of its 70th anniversary and fruitful career, was made. As a result, and as part of the celebration, the RA N3 V8 is a special issue on issues related to the service life of concrete structures in her honor. This edition begins precisely with an account of historical events in the area of corrosion and durability, which expanded knowledge since late last century, which Carmen has lived and narrated in detail.

The first work of this issue comes from **South Africa**, where Mark Alexander presents an international overview of current knowledge and progress in service life design and modelling of concrete structures. It explores why service life modelling is needed, and indicates that modern demands for longevity, durability, and sustainability of concrete structures cannot be fulfilled without service life modelling. It addresses the current approaches to durability design and specification and concludes that a move to performance-based approaches is imperative for progress to be made. Examples from international experience are cited to illustrate progress that has been made. Lastly, the paper discusses ways of moving forward, recognizing that the philosophical bases are already in place in the form of general code formulations, but which need to be converted into useful approaches.

In the second work, coming from **United Kingdom-China**, M. Basheer and colleagues make a review of techniques, highlighting the challenges and opportunities to evaluate the high performance concrete transport properties. They confirm that the in-situ characterization of the permeability properties of concrete is the most viable means to assess durability and has become increasingly important in the last 20 years. They show and describe a variety of methods that provide a range of parameters, such as air permeability, water absorption, capillary absorption, and the migration coefficient of chlorides.

In the third article from **Spain**, Carmen Andrade describes the use of concrete electrical resistivity as durability performance parameter and the complementary information that resistivity can provide like: setting period, mechanical strength and degree of curing. Also, it is explained how to design the concrete mix to obtain a target resistivity. Current codes have requirements for the durability design of concrete based on compressive strength and provisions related to cement content and water/cement ratio. For reinforcement corrosion the codes also specify the maximum flexural crack widths. However, modern trends specify the performance rather than the concrete characteristics. This performance approach demands to define a durability controlling parameter, such as the chloride diffusion coefficient, with its corresponding test and model to predict the time to steel corrosion

The fourth article, by Pedro Castro Borges and Paulo Helene, comes from **Mexico-Brazil**; they analyze and discuss a conceptual approach that considers the holistic character of concrete service life but splits it into seven time-stages that can be compared, for understanding purposes, with those of a human being. The paper discusses the overlapping of the different time-stages as well as the reasons why the prediction models can fail.

The fifth work in this issue is written by Enio Pazini and Carmnen Andrade from **Brazil-Spain**, they evaluate the influence of five different types of coatings applied on the rebar on apparent diffusion coefficient of oxygen ($D_{ap}(O_2)$) and on the corrosion intensity (I_{corr}) in comparison with a reference coating composed of a cement-sand mortar. The apparent diffusion coefficient values ($D_{ap}(O_2)$) ranged from $2.1 \times 10^{-6} \text{ cm}^2/\text{s}$ to $4 \times 10^{-9} \text{ cm}^2/\text{s}$, causing variations in the corrosion intensity measurements (I_{corr}), due to the cathodic corrosion process control.

In the sixth work, from **Argentina**, Yuri Villagran and colleagues present an analysis of experimental data from conventional concrete regarding sorptivity and penetrability under pressure comparing these parameters to chloride diffusion rate determined in the laboratory and in actual marine environment. The results show the limitations of both parameters as prescriptive indexes, with capillary absorption rate showing some advantages over water penetration under pressure.

In the seventh work, from **Venezuela-Mexico**, Oladis Troconis de Rincón and colleagues evaluate the correlation between crack width and apparent corrosion rate in reinforced concrete specimens exposed for more than six years to a tropical marine environment, at the natural test site La Voz, Venezuela. An empirical correlation between surface crack propagation rate and i_{CORR} was established, which may help to indirectly estimate the value of i_{CORR} , if values of maximum surface crack widths due to reinforcement corrosion are obtained in at least one-year period of monitoring.

The eighth article, by Paulo Helene and colleagues, comes from **Brazil**; they present results of concrete compression resistance control with Brazilian standardization, as well as comparisons with the controls proposed by ACI 318-14 and EN 206. For this article a real case study was carried out, where a concrete dosage was used with $f_{ck} = 40\text{MPa}$, self-consolidable, produced during 2 years and 9 months and applied in the structure of a building in the city of São Paulo.

The article that closes the edition is by Miguel Martínez and colleagues from **Mexico-United States**, who present a live load test and a qualification analysis on a pier damaged by corrosion in the Gulf of Mexico to assess its structural integrity. The results showed that corrosion damage did not represent an extreme structural threat; however, it was discovered that the structural elements of several pillars are currently overloaded and need to be reinforced externally. The procedures for testing, analysis and data handling are described.

This third issue closes with the news that RA has met the quality requirements to continue to be an international level journal on the CONACYT evaluation.

As an interesting fact, this edition increases the number of articles according to the expected trend. Likewise, the international nature of RA with articles from Argentina, Brazil, China, Spain, the United States, Mexico, the United Kingdom, South Africa and Venezuela is again manifested, four of them being international collaborations, which, of course, will increase the impact of RA.

We are confident that the articles in this issue will constitute an important reference for those readers involved with modeling and service life issues. We thank the authors participating in this issue for their willingness and effort to present quality articles and meet the established times.

For the Editorial Board

A handwritten signature in black ink, appearing to read 'Pedro Castro Borges', written over a circular stamp or seal.

Pedro Castro Borges
Editor in Chief

BRIEF HISTORICAL NOTES

C. Andrade¹

¹International Center for Numerical Methods in Engineering. CIMNE. UPC, Spain.

candrade@cimne.upc.edu

ABSTRACT

Anniversaries are a good excuse to make some summaries of historical events. Very briefly, some advances made from the initial research in the specialty of reinforcement corrosion which started in the 60's are summarized. The use of electrochemical techniques was a milestone which enabled, from the decade of the 1970, to study the effect of each variable with much more rigor. The studies on service life started in the decade of 1980, although they were not of general interest until the next decade. From 1990 RILEM Committees and the Iberoamerican Program on Corrosion of CYTED extended the knowledge so widely that in the XXI century the subject attracts much research interest.

Keywords: electrochemical techniques; service life; corrosion; reinforcement.

BREVES NOTAS HISTÓRICAS

RESUMEN

Los aniversarios son una buena excusa para hacer algunos resúmenes de eventos históricos. Muy brevemente, se resumen algunos avances realizados a partir de la investigación inicial en la especialidad de la corrosión por armadura que comenzó en los años 60. El uso de técnicas electroquímicas fue un hito que permitió, desde la década de 1970, estudiar el efecto de cada variable con mucho más rigor. Los estudios sobre la vida útil comenzaron en la década de 1980, aunque no fueron de interés general hasta la próxima década. A partir de 1990 los Comités RILEM y el Programa Iberoamericano de Corrosión de CYTED ampliaron el conocimiento de manera tan amplia que en el siglo XXI el tema atrae mucho interés de investigación.

Palabras clave: técnicas electroquímicas; vida de servicio; corrosión; reforzamiento.

BREVE NOTAS HISTÓRICAS

RESUMO

Aniversários são uma boa desculpa para fazer alguns resumos de eventos históricos. Muito brevemente, alguns avanços da pesquisa inicial na especialidade de corrosão de reforço que começou nos anos 60 estão resumidos. O uso de técnicas eletroquímicas foi um marco que permitiu, a partir da década de 1970, estudar o efeito de cada variável com muito mais rigor. Os estudos sobre vida de serviço começaram na década de 1980, embora não fossem de interesse geral até a década seguinte. A partir de 1990, os Comitês RILEM e o Programa Ibero-americano de Corrosão de CYTED ampliaram o conhecimento de forma tão ampla que, no século XXI, o assunto atraiu muito interesse de pesquisa.

Palavras-chave: técnicas eletroquímicas; vida de serviço; corrosão; reforço.

1. INTRODUCTION

The corrosion of the reinforcement is currently one of the subjects in which more resources are invested to investigate and it is also recognized as the main problem for the durability of concrete. I have lived the development of the concrete corrosion research since the beginning. First I make a very brief account of some research milestones in a sequential historical way before developing the subject with which I contributed to this special issue.

2. RESEARCH TO 1980

When I began my research by suggestion of José Calleja at the "Eduardo Torroja" Institute of Construction and Cement, there were no more than 30 citations in all the bibliography that I consulted (Gouda and Monfore, 1965; Stratfull, 1964; Cigna et al, 1966). His suggestion came because they had detected corrosion due to the use of CaCl_2 to accelerate the setting of concrete. The corrosion of armors was a matter of completely marginal interest in the decade of 1960-70, when the constructed park was still very limited. In my bachelors and in my thesis (Hausmann, 1964) I studied a total of 8 cements with additions of CaCl_2 and NaNO_2 , the latter as a possible corrosion inhibitor, manufacturing pre-stressed joists 2 m long with 6 embedded wires. The results clearly showed the corrosive effect of CaCl_2 and the inhibitory capacity of Nitrite. To measure corrosion, the non-destructive measuring technique called Polarization Resistance was applied for the first time in concrete, which would later be recognized along with other novel results by the RILEM when the author was awarded the Robert L'Hermite Medal.

Figure 1 shows the specimens and joists used in the thesis of the author, as a curiosity, on the right side the devices used for measurements during the thesis are shown, one of which had already been used in the dissertation and another, the galvanostatic indicated with a G in the photograph, was manufactured by Jose M^a Tobio of the IETcc with the drawings yielded by Sebastián Feliú of the CENIM who is the one who had suggested using the R_p that was a very novel measurement technique.

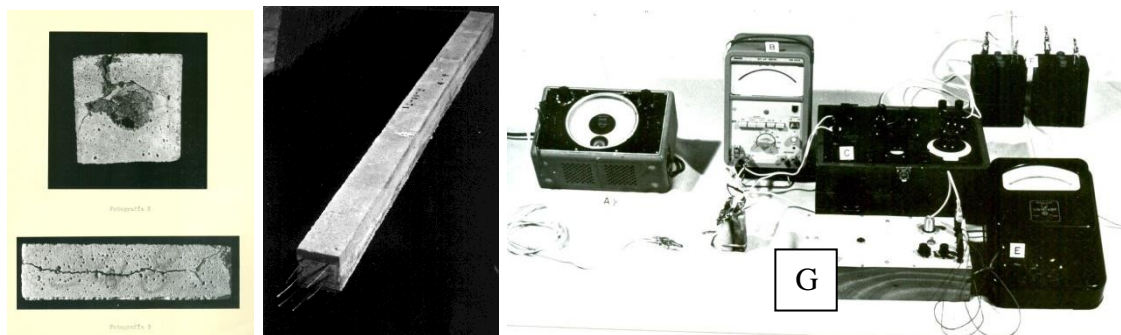


Figure 1. Used corroded probes during the thesis of the author and the beam made in the Doctoral thesis (Hausmann, 1964) presented the year 1973 in the Complutense University of Madrid.

Apparatus used in the doctoral thesis (Andrade, 1973)

The techniques that had been applied up to that moment to study the corrosion of the armor were of an accelerated type, mainly polarization curves (Gouda and Monfore, 1965) that were embodied in a potentiation test proposed by Kaesche and Bäumel (Andrade, 1970; Andrade, 1978) later standardized by DIN and by CEN for the detection of corrosive substances in concrete additives. Also outstanding in those years are Hausmann's works (Andrade, 1978) which establishes the critical relation of chlorides with respect to the pH of concrete at a value of $\text{Cl} / \text{OH} = 0.6$. Value

that has remained valid to this day. Also, the works of Gouda (Gouda and Monfore, 1965) and Treadaway (Kaesche, 1959) all on electrochemical techniques to detect the corrosiveness of the additives and the protection of the inhibitors.

3. DECADES OF 1980-2000

The use of electrochemical techniques was a fundamental milestone that allowed (Baumel, 1959) from 1970 to approach the studies with much more rigor on the effect of each variable. This is how they began to study the effects of carbonation (González, Algaba and Andrade, 1980) and the possible methods to avoid corrosion, mainly hot galvanizing, inhibitors, epoxy coatings for reinforcements and cathodic protection.

It is however in the 1980s when the calculation of useful life was addressed, which was not the subject of general attention until 1990. Thus K. Tuutti publishes his doctoral thesis (González, Algaba and Andrade, 1980) in 1982 with the diagram shown in figure 3 and that has articulated all subsequent studies. Figure 3 also shows K. Tuutti during a meeting of the Rilem Committee 60-CSC- "Corrosion of Steel in concrete" (Tuutti, 1982). Both this committee and subsequent ones, as well as the Subprogram "Durar" of CYTED (Schiessl, 1988) and the publication of Page and Treadaway in Nature (Page and Treadaway, 1982) supposed a disclosure of the problem in its basic aspects that contributed significantly to the multiplication of congresses and publications.

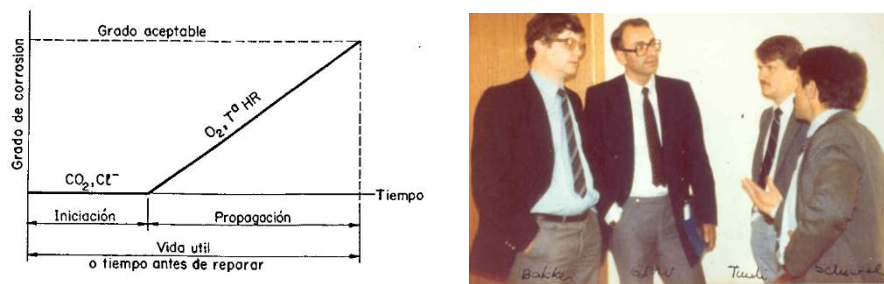


Figure 3. Left: Tuutti's life-time diagram. Right: from left to right Rob Bakker (Holland), O. Gjorv (Norway), K. Tuutti (Sweden) and P. Schiessl (Germany).

During the 1990s, enormous advances were made in basic knowledge, among which the possibility of in situ measurement (GECOR corrosion meter that allows measuring on site through confinement of the current (Page and Treadaway, 1982)) can be mentioned (Figure 4): the practice of cathodic protection both in new structures (Feliú et al, 1990) and already deteriorated, and the detection of problems with epoxy coatings (Lazzari and Pedferri, 2006).

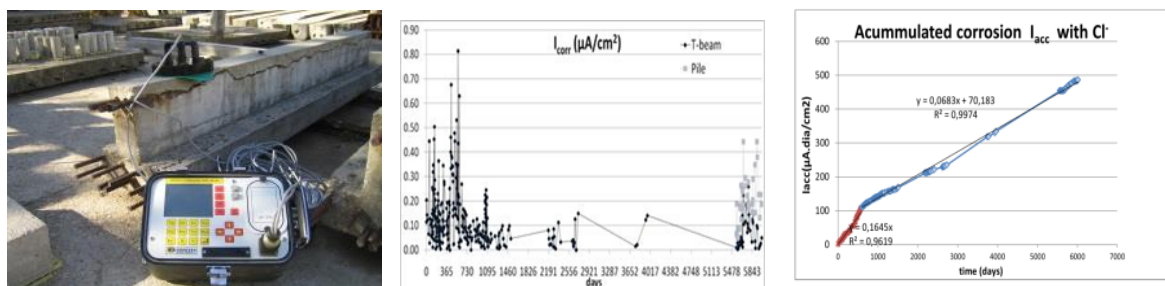


Figure 4. Aspect of the Gecor 08 portable corrosion meter and measurements of instantaneous corrosion rate taken on the beam of the figure as well as the calculation of corrosion penetration (accumulated corrosion) from the integration in time of these measurements.

In those years RILEM established several committees, both on measurement techniques (TC-154), and on the models based on the diffusion of chlorides and carbonation (TC-178 and TC-213). In this regard, it is worth mentioning the contribution of D. Whiting proposing in the 1980s to reduce the duration of the chloride resistance test (Sagüés et al, 2001) by applying a potential difference to the concrete. These works led to an intense debate that led to the work (Whiting, 1981) that allowed to lay the theoretical basis for the diffusion of chlorides and their migration through electric fields, which have led to the profusion of numerical models on concrete life.

4. FROM 2000 TO THE PRESENT DAY

The most remarkable thing in these years can be summarized in the work done in the DURAR project (Andrade, 1993) in terms of the disclosure of basic principles. The CONTECVET Manual (CONTECVET IN30902I, 2001) which considers how to calculate the residual structural capacity when the structures are corroded and the probabilistic treatment of the models and calculation of the useful life, of which we can mention as a summary all the work carried out in the DURACRETE project (DURACRETE, 2000) that has led to the incorporation of the fib Model Code of the probabilistic durability treatment.

One area in which a lot of technology has been developed is related to repair methods, given the growing number of structures that have had to be repaired. However, in the 21st century, the corrosion of armor is one of the areas that constantly attracts research interest, there are many aspects to be clarified, especially in the effectiveness of repairs and in the calibration of life models.

5. REFERENCES

- Andrade, C. (1970), *Aportación al estudio de la corrosión de armaduras en el hormigón armado*. Tesina de licenciatura, Universidad Complutense. Facultad de Químicas, Madrid, Julio.
- Andrade, C. (1973), *Nueva técnica electroquímica de medida de la corrosión de armaduras en hormigones armados y pretensados. Empleo de aditivos inhibidores como método de protección*. Universidad Complutense, Facultad de Químicas – Junio.
- Andrade, C. and González, J. A. (1978), *Quantitative measurements of corrosion rate of reinforcing steels embedded in concrete using polarization resistance measurements*, Materials and Corrosion, 29 (8), pp. 515. <https://doi.org/10.1002/maco.19780290804>
- Andrade, C. (1993), *Calculation of chloride diffusion-coefficients in concrete from ionic migration measurements*. Cement and Concrete Research 23 (3), pp. 724-742. [https://doi.org/10.1016/0008-8846\(93\)90023-3](https://doi.org/10.1016/0008-8846(93)90023-3)
- Baumel, A. (1959), *The effect of additives on the corrosion behaviour of steel in concrete*, Zement-Kalk-Gips, July, no.7 pp 294.
- Cigna, R., Maraghini, M., Schippa, G. (1966), *Effeto del contenuto di Ca_2Cl sul comportamento dei ferri affogati in malte cementizie*. L'Industria italiana del Cemento Marzo, p 139.
- CONTECVET IN30902I (2001) “*A validated user’s manual for assessing the residual life of concrete structures*”, DG Enterprise, CEC, (The manual for assessing reinforced structures affected by reinforcement corrosion can be seen at the web sites of IETcc (www.ietcc.csic.es) and GEOCISA (www.geocisa.es))
- DURACRETE. (2000), *Probabilistic performance based on durability design of concrete structures. EU-Brite EuRam Project BE95-1347*. A number of reports available from CUR Centre for Civil Engineering Research and Codes, Gouda, The Netherlands.

- Feliú, S., González, J. A., Feliú Jr., S., Andrade, C. (1990), "*Confinement of the electrical signal or in-situ measurement of Polarization Resistance in Reinforced concrete*," ACI Materials Journal. 87(5), pp. 457-460.
- González, J. A., Algaba, S., Andrade, C. (1980), *Corrosion of reinforcing bars in carbonated concrete*, British Corrosion Journal, 3 135-139.
- Gouda, V. K., Monfore, G. E. (1965), *A rapid method for studying corrosion inhibition of steel in concrete*, Journal Portland Cement Association, Septiembre, n° 3, 24.
- Hausmann, D. A. (1964), "*Electrochemical behaviour of steel in concrete*", Journal A. C. I., 171.
- Kaesche, H. (1959) *Testing corrosion danger of steel reinforcement due to admixtures in concrete*, Zement-Kalk-Gips, July, no.7 pp 289.
- Lazzari, L., Pedferri, P. (2006), *Cathodic Protection*, Milano: Polipress.
- Page, C. L., Treadaway, K. W. J. (1982), *Aspects of the electrochemistry of steel in concrete*. Narute 297 No. 5862, 109-115. <https://doi.org/10.1038/297109a0>
- Sagüés, A. A., Powers, R. G., Kessler, R. (2001) "*Corrosion Performance of Epoxy-Coated Rebar in Florida Keys Bridges*," NACE International. CORROSION 2001, 11-16 March, Houston, Texas. ID: NACE-01642
- Schiess, P. (1988) *Corrosion of steel in concrete: report of the Technical Committee 60 CSC, RILEM (the International Union of Testing and Research Laboratories for Materials and Structures)*, London, New York, Chapman and Hall.
- Stratfull, R.F. (1964), *Effect of reinforced concrete in ClNa and SO₄Na₂ environments*. Materials Protection, Dic, p 75.
- Tuutti, K. (1982), "*Corrosion of steel in concrete*", Swedish Cement and Concrete Institute (CBI) n° 4-82. Stockholm.
- Whiting, D. 1981, "*Rapid determination of the chloride permeability of concrete*", Federal Highway Administration, Report FHWA/RD-81/119.



CONTENT

REVIEW

- | | Página |
|---|---------------|
| M. G. Alexander: Service life design and modelling of concrete structures – background, developments, and implementation. | 224-245 |
| K. Yang, S. Nanukuttan, W. J. McCarter, A. Long, P. A. M. Basheer: Challenges and opportunities for assessing transport properties of high-performance concrete. | 246-263 |
| C. Andrade: Design and evaluation of service life through concrete electrical resistivity. | 264-279 |

BASIC RESEARCH

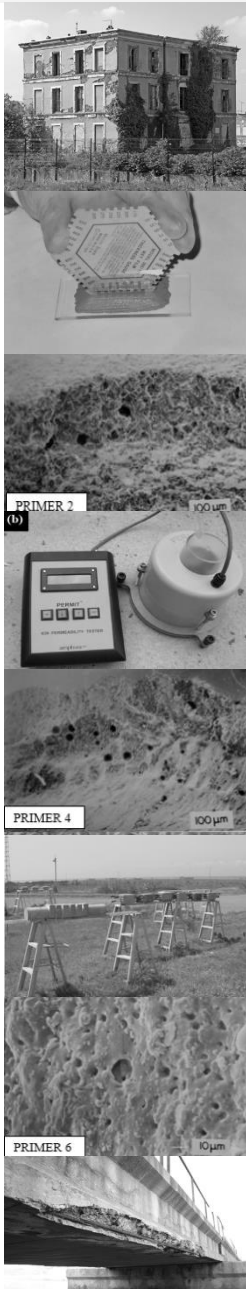
- | | |
|--|---------|
| P. Castro-Borges, P. Helene: A holistic conceptual approach to concrete service life: a split into different time-stages. | 280-287 |
| E. Pazini Figueiredo, C. Andrade: Apparent diffusion coefficient of oxygen and corrosion control of reinforcement rebar coated with primers. | 288-300 |
| Y. A. Villagrán Zaccardi, M. E. Sosa, Á. A. Di Maio: Limitations of sorptivity and water permeability for the estimation of the chloride penetration rate in concrete regarding the accomplishment of prescriptive design for durability in the marine environment. | 301-316 |

APPLIED RESEARCH

- | | |
|---|---------|
| O. Troconis de Rincón, V. Milano, A. A. Torres-Acosta, Y. Hernández-López: Cracks width-corrosion rate correlation on the durability of reinforced concrete in a very high aggressiveness tropical marine environment. | 317-332 |
|---|---------|

STUDY CASE

- | | |
|---|---------|
| R. Boni, C. Britez, P. Helene: Concrete strength control: ABNT, ACI and EN comparative procedures. Site study case. | 333-346 |
| M. Martínez-Madrid, A. A. Torres-Acosta, S. Aschermann, B. Commander, J. Grimson, P. Castro-Borges: Load rating assessment of a corroded pier structure in the Gulf of Mexico. | 347-362 |



Service life design and modelling of concrete structures – background, developments, and implementation

M. G. Alexander^{1*}

*Contact author: mark.alexander@uct.ac.za

DOI: <http://dx.doi.org/10.21041/ra.v8i3.325>

Reception: 21/03/2018 | Acceptance: 05/07/2018 | Publication: 31/08/2018

ABSTRACT

The paper presents an international overview of current knowledge and progress in service life design and modelling of concrete structures. It explores why service life modelling is needed, and indicates that modern demands for longevity, durability, and sustainability of concrete structures cannot be fulfilled without service life modelling. It addresses the current approaches to durability design and specification and concludes that a move to performance-based approaches is imperative for progress to be made. Examples from international experience are cited to illustrate progress that has been made. Lastly, the paper discusses ways of moving forward, recognizing that the philosophical bases are already in place in the form of general code formulations, but which need to be converted into useful approaches.

Keywords: service life modelling; performance-based specifications; concrete durability; durability indicators; model code.

Cite as: Citation: M. G. Alexander (2018) “*Service life design and modelling of concrete structures – background, developments, and implementation*”, Revista ALCONPAT, 8 (3), pp. 224-245, DOI: <http://dx.doi.org/10.21041/ra.v8i3.325>

¹ CoMSIRU, Department of Civil Engineering, University of Cape Town, Cape Town, South Africa.

Legal Information

Revista ALCONPAT is a quarterly publication by the Asociación Latinoamericana de Control de Calidad, Patología y Recuperación de la Construcción, Internacional, A.C., Km. 6 antigua carretera a Progreso, Mérida, Yucatán, 97310, Tel.5219997385893, alconpat.int@gmail.com, Website: www.alconpat.org

Responsible editor: Pedro Castro Borges, Ph.D. Reservation of rights for exclusive use No.04-2013-011717330300-203, and ISSN 2007-6835, both granted by the Instituto Nacional de Derecho de Autor. Responsible for the last update of this issue, Informatics Unit ALCONPAT, Elizabeth Sabido Maldonado, Km. 6, antigua carretera a Progreso, Mérida, Yucatán, C.P. 97310.

The views of the authors do not necessarily reflect the position of the editor.

The total or partial reproduction of the contents and images of the publication is strictly prohibited without the previous authorization of ALCONPAT Internacional A.C.

Any dispute, including the replies of the authors, will be published in the second issue of 2019 provided that the information is received before the closing of the first issue of 2019.

Diseño y modelado de vida útil de estructuras de hormigón: antecedentes, desarrollos e implementación

RESUMEN

El documento presenta una visión general internacional del conocimiento actual y el progreso en el diseño de vida útil y el modelado de estructuras de hormigón. Explora por qué es necesario el modelado de la vida útil e indica que las demandas modernas de longevidad, durabilidad y sostenibilidad de las estructuras de hormigón no pueden cumplirse sin un modelo de vida útil. Aborda los enfoques actuales del diseño y la especificación de la durabilidad y concluye que es imperativo avanzar hacia enfoques basados en el desempeño para avanzar. Se citan ejemplos de la experiencia internacional para ilustrar el progreso que se ha logrado. Por último, el documento analiza formas de avanzar, reconociendo que las bases filosóficas ya están en su lugar en la forma de formulaciones de código general, pero que deben convertirse en enfoques útiles.

Palabras clave: modelado de vida de servicio; especificaciones basadas en el desempeño; durabilidad del concreto; indicadores de durabilidad; código modelo.

Construindo um projeto de vida útil de estruturas de concreto - histórico, desenvolvimentos e implementação

RESUMO

O artigo apresenta uma visão internacional do conhecimento atual e do progresso na modelagem de um projeto de vida útil de estruturas de concreto. Explora porque a modelagem da vida útil é necessária e mostra que as demandas modernas de longevidade, durabilidade e sustentabilidade das estruturas de concreto não podem ser atendidas sem uma correta modelagem da vida útil. Discute as abordagens atuais de projeto e especificação da durabilidade e conclui que uma mudança para uma abordagem baseada em desempenho é imperativa para que um desenvolvimento significativo seja logrado. Exemplos da experiência internacional são citados para ilustrar o progresso que tem sido obtido. Por último, é discutido como avançar, reconhecendo que as bases filosóficas já estão em vigor na forma de formulações gerais nas normas prescritivas e de desempenho, mas que precisam ser transformadas em abordagens úteis ao exercício profissional.

Palavras-chave: modelagem do projeto de vida útil; especificações baseadas em desempenho; durabilidade do concreto; indicadores de durabilidade; norma modelo.

1. INTRODUCTION – WHY THE NEED FOR SERVICE LIFE MODELLING?

Concrete structures can deteriorate prematurely, giving rise to poor durability performance. Reasons include poor understanding of deterioration processes, inadequate acceptance criteria of site concrete, and changes in cement properties and construction practices with time (Neville, 1987). Durability problems in concrete structures cover a wide range including external destructive agents (e.g. sulphates), internal material incompatibilities (e.g. alkali-aggregate reaction), and aggressive environments such as freeze-thaw. The greatest threat for reinforced concrete is corrosion of reinforcing steel, leading to cracking, staining, and spalling of the concrete cover – see Figure 1. This in turn can lead to unserviceable structures that may be compromised in respect of safety, stability, and aesthetics. Such structures become a liability to their owners or managers, resulting in substantial economic loss, as well as being unsustainable by wasting valuable natural resources.



Figure 1. Corrosion-induced damage on a concrete bridge exposed to air-borne chlorides close to the shore in Cape Town

Currently, there is a ‘crisis of concrete durability’. This has several consequences: for infrastructure owners who increasingly require longer service life; for the imperative of proper stewardship of public infrastructure funding; and for developing engineering solutions that establish a basis for confidence in future infrastructure provision. These consequences are serious and need continual and urgent attention from the concrete community.

1.1 Durability and corrosion of reinforced concrete structures

As mentioned, the greatest threat to reinforced concrete (RC) durability is corrosion of the reinforcing steel. Corrosion is initiated by a change in the pore solution surrounding the steel, due either to acidification such as from carbonation, or more seriously, to ingress of chloride ions from a saline environment (e.g. marine or de-icing salts). Reinforcing steel is protected from the environment by a relatively thin cover layer, which must ‘guarantee’ the service life of the structure. Durability is therefore largely controlled by the quality of the cover, which is susceptible to the deteriorating influences of poor curing, early-age drying, inadequate compaction, and penetration of aggressive environmental agents. The durability problem in RC thus reduces largely to one of controlling the cover layer thickness and quality, which is a function of both design and construction decisions and actions. Figure 2 gives a schematic of the concrete cover layer, illustrating the important elements.

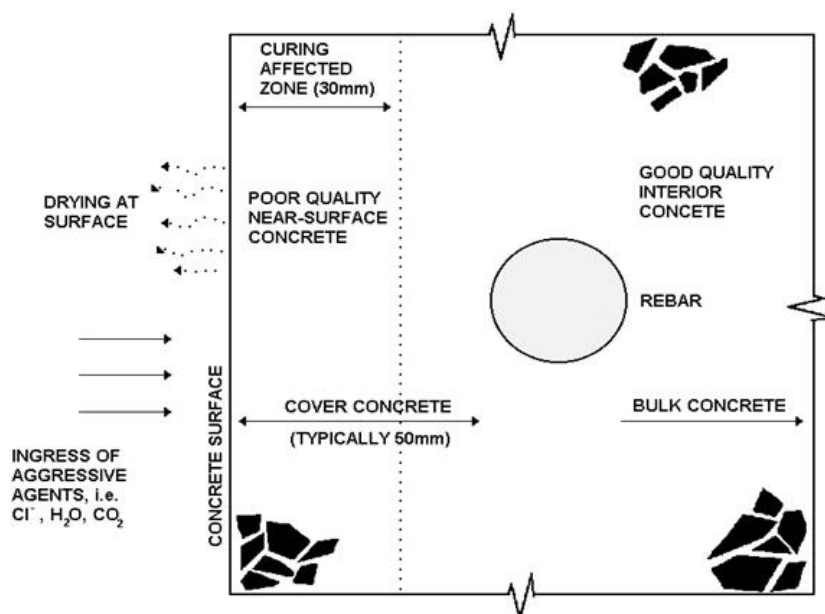


Figure 2. Schematic of cover layer of concrete

Consequently, durability strategies that are likely to give the greatest benefits must directly address the quality and quantity (depth) of the cover concrete. ‘Quality’ refers mainly to its ability to resist the ingress of aggressive fluids from the external environment, which is a function of the binder type and w/b ratio, assuming curing is effectively carried out (a false assumption in many cases, as it turns out!). The binder system is important because its chemical composition governs interaction and immobilisation of aggressive ions such as chlorides. For designers, this relates to two aspects: the ability to (i) quantify cover layer properties for specification purposes, and (ii) undertake service life prediction, which means being able to predict the rate of deterioration of a concrete structure. For constructors, the issue is to select the appropriate concrete materials and proportions, and to implement suitable site practices that ensure the specified cover properties are achieved in actual construction.

1.2 Service life

Engineers need tools for modelling or predicting the deterioration of RC structures over their service life. ‘Service Life Modelling’ (SLM) is intended to allow quantification of the design service life of structures, for purposes of economic optimisation, operational efficiency, and sustained structural and aesthetic performance. Thus, ‘service life modelling’ and ‘service life design’ are closely related: rational design needs good models, and models inform design. (Models are also used for other purposes such as research and diagnosis).

The fib Model Code for Service Life Design (fib, 2006) defines ‘Design service life’ as the assumed period for which a structure or part of it is to be used for its intended purpose, and in which:

- deterioration and material performance are quantified as far as possible (including kinetics or rate effects)
- a suitable ‘risk’ approach is adopted, usually based on probability which leads to measures of reliability
- quantifications, costs, interventions (e.g. maintenance) and the like can be rationally considered.

While the training and experience of structural engineers focuses largely on mechanical and physical aspects of design and specification, the ‘new demand’ is for a more comprehensive toolbox containing ‘tools’ for practical solutions to problems of time-based deterioration. This should also include provisions for deterioration and maintenance costs which can be substantial, easily amounting to several percentage points of GDP and often exceeding 50% of construction budgets. Much more is now required of modern engineers, and service life modelling is one of the ‘new’ demands.

2. HOW DO WE DESIGN FOR SERVICE LIFE?

Practically, how do we design for a service life of, say, 50 or 100 years, when we have no objective evidence on which to base our decisions? Undertaking rational SLM is complicated by changing environments (e.g. global warming), rapidly changing materials (e.g. new cements), inadequate knowledge and models, variable construction quality, differing perceptions of what ‘service life’ means, and the impossibility of verifying our designs in the long term. Clearly, the problem is not simple! A historical example is the Coignet House in Paris, France, shown in Figure 3. This was probably the first reinforced concrete house, built in 1853, and now more than 160 years old. To place this in context: how should such a house have been designed in the 19th Century to conform to requirements of the 21st Century? Much can change over the service life of a structure that might render even the best attempts at SLM rather meaningless.



Figure 3. Coignet House in Paris, France. The world's first RC house, 1853.

Service life of a RC structure is illustrated schematically in Figure 4, which shows the progress of deterioration over time of a structure (A), as it begins to deteriorate from its initial as-built condition (at time zero). Ideally, the time at which the structure reaches an unacceptable level of damage should equal or exceed the design service life and should be able to be modelled. However, many structures deteriorate prematurely, as in B in Figure 4, displaying inadequate durability and rapid deterioration, requiring rehabilitation during its service life. This deterioration is often unanticipated, which illustrates the need to accurately predict the performance of concrete structures during their service lives. The increasing frequency of inadequate durability and the associated high costs of repair mean that infrastructure owners are requiring that designers and contractors provide assurance of a pre-defined, repair-free service life of concrete structures.

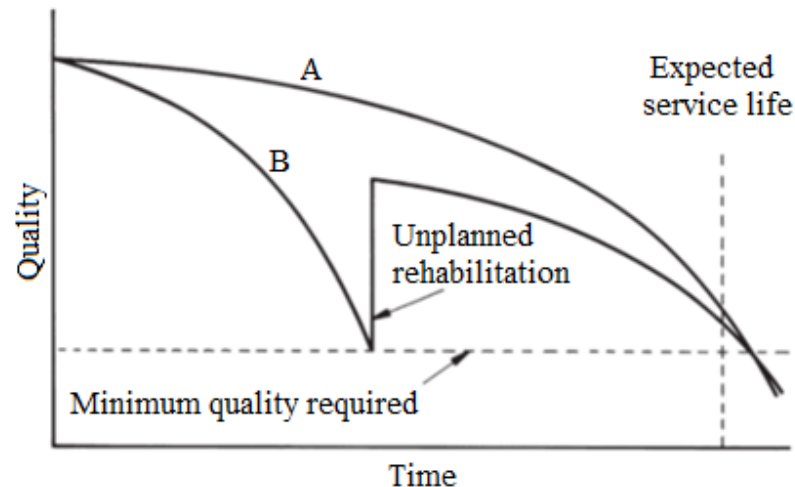


Figure 4. Schematic illustration of the concept of 'service life' of a structure

To summarise: service life design requires service life modelling and service life prediction. Service life is essentially about adequate serviceability over the design life, which implies that the structure must have adequate durability, as a serviceability limit state condition (SLS), or preferably as a durability limit state condition (DLS) which can be thought of as a sub-limit of the SLS criteria. Therefore, in the context of this paper, it is necessary to review current durability design and specification.

2.1 Current durability design and specification

Durability design of RC structures is the process of determining the most appropriate combination of materials and structural details to ensure durability (serviceability) of the structure over its design life and in its design environment (Alexander and Santhanam, 2013). This should be framed in terms of acceptable reliability or probability of the structure performing satisfactorily. The problem involves weighing the risk of undue deterioration with the economics of ensuring durability and may include planned maintenance and repair.

Durability specifications are closely linked to design. The specification sets out requirements to ensure that the structure is constructed according to the intent of the design and should give clear information on the desired nature or outcomes of the construction. There are two main types of specifications:

1. Prescriptive, setting out methods, materials, processes, and procedures that instruct exactly *how* to carry out the work. The constructor has few options and must simply carry out the specification instructions, leaving little room for innovation.
2. Performance, outlining *what* is required as a finished product, i.e. the desired *outcomes* of construction, defining these outcomes clearly in terms of measurable performance criteria.

2.1.1 Critique of current durability design

Currently, there is very little true durability design carried out for RC structures. Any durability ‘design’, if it does occur, is usually limited to rather vague specification clauses (or conversely, complex specifications that are unrealisable), in the hope that if the specification is adhered to, the structure’s durability should be ensured (i.e. a ‘deemed-to-satisfy’ approach). Further, durability specifications are often mired in outdated approaches and unrealistic assumptions. However, there are some notable examples of rational durability design (see for example Part Three of (Alexander, 2016a), which deals with practical case studies such as, inter alia, The Confederation Bridge in Canada, Marinas in the Gulf region, The Danish Strait Crossing Bridges, the Hong Kong- Zhuhai- Macau Sea Link project, and the New Panama Canal).

Current practice considers that compressive strength is the crucial factor, often used as a proxy for durability (Alexander, et al, 2008). However, different methods of achieving the same concrete strength do not all result in the same durability. In addition, strength of fully compacted, fully cured laboratory specimens cannot account for construction processes such as placing, compaction and curing, which affect the quality of the concrete cover. The important rate-controlling deterioration factors are the concrete material constituents, the cover quality of the as-built concrete, and the aggressiveness of the environment. It is usually impractical to control or modify the exposure conditions; therefore, strategies for improving service life must focus on the materials and the quality of construction. Such strategies require service life models and appropriate durability performance specifications (Mackechnie and Alexander, 2002). These developments facilitate innovative and responsive durability design, which is largely lacking at present.

2.2 Need for a new approach: from prescriptive to performance-based design and specification

While most specifications are still prescriptive, there are concerted international efforts to move from prescriptive to performance specifications, for example the P2P initiative of the US National Ready-mix Concrete Association (NRMCA, n.d.) and the French PERFDUB Programme (Linger & Cussigh, 2018). There are major benefits in moving from prescriptive to performance-based specifications, not least that the latter represents a more rational approach to improving concrete performance (Simons, 2004, Day, 2005, Bickley et al, 2006). Although the general philosophy of performance-based specifications is well established (Lobo et al, 2005, CAN/CSA, 2004), divergence remains on appropriate definitions and reliable measures of quality parameters. Appropriate test methods are crucial, and without these, little true progress can be made. Test

approaches have been reviewed by RILEM TC-NEC (RILEM, 2005), and further developments can be expected. While some tests are well established, such as the rapid chloride permeability test (RCPT) (ASTM C1202, 2010), the challenge will be to standardise newer and improved test methods, and general acceptance in the concrete industry.

2.2.1 Critique of prescriptive specifications

Structural concrete is designed to meet specific criteria for workability, strength, durability, and so on. As indicated, current specifications are largely prescriptive, laying down values for limiting parameters such as minimum binder content, maximum w/b ratio, minimum compressive strength, amount of entrained air, etc. Prescriptive specifications work on a ‘deemed-to-satisfy’ basis, where if the requirements are met (which is frequently not verifiable in practice), the structure is ‘deemed-to-satisfy’ the durability requirements. Prescriptive specifications are usually obscure on issues such as exposure conditions for the structure. They hark from a previous period when material complexity was less, and durability was not the critical issue which it now is. Their main drawback is that they specify parameters that are often unverifiable in practice, more particularly on the as-built structure, and thus cannot be verified objectively. Usually, once the concrete has been mixed and placed, only the compressive strength is measured to ensure compliance with the design requirements and specifications, using specially prepared samples made, cured and tested under conditions that bear little resemblance to those in the actual structure.

Taking compressive strength as a proxy for durability ignores the fact that strength and durability are not necessarily directly related. For example, the compressive strength test is not able to account for the physico-chemical nature of different binders and their resistance to the deteriorative effects of the environment. Also, strength is governed by the internal bulk of the concrete, whereas RC durability is primarily controlled by the thin cover zone, which is critically affected by handling, placement, consolidation, and curing. A reliable measure of the quality of the cover zone can be obtained only by assessing the concrete after hardening in the structure, rather than on companion strength specimens.

The dis-connect between durability and compressive strength is given in Figure 5, showing correlations between a durability parameter (oxygen permeability index OPI (log scale)) measured on actual structures and cube compressive strength measured on standard moist-cured lab cubes from the same concretes placed in the structures. It is clear – there is no correlation! This illustrates powerfully that measurements on actual structures are the only reliable way to assess and verify concrete durability.

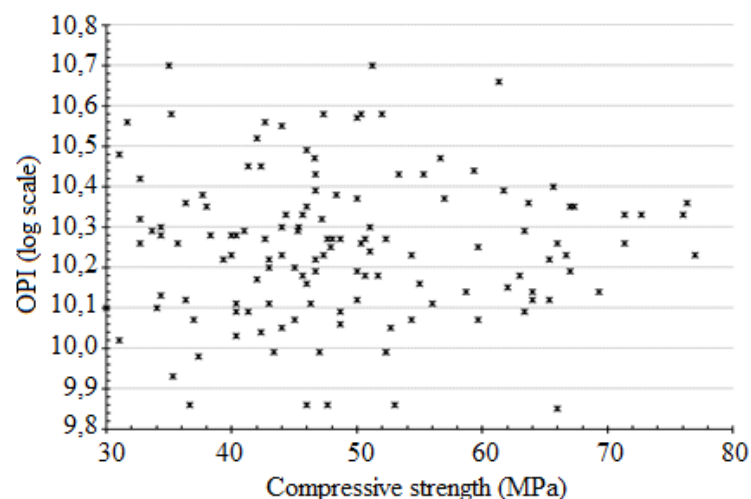


Figure 5. Lack of correlation between standard cube compressive strength, and oxygen permeability (log scale) measured on actual structures (Nganga et al, 2013)

Day (Day, 2005) suggests that prescriptive specifications offer little advantage to the concrete producer, because they limit the extent to which newer developments in materials technology and mixture proportioning techniques can be applied. Simply put, prescriptive specifications stifle innovation in the manufacture and use of concrete.

Notwithstanding the above, some elements of prescriptive specifications are still useful, for example guidance on processes such as compaction and curing. In practice therefore, and in the foreseeable future, a hybrid approach for specifications, with greater emphasis on performance criteria, is appropriate, where the owner and designer decide on the desired performance level in the service environment and propose appropriate ‘index’ or indicator tests (see later), which are used to prepare specifications. The supplier and contractor then provide a concrete system (prequalified using tests conducted before actual construction) that satisfies the index parameters or limits set by the owner/designer. The ‘concrete system’ not only describes the mixture requirements, but also encompasses the concreting procedures adopted.

2.2.2 Performance-Based Specifications

The discussion above indicates deficiencies in prescriptive specifications and raises the importance that key durability-related parameters are measured on actual *as-built* constructions. Thus, performance-based specifications are gaining ground, which assist in assessing and ensuring the required level of concrete quality for long-term durability in the given service environment. Lobo et al. (2005) describe performance specifications as ‘a set of clear, measurable, and enforceable instructions that outline the application-specific functional requirements for hardened concrete’. Performance-based specifications also shift the locus of responsibility for design and construction. In a prescriptive specification, the primary risk is placed on the owner and designer, while performance specifications separate and allocate risk and responsibility more clearly to owner/designer, concrete producer, and constructor (Taylor, 2004). By specifying and testing the concrete at the point of supply, and after placement and early hardening in the structure, the risk and responsibility appropriate to the supplier of the concrete is distinguished from that of the constructor who places and cures the concrete.

The main drawback for performance-based specifications is the lack of agreement, consistency, or standardisation on tests for measuring the concrete cover properties (or other criteria of the specification). For example, EN 206-1 (2013), which deals with specification, performance, production and conformity for concrete construction, ‘avoids’ a performance-based approach on the ground of lack of agreement on test methods.

As argued earlier, compressive strength is not an adequate indicator of durability. Rather, tests and parameters are needed that reflect rate-controlling deterioration factors, such as material constituents, the cover quality of the finished concrete, and the aggressiveness of the environment. Therefore, durability specifications for RC must rely on measuring transport properties of the cover zone. Such developments pave the way for crafting innovative performance specifications.

To summarise: the key to improving reinforced concrete durability is to require that as-built structures meet certain critical performance criteria in respect of probable modes of deterioration, notably reinforcement corrosion. The purpose is to ensure that the structure, during its service life, does not approach a “limit state” beyond which serviceability of the structure becomes compromised. The goal of performance-based specifications is to ensure that an acceptable probability of durability performance is achieved. A shift from prescriptive to performance specifications is one of the important steps necessary to address the shortcomings that are often apparent in current reinforced concrete construction.

2.2.3 Durability indicators, or durability indexes

The concept of ‘durability indicators’ or ‘durability indexes’ (DIs) originated in the 2000s from work of, inter alia, Andrade (Andrade & Izquierdo, 2005), Alexander (Alexander et al, 2001) and

Baroghel-Bouny and co-workers (Baroghel-Bouny, 2004), all of whom proposed the use of ‘indicators’ or ‘indexes’ for control of durability. Such DIs are intended to describe, and hence control, a range of deterioration problems, and include physical, chemical, and electro-chemical parameters. DIs generally describe a transport property or deterioration mechanism and may be used to characterise the concrete in terms of its ‘potential’ durability (Alexander, et al, 2017). ‘Potential’ durability refers to the potential for the concrete to be durable in the given environment, provided it is properly proportioned with the correct constituents and then cured appropriately *ab initio*. To obtain durable concrete structures using this concept, various parameters are needed that can serve as ‘indexes’ of the durability of the material or structure. By measuring these in the short-term, they can be used as indicators of the likely durability performance of the structure in the long-term. They should be fundamental material parameters that relate to transport mechanisms and deterioration processes. These parameters should characterise the key material property (or properties) that govern the durability issue of concern, measurable in tests that are relatively simple, quick, and accurate in the sense that they properly represent the ‘real’ durability problem. The usefulness of indicators or indexes will be assessed ultimately only by reference to actual durability performance of structures built using the indexes for quality control purposes - a long-term undertaking. Thus, a framework for durability studies should incorporate at least the following elements: early-age material indexing, direct durability testing, and observations of long-term durability performance; these elements should be linked by the relevant DI(s), so that an integrated approach emerges that can be used in durability design and specification of concrete structures (Alexander & Ballim, 1993).

2.3 Service life modelling and prediction

Service life modelling for reinforced concrete structures involves quantitative calculations or estimates to predict the time to unacceptable damage (e.g. cracking, corrosion, loss of section, etc.) for a given environment. Service life models are often semi-empirical in nature, based on laboratory and site data that are necessary for calibration. Alternatively, SLMs can be constructed from ‘first principles’, using ionic or reactive transport models and principles of flow in porous media (Van der Lee, et al., 2008); these models elaborate the ‘transport-interaction’ aspects of fluid or ionic flow in the concrete, with approaches based on thermodynamic and geochemical principles (Guillon et al, 2013). However, such models are not necessarily more accurate or reliable in their predictions, and the added complexity does not always justify the results obtained. In any event, these models must also be calibrated from laboratory and site data, and herein lies the rub: in almost all cases, concretes of a range of mix constituents and proportions need to be tested in appropriate environments to collect data which can be used to calibrate or construct the model, and subsequently to predict the ingress of harmful substances. SLMs are also useful in ‘back-analysis’ of existing structures when the penetration of contaminants such as chlorides is known for a particular concrete and environment at a particular time; it is then possible to use the model to determine the time to corrosion and possibly damage as well if there is a linked damage model. For a full probabilistic approach, variability also needs to be considered (Muigai, et al, 2009).

2.3.1 The two-stage conceptual service life model

The well-accepted conceptual ‘model’ for service life is the two-stage model proposed by Tuutti, (Tuutti, 1992). Deterioration is conceptualised into two distinct phases, the initiation phase and the propagation phase – see Figure 6. During the initiation period, contaminants enter the concrete to the depth of the reinforcing (in sufficient concentration), at which stage the protective passive layer on the steel is depassivated, resulting in an active corrosion state. The length of this period depends on concrete quality, cover depth, exposure conditions and the threshold or critical concentration required to initiate corrosion. Once corrosion initiates, the corrosion propagation phase commences in which active corrosion ensues, leading in time to structural damage. Figure 6 shows that the

propagation period can be further sub-divided into different limit states, namely the onset of corrosion, cracking due to expanding corrosion products, delamination and spalling of concrete cover, and possible ultimate collapse of the structure.

2.3.2 Practical service life models

Various service life models exist in different parts of the world, largely in response to conditions in the various localities where the SLMs were developed. Most models cover both chloride and carbon dioxide ingress into concrete, such as the European model “DuraCrete” (DuraCrete, 1998) and the North American “LIFE-365” (2005). In South Africa, carbonation and chloride ingress models have also been developed (Mackechnie & Alexander, 2002).

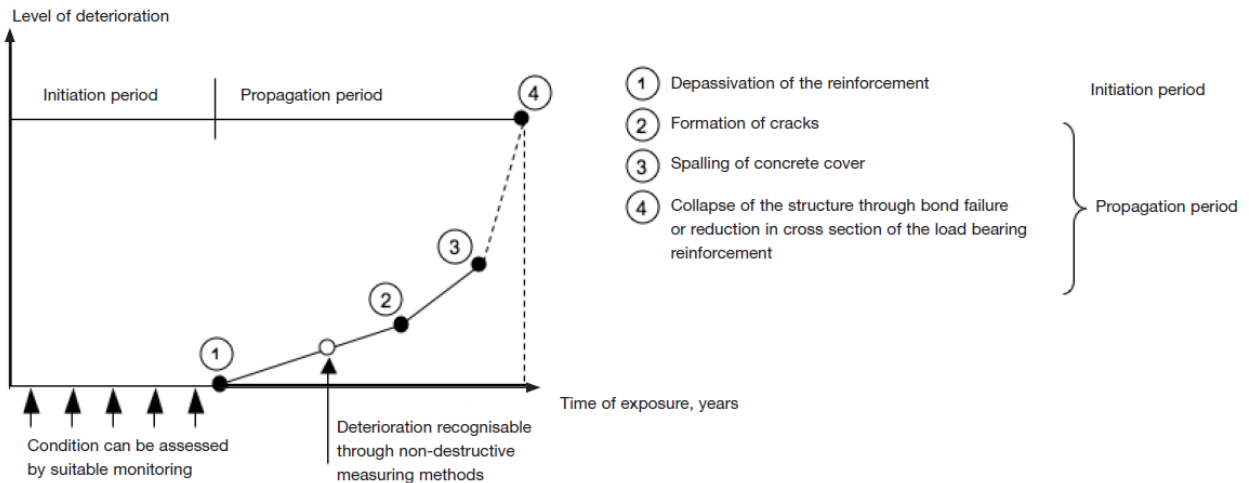


Figure 6: Two-stage Tuutti model

Table 1 provides a summary of some of the more prominent service life models available at present. Chloride modelling is commonly represented, with carbonation modelling also evident. (Further details on SLMs is given in the section on International efforts.)

Table 1. Summary of some service life models for reinforced concrete

Model	Characteristics	Reference
Life-365®	Chloride diffusion model, based on Fick’s law. Semi-probabilistic. Provides life-cycle cost analysis.	Free software. www.Life365.org
Stadium®	Multi-ionic model, based on Nernst-Planck equation. Provides chloride ingress rate and corrosion initiation. Also provides carbonation and sulphate profiles. Full probabilistic.	Proprietary software www.simcotechologies.com
fib Bulletin 34	Based on Fick’s 2 nd law. Deals primarily with chloride ingress and carbonation. Used in fib Model Code 2010. Full probabilistic.	Open source bulletin: ISBN: 978-2-88394-074-1
ConcreteWorks	Based on Fick’s law. Predicts strength, chloride ingress, thermal cracking	www.texasconcreteworks.com (Folliard et al, 2008)
ClinConc	Chloride diffusion model.	(Tang, 2008)

2.4 International efforts in developing SLMs and performance-based specifications

This section outlines developments in SLMs and performance-based specifications in various parts of the world. Most models are concerned with prediction of onset of steel corrosion in concrete, and therefore with ingress of carbon dioxide or chlorides, and so the discussion will be limited to these deterioration mechanisms. General remarks are given first, followed by salient details for each country or region.

The European, Scandinavian and South African chloride prediction models are performance-based approaches, i.e. they are based on actual measurement of material properties of the concrete mix or structure under consideration. The onset of corrosion is predicted using Fick's second law of diffusion which permits chloride profiles to be modelled using a relevant diffusion coefficient, the exposure conditions, and the chloride surface concentration. Diffusion coefficients based on various materials and mix proportions are experimentally determined or obtained from experience. Different test methods are used in different parts of the world to estimate chloride diffusion coefficients. The European and Scandinavian models apply the Rapid Chloride Migration (RCM) test (NTBUILD 492, 1999) while the chloride conductivity index (CCI) test (Streicher and Alexander, 1995) is used in South Africa. For carbonation models, the carbonation resistance of concrete is usually found from accelerated carbonation tests typically using laboratory-cured specimens.

By contrast, the North American "LIFE-365" model is based on computer simulations and does not involve testing. The service life and life-cycle costs of reinforced concrete structures are estimated from input parameters such as mix proportions and materials, preventative measures (corrosion inhibitors, coatings, stainless or epoxy-coated steel) and environmental conditions.

Several countries around the world have, to varying degrees, adopted the use of performance-based specifications for concrete construction, and are discussed below.

2.4.1 Canada and Australia

Bickley et al. (2006) give a brief review of the use of performance specifications in Australia and Canada. A common factor in these countries is the refinement of the definitions of exposure classes, enabling a clear description of the type of performance desired in a specific situation. The Australian concrete specification (AS, 2007) provides for special grade concrete that can be ordered using either performance or prescriptive criteria. According to Day (2005), Australian specifications provide a good platform for competent concrete producers, with the producer conducting the main tests on the concrete and independent labs performing only limited checks for quality assurance. An essential component of this arrangement is the presence of a good 'quality system' that monitors the concrete throughout and allows control of deviations. However, the main thrust of these specifications remains control of concrete strength, rather than overt attempts to measure 'durability' directly.

The Canadian concrete standards (CAN/CSA, 2004) give the choice to specify either performance or prescriptive criteria. Exposure classes have been extensively defined, and limits are suggested for constituents or properties that will lead to the production of durable concrete for the specific exposure condition. These limits can be interpreted in both prescriptive or performance specifications; in the former, compliance to the limits would be required, while for the latter, limits would serve as a valuable guideline to the supplier.

Bickley et al. (2006) indicate that the Canadian standards use performance requirements such as total charge passed (Coulombs) for special categories of chloride exposure, in addition to the routine prescriptive requirements. Several standardized testing methods are available to use in performance specifications, namely, the RCPT (ASTM C1202, 2010), air void system (ASTM C457, 2010), sorptivity (ASTM C1585, 2004), and chloride bulk diffusion (ASTM C1556, 2004). These tests can be conducted either on samples cast during concreting or from drilled cores. However, not all these tests are useful for routine quality control purposes.

2.4.2 USA

As mentioned, the North American “LIFE-365” service life model for chloride ingress is based on computer simulations and does not involve testing directly. However, Thomas et al showed that the model successfully predicted the ingress of chlorides into different concretes in a marine exposure site in Maine, USA (Thomas et al, 2012, Alexander and Thomas, 2015). For other types of deterioration, Simons (2004) outlined experience with performance specifications in New Mexico, where there is a high risk of alkali silica reaction in concrete. From a specification that prescribed safety against only ASR, freezing and thawing, and salt related damage, newer specifications were developed that addressed issues of variability in aggregate quality around the state, differences in operating equipment and procedures, and minimization of cracking, in addition to the three durability issues stated earlier. This led to controls on the cement quantity as well as controlled gain of strength of concrete. In the newer specifications, references to minimum cement content, maximum water content, and sand-aggregate ratio were removed, while appropriate tests for measuring ASR potential, permeability, and freeze–thaw were outlined. The older specifications could not ‘guarantee’ protection against the durability issues, as there was no direct testing.

2.4.3 Scandinavia

In Scandinavia, the “ClinConc” chloride ingress model has been developed (Nilsson et al, 1996, Tang, 2008). It models chloride transport in the concrete pore structure, taking free chlorides as the diffusion potential, and then calculates the total chloride content taking into account non-linear chloride binding. It is therefore a type of ‘transport-interaction’ model.

In Norway, Gjrv pioneered an approach to probability-based durability design using DuraCrete guidelines but expressed in a probability-based model called DuraCon (Gjrv, 2014). Using a modified Fick’s second law and a Monte Carlo simulation, the probability of corrosion during a certain “service period” for the structure in the given environment is obtained, with the following input parameters:

1. Environmental loading: chloride loading, age at chloride loading, and temperature
2. Concrete quality: chloride diffusivity, time dependence of the chloride diffusivity, and critical chloride content
3. Nominal concrete cover

A certain “service period” is specified before the probability for onset of steel corrosion exceeds an upper serviceability level of 10%, which is in accordance with current standards for reliability of structures. Based on the calculations, a combination of concrete quality and concrete cover can be selected, which will meet the specified “service period.” In the case of North Sea offshore concrete platforms, performance requirements based on chloride diffusivity (measured in the NT Build 492 “Rapid chloride migration test”) and concrete resistivity, as well as cover thickness were specified. Gjrv suggests that resistivity can be used to assess chloride diffusivity of the structural concrete, as well as for site quality control.

2.4.4 Spain

In Spain, Andrade et al (1993) proposed the use of electrical resistivity to characterize mass transport processes universally in concrete, i.e. for both chloride diffusion and gas permeation. Resistivity provides a fast, easy and cheap measure of concrete penetrability, also suitable for on-site use for quality control of new structures. A test limitation is that it cannot consider the influence of the binding capacity on transport mechanisms. Resistivity has the advantage of enabling assessment of existing structures through systematic mapping, described in the RILEM TC 154-EMC Recommendation (Andrade et al, 2004). In addition to resistivity measurements and RCPT, Andrade proposed the use of half–cell potential measurements and site determination of the corrosion rate using Polarization Resistance (Andrade et al, (2004).

Service life models (SLM) for the initiation and propagation period of corrosion, based on electrical resistivity, have been developed and are reported in Andrade (2004) and Andrade and d'Andrea (2010). The SLM considers the reaction or retarder factor of chlorides (r_{cl}) for different cement types accounting for chlorides that are immobilized by cement phases through binding, environmental factors (k_{cl,CO_2}) based on exposure classification as in EN 206, and the aging factor (ρ_i). The input parameters in the model are the cement type which determines the value of r_{cl} , exposure class from which a value of k_{cl,CO_2} is obtained, service life e.g. 100 years, cover depth and the aging factor. From these input parameters, the resistivity is obtained as a corrosion indicator (or durability indicator) that can be used to assess performance of a structure.

2.4.5 Switzerland

The Swiss Standard SN 505 262/1:2013 incorporates several DIs, prescribing limiting values for compliance by the concrete producers. Among them are a chloride migration test (similar to NT Build 492 (1999)) and an accelerated carbonation test, for chloride- and carbonation-induced corrosion respectively. A DI is also prescribed for conformity control of the end-product, using the site air-permeability test developed by Torrent, (Torrent, 1992) with limiting values for chloride- and carbonation-induced corrosion.

Rules for the application of the Torrent air permeability test for quality and durability control are provided in Swiss Standard SN 505 262/1 (2013), summarized by Torrent et al (2012). Limiting coefficient of permeability values, k_T , are provided based on the exposure conditions in EN 206-1. The in-situ concrete should be tested at 28 to 90 days after placing. For slow-reacting cements such as with fly ash, a minimum test age of 60 days should be considered. Precautions should be taken to avoid testing concrete at very low temperatures or with high degrees of saturation. Moisture content is checked using an electrical impedance-based instrument, with an upper moisture limit of 5.5% (by mass). Further details on conformity evaluation and acceptance testing are given in the Swiss Standard or in (Jacobs et al., 2009), (Torrent and Jacobs, 2014).

2.4.6 South Africa

The South African concrete industry has been experimenting with performance specifications and durability design for two decades now (Alexander et al, 2001). A “durability index” approach has been developed to improve the quality of reinforced concrete construction, i.e. it specifically aims to control rebar corrosion. It is based on measurement of transport properties of the cover layer, for either laboratory or in-situ concrete, which reflect the dual aspects of material potential and construction quality. Key stages in formulating this approach were developing suitable test methods to measure durability indexes, characterising a range of concretes using these tests, studying in-situ performance, and applying the results to practical construction. The approach has progressed to the point where rational durability design and performance-based durability specifications exist and are being applied in actual construction.

The Durability Index (DI) approach, is based on the following principles:

- Reinforced concrete durability depends primarily on the quality of the cover or surface layer, i.e. its ability to protect the reinforcing steel.
- Improved durability can only be assured if a relevant durability parameter(s) can be measured.
- The quality of the cover layer should be characterised using parameters that influence deterioration processes and that are linked with relevant transport mechanisms.
- Index tests are needed to cover the range of durability problems, each index test being linked to a transport mechanism relevant to that process.
- The usefulness of index tests is assessed by reference to actual durability performance of structures built using the indexes for quality control purposes.

Three DI tests have been developed: oxygen permeability index, chloride conductivity index, and water sorptivity index tests (see Table 2). DIs are quantifiable ‘engineering’ parameters that characterise concrete in the as-built structure (or from the lab), and are sensitive to material, processing, and environmental factors such as cement type, water: binder ratio, type and degree of curing, etc. Material indexing provides reproducible engineering measures of microstructure and key properties of concrete at a relatively early age (e.g. 28 days).

Testing for DI values is done on cores that are removed either from laboratory specimens, or from test panels or actual structures. Rigorous site proving trials have shown that coring from site cubes is not adequate, with test panels being more representative of in-situ construction (Ronny and Everitt, 2010). Typically, test panels (400 mm wide, 600 mm high and 150 mm thick) are constructed adjacent to the structure with the same concrete, shutter type, compaction and curing methods used for the actual structure, and at the same time as the actual structure. Cores are removed at 28 – 35 days and taken to an approved laboratory for durability testing. For precast median barriers, samples for testing are obtained directly from the actual elements.

The approach has also derived correlations between durability indexes, direct durability testing results, and actual structural performance, and the indexes can therefore be used as follows:

- For controlling a particular property or quality of the cover zone, reflected by a construction specification in which limits to index values are specified
- For assessing the quality of construction for compliance with a set of performance criteria
- For fair payment for the achievement of concrete quality.
- For predicting the performance of concrete in the design environment, by being linked with Service Life Models. Two SLMs incorporating the relevant durability indexes have been developed for SA conditions – a carbonation ingress model, and a chloride ingress model (Mackechnie and Alexander, 2002).

Importantly, the South African work represents an ‘integrated’ approach in which measured durability indexes giving actual material quality either in pre-trials, lab situations, or the as-built structure, are linked to the construction specifications for quality control purposes and to rational service life prediction models used in design. Such an approach allows complete integration and consistency between design, specification, and construction quality. (Implementation of the South African approach is further explored later).

2.5 Summary: performance-based approaches

Table 2 summarises provisions in selected countries for performance-based specifications.

Table 2 indicates that there has indeed been progress towards performance-based methods in various parts of the world. Problems still exist, and it is doubtful that a universal approach will easily emerge soon. However, it is probably more appropriate that local or regional solutions be found which can assist in moving concrete construction forward in those localities.

There is an important caveat, however: performance specifications must require *as-built* assessment of concrete quality in relation to durability to be regarded as truly ‘performance-based’. Pre-qualification and testing of laboratory mixes is not sufficient, which means that many of the so-called ‘performance’ approaches are only partial at this stage. (Further information on implementation of performance-based approaches in parts of the world can be found in Chapter 6 of Alexander et al, 2017).

Table 2. Summary of durability performance-based approaches in various countries (based on durability indicators or indexes) (Details in Alexander (2016b))

Country	Durability parameter (Indicator or index)	Service life model	Durability test method
Canada	Chloride ion penetrability	None identified	ASTM C 1202 Chloride penetration test
France	Chloride diffusion coefficient - effective and apparent - Apparent gas permeability - Liquid water permeability - Initial Ca (OH) ₂ content - Water-accessible porosity	LCPC Empirical models	Chloride diffusion - migration and diffusion tests Air and water permeability
Netherlands	Chloride ion penetration	DuraCrete Probability-based durability design	NT Build 492, rapid chloride migration test Two Electrode Method (TEM)
Norway	Chloride diffusivity	DuraCon Probability based durability design	NT Build 492, rapid chloride migration test Two Electrode Method (TEM)
Spain	Electrical resistivity	Resistivity-based model LIFEPRED	Two-point or Wenner four point resistivity test
Switzerland	Chloride Migration Accelerated Carbonation Air permeability on site	None identified	Max Limits: SN 505 262/1-B (NT Build 492) Max Limits: SN 505 262/1-I Max Limits: SN 505 262/1-E (Torrent k _T)
South Africa	Oxygen permeability Water sorptivity Chloride conductivity Lab or site	Chloride- and Carbonation-induced corrosion initiation models	Oxygen permeability index OPI Chloride conductivity index CCI Water sorptivity index WSI

3. WAY FORWARD, AND PRACTICAL STEPS

‘Service Life Modelling’ and ‘Service Life Design’ are related: i) they both involve assessing durability performance of a structure over its design life, ii) rational design for durability needs predictive deterioration models that provide the chemistry and kinetics of the problem by way of rate equations, and iii) predictive modelling provides the basis for design.

However, ultimately, design engineers work to Codes of Practice and other standards such as specification documents. Thus, predictive models need to be linked to Codes and Standards either implicitly by being incorporated into them, or explicitly by being accepted as suitable models for design that link with the design code requirements. Practically, ‘real progress’ will occur only with the formulation and ratification of design codes and standards.

This section reviews aspects of current codification for durability design and provides an example from South African practice of the implementation of a durability performance specification.

3.1 Moves toward codification of service life design

The fib Model Code for Service Life Design (SLD) (2006) categorizes approaches for service life design as: full probabilistic, partial factor design, deemed-to-satisfy, and avoidance of deterioration (see also later). Any of these approaches can be used, although a full probabilistic approach is desirable for large public infrastructure projects or prestigious structures.

Currently, approaches for rational durability design are limited and of variable implementation. For example, the approaches in the European DuraCrete, (1998) and Life-365 (2005), while useful, are location specific and do not fully represent an integrated approach, which requires site-measurable durability parameters which are used in a performance specification and coupled with Service Life Models. Durability design also needs a specification for implementation during construction, to ensure that the design assumptions for concrete quality and composition are achieved. Since the approaches mentioned are not ‘codified’, design and specifying authorities find limited justification to use them, especially if they do not have the needed expertise.

3.1.1 Service life design approaches and limit states

Walraven suggests that practical application of a performance-based approach for service life assessment and codification requires the following elements (Walraven, 2008): (i) limit state criteria, (ii) a defined service life, (iii) deterioration models, (iv) compliance tests, (v) maintenance and repair strategies, and (vi) quality control systems. Limit state criteria for concrete durability should be quantified, with clear physical meaning such as percentage of cracking or loss of surface, and the like. Deterioration models are generally mathematical and should include parameters that are linked to the performance criteria.

As indicated, the importance of codes of practice makes it essential that any usable approach be codified. Structural codes, which include durability provisions, are often slow in being updated so that new knowledge from research and practice takes a long time to enter the standards. As an example of performance-based durability design, (ISO 13823, 2008) outlines a limit-state methodology, summarised in Figure 7, which is related to different service life design approaches.

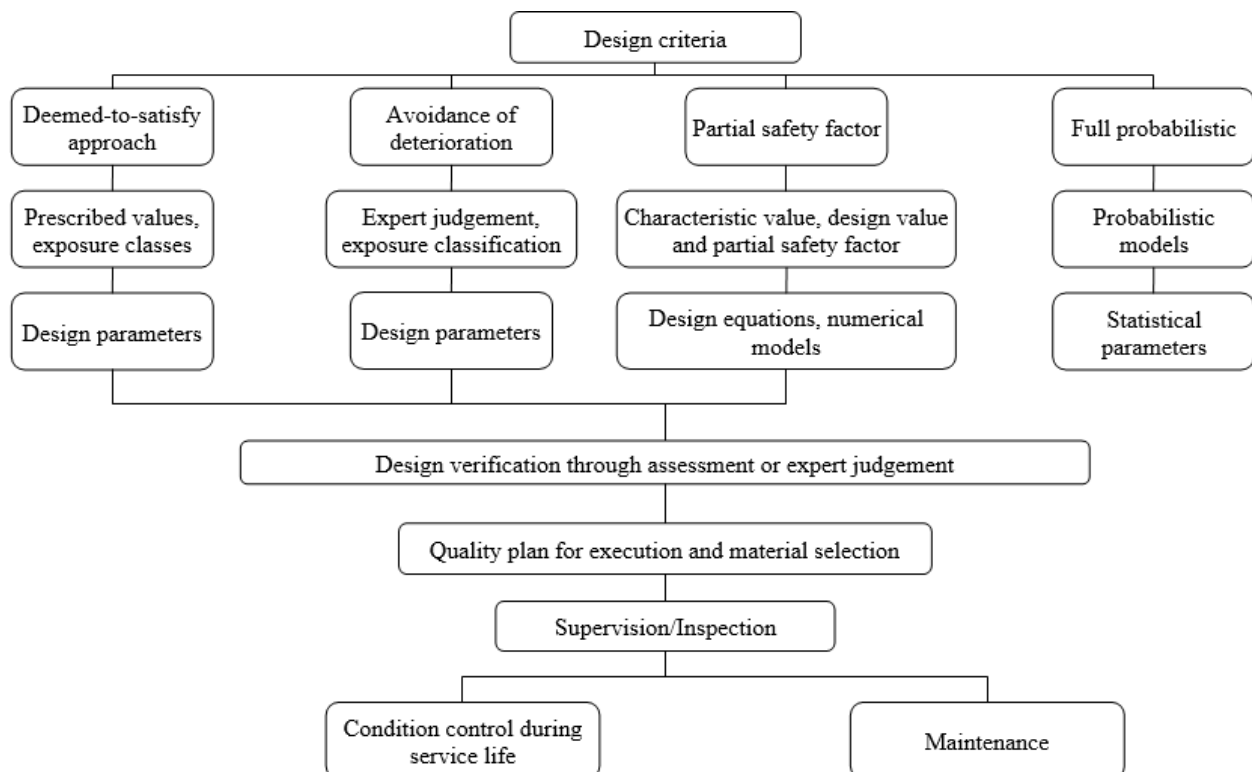


Figure 7. Summary of service life design approaches (ISO 13823, 2008)

Figure 7 is also reflected in the fib Model Code (2010), with several approaches to service life design. In principle, the design approaches in the Model Code avoid or minimise deterioration caused by environmental action, similar to present approaches to design for loading; they are therefore ‘intelligible’ to structural design engineers. Based on quantifiable models for the “loading” (i.e. environmental actions) and the resistance (i.e. resistance of the concrete against the considered environmental action), the design options as given earlier in the fib SLD Model Code are mirrored, viz. full probabilistic approach; semi-probabilistic approach (partial safety factor design); deemed-to-satisfy rules; and avoidance of deterioration.

The full probabilistic approach should be used for exceptional structures only and is based on probabilistic models that are sufficiently validated to give realistic and representative results of deterioration mechanisms and material resistance. The basis is formed by appropriate test methods and statistical evaluation models, both of which lack significantly at present. The first two options involve quantitative evaluation of the performance of a structure using limit-state theory, documented in ISO 2394 (2015), with three limit states: ultimate limit-state (ULS), serviceability limit-state (SLS), and durability-limit-state (DLS). The ULS addresses the safety and stability of the structure (see e.g. EN 1990-1: 2002). The SLS considers failure due to material deterioration (e.g. sulphate attack) or excessive deflection, cracking and vibration. The DLS marks the onset of durability failure e.g. corrosion initiation in a RC structure (ISO 13823: 2008). Each of the three limit states is characterized by an inequality: the performance (R) (‘Resistance’) of the structure should be larger than the target design requirements (S) (‘Loading’, in this case, environmental loading). This is expressed by Equation (1).

$$R - S > 0 \quad (1)$$

The task of the designer is to carry out performance verification of a structure to ensure that the chosen design variables are such that the specified limit-state is not reached within the design working life. The performance verification depends on the probabilistic approach used i.e. full probabilistic or partial safety factor (semi-probabilistic) approaches.

Discussing further the partial safety factor approach, the probabilistic nature of the problem (scatter of material resistance and load data) is considered through partial safety factors. It is based on the same models as the full probabilistic approach and is intended to present a practical, statistically reliable design tool.

The deemed-to-satisfy approach is comparable to durability specifications given in most current codes and standards, i.e. prescriptive specifications based on a selection of certain design values (dimensioning, material and product selection, execution procedures) depending on environmental classes. The difference between the deemed-to-satisfy approach in the fib Model Code and traditional service life design rules is that the latter are commonly not based on physical and chemical models for concrete, but largely on practical experience, whereas the fib method is intended to be calibrated against the full probabilistic approach. The limiting values for design, material selection and execution, are determined either (i) from statistical evaluation of experimental data and field observations, and/or (ii) from calibration with long-term experience of building tradition. However, a specific service life estimate is not required in the ‘deemed-to-satisfy’ approach, rendering it not a performance-based approach, although if the specified limits relate to actual performance criteria such as a relevant durability indicator, it is a step in the right direction. Nevertheless, it remains largely prescriptive. For example, the European Standard EN 206-1:2013 adopts a deemed-to-satisfy approach and prescribes minimum cement content, maximum w/c ratio, and minimum compressive strength class for concrete components in various environmental exposure classes.

The fourth level of service life design (avoidance of deterioration) requires use of deterioration-resistant materials such as stainless steel, or concrete protection systems such as coatings, thus limiting or eliminating deterioration of the structure. Maintenance may still be required such as renewal of coatings from time to time.

Further, many structures or portions of structures are not exposed to severe environmental or operating deterioration mechanisms, in which case simple attention to good construction practices, which should include good mix design, compaction, curing and so on, should help to ensure adequate durability. This is exemplified in the exposure category XO of EN 206-1: 2013, described as: “Concrete with reinforcement or embedded metal: Very dry”, i.e. “Concrete inside buildings with very low air humidity”, which represents a large proportion of concrete construction in mild or benign environments.

3.2 Implementation example: The South African DI approach in practice

The approach to durability design and modelling in South Africa was reviewed earlier, and this section briefly outlines an implementation example (Alexander, 2016b). The approach has progressed to the point that both rational durability design and performance-based durability specifications are in place and being applied in actual construction (Nganga et al, 2013, Alexander et al, 2001, Gouws et al, 2001, Raath, 2004). The approach allows material and production variability to be quantified in deciding on suitable DI limits to be achieved by both concrete producer and concrete constructor, based on statistical principles (Alexander et al, 2008).

3.2.1 Durability Index performance-based implementation on major freeway bridge projects

A significant and large-scale implementation using the DI performance-based approach was undertaken in a major infrastructure project – the Gauteng Freeway Improvement Project (GFIP) – which upgraded the freeway system in urban Gauteng Province between 2007 and 2012 to alleviate traffic congestion. Work involved freeway widening by addition of traffic lanes and construction of interchanges with associated bridges at a cost of about US \$2 billion. Due to the inland environment, the DI approach required only the OPI and sorptivity tests to be performed on site concrete. Limiting values adopted were a minimum of 9.70 for OPI, and a maximum sorptivity of 10 mm/ $\sqrt{\text{hr}}$. Cover depths were also monitored (see Table 3).

The specified limiting values and reduced payment criteria applied in the GFIP are summarized in Table 3. For the water sorptivity test, no reduced payment criterion was applied as the test was used only as an internal control to monitor the effectiveness of curing.

Table 3. Limiting values used in DI-based performance specifications and the reduced payment criteria applied for GFIP (SANRAL, 2010)

	Oxygen Permeability Index (OPI)		Concrete cover	
	OPI (log scale)	Percentage payment	Overall cover (mm)	Percentage payment
Full acceptance	> 9.70	100%	$\geq 85\%$ <(100%+15mm)	100%
Conditional acceptance^a	$> 8.75 \leq 9.70$	80%	$< 85\% \geq 75\%$	85%
Conditional acceptance^b	-	-	$< 75\%$	70%
Rejection	< 8.75	Not applicable	$< 65\%$	Not applicable

^a with reduced payment

^b with remedial measures as approved by engineer and reduced payment

It was found that, although the limiting values were generally achieved on average, individual sets of results (from different sub-projects) showed high variability, illustrated in Table 4. The spread of variability obtained in selected sub-projects is clear, and the differences between construction ‘quality’ (here represented by variability) are quite stark. Only sub-project 9 (a precast median barrier construction yard) achieved acceptable low variability with all results meeting the project specifications. The in-situ results from the other sub-projects are a good illustration of the variability that can be introduced into as-built structures by site construction processes, since essentially the concretes all came from the same source.

4. CLOSURE

It is clear that, for service life design and modelling of concrete structures, considerable progress has been made in recent decades, although much remains to be done. The need for performance-based approaches, without which service life design cannot be implemented, is now reasonably well recognised, but not always by concrete practitioners.

Table 4. Numerical summary of OPI test results – GFIP (Nganga et al, 2013)

Sub-project	OPI (log scale)						Proportion of defectives* (%)
	n	Mean	Max	Min	s	CoV (%)	
1	172	9.75	10.41	9.07	0.28	2.84	40.1
2	94	9.91	10.42	9.37	0.22	2.24	13.8
4	116	9.87	10.40	9.39	0.23	2.33	18.1
6	91	10.06	11.10	8.83	0.46	4.60	26.4
9	132	10.25	10.70	9.85	0.18	1.75	0

* Values that fail to comply with the limit value of 9.70

Approaches have emerged in different parts of the world largely in response to perceived needs for better durability of concrete structures. However, a truly universal approach is still lacking, although the Model Code documents of the fib have outlined the basic philosophy and needed approaches. Major progress can be expected in this important area of concrete design and construction in the coming years.

5. REFERENCES

- Alexander, M. G. & Ballim, Y. (1993), “*Experiences with durability testing of concrete: a suggested framework incorporating index parameters and results from accelerated durability tests*”. Proc. 3rd Canadian Symp. on Cement and Concrete, Ottawa, August 1993, Nat. Res. Council, Ottawa, Canada, 1993: 248-263.
- Alexander, M. G., Mackechnie, J. R., Ballim, Y. (2001), “*Use of durability indexes to achieve durable cover concrete in reinforced concrete structures*, Chapter, Materials Science of Concrete, V. VI, Ed. J. P. Skalny and S. Mindess, American Ceramic Society, pp 483 – 511.
- Alexander, M. G., Ballim, Y., Stanish, K. (2008), “*A framework for use of durability indexes in performance-based design and specifications for reinforced concrete structures*”, Materials & Structures, V. 41, No. 5, pp. 921-936.

- Alexander, M. G., Santhanam, M. (2013), “Achieving durability in reinforced concrete structures: durability indices, durability design and performance-based specifications”. Keynote paper at International Conferences on Advances in Building Sciences & Rehabilitation and Restoration of Structures, IIT Madras, Chennai, India, 21pp.
- Alexander, M. G. & Thomas, M. (2015), “Service Life Prediction and Performance Testing – Current Developments and Practical Applications”. Cement & Concrete Research, Vol 78, pp. 155-164.
- Alexander, M. G. Ed. (2016a), “Marine concrete structures. Design, durability and performance”. Ed. M.G. Alexander, Cambridge: Woodhead Publishers (Imprint of Elsevier). 400 pp.
- Alexander, M. G. (2016b), “Performance-based concrete durability design and specification in South Africa – background, implementation, and quo nunc?” Proceedings fib Symposium, Cape Town, Lausanne, fib, pp. 52-62.
- Alexander, M. G., Bentur, A., Mindess, S. (2017), “Durability of Concrete: Design and Construction”. CRC Press, Taylor & Francis Group, U.K.
- Andrade, C., Alonso, C., Goni, S. (1993), “Possibilities for electrical resistivity to universally characterize mass transport processes in concrete”. In Concrete 2000 Economic and durable construction through excellence Volume Two: Infrastructure, research, new applications. Dhir, R. K. and Jones, M. R. ed. Scotland, UK: E & FN SPON, pp. 1639–1652.
- Andrade, C. (2004), “Calculation of initiation and propagation periods of service life of reinforcements by using the electrical resistivity”. In International Symposium: Advances in Concrete through Science and Engineering. Evanston, Northwestern University, USA, (2004) p. 8.
- Andrade C, Alonso C, Gulikers J, Polder R, Cigna R, Vennesland Ø, Salta M, Raharinaivo A, Elsener B. (2004), “RILEM TC 154-EMC: Electrochemical Techniques for Measuring Metallic Corrosion. Recommendations Test methods for on-site corrosion rate measurement of steel reinforcement in concrete by means of the polarization resistance method”, Materials & Structures V. 37, No. 273, pp. 623-643.
- Andrade, C., Izquierdo, D. (2005), “Benchmarking through an algorithm of repair methods of reinforcement corrosion: the Repair Index Method”, Cement & Concrete Composites, V. 27, No. 6, pp.727-733.
- Andrade, C., d’ Andrea, R. (2010), “Electrical resistivity as microstructural parameter for modelling of service life of reinforced concrete structures”, In 2nd International symposium on service life design for infrastructure. pp. 379–388.
- Australian Standard (AS) (2007), AS 1379: “Specification and Supply of Concrete”. Sydney: Standards Australia.
- ASTM International. (2010). ASTM C457/C457M-10a Standard Test Method for Microscopical Determination of Parameters of the Air-Void System in Hardened Concrete. Retrieved from https://doi.org/10.1520/C0457_C0457M-10A
- ASTM International. (2010). ASTM C1202-10 Standard Test Method for Electrical Indication of Concrete’s Ability to Resist Chloride Ion Penetration. Retrieved from <https://doi.org/10.1520/C1202-10>
- ASTM International. (2004). ASTM C1556-04 Standard Test Method for Determining the Apparent Chloride Diffusion Coefficient of Cementitious Mixtures by Bulk Diffusion. Retrieved from <https://doi.org/10.1520/C1556-04>
- ASTM International. (2004). ASTM C1585-04e1 Standard Test Method for Measurement of Rate of Absorption of Water by Hydraulic-Cement Concretes. Retrieved from <https://doi.org/10.1520/C1585-04E01>
- Bickley, J. A., Hooton, D. and Hover, K. C. (2006), “Performance specifications for durable concrete”. Concrete International, 28(9): 51-57.

- Canadian Standards Association (2004), *CAN/CSA-A23.1-04/A23.2-04: Concrete Materials and Methods of Concrete Construction/Methods of Test and Standard Practices for Concrete*, Toronto, 516 pp.
- Day, K. W. (2005), “Prescriptive on prescriptions”, *Concrete International*, V. 7, pp.27–30.
- DuraCrete (1998), “Probabilistic performance-based durability design: modelling of degradation”, Document, D. P. No. BE95-1347/R4-5, The Netherlands.
- EN 1990-1 (2002), Eurocode: “Basis of structural design”, CEN, Brussels, 2002.
- EN 206-1 (2013), “Concrete - Part 1: Specification, performance, production and conformity”, CEN, Brussels, 2013.
- fib Model Code for Service Life Design (2006) *fib Bulletin 34*, fib, EPFL Lausanne, 116 pp.
- fib Model Code (2010, 2013), International Federation for Structural Concrete (fib), Lausanne, Switzerland.
- Gjørsv, O. E. (2014), “Durability Design of Concrete Structures in Severe Environments”, 2nd edition, Taylor & Francis, CRC Press, London.
- Gouws, S. M., Alexander, M. G., Maritz, G. (2001), “Use of durability index tests for the assessment and control of concrete quality on site”, *Concrete Beton*, 98 pp. 5-16.
- Guillon, E., Le Bescop, P., Lothenbach, B., Samson, E. and Snyder, K. (2013), “Modelling degradation of cementitious materials in aggressive aqueous environments”, Part II in Star 211-PAE, Performance of cement-based materials in aggressive aqueous environments, pp. 1- 39. Springer.
- ISO 13823-1 (2008), “General Principles on the design of structures for durability”, International Organization for Standardization, Geneva.
- ISO 2394 (2015), “General Principles on Reliability for Structures”, International Organization for Standardization, Geneva, 111pp.
- Jacobs, F., Leemann, A., Denarié, E., Teruzzi, T. (2009), SIA 262/1. “Recommendation for the quality control of concrete with air permeability measurements”, VSS report, Zurich. 22 pp.
- LIFE-365 (2005). ACI-Committee-365, “Service life prediction model, Computer program for predicting the service life and life-cycle costs of reinforced concrete exposed to chlorides”. American Concrete Institute.
- Linger, L., Cussigh, F. (2018), “PERFDUB: A New French Research Project on Performance-Based Approach for Justifying Concrete Structures Durability”. In High Tech Concrete: Where Technology and Engineering Meet.1. <https://doi.org/10.1007/978-3-319-59471-2>
- Lobo, C., Lemay, L. and Obla. K. (2005), “Performance-based specifications for concrete”. *The Indian Concrete Journal*, 79(12): 13-17.
- Mackechnie, J. R, Alexander, M. (2002), “Durability predictions using early-age durability index testing”. Proceedings, 9th Durability and Building Materials Conference, Australian Corrosion Association, Brisbane, (2002) 11pp.
- Muigai, R. N., Alexander, M. G., Moyo, P. (2009), “Use of chloride conductivity index in probabilistic modelling for durability design of RC members”. *Restoration of Building Monuments Journal*, V. 15, No. 4, pp. 267-276.
- National Ready-mix Concrete Association, (NRMCA), n.d. www.nrmca.org/P2P
- Neville, A. M. (1987), “Why we have concrete durability problems”, ACI SP-100, Katherine and Bryant Mather International Conference on Concrete Durability, American Concrete Institute, Detroit, USA, pp. 21-48.
- Nganga, G., Alexander, M. G., Beushausen, H. (2013), “Practical implementation of the durability index performance-based design approach”. *Construction & Building Materials*, Published online: 6-MAY-2013. *Construction and Building Materials*. V. 45, pp. 251-261.
- Nilsson, L. O., Poulsen, E., Sandberg, P., Sørensen, H.E., Klinghoffer, O. (1996), “Chloride penetration into concrete”, State of the Art, Transport processes, corrosion initiation, test methods and prediction models, Copenhagen: Danish Road Directorate, pp.23-25.

- NTBUILD 492, (1999), *“Concrete, mortar and cement based repair materials: chloride migration coefficient from non-steady state migration experiments”*. Esbo, Finland: Nordtest.
- Raath, B. (2004), *“Practical Issues of Concrete Specification”*. Concrete Society of Southern Africa, National Seminar: Specifying Concrete for Durability - State of the Art of South African Practice, Presented at Johannesburg Durban, Port Elizabeth and Cape Town, South Africa.
- RILEM TC 189-NEC (2005), *“Non-destructive evaluation of the concrete cover: Comparative test - Part I: Comparative test of ‘penetrability’ methods”*. Materials and Structures (284), 2005.
- Ronny, R., Everitt, P. (2010), *“Durability specification and testing results from four bridge structures in Kwa Zulu-Natal”*, In Concrete for a sustainable environment, Emperor's Palace, Kempton Park, Gauteng, South Africa.
- The South African National Roads Agency Limited (SANRAL) (2010), *“Project document: Project specifications”*.
- Simons, B. (2004), *“Concrete performance specifications: New Mexico Experience”*. Concrete International, 26(4): 68-71.
- Streicher, P., Alexander, M. G. (1995), *“A chloride conduction test for concrete.”* Cement and Concrete Research, V. 25, No. 6, pp 1284-1294.
- Swiss Standard SN 505 262/1 (2013), *“Concrete Construction – Complementary Specifications”*, Schweizer Norm, 52 p. (in German and French)
- Tang, L. (2008), *“Engineering expression of the ClinConc model for prediction of free and total chloride ingress in submerged marine concrete”*, Cement and Concrete Research, 38(8–9), 1092–1097.
- Taylor, P. (2004), *“Performance-Based Specifications for Concrete”*, Concrete International, 8: 91 – 93.
- Thomas, M. D. A., Green, B., O’Neal, E., Perry, V., Hayman, S. Hossack, A. (2012), *“Marine Performance of UHPC at Treat Island”*, Proceedings of Hipermat, 3rd International Symposium on UHPC and Nanotechnology for High Performance Construction Materials (Editors Michael Schmidt et al), Kassel, pp. 365-370.
- Torrent, R. J. (1992), *“A two-chamber vacuum cell for measuring the coefficient of permeability to air of the concrete cover on site”*, Materials & Structures, V. 25, No. 6, pp.358-365.
- Torrent, R., Denarié, E., Jacobs, F., Leemann, A., Teruzzi, T. (2012), *“Specification and site control of the permeability of the concrete cover: The Swiss approach”*, Materials and Corrosion, V. 63, No. 12, pp.1127-1133.
- Torrent, R., Jacobs, F. (2014), *“Swiss Standards 2013: World's most Advanced Durability Performance Specifications”*, 3rd Russian Intern. Confer. on Concrete and Ferrocement, Moscow.
- Tuutti, K. (1992), *“Corrosion of steel in concrete”*. Swedish Cement and Concrete Research Institute, CBI Research Report, No. 4 p 82.
- Van der Lee, J., De Windt, L., Lagneau, V. (2008), *“Application of reactive transport models in cement-based porous media”*. Proceedings in the International RILEM Symposium on Concrete Modelling – CONMOD’08, Delft, The Netherlands.
- Walraven, J. (2008), *“Design for service life: how should it be implemented in future codes”*, International Conference on Concrete Repair, Rehabilitation and Retrofitting, Proceedings ICCRRR Cape Town, (2008) pp. 3-10.

Challenges and opportunities for assessing transport properties of high-performance concrete

K. Yang^{1,2}, S. Nanukuttan³ , W. J. McCarter⁴ , A. Long³ ,
P. A. M. Basheer^{2*} 

*Contact author: P.A.M.Basheer@leeds.ac.uk

DOI: <http://dx.doi.org/10.21041/ra.v8i3.301>

Reception: 03/03/2018 | Acceptance: 04/07/2018 | Publication: 31/08/2018

ABSTRACT

In this paper, a review of techniques is given so that both, the challenges and opportunities for assessing transport properties of high-performance concrete, are highlighted. A knowledge of performance of structural concrete is required for design and compliance purposes. One driving force for the use of high performance concretes (HPC) is enhanced durability yet it would be wrong to assume that all HPCs can deliver the desired performance level. In situ characterisation of the permeation properties of concrete is the most viable means for assessing durability and has become increasingly important over the past 20 years. A variety of methods exist that provide a range of parameters, e.g. air permeability, water absorption rate, sorptivity and chloride migration coefficient.

Keywords: high-performance concrete; permeation properties; performance-based specification; NDT test methods; reliability.

Cite as: K. Yang, S. Nanukuttan, W. J. McCarter, A. Long, P. A. M. Basheer (2018), “Challenges and opportunities for assessing transport properties of high-performance concrete”, Revista ALCONPAT, 8 (3), pp. 246-263, DOI: <http://dx.doi.org/10.21041/ra.v8i3.301>

¹ School of Materials Science and Engineering, Chongqing University, China

² School of Civil Engineering, University of Leeds, United Kingdom.

³ School of Natural and Built Environment, Queen’s University Belfast, United Kingdom.

⁴ School of Energy, Geoscience, Infrastructure and Society, Heriot-Watt University, United Kingdom.

Legal Information

Revista ALCONPAT is a quarterly publication by the Asociación Latinoamericana de Control de Calidad, Patología y Recuperación de la Construcción, Internacional, A.C., Km. 6 antigua carretera a Progreso, Mérida, Yucatán, 97310, Tel.5219997385893, alconpat.int@gmail.com, Website: www.alconpat.org

Responsible editor: Pedro Castro Borges, Ph.D. Reservation of rights for exclusive use No.04-2013-011717330300-203, and ISSN 2007-6835, both granted by the Instituto Nacional de Derecho de Autor. Responsible for the last update of this issue, Informatics Unit ALCONPAT, Elizabeth Sabido Maldonado, Km. 6, antigua carretera a Progreso, Mérida, Yucatán, C.P. 97310.

The views of the authors do not necessarily reflect the position of the editor.

The total or partial reproduction of the contents and images of the publication is strictly prohibited without the previous authorization of ALCONPAT Internacional A.C.

Any dispute, including the replies of the authors, will be published in the second issue of 2019 provided that the information is received before the closing of the first issue of 2019.

Desafios e oportunidades para conhecer as propriedades dependentes dos mecanismos de transporte nos concretos de alto desempenho

RESUMO

Neste artigo, é feita uma revisão dessas técnicas, destacando os desafios e as oportunidades para avaliar as propriedades de transporte do concreto de alto desempenho. O conhecimento do desempenho do concreto estrutural é necessário para propósitos de projeto e conformidade. Uma das fortes vantagens para o uso de concreto de alto desempenho (HPC) é obter uma durabilidade destacada, mas seria errado supor que todos os HPCs podem fornecer, automaticamente, um nível de desempenho desejado. A caracterização in loco das propriedades de permeabilidade do concreto é o meio mais viável para avaliar a durabilidade e tem se tornado cada vez mais importante nos últimos 20 anos. Existe uma variedade de métodos que fornecem uma gama de parâmetros, como, por exemplo, permeabilidade ao ar, absorção de água, absorção capilar, e coeficiente de migração de cloratos.

Palavras-chave: concreto de alto desempenho; permeabilidade; especificação por desempenho; ensaios não destrutivos NDT; confiabilidade.

Retos y oportunidades para evaluar las propiedades de transporte del concreto de alto rendimiento

RESUMEN

En este artículo, se hace una revisión de estas técnicas, destacando los desafíos y las oportunidades para evaluar las propiedades de transporte del concreto de alto desempeño. El conocimiento del desempeño del concreto estructural es necesario para propósitos de diseño y conformidad. Una de las fuertes ventajas para el uso de concreto de alto rendimiento (HPC) es obtener una durabilidad destacada, pero sería erróneo suponer que todos los HPC pueden proporcionar automáticamente un nivel de rendimiento deseado. La caracterización in situ de las propiedades de permeabilidad del concreto es el medio más viable para evaluar la durabilidad y se ha vuelto cada vez más importante en los últimos 20 años. Hay una variedad de métodos que proporcionan una gama de parámetros, como la permeabilidad al aire, la absorción de agua, la absorción capilar, y el coeficiente de migración de los cloruros.

Palabras clave: concreto de alto rendimiento; permeabilidad; especificación por rendimiento; ensayos no destructivos NDT; confiabilidad.

Nomenclature

A	the cross section area subjected to the flow (m^2)
ΔC	the concentration difference (g/m^3)
C	the concentration at the depth x (g/m^3)
C_0	ion concentration at the exposed surface (g/m^3)
D_c	the carbonation diffusion coefficient ($m/s^{0.5}$)
D_g	the gas diffusion coefficient (m^2/s)
D_v	the vapour diffusion coefficient (m^2/s)
D_{is}	the ion diffusion coefficient (m^2/s)
D_{ia}	the diffusion coefficient (m^2/s)
D_{js}	the migration coefficient (m^2/s)

D_{in}	the migration coefficient (m^2/s)
d	depth of penetration (m) at time t (s)
d_c	the carbonation depth (m)
ΔE	the applied potential difference (V)
F	Faraday constant (c/mol)
ΔH	the pressure difference expressed in water head (m)
i	the volume absorbed per unit area (mm)
J_g	gas mass flux ($g/m^2 \cdot s$)
J_v	vapour mass flux ($g/m^2 \cdot s$)
J_s	ion mass flux ($g/m^2 \cdot s$)
J_j	the flux of species ($kg/m^2 \cdot s$)
K_{gs}	the permeability coefficient (m^2)
K_{gn}	the permeability coefficient (m/s)
K_{ws}	the water permeability coefficient (m/s)
K_{wn}	permeability coefficient (m/s)
L	the thickness of the specimen (m)
P_e	the upstream pressure (N/m^2)
P_s	the downstream pressure (N/m^2)
P_i	the pressure at the start of test (N/m^2)
P_t	the pressure at the end of test (N/m^2)
Q_s	the steady-state volume flow rate (m^3/s)
R	universal gas constant ($J/mol \cdot K$)
S_w	the sorptivity of materials ($mm/min^{0.5}$)
S_d	the sorptivity ($mm/min^{0.5}$)
T	the absolute temperature (K)
t	time elapse (s)
t_r-t_i	the test duration (s)
v	porosity of the sample
V_c	the volume of the test chamber (m^3)
erf	the error function
x	ion penetration depth (m)
Z_j	the electrical charge of species
μ	the dynamic viscosity of the gas (Ns/m^2)

1. INTRODUCTION

In the design of concrete structures, durability and service life prediction have increasingly gained importance in recent years. This is due to inadequate durability performance of many reinforced concrete structures built in the past few decades, which places considerable strain on construction budgets. This is a worldwide problem (Beushausen and Luco, 2016). The use of high-performance concrete (HPC) is an established approach to enhancing the durability of reinforced and pre-stressed concrete structures (Aitcin, 1998). However, with performance levels of HPC typically assessed on laboratory-based testing, the long-term, in-service performance of concrete structures is largely dependent on factors such as construction quality. Set against this background, the ability to undertake accurate, *in situ* quality assessment of HPC is critical.

When discussing testing of concrete durability, it is the permeation and mass transport properties which are of significance and terms such as adsorption¹, diffusion, migration, absorption and permeability are used in this respect. Tests are normally undertaken on 150×300 mm cylinders using standard test methods, generally at the age of 28 days. It should be remembered that transport properties can be determined by laboratory techniques and/or *in situ* techniques (Basheer et al., 2008; McCarter et al., 2017). Laboratory techniques are easy to perform and most have been standardised to determine the compliance of structures with their design (Dhir et al., 1989; Zhang et al., 2017).

In situ permeation tests can be used to obtain much information; however, this does not suggest stopping laboratory measurements completely as noted in the Concrete Society Technical Report-31 (2008). There is clearly a demonstrable need for *in situ* testing to provide an owner with documentation (and reassurance) of the acceptability of the finished structure comparable to the documentation required for other aspects of concrete quality control/assurance (Bentur and Mitchell, 2008).

Numerous techniques have been applied to assess the permeation properties of normal concrete (NC), but few of them are suitable for distinguishing HPCs. There are two technical challenges for current testing techniques: firstly, the characteristics of HPC due to its dense pore structure, and secondly, the difficulty in controlling the test conditions before and during the measurements. This paper reviews the current permeation testing techniques with the aim of identifying a reliable method for HPCs. The scope of the test methods reviewed is confined to direct permeation methods.

2. TECHNIQUES FOR TESTING AND MONITORING PERFORMANCE OF CONCRETE STRUCTURES

2.1 Laboratory methods for assessing permeation properties

2.1.1 Permeability methods

The techniques to determine permeability of concrete can be broadly divided into two categories, gas (air) permeability tests and water permeability tests. Gas permeability coefficients can be determined by either measuring the flow of gas at a constant pressure or by monitoring the pressure decay over a specified time interval (Basheer, 2001). The rate of outflow is measured for the steady-state gas permeability test. The other type of air test, referred to as falling pressure test, utilises the pressure decay to compute a gas permeability coefficient. Gas permeability tests became popular because of short test duration and the limited effect the test variables have on the pore structure during measurements (Torrent, 1992; Basheer, 2001; Yang et al., 2013).

Water permeability can be determined by either steady-state or non-steady state water flow measurements as well as water penetration under the influence of an external pressure head (Basheer, 1993; Yang et al. 2013). The main difference between them is the test duration. The time required to obtain a steady-state flow varies from a few days to several weeks or months depending on the quality of concrete (Hearn and Morley, 1997; El-Dieb and Hooton, 1995), while the test duration of non-steady state tests is much shorter, generally less than 3 days. The test developed by El-Dieb and Hooton (1995) needs to be highlighted due to its novelty. Compared to other methods, it provides a wide range of test pressure from 0.5 MPa to 3.5 MPa and improves the accuracy of the flow measurement. The range of water permeability coefficient of HPC determined by Nokken and Hooton (2007) varied from 10^{-13} to 10^{-15} m/s, which is in agreement with the results reported by others using similar test arrangements (Galle et al., 2004; Reinhardt and Jooss, 2003). As the steady state tests require long test duration to achieve the steady state, the depth of water

¹ Adsorption is not discussed here, as this parameter is not commonly used as a durability indicator.

penetration in concrete also has been used to determine the water permeability coefficient for low permeability concretes. This method has been standardised and is outlined by BS-EN 12390-8 (2009). Chia and Zhang (2002) and Pocock and Corrans (2007) found that the scatter of results is quite high and the coefficient of variation of the test results is above 100%. Table 1 gives a summary of typical values and their variance for different test methods.

Table 1. Summary of typical values and variance of permeability coefficients determined by different test methods

Permeability coefficient	Concrete			Variance (CoV)
	Poor	Normal	Good	
K_{gs} (m ²)	$>10^{-13}$	10^{-14} - 10^{-15}	$<10^{-16}$	15%-30%
K_{ws} (m/s)	$>10^{-11}$	10^{-11} - 10^{-13}	$<10^{-14}$	20%-40%
K_{wn} (m/s)	$>10^{-10}$	10^{-10} - 10^{-12}	$<10^{-13}$	40%-100%

2.1.2 Ion diffusion

The transport of chloride ions can be assessed by means of an ionic diffusion test (Basheer, 2001; Tang et al., 2011). Such tests can be grouped into two categories; diffusion based and migration based methods. Diffusion tests simulate the movement of chloride ions under the influence of a concentration gradient and the traditional set-up includes either diffusion cells (steady-state and non-steady state), or immersion/ponding (non-steady state). In the case of steady-state tests, the rate of ionic transport is measured and using Fick's first law of diffusion, the diffusion coefficient is calculated. In the case of non-steady state tests, the depth of penetration of chlorides is used to calculate the diffusion coefficient by using the error function solution of Fick's second law of diffusion. The steady-state diffusion test, typically, requires six months or more to achieve a steady-state of flow. The duration is short for non-steady state tests. The immersion and ponding tests usually take around 90 days, which can be used to assess chloride resistance for most construction projects if time is available.

Since the 1980's, many techniques have been proposed which apply an external electrical field to accelerate the ingress of chloride ions. Some of the tests have utilised a high concentration of chloride source solution to further expedite ionic movement (Tang et al., 2011). One of the first tests in this category is the Rapid Chloride Permeability Test (RCPT) and this was adopted as a standard test by AASHTO T277 (2015) and ASTM C1202 (2017). In this test, the resistance of concrete against chloride is categorised by the total charge passing through the specimen during the first 6 hours. As charge is carried by all ions and not just chlorides, this test has been criticised by some researchers in 1990s (Andrade, 1993; Tang and Nilsson, 1992). The most recent test is the steady-state migration test. The test arrangement is similar to RCPT, however, in this instance, the chloride concentration of the anolyte is measured instead of the charge passed. The migration coefficient is calculated using a modified Nernst-Planck equation (Tang et al., 2011). Tang and Nilsson (1992) proposed a rapid test based on the non-steady state chloride migration theory, known as the rapid chloride migration (RCM) test. The chloride migration coefficient is calculated from the chloride depth and using a modified Nernst-Planck equation. Currently, this method is included in the Nordic standards NT-Build 492 (1999). Due to short test duration and simplicity, the three migration based methods have an advantage over diffusion based tests for determining the chloride transport resistance of concrete. However, as stated earlier, the RCPT has several inherent problems. It is reported that this method measures conductivity of the pore solution, rather

than chloride transport properties (Andrade, 1993; Basheer et al., 2005). The temperature rise due to the high voltage can significantly affect the conductivity of ions and, hence, the final result in Coulombs. Therefore, the RCPT cannot provide a reliable indication of chloride migration. The other two methods are based on the well-established theory and widely accepted by researchers to assess HPCs. The typical results of ionic diffusion/migration coefficients are given in Table 2.

Table 2. Summary of typical values and variance of ion diffusion/migration coefficients determined by different test methods

Diffusion coefficient	Concrete			Variance (CoV)
	Poor	Normal	Good	
D_{is} (m ² /s)	$>10^{-11}$	10^{-11} - 10^{-12}	$<10^{-12}$	15%-25%
D_{ia} (m ² /s)	$>10^{-11}$	10^{-11} - 10^{-12}	$<10^{-13}$	20%-35%
D_{js} (m ² /s)	$>10^{-11}$	10^{-11} - 10^{-12}	$<10^{-13}$	20%-35%
D_{in} (m ² /s)	$>10^{-11}$	10^{-11} - 10^{-12}	$<10^{-13}$	20%-35%

2.1.3 Sorptivity methods

Sorptivity is the parameter to estimate the ability of liquid penetration due to capillary potential (Basheer, 2001; McCarter et al., 2009). Two kinds of tests are used to measure sorptivity: (1) weight gain method; and (2) water penetration depth. The weight gain method has been accepted as a European standard method: EN-13057 (2002). Basheer (2001) has reviewed the results for NC, which vary from 0.05 and 0.15 mm/min^{0.5}. The depth of water penetration – estimated using a sample splitting technique - caused by capillary suction can also be used to evaluate the sorptivity (McCarter et al., 1995). However, the need for multiple samples is the main drawback for this method. It is also difficult to observe a clear water-front for concrete containing fly ash and microsilica. Ganjian and Pouya (2009) studied the effects of supplementary cementitious materials (SCMs) on sorptivity of HPCs and found no significant difference among different HPCs. Similar results have also been reported by other researchers (Elahi et al., 2010) hence sorptivity is not a sufficiently sensitive parameter in assessing the performance of HPCs.

2.1.4 Considerations of assessing permeation properties of HPCs by laboratory techniques

To assess the permeation properties of HPCs using laboratory test techniques, steady-state water permeability and ion diffusion tests offer a simple analysis procedure. However, they have a common limitation, the long test duration, which may lead to coupled chemical and physical interactions. Non-steady state tests perform better in this aspect and could be used to evaluate HPC. Another point that should be highlighted is the initial condition of a specimen, including moisture content and distribution, which has a predominant effect on results and has to be assessed prior to measurements. Table 3 summarises laboratory test techniques and their governing equations along with recommendations to assess HPC.

Table 3. Summary of laboratory permeation test techniques and governing equations

Transport mechanism	Testing medium	Moisture condition	Theory	Governing equation	Suitable to test HPCs
Permeability	Gas	Dry	Steady-state	$K_{gs} = 2\mu LP_s Q_s / A(P_e^2 - P_s^2)$	Yes
			Non-steady state	$K_{gn} = V_c L / RTA \times \ln \frac{P_i}{P_t} / (t_t - t_i)$	Yes
	Water	Saturated	Steady-state	$K_{ws} = Q_s / A \times L / \Delta H$	No
			Non-steady state	$K_{wn} = d^2 v / t \Delta H$	Yes
Diffusivity and Migration	Gas	Dry	Steady-state	$D_g = J_g L / \Delta C$	No
			Non-steady state	$D_c = d_c / t^{0.5}$	Yes
	Vapour	Dry	Steady-state	$D_v = J_v L / \Delta C$	No
		Saturated	Steady-state		
	Ion diffusivity	Saturated	Steady-state	$D_{is} = J_s L / \Delta C$	No
			Non-steady state	$C = C_0 [1 - \text{erf}(x / 2\sqrt{D_{ia}t})]$	Yes
	Ion migration	Saturated	Non-steady state	Classification of chloride resistance according to the total charge passing through a specimen	No
			Steady-state	$D_{js} = J_j / C_j \times RT / Z_j F \times L / \Delta E$	Yes
			Non-steady state	$D_{in} = RT / Z_j F \Delta E \times (x_d - 1.061x_d^{0.589}) / t$	Yes
Sorption	Water	Dry	Non-steady state	$S_w = i / t^{0.5}$	No
			Non-steady state	$S_d = d / t^{0.5}$	No

2.2 Field methods

2.2.1 *In situ* air permeability tests

Air permeability tests have gained popularity due to their short test duration and the fact that concrete pore structure is unaffected during the test. Schonlin and Hilsdorf (1987) developed a surface-mounted air permeability test method that could measure the pressure drop to calculate an air permeability index. This falling pressure method is extremely fast and can be performed by a single operator. Later, numerous researchers modified the setup and theory of this technique. One modification that needs to be highlighted is Torrent's method (1992) which introduced a guard ring to develop a double-chamber apparatus. By assuming a unidirectional flow of air through the concrete in the inner chamber, the air permeability coefficient is calculated from the pressure change in the inner chamber. Similarly, Guth and Zia (2001) used flow patterns through a two-concentric-chamber cell to determine air permeability of concrete. The application of a guard ring was proposed for the *in situ* water absorption test. In the strictest sense, the guard ring cannot guarantee unidirectional air flow across the whole section, as the flow simulation carried out by Yang et al. (2015) has indicated that the guard ring can confine the flow at the near surface and a uni-directional flow is not achievable for the whole depth of the test specimen. However, Torrent's method may serve as a conservative approximation of air permeability with the simplifying assumptions. The other type of surface-mounted air permeability test is the constant head test. Whiting and Cady (1992) applied the vacuum technique to measure the air permeability on site, named as surface air flow test (SAF). The steady-state air flow rate under a constant vacuum level is regarded as an indicator of air permeability.

This type of surface-mounted air permeability tests can identify the effects of w/b, curing duration and curing temperature on permeability under controlled test conditions. The Torrent method, Guth-Zia's device and Autoclam have been used to attempt to measure the permeability of HPCs. Romer (2005) reported that misleading results were obtained using the Torrent test when moist concrete specimens were tested. A similar finding was also reported by Guth and Zia (2001) and Elahi et al. (2010). The modified Autoclam (Low volume test method) was designed to measure *in situ* air permeability of HPCs (Yang et al., 2015) and Figure 1 highlights the development progress of AutoClam test and typical results to measure air permeability of 1 NCs and 5 HPCs. The research confirmed strong positive relationships between the proposed test method and existing standard permeability assessment technique and strong potential to become recognized as international methods for determining the permeability of HPCs.

Figg (1973) developed the drill hole suction test during his work at the Building Research Establishment. A hypodermic needle is pushed into the cavity and connected to a mercury filled manometer and hand vacuum pump. After applying vacuum in the cavity, the time taken for the air pressure increase from 15 to 20 kN/m² is regarded as a measure of the air permeability of concrete. Two similar test methods are also found in the literature: one developed by Parrott and Hong (1991) at the British Cement Association, and the other developed by Dinku and Reinhardt (1997) at the University of Stuttgart. One issue noted by Figg (1973) is that microcracks are induced by application of the hammer-action drill and may affect the results significantly. For HPCs, the situation may become even more severe due to the high brittleness and difficulty of drilling very high strength concrete (Aitcin, 1998). It is evident from the literature that there is a paucity of data on air permeability measurements for HPCs.

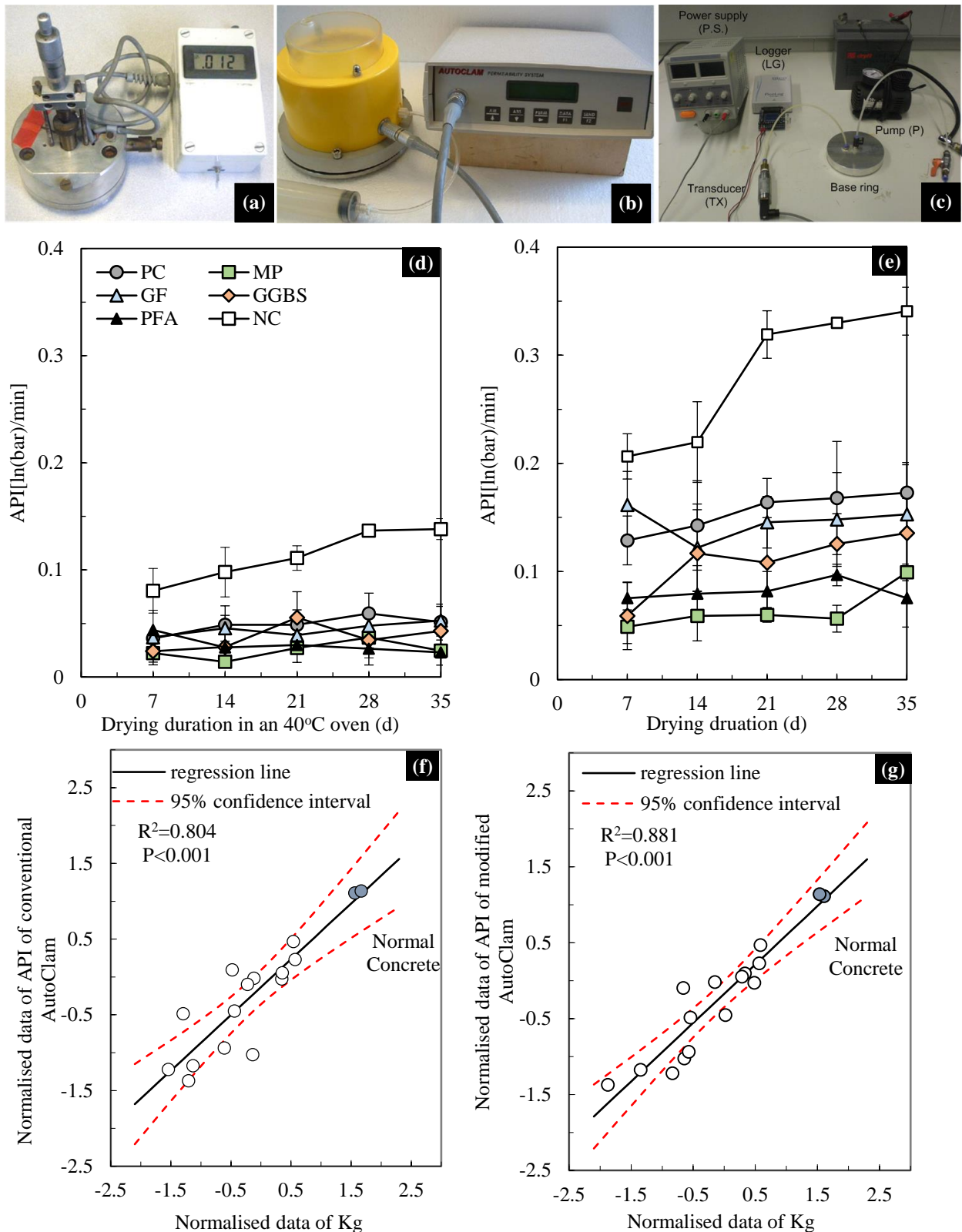


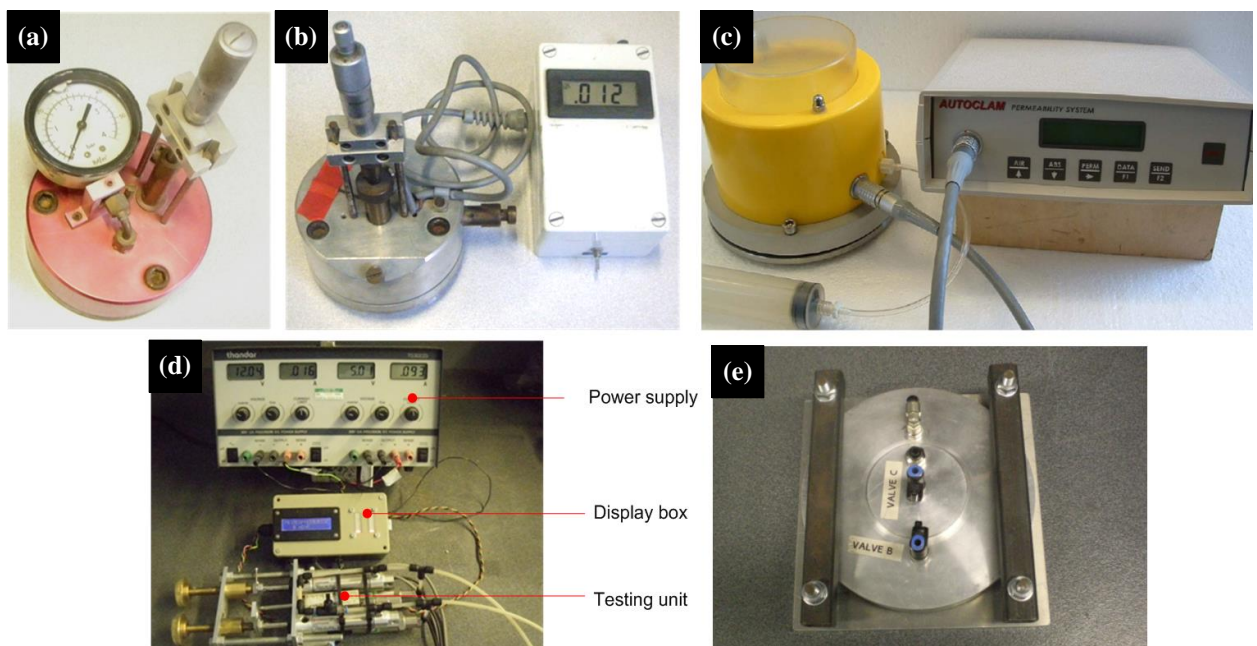
Figure 1. Development of Autoclam air permeability test (a) Universal CLAM air test (1985), (b) Autoclam air test (1992), (c) modified Autoclam air test (2011), (d) conventional Autoclam air test results, (e) modified Autoclam air test results, (f) conventional Autoclam Vs RILEM air test, (g) modified Autoclam Vs RILEM air test

2.2.2 *In situ* water permeability tests

It should be noted that in order to yield reliable results, the concrete should be in a moisture state equivalent of 21 days of drying in an oven at 40°C (Yang et al., 2013). This can be ensured by achieving a relative humidity of less than 60% in the near-surface region of approximately 40mm thickness (Basheer, 2001; Yang et al., 2013). This moisture condition is not easy to achieve *in situ*, especially in most parts of northern Europe, where annual rainfall averages from 80 to 110 times and annual precipitation varies from 600 to nearly 2000 mm (Perry and Hollis, 2003). Therefore, it is logical that concrete in structures should be tested when it is in a saturated condition rather than in a dry state and, in this respect, *in situ* water permeability tests are preferable to air permeability tests for assessing the quality of concrete in these regions.

The first standardised test aimed at measuring the field absorption property of concrete was the initial surface absorption test (ISAT) in BS:1881-208 (1996): Testing concrete - Recommendations for the determination of the initial surface absorption of concrete. Initial surface absorption is defined as the rate of water flow into concrete per unit area under a constant pressure head. The Autoclam uses the same test procedure and can measure both the water absorption and sorptivity of concrete (Basheer et al., 1994). Figg (1973) and Dhir et al. (1989) developed drill-hole methods that are able to perform water absorption measurements, but it is not appropriate to estimate the sorptivity using the intrusive methods, as the water absorption process is initiated from the drilled hole, not from the surface. The ISAT can be used to study the sorptivity of concrete, while the Autoclam is a direct, easy and fast way to determine this property. As discussed in section 1, however, sorptivity is not a sensitive parameter to test HPCs.

The Clam test, first reported by Montgomery and Adams (1985), for measuring the water permeability of *in situ* concrete was modified by Basheer et al. (1994), which is currently available as the Autoclam Permeability System (Figure 2). It is a constant head permeability test and the water permeability is estimated either by the steady state or non-steady state flow theory. In the latest version, a test pressure of 7 bar can be selected to assess HPCs and improve the repeatability and accuracy of the measurements (Yang et al., 2015), results of which are given in Figure 2.



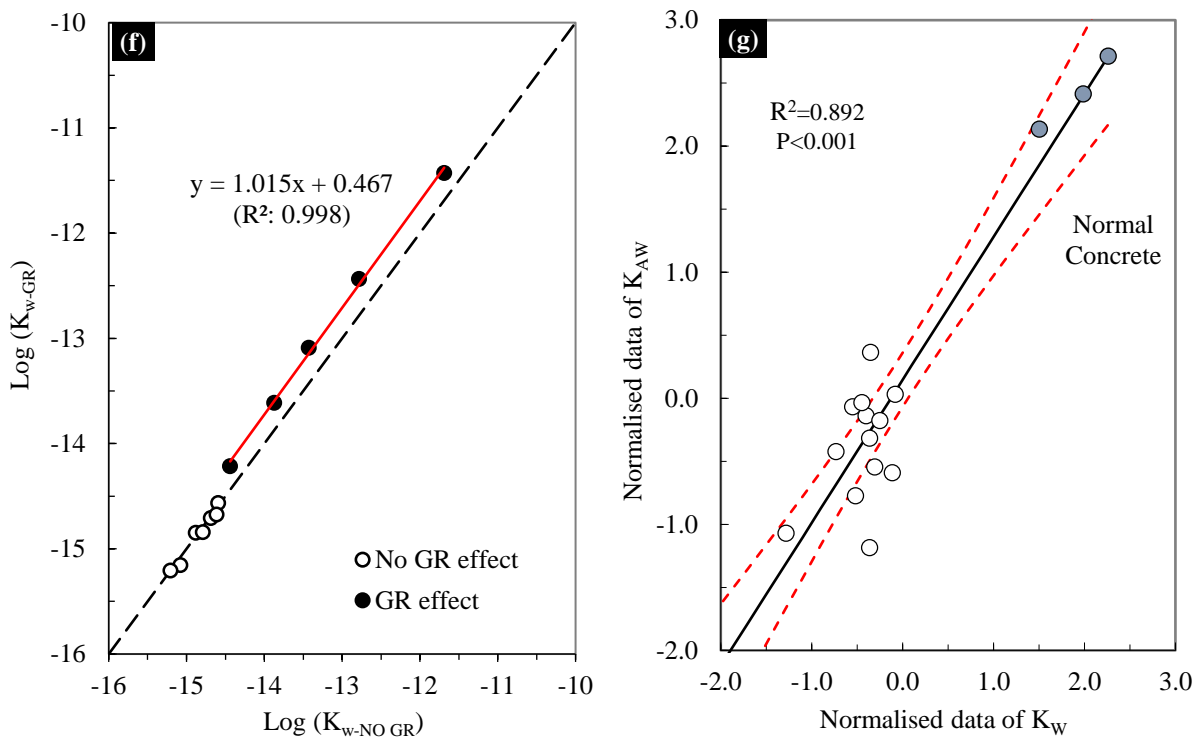


Figure 2. Development of CLAM water permeability tests (a) CLAM test (1985), (b) Universal CLAM test (1989), (c) Autoclam Test (1992), (d) High pressure CLAM water test (2012), (e) test head with the guard ring, (f) relationship between permeability coefficient from tests with and without the guard ring, (g) high pressure CLAM water test (K_{AW}) Vs BS-EN water penetration test (K_W)

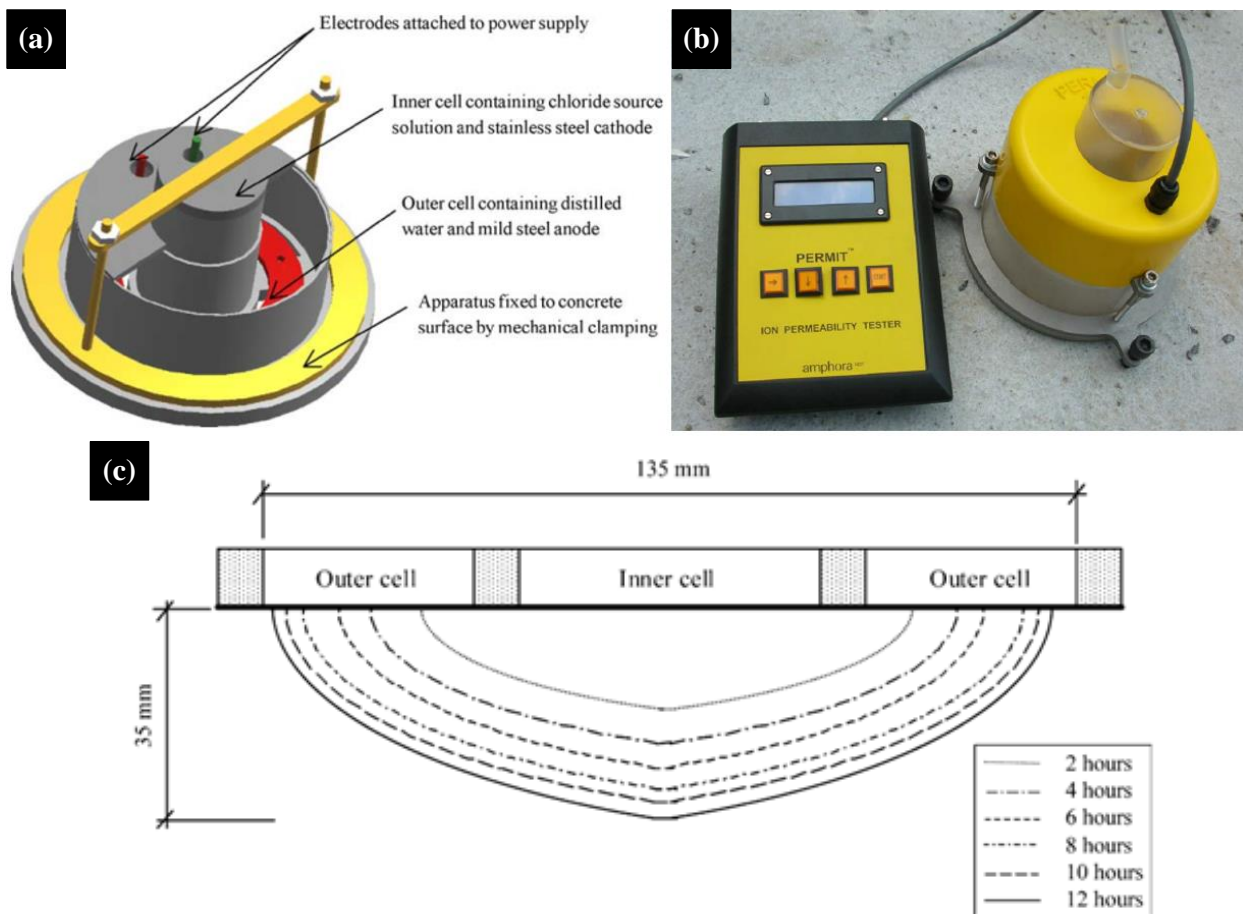
A field permeability test (FPT) developed by Meletiou et al. (1992) uses a steady-state, drill-hole water permeability procedure and to remove the influence of moisture on test results, vacuum saturation is applied before measurements. The water flow is monitored by the water level in the manometer tube. Flow is assumed to stabilise after 2 hours and the steady-state flow rate is used to calculate the coefficient of permeability. The results indicate that the effect of moisture variations is nearly removed after applying vacuum saturation, although the additional potential influence of microcracks induced by drilling is not fully addressed.

2.2.3 *In situ migration tests*

Steady state diffusion tests are not suitable for *in situ* application due to their long test duration. An external electric field can accelerate ionic transport and, as a consequence, some migration tests have been designed as field-test techniques. Such test methods include the Coulomb test developed by Whiting (1981), the *in situ* rapid chloride migration test (RCM test) (Tang et al., 2011) and the PERMIT ion migration test (Nanukuttan et al., 2015).

Whiting (1981) developed the Coulomb test on the basis of the RCPT method. The charge passed is considered as an index to assess the diffusivity of concrete. As discussed before, the Coulomb test provides an estimate of the charge carried by all ions and not just chlorides. Moreover, this technique does not provide a migration coefficient. The second field method was developed by Tang and Nilsson (Tang et al., 2011) and based on the rapid chloride migration (RCM) test. An external potential is applied through the reinforcement bar and cathode in the chamber. After the measurement, a core is taken from the test position and the chloride penetration front is examined by the colorimetric technique. As cores are required for interpretation of the *in situ* RCM method there is no obvious advantage compared with laboratory methods.

The PERMIT ion migration test (Figure 3) was developed by Nanukuttan et al. (2009). Both the anolyte and the catholyte chambers are in the form of concentric cylindrical reservoirs. The chloride ions move from the catholyte towards the anolyte through the concrete influenced by the potential difference created by the external electric field. The change in conductivity of the anolyte is used as a means to monitor the chloride movement. The *in situ* migration coefficient is evaluated by using a modified Nernst-Planck equation. Validation of the PERMIT has been carried out by comparing the coefficients from PERMIT test against the one-dimensional chloride migration test, the effective diffusion coefficient from the normal diffusion test and the apparent diffusion coefficient determined from chloride profiles (Basheer et al., 2005; Nanukuttan et.al. 2015). The results show that for a wide range of concrete mixes, a high degree of correlation exists between the *in situ* migration test and the laboratory based tests, the results of which are given in Figure 3. Note that the performance of the PERMIT is confirmed in the laboratory and for site application, as test area is saturated by ponding for 24 hours, it is not possible to achieve full saturation from the surface to 30mm, especially for HPCs. Therefore, PERMIT needs to be validated for its ability to assess HPCs on site.



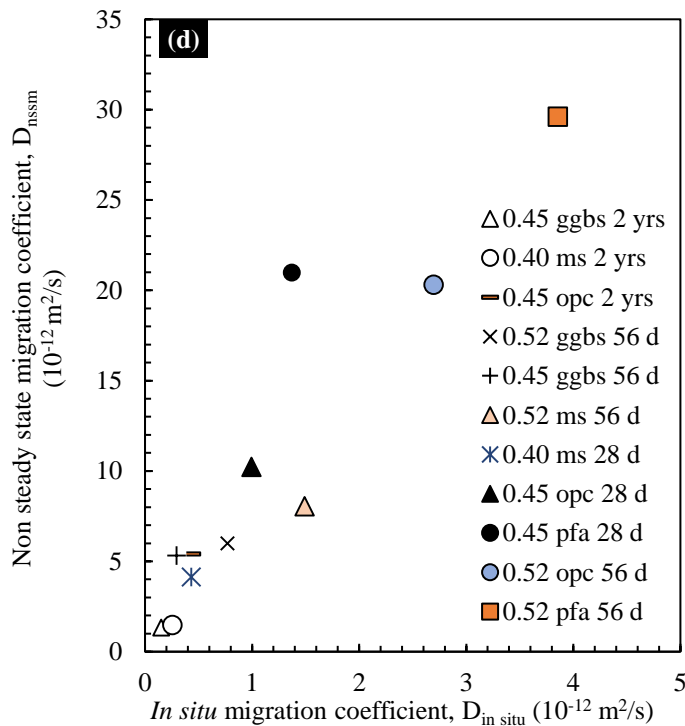


Figure 3. Development of PERMIT (a) schematic of PERMIT test, (b) the PERMIT ion migration test apparatus (2005), (c) flow area of chloride at different test duration, (d) PERMIT Vs non-steady migration test

The commercially available techniques are grouped into permeability tests, diffusion tests and sorptivity (water absorption) tests, similar to the laboratory methods, main features of which are summarised in Table 4.

Table 4 Summary of *in situ* test method to assess permeation properties of concrete

Name	Penetrating Medium	Approach to control moisture effect	Parameters determined	Accuracy	Cost per test	Surface mounted or Intrusive methods
Schonlin and Hilsdorf	Air	Use of a heat gun to remove moisture	Pressure decay	Good	Low	Surface mounted
Torrent	Air	Resistivity measurement	Pressure decay	Good	Relative low	Surface mounted
Guth and Zia	Air	No requirement	Pressure decay	Fair	Low	Surface mounted
SAF	Air	No requirement	Flow rate	Good	High	Surface mounted
Autoclam	Water , Air	RH requirement	Pressure decay or water volume	Good	Relative low	Surface mounted
LV Autoclam	Air	RH Measurement	Pressure decay	Good	Low	Surface mounted

Figg	Water, Air	No requirement	Pressure decay	Good	Low	Intrusive methods
Parrot	Air	RH measurement	Pressure decay	Good	Relative low	Intrusive methods
Dinku and Reinhardt	Air	Use of high pressure	Pressure decay	Good	Relative low	Intrusive methods
Dhir	Air	Use of vacuum to remove moistures	Pressure decay	Good	Low	Surface mounted
CLAM	Water	Ponding for 24 hours	Water volume	Good	Relative low	Surface mounted
High pressure CLAM	Water	Vacuum saturation	Water volume	Good	Relative low	Surface mounted
GWT	Water	RH measurement	Flow rate	Fair	Relative low	Surface mounted
ISAT	Water	Protect tested surface from water for at least 48h	Water volume	Fair	Low	Surface mounted
FPT	Water	Vacuum saturation	Flow rate	Good	High	Intrusive methods
CAT	Water	No requirement	Water volume	Fair	Relative low	Intrusive methods
PERMIT	Ion	Ponding for 24 hours	Conductivity	Good	Relative low	Surface mounted
<i>In situ</i> RCM	Ion	No requirement	Penetration depth	Fair	High	Surface mounted
Coulomb test	Ion	Vacuum saturation	Coulomb	Fair	Relative low	Surface mounted

Note: Some *in situ* test methods are not included in this table because there is no enough information to support their products.

2.2.4 Recommendation of *in situ* permeation methods in the context of assessing HPCs

Two questions always arise for *in situ* testing. One is whether it can provide the information that is actually needed, as an obvious objection is that most techniques measure something related to the transport properties other than intrinsic permeation characteristics. The other concerns the capability of these techniques for testing new cementitious materials. Due to the difference in the microstructure between NC and HPCs, the performance characteristics of the test apparatus need to be carefully examined and validated. With respect to the permeation methods discussed above, some points are briefly highlighted below:

- 1) The drill-hole method is a partially destructive method as repairs are unavoidable after carrying out measurements. More importantly, the percussion action of the hammer-drill used to drill the hole may create a detrimental and uncontrollable damage of concrete in the vicinity of the hole. This can cause discrepancies of test results. As such, this type of method is not recommended. The surface-mounted method can overcome the above disadvantages. The flow of most surface based methods is axi-symmetric, not unidirectional. This means multi-dimensional flow analysis is needed to examine test results.

- 2) The differences in permeability of HPCs are much smaller and this challenges most *in situ* test apparatus to differentiate between them. Both the falling-pressure and the constant-pressure air tests are possible for characterising HPCs. The former requires the pressurised reservoir geometry to be known and recording of the decrease in pressure within the reservoir, while the latter needs a knowledge of the testing geometry, flow rate and pressure. The high-pressure water test and modified air test are designed based on these concepts to measure permeability of HPCs.
- 3) The success of field assessments is greatly influenced by the water-content and moisture gradients in the concrete. The importance of the initial condition before the measurements has to be highlighted. Either ‘dry’ or ‘saturated’ samples are preferred for measuring the transport properties. Moreover, the presence of cracking and heterogeneity in concrete can also greatly affect flow rates.
- 4) Most work focusses on *in situ* permeability tests, while only three ion migration tests have been trialled for field application. More effort should be given on the laboratory investigation to fully improve the effectiveness of these methods for field application, as site ion migration tests are able to assess the quality of coverconcrete from the surface to 30 mm.

3. CONCLUSIONS

If testing has been undertaken earlier in the construction process, then potential problems could have been identified and appropriate measures taken early in the life of structures. Both *in situ* and laboratory permeation testing methods show potential for assessing the durability performance of HPCs. Although cores extracted from structures in-service could be tested in the laboratory under controlled temperature and moisture conditions, reliable *in situ* permeation tests have the advantage of carrying out numerous tests at the same test location, without damaging the structure. These test methods could form the basis of developing a performance-based specification strategy for concrete structures, but they all have their own specific benefits as well as drawbacks. Furthermore, several interesting aspects have not fully been addressed in previous studies, e.g. the coupled influence of deterioration and loading, influence of cracking, relationship between microstructure and permeation properties, suitability of conventional permeation test methods to assess new multi-functional cementitious materials. Therefore, further research is required to clarify these factors. The established knowledge and techniques for assessing permeation properties of normal Portland cement concretes is an area which requires development, if they are to be used in evaluating the performance of HPCs.

4. ACKNOWLEDGEMENTS

This paper has been prepared based on research carried out by the authors along with their colleagues and students. It has not been possible to list all contributors as authors, but their input in discussions and contributions to the content of this paper is gratefully acknowledged. Funding for the work was received from a range of sources, including Engineering and Physical Sciences Research Council, Technology Strategy Board and National Science Foundation of China.

5. REFERENCES

- Aitcin, P. C. (1998), *High performance concrete*. Spon Press.
- American Association of State Highway and Transportation Officials (2015,) *AASHTO T-277, Electrical Indication of Concrete's Ability to Resist Chloride Ion Penetration*, 15 pages.

- Andrade, C. (1993), *Calculation of chloride diffusion coefficients in concrete from ionic migration measurements*, Cement and Concrete Research, vol 23, 724-742. [https://doi.org/10.1016/0008-8846\(93\)90023-3](https://doi.org/10.1016/0008-8846(93)90023-3)
- ASTM C-1202(a) (2017), *Standard Test Method for Electrical Indication of Concrete's Ability to Resist Chloride Ion Penetration*, ASTM, 8 pages.
- Basheer, P. A. M. (1993), *A brief review of methods for measuring the permeation properties of concrete in-situ*, Structures and Buildings, Proceedings of the ICE, vol 99, 74-83. <https://doi.org/10.1680/istbu.1993.22515>
- Basheer, P. A. M., Long, A. E. and Montgomery, F. R. (1994), *The Autoclam - a new test for permeability*, Concrete, vol 28, 27-29.
- Basheer, P. A. M. (2001), *Permeation analysis*, in *Handbook of Analytical Techniques in Concrete Science and Technology: Principles, Techniques and Applications*, Editors V.S. Ramachandran and J. J. Beaudoin, Noyes Publications. 658-727.
- Basheer, P. A. M., Andrew, R. J., Robinson, D., Long, A. E. (2005), *'PERMIT' ion migration test for measuring the chloride ion transport of concrete on site*, NDT & E International, vol 38, 219-229. <https://doi.org/10.1016/j.ndteint.2004.06.013>
- Basheer, L., Cleland, D. J. and Basheer, P. A. M. (2008), *Autoclam Permeability System to assess the protection provided by surface treatments*. In: JIN W.-L., UEDA T. & BASHEER P.A.M., eds. *Advances in Concrete Structural Durability*, Proceedings of the International Conference on Durability of Concrete Structures, 26-27 November Zhejiang University, Hangzhou, China. Zhejiang University Press, 1186-1192.
- Bentur, A. and Mitchell, D. (2008), *Materials performance lessons*, Cement Concrete Research, vol 38, 259-272. <https://doi.org/10.1016/j.cemconres.2007.09.009>
- Beushausen, H. and Luco, L. F. (2016), *Performance-based specifications and control of concrete durability*, RILEM TC 230-PSC State-of-the-Art report, 373 pages.
- BS 1881-208 (1996), *Testing concrete. Recommendations for the determination of the initial surface absorption of concrete*, BSI, 14 pages.
- BS-EN 12390-8 (2009), *Testing hardened concrete. Depth of penetration of water under pressure*, BSI, 10 pages.
- BS-EN 13057 (2002), *Products and systems for the protection and repair of concrete structures. Test methods. Determination of resistance of capillary absorption*, BSI, 16 pages.
- Chia, K. S. and Zhang, M. H. (2002), *Water permeability and chloride penetrability of high-strength lightweight aggregate concrete*. Cement and Concrete Research, vol 32, 639-645. [https://doi.org/10.1016/S0008-8846\(01\)00738-4](https://doi.org/10.1016/S0008-8846(01)00738-4)
- Concrete Society Technical Report: No. 31, *Permeability testing of site concrete*. 2008, 90 pages.
- Dhir, R. K., Hewlett, P. C., Chan, Y. N. (1989), *Near-surface characteristics of concrete prediction of carbonation resistance*. Magazine of Concrete Research, vol 41, 137-43. <https://doi.org/10.1680/mac.1989.41.148.137>
- Dinku, A. and Reinhardt, H. (1997), *Gas permeability coefficient of cover concrete as a performance control*. Materials and Structures. 30: 387-393. <https://doi.org/10.1007/BF02498560>
- Elahi, A., Basheer, P. A. M., Nanukuttan, S. V. and Khan, Q. U. Z. (2010), *Mechanical and durability properties of high performance concretes containing supplementary cementitious materials*. Construction and Building Materials, vol 24, 292-299. <https://doi.org/10.1016/j.conbuildmat.2009.08.045>
- El-Dieb, A. E. and Hooton, R. D. (1995), *Water permeability measurement of high performance concrete using a high pressure triaxial cell*. Cement and Concrete Research, vol 25, 1199-1208. [https://doi.org/10.1016/0008-8846\(95\)00112-P](https://doi.org/10.1016/0008-8846(95)00112-P)
- Figg, J. W. (1973), *Methods of measuring the air and water permeability of concrete*. Magazine of Concrete Research, 25: 213-219. <https://doi.org/10.1680/mac.1973.25.85.213>

- Galle, C., Peycelon, H. and Bescop, P. L. (2004), *Effect of an accelerated chemical degradation on water permeability and pore structure of cement-based materials*. *Advances in Cement Research*, vol 16, 105-114. <https://doi.org/10.1680/adcr.2004.16.3.105>
- Guth, D. L. and Zia, P. (2001), *Evaluation of New Air Permeability Test Device for Concrete*. *ACI Materials Journal*, vol 98: p. 44-51.
- Ganjian, E. and Pouya, H. S. (2009), *The effect of Persian Gulf tidal zone exposure on durability of mixes containing silica fume and blast furnace slag*. *Construction and Building Materials*, vol 23(2): p. 644-652. <https://doi.org/10.1016/j.conbuildmat.2008.02.009>
- Hearn, N. and Morley, C. T. (1997), *Self-sealing property of concrete—Experimental evidence*. *Materials and Structures*, vol 30, 404-411. <https://doi.org/10.1007/BF02498563>
- McCarter, W. J., Emerson, M. and Ezirim, H. (1995), *Properties of concrete in the cover zone: developments in monitoring techniques*, *Magazine of Concrete Research*, vol 47, 243-251. <https://doi.org/10.1680/mac.1995.47.172.243>
- McCarter, W. J., Starrs, G., Kandasami, S., Jones, M. R. and Chrisp, M. (2009), *Electrode configurations for resistivity measurements on concrete*, *ACI Materials Journal*, vol 106, 258-264.
- McCarter, W. J., Suryanto, B., Taha, H. M., Nanukuttan, S. and Basheer, P. A. M. (2017), *A Testing Methodology for Performance-Based Specification*, *Journal of Structural Integrity and Maintenance*, vol 2, 78-88.
- Meletioui, C. A., Tia, M. and Bloomquist, D. (1992), *Development of a field permeability test apparatus and method for concrete*. *ACI Materials Journal*. 89: 83-89.
- Montgomery, F. R. and Adams, A. E. (1985), *Early experience with a new concrete permeability apparatus*, *Proceeding of Structural Faults*, ICE London, 359-363.
- Nanukuttan, S. V., Basheer, P. A. M., McCarter, W. J., Tang, L., Holmes, N., Chrisp, T. M., Starrs, G. and Magee, B. (2015), *The performance of concrete exposed to marine environments: predictive modelling and use of laboratory/on site test methods*, *Construction and Building Materials*, vol 93, pp. 831-840.
- Nokken, M. R. and Hooton, R. D. (2007), *Using pore parameters to estimate permeability or conductivity of concrete*. *Materials and Structures*, vol 41, 1-16. <https://doi.org/10.1617/s11527-006-9212-y>
- NT Build-492 (1999), *Concrete, mortar and cement-based repair materials: Chloride migration coefficient from non-steady-state migration experiments*, Nordtest method, 8 pages.
- Parrott, L. J. and Hong, C. Z. (1991), *Some factors influencing air permeation measurements in cover concrete*. *Materials and Structures*. vol 24: 403-408. <https://doi.org/10.1007/BF02472013>
- Perry, M. and Hollis, D. (2003), *The generation of monthly gridded datasets for a range of climatic variables over the United Kingdom*. Met Office.
- Pocock, D. and Corrans, J. (2007), *Concrete durability testing in Middle East construction*. *Concrete Engineering International*, 52-54.
- Reinhardt, H. and Jooss, M. (2003), *Permeability and self-healing of cracked concrete as a function of temperature and crack width*. *Cement and Concrete Research*, vol 33, 981-985. [https://doi.org/10.1016/S0008-8846\(02\)01099-2](https://doi.org/10.1016/S0008-8846(02)01099-2)
- Romer, M. (2005), *Effect of moisture and concrete composition on the Torrent permeability measurement*. *Materials and Structures*, vol 38 (279): 541-547. <https://doi.org/10.1007/BF02479545>
- Schonlin, K. and Hilsdorf, H. K. (1987), *Evaluation of the effectiveness of curing of concrete structures*, in *Concrete Durability: Katharine and Bryant Mather International Conference*, Scanlon J. M. (Editor). ACI, 207-226.
- Tang, L. and Nilsson, L. O. (1992), *Rapid determination of the chloride diffusivity in concrete by applying an electric field*. *ACI Materials Journal*, vol 89, 49-53.

- Tang, L., Nilsson, L. O. and Basheer, P. A. M. (2011), *Resistance of Concrete to Chloride Ingress: Testing and modelling*. Spon Press.
- Torrent, R. T. (1992), *A two-chamber vacuum cell for measuring the coefficient of permeability to air of the concrete cover on site*. *Materials and Structures*, vol 25, 358-365. <https://doi.org/10.1007/BF02472595>
- Whiting, D. (1981), *Rapid Determination of the Chloride Permeability of Concrete*. in FHWA/RD-81/119. Federal Highway Administration. 173 pages.
- Whiting, D. and Cady, P. D. (1992), *Condition Evaluation of Concrete Bridges Relative to Reinforcement Corrosion*. Strategic Highway Research Program: Washington, D.C. 93 pages.
- Yang, K., Basheer, P. A. M., Magee, B. and Bai, Y. (2013), *Investigation of moisture condition and Autoclam sensitivity on air permeability measurements for both normal concrete and high performance concrete*, *Construction and Building Materials*, vol 48, 316-331. <https://doi.org/10.1016/j.conbuildmat.2013.06.087>
- Yang, K., Basheer, P. A. M., Magee, B., Bai, Y. and Long, A. E. (2015), *Repeatability and Reliability of New Air and Water Permeability Tests for Assessing the Durability of High-Performance Concretes*, *Journal of Materials in Civil Engineering*, vol 27, 11 pages. [https://doi.org/10.1061/\(ASCE\)MT.1943-5533.0001262](https://doi.org/10.1061/(ASCE)MT.1943-5533.0001262)
- Yang, K., Basheer, P. A. M., Bai, Y., Magee, B. and Long, A. E. (2015), *Assessment of the effectiveness of the guard ring in obtaining a uni-directional flow in an in situ water permeability test*, *Materials and Structures*, vol 48, 167–183. <https://doi.org/10.1617/s11527-013-0175-5>
- Zhang, P., Wittmann, F. H., Vogel, M., Müller, H. S. and Zhao, T. J. (2017), *Influence of freeze-thaw cycles on capillary absorption and chloride penetration into concrete*, *Cement and Concrete Research*, vol 100, 60-67. <https://doi.org/10.1016/j.cemconres.2017.05.018>

Design and evaluation of service life through concrete electrical resistivity

C. Andrade^{1*} 

*Contact author: candrade@cimne.upc.edu

DOI: <http://dx.doi.org/10.21041/ra.v8i3.349>

Reception: 26/07/2018 | Acceptance: 24/08/2018 | Publication: 31/08/2018

ABSTRACT

This paper describes the use of concrete electrical resistivity as durability performance parameter and the complementary information that resistivity can provide like: setting period, mechanical strength and degree of curing. Also, it is explained how to design the concrete mix to obtain a target resistivity. Current codes have prescriptive requirements for the durability of concrete and reinforcement corrosion. However, modern trends specify the performance rather than the concrete characteristics. This performance approach demands to define a durability controlling parameter, such as the chloride diffusion coefficient, with its corresponding test and the model to predict the time to steel corrosion.

Keywords: concrete electrical resistivity; durability performance; chloride diffusion coefficient.

Cite as: C. Andrade (2018), “*Design and evaluation of service life through concrete electrical resistivity*”, Revista ALCONPAT, 8 (3), pp. 264-279, DOI: <http://dx.doi.org/10.21041/ra.v8i3.349>

¹ International Center for Numerical Methods in Engineering. CIMNE. UPC, Spain.

Legal Information

Revista ALCONPAT is a quarterly publication by the Asociación Latinoamericana de Control de Calidad, Patología y Recuperación de la Construcción, Internacional, A.C., Km. 6 antigua carretera a Progreso, Mérida, Yucatán, 97310, Tel.5219997385893, alconpat.int@gmail.com, Website: www.alconpat.org

Responsible editor: Pedro Castro Borges, Ph.D. Reservation of rights for exclusive use No.04-2013-011717330300-203, and ISSN 2007-6835, both granted by the Instituto Nacional de Derecho de Autor. Responsible for the last update of this issue, Informatics Unit ALCONPAT, Elizabeth Sabido Maldonado, Km. 6, antigua carretera a Progreso, Mérida, Yucatán, C.P. 97310.

The views of the authors do not necessarily reflect the position of the editor.

The total or partial reproduction of the contents and images of the publication is strictly prohibited without the previous authorization of ALCONPAT Internacional A.C.

Any dispute, including the replies of the authors, will be published in the second issue of 2018 provided that the information is received before the closing of the first issue of 2018.

Diseño y evaluación de la vida útil a través de resistividad eléctrica concreta

RESUMEN

Este artículo describe el uso de la resistividad eléctrica del concreto como parámetro de desempeño de durabilidad y la información complementaria que puede proporcionar la resistividad, como: período de fraguado, resistencia mecánica y grado de curado. Además, se explica cómo diseñar la mezcla de concreto para obtener una resistividad objetivo. Los códigos actuales aún tienen requisitos prescriptivos para el diseño por durabilidad del concreto y para la corrosión del refuerzo. Sin embargo, las tendencias modernas especifican el desempeño más que las características del concreto. Este enfoque de desempeño exige definir un parámetro de control de la durabilidad, como el coeficiente de difusión del cloruro, con su prueba correspondiente y el modelo para predecir el tiempo de corrosión del acero.

Palabras clave: resistividad eléctrica concreta; desempeño de durabilidad; coeficiente de difusión de cloruro.

Projeto e avaliação da vida útil através da resistividade elétrica do concreto

RESUMO

As normas atuais têm requisitos para o projeto de durabilidade do concreto com base na resistência à compressão e provisões relacionadas ao teor de cimento e à relação água-cimento. Para corrosão da armadura, os códigos também especificam as larguras máximas das fissuras de flexão. No entanto, as tendências modernas preferem especificar o desempenho em vez das características do concreto. Essa abordagem de desempenho exige definir um parâmetro de controle de durabilidade, como o coeficiente de difusão de cloreto, com seu teste correspondente e o modelo para prever o tempo de corrosão do aço. Este artigo descreve o uso da resistividade elétrica do concreto a ser usada como parâmetro de desempenho de durabilidade e as informações complementares que a resistividade pode fornecer como é: o período de ajuste, a resistência mecânica e o grau de cura. Além disso, é explicado como projetar a mistura de concreto para obter uma resistividade alvo.

Palavras-chave: resistividade elétrica do concreto; desempenho em durabilidade; coeficiente de difusão de cloretos.

1. INTRODUCTION

Concrete electrical resistivity was measured comparatively early with respect to the application of other electrochemical techniques in concrete because studies are reported from the 40-50's (Hammond and Robson, 1955; Monfore, 1968) related to the characterization of concrete as an electrical insulator to be used in train sleepers and because it was applied to non-destructive measurement of cement setting (Calleja, 1953). It is in the decade of the 60's when reinforcement corrosion was started to appear as an important potential distress and electrochemical techniques started to be applied, in particular polarization curves (Gjorv et. al 1986; Gouda and Monfore 1965).

However, its role in these electrochemical experiments was not appraised until Polarization Resistance technique, R_p , was used to measure the instantaneous corrosion rate (Andrade and González 1978; González et.al 1980), because their values could be very much affected by the ohmic drop if not removing resistive component from the recorded value. The systematic measurement of the ohmic drop affecting R_p measurements enabled the evidence that the concrete resistivity is a direct function of concrete porosity and its degree of water saturation (Andrade et. al 2000a; McCarter and Garvin 1989) and then, the corrosion rate results a direct function of

resistivity with the consequence that ohmic control is the key rate controlling mechanism of reinforcement corrosion.

It is in the decade of the 90's when the interest on resistivity arises again when the relation between chloride diffusion and concrete resistivity is demonstrated (Andrade et al, 2000b). To explore this relation was not appreciated and instead, most of the researchers focused to develop models and tests on chloride migration (Andrade, 1993; Tang, 1996). However, the author of this communication has been attracted by the potential numerous applications of concrete resistivity and in particular has identified that it is the key parameter linking microstructure with transport ability of concrete and has studied in depth the fundamentals of resistivity in particular the possibility to predict the reinforcement service life from its characterization (Andrade et al, 1993; Andrade, 2004). In present work some of the microstructural bases of the resistivity as universal parameter controlling transport processes in concrete as porous medium are described as well as the relation between reinforcement corrosion and degree of saturation which makes to vary concrete resistivity.

2. CONCRETE RESISTIVITY FUNDAMENTALS

Concrete electrical resistance, R , is the relation between the voltage drop, V , applied to a conductive body and the current, I , induced by it.

$$R = \frac{V}{I} = \rho \frac{d}{A} \quad (1)$$

This Resistance, if standardized to a regular geometry, enables to know the resistivity through Ohm's law which is given in equation 1 (d = the distance between electrodes and A is the cross-section area in figure 1).

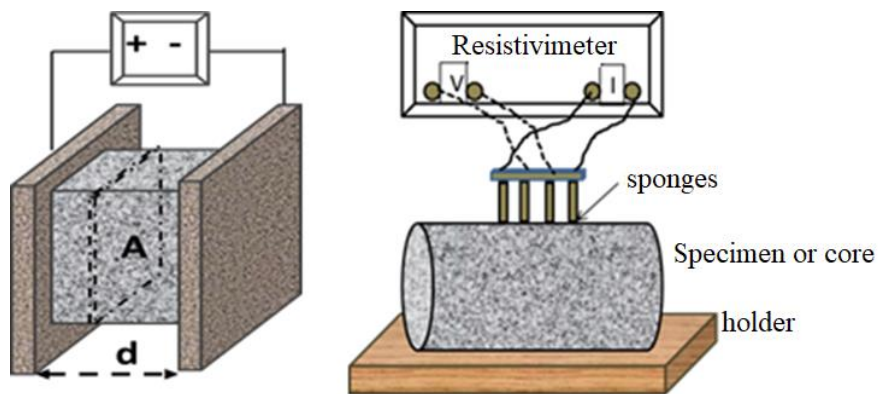


Figure 1. Left: direct, method to measure resistivity (the pore network is made evident for the sake of the representation). Right: four points or Wenner method. Concrete resistivity is an indication of the concrete porosity and degree of water saturation.

The most common method of measurement of resistivity is the “direct” or “bulk” method (figure 1-left). Two electrodes as placed in two parallel faces of a concrete specimen or disc and voltage is applied. The other common method is that known as “four points or Wenner method” shown right in the same figure.

2.1 Evolution of resistivity during setting and hardening

When water is mixed with the cement powder the paste formed is very fluid and then the resistivity is very low (figure 2), however as soon as the paste is setting, the resistivity increases following

cement hydration (Calleja, 1953). The increase continues during hardening as porosity evolves with cement hydration. This increase with time serves to monitor the “aging factor of hydration” which will be addressed later.

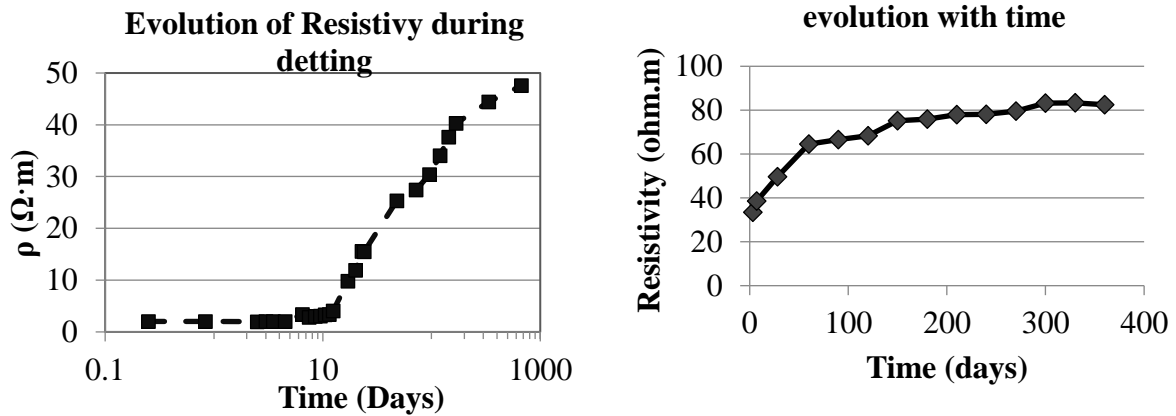


Figure 2. Left: Evolution of resistivity of mortar with w/c ratio of 0.65 during cement setting. Right: example of evolution of concrete resistivity during hardening

2.2 Relation resistivity and mechanical strength

The increase of resistivity with time is parallel to that of mechanical strength due both parameters depend on concrete porosity. In figure 3 is shown their relation for numerous concretes which indicates that the resistivity may be used to predict mechanical strength when the specimens are of the same cement type and cured in standardized conditions.

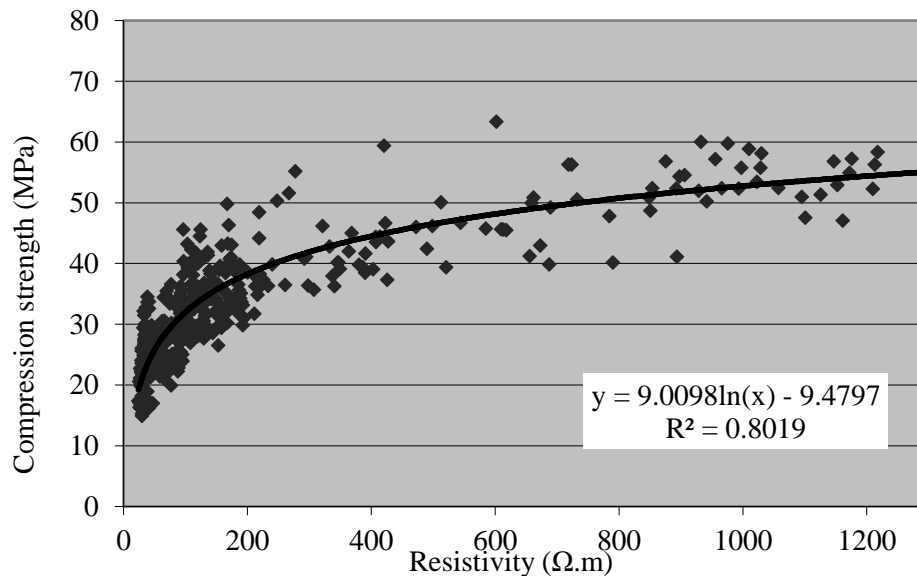


Figure 3. Relation of compressive strength of concretes at different ages and resistivity.

2.3 Relation of Resistivity with pore microstructure and water saturation

Concrete is a porous body in which the solid phases are non-conductive being the pores filled with a solution which is the conductive phase. Then the resistivity/conductivity of the concrete will depend on the total pore volume and on its pore size distribution. As higher is the porosity, lower is the resistivity providing the concrete is water saturated. If the concrete is not saturated then, the resistivity is an indication of concrete degree of saturation (McCarter and Garvin, 1989; Andrade et. al, 2000b). This relation can be expressed through a modification of Archie’s law (Archie,

1942), where ρ_0 = the resistivity of the pore solution (average value from 10 to 50 Ω .cm), W is the volumetric fraction of water and τ is the tortuosity factor, τ :

$$\rho = \rho_0 \cdot W^{-\tau} \quad (2)$$

Regarding the influence of the chemical composition of pore solution, ρ_0 , its impact in the total resistivity following equation 2 is small providing the concrete remains alkaline. If concrete is carbonated then, the value of ρ_0 is much higher.

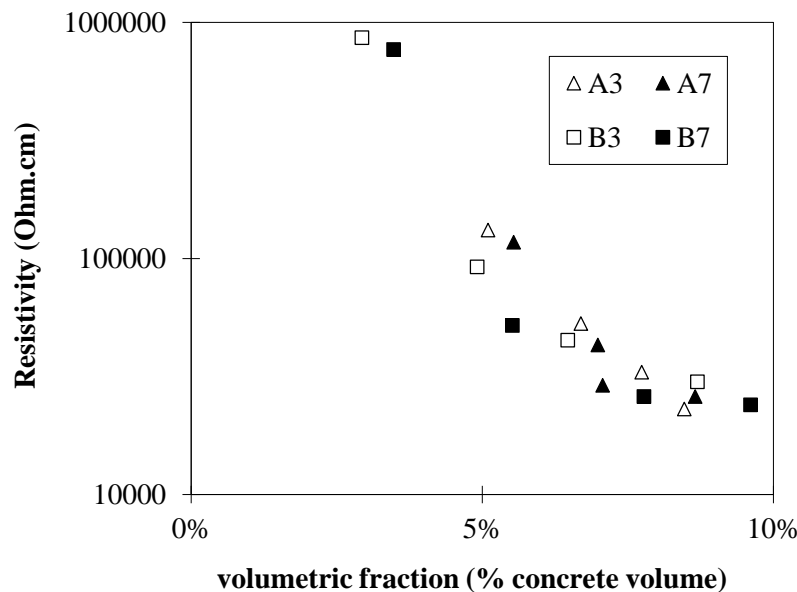


Figure 4. Relation between volumetric fractions of porosity saturated with water and resistivity of four different mixes. The value of τ of equation 2 is 2.52 in the figure (Andrade, Bolzoni, Fullea, 2011)

An illustration of this empirical relation is given in figure 4 (Andrade, Bolzoni, Fullea, 2011) where four concrete mixes have been conditioned to several relative humidities in which the resistivity was measured together with the weight. It indicates that below a RH of 65% the resistivity rises exponentially while it is above 85-90% RH when it reaches the minimum values due to the capillary pores that are starting to be filled with evaporable water.

2.4 Influence of temperature in the Resistivity

With respect to the influence of temperature, it has an important effect on resistivity: resistivity increases when temperature decreases. This effect only can be generalized if the ρ values are standardized to a reference temperature that it is proposed to be 25°C. Other possibility is the use of Arrhenius law; however, it has been detected that the Activation energy depends on the degree of saturation and a single value seems not exiting (Andrade, Zuloaga, et. al, 2011). For practical applications, however the effect can be neglected if the temperature is varying from 18 to 22°C. Larger variations may need standardization.

On the other hand, an increase in temperature usually means evaporation of pore water, which in turn means increase of resistivity. That is, the final effect of temperature in the corrosion is counter-influencing as an increase in temperature may produce a slowing of the Diffusion coefficient and the corrosion rate due to the drying. Therefore, the incorporation of temperature effects on models is very premature and more results are needed.

3. RELATION BETWEEN RESISTIVITY, DIFFUSIVITY AND CORROSION RATE

3.1 Resistivity-Diffusivity

Being concrete a porous material, Resistivity is related to its ionic transport ability by applying Einstein law on conductivity-diffusivity which relates the movement of electrical charges to the conductivity of the medium (Andrade, 1993) as represented in figure 5 in a log-log graph:

$$D_e = \frac{F}{\rho_{ef}} = F \cdot \sigma = \frac{2E-4}{\rho_{ef}} \quad (3)$$

Where:

D_e = effective diffusion coefficient

F = a factor, which depends on the external ionic concentration

ρ_{ef} = “effective” resistivity (in this case of concrete saturated with water)

σ = conductivity (inverse of resistivity)

A value of kCl of 20×10^{-5} can be used for external chloride concentrations of 0.5 to 1 M.

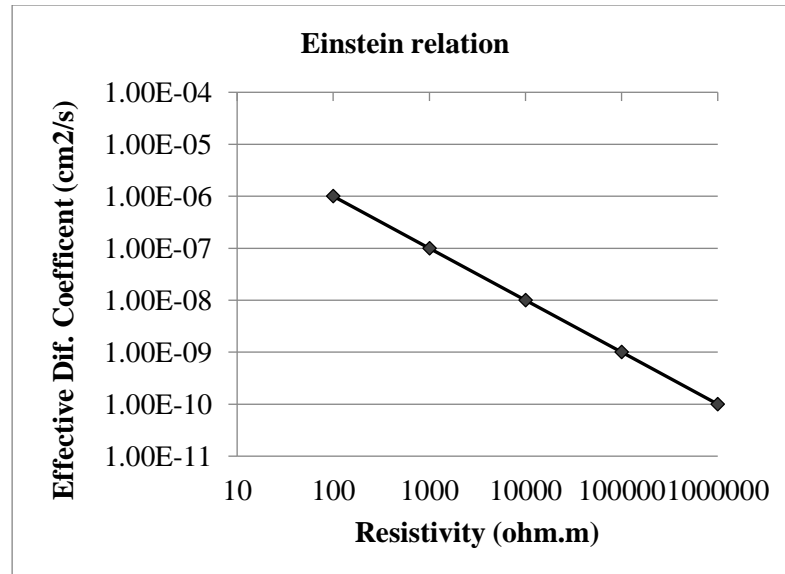


Figure 5. Relation between resistivity and diffusivity as calculated from Einstein law.

3.2 Resistivity- Corrosion Rate

It is the dependence with moisture of the resistivity which explains the relation between it and the reinforcement corrosion rate which is illustrated with the graph I_{corr} -resistivity (Andrade et. al. 2000a; Lambert et. al., 1991) of figure 6, in which it is illustrated the average relation and some values of a particular test. The inclined line in the figure 6 represents the expression:

$$I_{corr} \left(\frac{\mu A}{cm^2} \right) = \frac{26}{\rho (K\Omega \cdot cm)} \quad (4)$$

If the I_{corr} is given as V_{corr} in mm/year this expression 3 results in expression 4:

$$V_{corr} = \frac{0.0116 \cdot 26000}{\rho} = \frac{301.6}{\rho} \quad (5)$$

Where V_{corr} = (mm/year), 0.0116 = conversion factor between V_{corr} and I_{corr} and ρ = concrete resistivity (ohm-cm).

This relation has opened the door to derive the corrosion rate from resistivity providing the corrosion is in active state, because when the steel is passive the resistivity cannot be used to forecast corrosion rates.

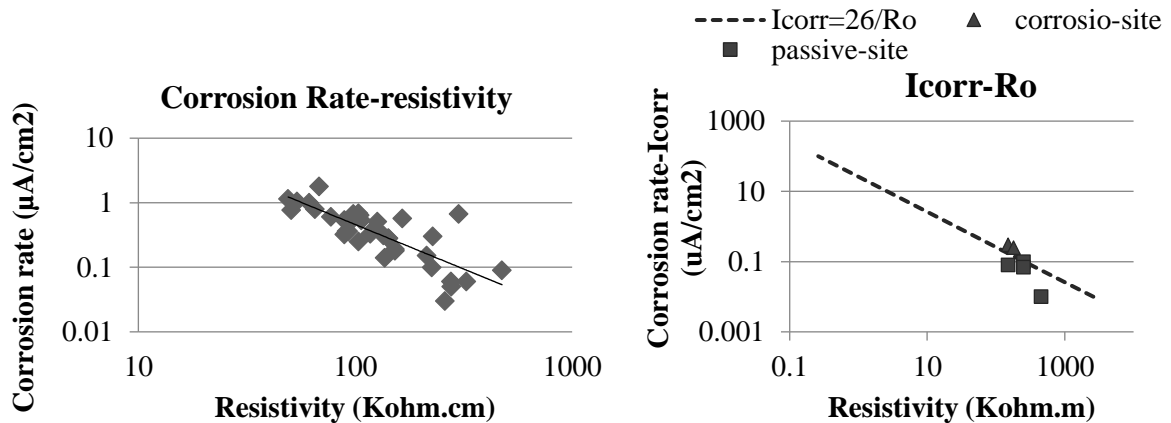


Figure 6. Two examples of the Graph I_{corr} - ρ_{ef} which indicates the relation between the I_{corr} and the degree of concrete saturation.

3.3 Diffusion Coefficient-Corrosion Rate

It is apparent that equation 3 and equation 4 are very similar in spite that one (that of the diffusivity) is based in the well based theory of movement of electrical charges and the other (that of the I_{corr}) is empirical and developed for concrete (perhaps it could be applied to some porous materials as corrosion of metals in soils). What is the physical meaning of that similarity?. The explanation found with respect to the equation of the I_{corr} - ρ was the well-known “resistance control” of the corrosion activity of the micro- and macro-galvanic cells. That is, the resistivity of the electrolyte controls the maximum rate of corrosion (either the movement of the produced iron ions and that of the hydroxides produced in the cathode) while in solution the corrosion activity rate is more controlled by the energy of activation (activation control) or the concentration of the ions oxidized in the anodic areas or reduced in the cathodic ones (concentration control). This resistance control is what expresses the equation 4 of the diffusivity: the ions cannot move faster that the resistivity of the solution allows. Being the movement of electrical charges (ions) involved in the corrosion and in the diffusion, both are controlled by the resistivity of the electrolyte.

Apart from the physical meaning, it has also to be considered the mathematical similarity. This is very interesting from a practical point of view because, in addition to make possible the calculation of the diffusion coefficient and the corrosion rate from the resistivity of the concrete, it also enables the calculation of the maximum corrosion rate to be produced in a concrete if the coefficient of diffusion is known and vice versa, the deduction of the coefficient of diffusion from a measurement of maximum corrosion rate.

Operating mathematically by equalizing both expression 3 and 4 and assuming that for the sake of simplification in equation 4 the value of $k = 2.6 \cdot 10^{-5}$ instead of $k = 2.3 \cdot 10^{-5}$, it can be deduced that:

$$\rho = \frac{26 \cdot 10^{-5}}{D_e} = \frac{26000}{I_{corr}} \quad (6)$$

which aims into:

$$I_{corr} = \frac{26000}{26 \cdot 10^{-5}} \cdot D_e = D_e \cdot 10^8 \quad (7)$$

And

$$D_e = I_{corr} \cdot 10^{-8} \quad (8)$$

Table 1 gives some calculations for different values of I_{corr} and D_{ef} .

Table 1. Equivalence between D_{ef} and I_{corr} for the value of $k=2.6E-5$

D_{ef} (cm ² /s)	0.1E-8	1E-8	10E-8
I_{corr} (µm/year)	0.1	1	10

It must be stressed that such relations are based in the so called “effective diffusion coefficient”, D_e which is a steady-state value and not in the Apparent D_{ap} that averages the evolution of the coefficient along the testing time and it is the result of a non-steady-state regime.

3.4 Relation between resistivity and water saturation

Following with analogies, it is possible to calculate the corrosion rate from the water saturation, as this one depends on the resistivity. Substituting equation 2 and 3 in 4 results in equation 6:

$$V_{corr} \left(\frac{mm}{year} \right) = 6 \cdot W^2 \quad (9)$$

Being: $W = S_w \cdot \varepsilon$, S_w = concrete water saturation degree, % and ε = porosity in volume, % This equation enables to deduce the maximum velocity of corrosion in a concrete in function of its volumetric fraction of pores saturated with water. Thus, as an example, for a $W = 0.05$ (50% of saturation degree in a concrete with 10% of porosity in volume), the maximum corrosion rate would be of 15 µm/year.

Then, in figure 7, all the concordances and analogies are summarized.

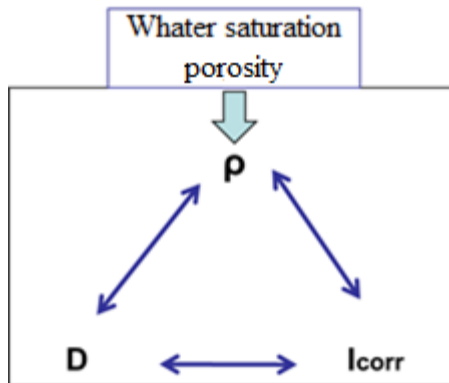


Figure 7. Relations between Resistivity-Diffusivity and Corrosion rate

4. SERVICE LIFE MODEL BASED IN THE RESISTIVITY MEASUREMENTS

Two main aspects must be taken into account when trying to calculate the service life from the resistivity (Andrade, 2004).

- It is necessary to introduce the relation of ρ with time
- The ρ is proportional to the effective diffusion coefficient, that is the reaction of chlorides with the hydrated cement phases has to be incorporated.

4.1 Relation with time

The resistivity can be introduced in a “square root law” enabling the relation between time and the resistivity. Thus, if using the standard square root law:

$$x = V_{CO_2,Cl} \cdot \sqrt{t} = \sqrt{2 \cdot D \cdot t} \quad (10)$$

Where x = depth of carbonation or chloride threshold penetration and t = time life. The model based in the resistivity was proposed (Calleja, 1953) by substituting the value of D by expression 7 which gives:

$$x = \sqrt{2 \cdot \frac{k}{\rho} \cdot t} \quad (11)$$

Based in this relation, a complete model has been developed (Calleja, 1953). For the sake of summarizing it is presented in equation 12 and equation 13:

$$t_l = t_i + t_p = \frac{x_i^2}{V_{CO_2,Cl}} \quad (12)$$

$$t_l = \frac{x^2 \cdot \rho_{ef}}{k_{Cl,CO_2}} \quad (13)$$

Where:

t_i = initiation period

t_p = propagation period

ρ_{ef} = effective resistivity (at 28 days of wet curing)

$k_{CO_2, Cl}$ = environmental factor depending on exposure class

Knowing the value of the resistivity in the same specimen than that used for mechanical strength at 28 days, this model enables the calculation of the time to corrosion and the corrosion propagation period, if some information on the reaction ability of the cement phases and the aging factor are known.

4.2 Consideration of chloride reaction and other factors

As has been mentioned, the ability of resistivity to quantify diffusivity is based in one of the Einstein laws which relates the movement of electrical charges to the conductivity of the medium (Andrade, 1993; Andrade et al, 1993; Andrade, 2004; Garboczi, 1990) (see equation 3). This expression only accounts for the transport of the chloride ions through the pore network which is

insufficient to characterize the transport through concrete where reaction of chlorides takes place and this reaction and the hydration make to evolve the porosity. Then some factors have to be applied to equation 3 to account for these effects together with the value of the k factor which takes into account the concentration of the chloride or aggressive substance.

The factors introduced in the equation 3 have been:

- *k* has been named “environmental factor”. It depends on chloride concentration and in the case of carbonation, on the concrete moisture content (Andrade, 1993; Andrade, 2004)
- *r_b* “retarder or reaction factor” (Andrade et al, 2014) which multiplies the resistivity to account for the “retarder” effect of chloride binding during penetration of chlorides. It can also be applied to the case of carbonation. This is due to carbonation progresses when the concrete is partially saturated. That is, as higher is the porosity or the empty pores due to dry conditions, higher the carbonation depth will be but a certain moisture level is necessary for the carbonation reaction to proceed.
- Finally, the “aging factor” *q* (Andrade, Castellote, D’Andrea, 2011) which accounts for the evolution with time of the porous microstructure.

These factors have been quantified to introduce them in an expression linking resistivity with time that will be described later.

Environmental factor *F*

The environmental factors *F_{Cl}* and *F_{CO2}* depend on the exposure conditions (Andrade, 1993; Andrade, 2004). Table 2 presents values that were calculated by inverse analysis of test results obtained on real structures.

Table 2. Values of environmental factors, *kCl* and *kCO2*, following the exposure classification of EN206

Exposure class	F (cm ³ Ω/year)
X0,XC1,XC2	200
XC3 moderate humidity	1000
XC4 cycles wet and dry	3000
XS1 (d > 500 m distance to the coast line)	5000
XS1 (d < 500 m distance to the coast line)	10000
XS2 submerged	17000
XS3 tidal	25000

Reaction factor *r_b*

The reaction factors *r_{Cl}* and *r_{CO2}* (Andrade et al, 2014) depend on the type and amount of cement and therefore on the reaction of the penetrating substance with the cement phases. Equation 3 can be expressed as:

$$D_{CO2} = \frac{F_{Cl,CO2}}{\rho_{ef} \cdot r_{Cl,CO2}} \tag{14}$$

The values can be calculated either by direct measurement, or indirectly by measuring the relation between the effective and apparent diffusion coefficients, or by calculation based on the cement composition. Table 3 presents examples of *r_{Cl}* values that were calculated based on test results obtained by comparing steady and non-steady diffusion coefficients.

Table 3. Examples of values of the reaction factor of chlorides, r_{Cl} , for 3 types of cement

Cement	r_{Cl}	Standard Deviation
CEM I	1.9	1.3
CEM I + silica fume	1.5	0.5
CEM IIA (with pozzolan and fly ash, in $\leq 20\%$)	3.0	2.1

Aging Factor q

It accounts for the refinement of the concrete pore system results in an increase of resistivity with time (Andrade, Castellote, D’Andrea, 2011). The resistivity evolves with time due to the progression of hydration, the combination of the cement phases with the chlorides or carbon dioxide which usually decreases the porosity and by the concrete drying out (depending on the environment. It can be calculated through the expression 15.

$$\rho_t = \rho_0 \left(\frac{t}{t_0} \right)^q \tag{15}$$

Where:

ρ_t = resistivity at any age t

ρ_0 = resistivity at the age of the first measurement t_0

Values of q found for different cement types are given in table 4.

Table 4. Values of the ageing factor

Cement	q	Standard Deviation
I	0.22	0.01
II/A -P	0.37	0.06
II/A-V	0.57	0.08

The relation between q and the aging factor n of the diffusion coefficient gives the expression 23:

$$q = 0.8 n \tag{16}$$

4.3 Propagation period

In the case of considering the propagation of corrosion (t_p), considering the loss in rebar diameter, or pit depth, (P_{corr}) as the limit corrosion attack, the service life of structure can be written by the expression 9:

$$I_{corr} \left(\frac{\mu A}{cm^2} \right) = \frac{K_{corr}}{\rho_{ef} (Kohm.cm)} \tag{17}$$

The relation for the service life prediction can be then formulated as follows (16):

$$t_l = \frac{P_{corr} \cdot \left(\rho_{ef} \left(\frac{t}{t_0} \right)^q \cdot W_s \right)}{K_{corr} \cdot 0.00116} \tag{18}$$

Where:

P_{corr} = steel cross section reached at the time t_p

ρ_{ef} = resistivity at 28 days in saturated conditions

q = aging factor of the resistivity (Table 4)

ξ = environmental factor of the corrosion rate (it can be of 10 ± 2 for carbonation and 30 ± 5 for chlorides)

K_{corr} = constant with a value of $26 \mu A/cm^2 \cdot k\Omega \cdot cm = 26 mV/cm$ relating the resistivity and the corrosion rate I_{corr}

Complete expression of the service life model based in the resistivity.

Then, the final expression of the service life model based on resistivity is:

$$t_l = t_i + t_p = \frac{x_i^2}{V_{CO_2,Cl}} + \frac{P_{corr}}{V_{corr}} \quad (19)$$

$$t_l = \frac{x^2 \cdot \rho_{ef} \left(\frac{t}{t_0}\right)^q}{F_{Cl,CO_2}} \cdot r_{Cl,CO_2} + \frac{P_{corr} \cdot \left(\rho_{ef} \cdot \left(\frac{t}{t_0}\right)^q \cdot W_s\right)}{K_{corr} \cdot 0.00116} \quad (20)$$

Example of application

For the initiation period the application of the above theory can be shown by way of example, assuming a concrete with a cover depth of 4 cm made with cement type I with silica fume (reaction factor = 1.5 and aging factor = 0,22) to be placed in exposure class XS3 (tidal and splash conditions). Considering a service life of 100 years, the values of the reaction, as well as the environmental and aging factors are presented in Table 5. The calculations indicate that the resistivity needed at 28 days of age, measured in saturated conditions, is 215 $\Omega \cdot m$.

Table 5. Input data for a calculation of the concrete resistivity

Cement type I with silica fume	$r_{Cl} = 1,85$
Exposure class (XS3)	$F (cm^3\Omega/year) = 25000$
Service life	$t (years) = 100$
Cover depth	$X_{Cl} (cm) = 4$
Ageing factor during 10 years	$q = 0.22$

$$4 = \sqrt{\frac{25000}{\rho_0 \left(\frac{100}{0.0767}\right)^{0.22} \cdot 1.5}} \cdot 100 \} \rho_0 (\Omega \cdot cm) = 21497 \rightarrow \rho_0 (\Omega \cdot m) = 215$$

With this resistivity the length of the propagation period following Table 6 is:

Table 6. Input data for the propagation period

Limit Diameter loss, P_{corr}	$100 \mu m = 0.01 cm$
ρ_{ef} at 28 days	$21.5 Kohm.cm$
q applied during 100 years	0.22
W_s in saturated conditions	1

$$t_l = \frac{0.01 \cdot \left(21.5 \cdot \left(\frac{100}{0.0767} \right)^{0.22} \cdot 1 \right)}{26 \cdot 0.00116} = 34.54 \text{ years}$$

This propagation period may be included in the 100 years or considered apart as an additional safe time until cracking is produced.

5. PRODUCTION OF CONCRETE FOR A SPECIFIED APPARENT RESISTIVITY

Once known the resistivity which is needed to reach a nominal service life, it remains to describe how the concrete producer can design a mix to fulfil the service life specification. This can be done (Andrade and D'Andrade, 2010) by considering a modification of Archie's law linking resistivity and porosity:

$$\rho_{28d} = \rho_o \cdot \varepsilon^{-\tau} \quad (21)$$

where ρ_{28d} is the resistivity of concrete under saturated condition at 28 days, τ is the tortuosity coefficient which is estimated by fit to the experimental data, and ε is the total porosity.

The coefficient τ depends on the concrete composition which is identified to the tortuosity, and could be determined from type or family of cement type by means of measuring the porosity and the resistivity. The values found in present research are. For type I cement $\tau= 1.9$, for type II-AV $\tau= 2.3$ and for type II AP $\tau= 1.6$.

From the specified resistivity the paste porosity can be obtained and through Power's relation on porosity and w/c ratio

$$\varepsilon_p (\% \text{volumen}) \approx \frac{\left(\frac{w}{c} \right) - 0,36\alpha}{\left(\frac{w}{c} \right) + 0,32} \times 100 \quad (22)$$

To use ρ_p in the model based on Archie's law, it must convert the porosity of the paste (ρ_p) to porosity of the concrete (ρ). For this, it is applied a simple method based on multiplying the percentage of capillary porosity of the paste by the volume of paste (γ) in the concrete.

$$\varepsilon = \varepsilon_p \cdot \gamma \quad (23)$$

It is feasible to prepare a mix with the needed effective resistivity at 28 days, providing the consideration of the type of cement and its retarder factor. The concrete producer should verify by testing the reaching of the specified resistivity while the cement producer should give the retarder factor of his cements.

So, the following concrete design methodology based on Archie's law model is proposed to achieve the prescribed value ρ_{28d} :

1. Select a type of cement. It fixes the values of reaction factor (r) and tortuosity (τ) are defined.
2. Select a w/c ratio and calculate porosity of the paste following Powers' model

3. Then calculate the expected resistivity through $\rho = \rho_o \cdot (\varepsilon_p \cdot \gamma)^{-\tau}$.

6. FINAL COMMENTS

Concrete is a very complex material but which is placed on site in many manners by relatively simple practices. It needs to be modelled by sophisticated models, but also by simple ones which could help to improve the quality and spread the tools for it. The electrical resistivity, being a non-destructive method simplifies very much the control of the durability. On the other hand, it enables multiple applications in concrete technology and the quantification of the expected life. It has been summarized some of the possible applications of the concrete electrical resistivity values. Its main advantage is that the measurement is non-destructive and the concrete can be monitored. Concrete resistivity is able to inform on:

- Porosity
- Degree of water saturation
- Degree of curing
- Cement setting time
- Concrete mechanical strength
- Reinforcement corrosion rate
- Gas and water permeability

In present paper is shown the fundamental relations of resistivity with diffusivity and with the reinforcement corrosion rate. Resistivity is the parameter enabling to link microstructure with the macro-performance Also has been summarized the model for service life prediction based in Einstein law relating electrical resistance or conductance with the diffusion coefficient. Making certain assumptions this basic law can be applied to the advance of carbonation front or chloride threshold, and to the representation of steel corrosion propagation. This model can be used for calculating cover thicknesses from actual resistivity values or the minimum resistivity for a certain cover thickness.

7. ACKNOWLEDGEMENTS

The authors would like to acknowledge the financing of the Ministry of Science and Innovation for the INGENIO 2010-CONSOLIDER Project on “Safety and Durability of Structures: SEDUREC”.

8. REFERENCES

- Andrade, C. (1993), *Calculation of chloride diffusion coefficients in concrete from ionic migration measurements*. Cement and Concrete Research, Volume 23, Issue 3, pp. 724-742. [https://doi.org/10.1016/0008-8846\(93\)90023-3](https://doi.org/10.1016/0008-8846(93)90023-3)
- Andrade, C. (2004), “*Calculation of initiation and propagation periods of service-life of reinforcements by using the electrical resistivity*”. International RILEM Symposium on Concrete Science and Engineering: A Tribute to Arnon Bentur, 22-24, RILEM Publications SARL.
- Andrade, C., Bolzoni F., Fullea, J. (2011), *Analysis of the relation between water and resistivity isotherms in concrete*, Materials and Corrosion, 62, no.2 130-138, <https://doi.org/10.1002/maco.201005777>
- Andrade, C., Castellote, M., D’Andrea, R. (2011) *Measurement of ageing effect of chloride diffusion coefficients in cementitious matrices*, Journal of Nuclear Materials, Volume 412, Issue 1, pp 209-216. <https://doi.org/10.1016/j.jnucmat.2010.12.236>

- Andrade C., D'Andréa, R. (2010), *Concrete mix design based on the electrical resistivity- 2nd International Conference on Sustainable Construction Materials and Technologies*. Ancona- Italy June. Ed. Coventry University UK.
- Andrade, C., D'Andrea, R., Rebolledo, N. (2014), “*Chloride ion penetration in concrete: The reaction factor in the electrical resistivity model*”, *Cement and Concrete Composites*, Volume 47, pp 41-46, <https://doi.org/10.1016/j.cemconcomp.2013.09.022>
- Andrade, C., Fullea, J., Alonso, C. (2000), *The use of the graph corrosion rate-resistivity in the measurement of the corrosion current- Proceedings of the International Workshop on “Measurement and interpretation of the on-site corrosion rate*. MESINA- RILEM Proc. No. 18. Ed. C. Andrade, C. Alonso, J. Fullea, J. Polimon and J. Rodriguez. Rilem Publications S.A.R.L. 157-166.
- Andrade C., Fullea J., Alonso C. (2000b), *The use of the graph corrosion rate-resistivity in the measurement of the corrosion current- Proceedings of the International Workshop on “Measurement and interpretation of the on-site corrosion rate*. MESINA- RILEM, Proc. No. 18. Ed. C. Andrade, C. Alonso, J. Fullea, J. Polimon and J. Rodriguez. Rilem Publications S.A.R.L. 157-166.
- Andrade, C. and González, J. A. (1978), *Quantitative measurements of corrosion rate of reinforcing steels embedded in concrete using polarization resistance measurements*, *Materials and Corrosion*, Volume 29, Issue 8, 515. <https://doi.org/10.1002/maco.19780290804>
- Andrade, C., Zuloaga, P., Martinez, I., Castillo, A., Briz, S. (2011), *Effect of temperature on the corrosion parameters and apparent activation energy measured by embedded sensors in a pilot container in “el Cabril” repository*. *Corrosion Engineering, Science and Technology: The International Journal of Corrosion Processes and Corrosion Control*, Vol 46, No 2, pp 182-189. <https://doi.org/10.1179/1743278211Y.0000000007>
- Andrade. C., Alonso, C., Goñi, S. (1993), *Possibilities for electrical resistivity to universally characterize mass transport processes in Concrete*. *Concrete 2000: Economic and Durable Construction Through Excellence*, V. 2, R.K. Dhir and M.R. Jones, eds., E&FN Spon, Cambridge, pp. 1639-1652.
- Archie, G. E. (1942), “*The electrical resistivity log as an aid in determining some reservoir characteristics*” *Transactions of the AIME*. 146, 54. <https://doi.org/10.2118/942054-G>
- Calleja, J. (1953), *Determination of settings and hardening time of high-alumina cements by electrical resistance techniques*. *Journal of ACI*, vol 25, pp. 249
- Dhir, R. K., Jones, M. R. (1999), “*Development of chloride-resisting concrete using fly ash*”, *Fuel*, Volume 78, Issue 2, pp. 137-142
- Garboczi, E. J. (1990), “*Permeability, Diffusivity and Microstructural Parameters: A Critical Review*”, *Cement and Concrete Research*, Volume 20, Issue 4, pp. 591-601. [https://doi.org/10.1016/0008-8846\(90\)90101-3](https://doi.org/10.1016/0008-8846(90)90101-3)
- Gjorv, O. E., Vennesland, O., El-Busaidy, A. H. S. (1986), *Diffusion of Dissolved Oxygen Through Concrete*, *Materials Performance*, Vol. 25, No. 12, December, pp. 39-44
- González, J. A., Algaba, S., Andrade, C. (1980), *Corrosion of reinforcing bars in carbonated concrete*, *British Corrosion Journal*, Volume 15, Issue 3. <https://doi.org/10.1179/bcj.1980.15.3.135>
- Gouda, V. K., Monfore, G. E. (1965), *A rapid method for studying corrosion inhibition on steel in concrete*. *Journal PCA*, vol 7 n. 3, pp. 24.
- Hammond, E., Robson, T. D. (1955), *Comparison of electrical properties of various cements and concretes*. *The Engineer*, vol 199, pp. 78-80 and pp. 114.115.
- McCarter, W. J., Garvin, S., (1989) “*Dependence of Electrical Impedance of Cement-Based Materials on their Moisture Condition*”, *Journal of Physics D Applied Physics*, Vol. 22 (11), pp. 1773 – 1776.
- Monfore, G. E. (1968), *The electrical resistivity of concrete*. *Journal P.C.A. Applied Research Section*. pp. 35.

- Lambert, P., Page, C. L., Vassie, P. R. W. (1991), “*Investigations of reinforcement corrosion, 2: Electrochemical monitoring of steel in chloride-contaminated concrete*”, *Materials and Structures*, 24 (5), pp. 351-358. <https://doi.org/10.1007/BF02472068>
- Page, C. L., Treadaway, K. W. J. (1982), *Aspects of the electrochemistry of steel in concrete*. *Nature* 297, pp. 109-115. <https://doi.org/10.1038/297109a0>
- Tang, L. (1996), *Chloride Transport in Concrete – Measurement and Prediction*, Chalmers University of Technology, Dept. of Building Materials. ISSN: 1104-893X

Design and evaluation of service life through concrete electrical resistivity

C. Andrade^{1*} 

*Contact author: candrade@cimne.upc.edu

DOI: <http://dx.doi.org/10.21041/ra.v8i3.349>

Reception: 26/07/2018 | Acceptance: 24/08/2018 | Publication: 31/08/2018

ABSTRACT

This paper describes the use of concrete electrical resistivity as durability performance parameter and the complementary information that resistivity can provide like: setting period, mechanical strength and degree of curing. Also, it is explained how to design the concrete mix to obtain a target resistivity. Current codes have prescriptive requirements for the durability of concrete and reinforcement corrosion. However, modern trends specify the performance rather than the concrete characteristics. This performance approach demands to define a durability controlling parameter, such as the chloride diffusion coefficient, with its corresponding test and the model to predict the time to steel corrosion.

Keywords: concrete electrical resistivity; durability performance; chloride diffusion coefficient.

Cite as: C. Andrade (2018), “*Design and evaluation of service life through concrete electrical resistivity*”, Revista ALCONPAT, 8 (3), pp. 264-279, DOI: <http://dx.doi.org/10.21041/ra.v8i3.349>

¹ International Center for Numerical Methods in Engineering. CIMNE. UPC, Spain.

Legal Information

Revista ALCONPAT is a quarterly publication by the Asociación Latinoamericana de Control de Calidad, Patología y Recuperación de la Construcción, Internacional, A.C., Km. 6 antigua carretera a Progreso, Mérida, Yucatán, 97310, Tel.5219997385893, alconpat.int@gmail.com, Website: www.alconpat.org

Responsible editor: Pedro Castro Borges, Ph.D. Reservation of rights for exclusive use No.04-2013-011717330300-203, and ISSN 2007-6835, both granted by the Instituto Nacional de Derecho de Autor. Responsible for the last update of this issue, Informatics Unit ALCONPAT, Elizabeth Sabido Maldonado, Km. 6, antigua carretera a Progreso, Mérida, Yucatán, C.P. 97310.

The views of the authors do not necessarily reflect the position of the editor.

The total or partial reproduction of the contents and images of the publication is strictly prohibited without the previous authorization of ALCONPAT Internacional A.C.

Any dispute, including the replies of the authors, will be published in the second issue of 2018 provided that the information is received before the closing of the first issue of 2018.

Diseño y evaluación de la vida útil a través de resistividad eléctrica concreta

RESUMEN

Este artículo describe el uso de la resistividad eléctrica del concreto como parámetro de desempeño de durabilidad y la información complementaria que puede proporcionar la resistividad, como: período de fraguado, resistencia mecánica y grado de curado. Además, se explica cómo diseñar la mezcla de concreto para obtener una resistividad objetivo. Los códigos actuales aún tienen requisitos prescriptivos para el diseño por durabilidad del concreto y para la corrosión del refuerzo. Sin embargo, las tendencias modernas especifican el desempeño más que las características del concreto. Este enfoque de desempeño exige definir un parámetro de control de la durabilidad, como el coeficiente de difusión del cloruro, con su prueba correspondiente y el modelo para predecir el tiempo de corrosión del acero.

Palabras clave: resistividad eléctrica concreta; desempeño de durabilidad; coeficiente de difusión de cloruro.

Projeto e avaliação da vida útil através da resistividade elétrica do concreto

RESUMO

As normas atuais têm requisitos para o projeto de durabilidade do concreto com base na resistência à compressão e provisões relacionadas ao teor de cimento e à relação água-cimento. Para corrosão da armadura, os códigos também especificam as larguras máximas das fissuras de flexão. No entanto, as tendências modernas preferem especificar o desempenho em vez das características do concreto. Essa abordagem de desempenho exige definir um parâmetro de controle de durabilidade, como o coeficiente de difusão de cloreto, com seu teste correspondente e o modelo para prever o tempo de corrosão do aço. Este artigo descreve o uso da resistividade elétrica do concreto a ser usada como parâmetro de desempenho de durabilidade e as informações complementares que a resistividade pode fornecer como é: o período de ajuste, a resistência mecânica e o grau de cura. Além disso, é explicado como projetar a mistura de concreto para obter uma resistividade alvo.

Palavras-chave: resistividade elétrica do concreto; desempenho em durabilidade; coeficiente de difusão de cloretos.

1. INTRODUCTION

Concrete electrical resistivity was measured comparatively early with respect to the application of other electrochemical techniques in concrete because studies are reported from the 40-50's (Hammond and Robson, 1955; Monfore, 1968) related to the characterization of concrete as an electrical insulator to be used in train sleepers and because it was applied to non-destructive measurement of cement setting (Calleja, 1953). It is in the decade of the 60's when reinforcement corrosion was started to appear as an important potential distress and electrochemical techniques started to be applied, in particular polarization curves (Gjorv et. al 1986; Gouda and Monfore 1965).

However, its role in these electrochemical experiments was not appraised until Polarization Resistance technique, R_p , was used to measure the instantaneous corrosion rate (Andrade and González 1978; González et.al 1980), because their values could be very much affected by the ohmic drop if not removing resistive component from the recorded value. The systematic measurement of the ohmic drop affecting R_p measurements enabled the evidence that the concrete resistivity is a direct function of concrete porosity and its degree of water saturation (Andrade et. al 2000a; McCarter and Garvin 1989) and then, the corrosion rate results a direct function of

resistivity with the consequence that ohmic control is the key rate controlling mechanism of reinforcement corrosion.

It is in the decade of the 90's when the interest on resistivity arises again when the relation between chloride diffusion and concrete resistivity is demonstrated (Andrade et al, 2000b). To explore this relation was not appreciated and instead, most of the researchers focused to develop models and tests on chloride migration (Andrade, 1993; Tang, 1996). However, the author of this communication has been attracted by the potential numerous applications of concrete resistivity and in particular has identified that it is the key parameter linking microstructure with transport ability of concrete and has studied in depth the fundamentals of resistivity in particular the possibility to predict the reinforcement service life from its characterization (Andrade et al, 1993; Andrade, 2004). In present work some of the microstructural bases of the resistivity as universal parameter controlling transport processes in concrete as porous medium are described as well as the relation between reinforcement corrosion and degree of saturation which makes to vary concrete resistivity.

2. CONCRETE RESISTIVITY FUNDAMENTALS

Concrete electrical resistance, R , is the relation between the voltage drop, V , applied to a conductive body and the current, I , induced by it.

$$R = \frac{V}{I} = \rho \frac{l}{A} \quad (1)$$

This Resistance, if standardized to a regular geometry, enables to know the resistivity through Ohm's law which is given in equation 1 (l = the distance between electrodes and A is the cross-section area in figure 1).

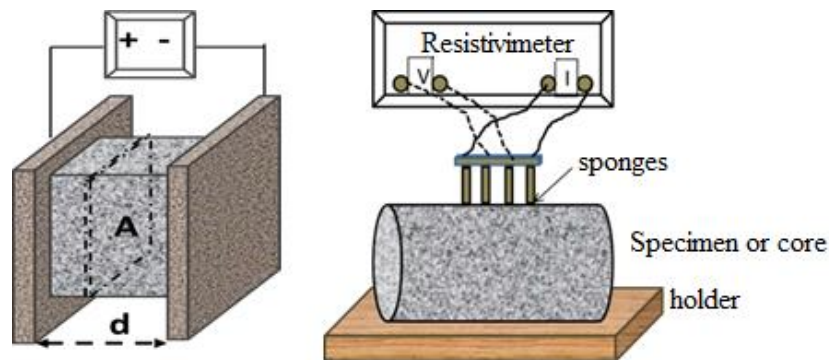


Figure 1. Left: direct, method to measure resistivity (the pore network is made evident for the sake of the representation). Right: four points or Wenner method. Concrete resistivity is an indication of the concrete porosity and degree of water saturation.

The most common method of measurement of resistivity is the “direct” or “bulk” method (figure 1-left). Two electrodes as placed in two parallel faces of a concrete specimen or disc and voltage is applied. The other common method is that known as “four points or Wenner method” shown right in the same figure.

2.1 Evolution of resistivity during setting and hardening

When water is mixed with the cement powder the paste formed is very fluid and then the resistivity is very low (figure 2), however as soon as the paste is setting, the resistivity increases following cement hydration (Calleja, 1953). The increase continues during hardening as porosity evolves

with cement hydration. This increase with time serves to monitor the “aging factor of hydration” which will be addressed later.

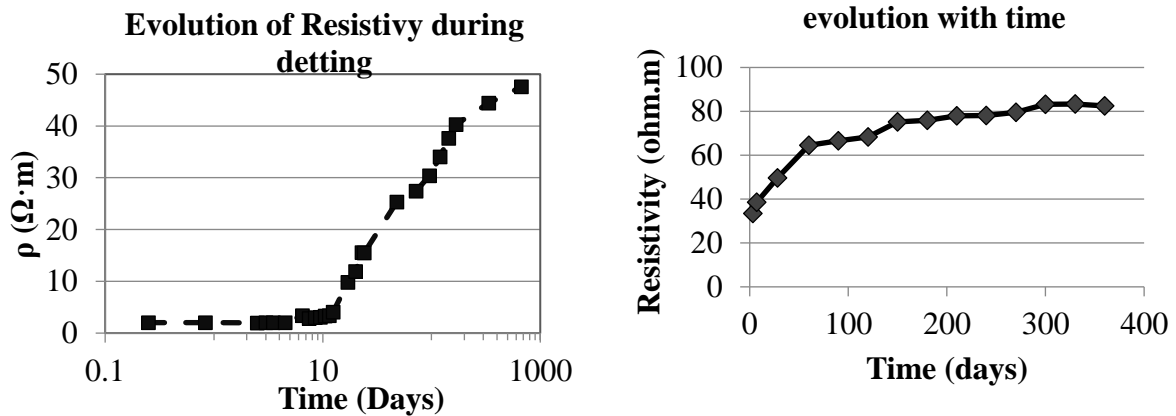


Figure 2. Left: Evolution of resistivity of mortar with w/c ratio of 0.65 during cement setting. Right: example of evolution of concrete resistivity during hardening

2.2 Relation resistivity and mechanical strength

The increase of resistivity with time is parallel to that of mechanical strength due both parameters depend on concrete porosity. In figure 3 is shown their relation for numerous concretes which indicates that the resistivity may be used to predict mechanical strength when the specimens are of the same cement type and cured in standardized conditions.

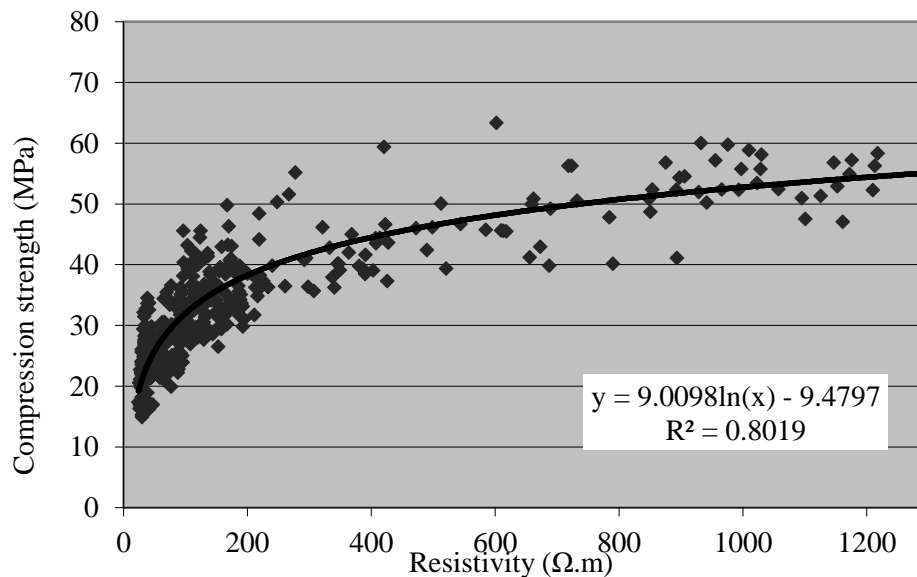


Figure 3. Relation of compressive strength of concretes at different ages and resistivity.

2.3 Relation of Resistivity with pore microstructure and water saturation

Concrete is a porous body in which the solid phases are non-conductive being the pores filled with a solution which is the conductive phase. Then the resistivity/conductivity of the concrete will depend on the total pore volume and on its pore size distribution. As higher is the porosity, lower is the resistivity providing the concrete is water saturated. If the concrete is not saturated then, the resistivity is an indication of concrete degree of saturation (McCarter and Garvin, 1989; Andrade et. al, 2000b). This relation can be expressed through a modification of Archie’s law (Archie,

1942), where ρ_0 = the resistivity of the pore solution (average value from 10 to 50 Ω .cm), W is the volumetric fraction of water and τ is the tortuosity factor, τ :

$$\rho = \rho_0 \cdot W^{-\tau} \quad (2)$$

Regarding the influence of the chemical composition of pore solution, ρ_0 , its impact in the total resistivity following equation 2 is small providing the concrete remains alkaline. If concrete is carbonated then, the value of ρ_0 is much higher.

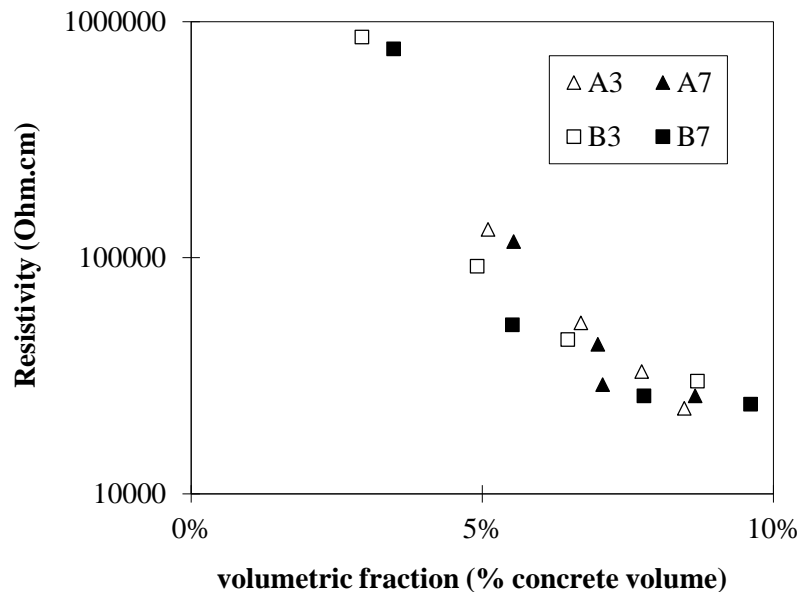


Figure 4. Relation between volumetric fractions of porosity saturated with water and resistivity of four different mixes. The value of τ of equation 2 is 2.52 in the figure (Andrade, Bolzoni, Fullea, 2011)

An illustration of this empirical relation is given in figure 4 (Andrade, Bolzoni, Fullea, 2011) where four concrete mixes have been conditioned to several relative humidities in which the resistivity was measured together with the weight. It indicates that below a RH of 65% the resistivity rises exponentially while it is above 85-90% RH when it reaches the minimum values due to the capillary pores that are starting to be filled with evaporable water.

2.4 Influence of temperature in the Resistivity

With respect to the influence of temperature, it has an important effect on resistivity: resistivity increases when temperature decreases. This effect only can be generalized if the ρ values are standardized to a reference temperature that it is proposed to be 25°C. Other possibility is the use of Arrhenius law; however, it has been detected that the Activation energy depends on the degree of saturation and a single value seems not exiting (Andrade, Zuloaga, et. al, 2011). For practical applications, however the effect can be neglected if the temperature is varying from 18 to 22°C. Larger variations may need standardization.

On the other hand, an increase in temperature usually means evaporation of pore water, which in turn means increase of resistivity. That is, the final effect of temperature in the corrosion is counter-influencing as an increase in temperature may produce a slowing of the Diffusion coefficient and the corrosion rate due to the drying. Therefore, the incorporation of temperature effects on models is very premature and more results are needed.

3. RELATION BETWEEN RESISTIVITY, DIFFUSIVITY AND CORROSION RATE

3.1 Resistivity-Diffusivity

Being concrete a porous material, Resistivity is related to its ionic transport ability by applying Einstein law on conductivity-diffusivity which relates the movement of electrical charges to the conductivity of the medium (Andrade, 1993) as represented in figure 5 in a log-log graph:

$$D_e = \frac{F}{\rho_{ef}} = F \cdot \sigma = \frac{2E-4}{\rho_{ef}} \quad (3)$$

Where:

D_e = effective diffusion coefficient

F = a factor, which depends on the external ionic concentration

ρ_{ef} = “effective” resistivity (in this case of concrete saturated with water)

σ = conductivity (inverse of resistivity)

A value of kCl of 20×10^{-5} can be used for external chloride concentrations of 0.5 to 1 M.

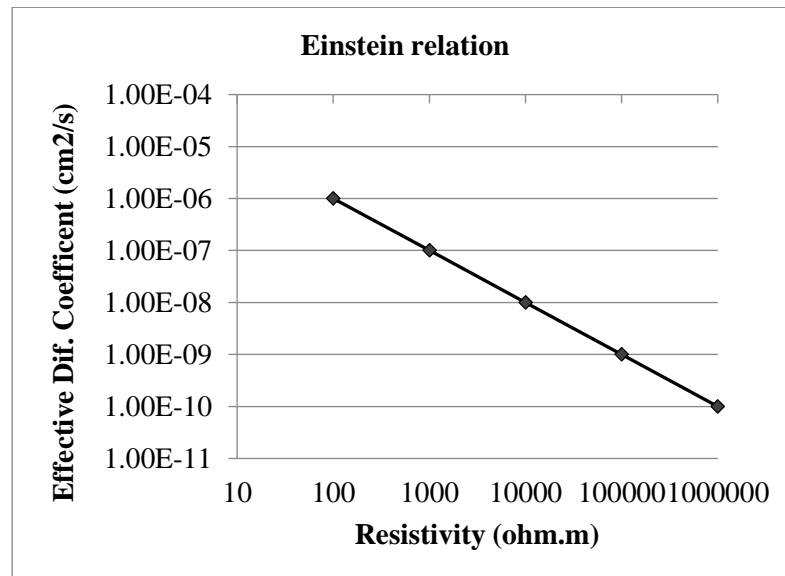


Figure 5. Relation between resistivity and diffusivity as calculated from Einstein law.

3.2 Resistivity- Corrosion Rate

It is the dependence with moisture of the resistivity which explains the relation between it and the reinforcement corrosion rate which is illustrated with the graph I_{corr} -resistivity (Andrade et. al. 2000a; Lambert et. al., 1991) of figure 6, in which it is illustrated the average relation and some values of a particular test. The inclined line in the figure 6 represents the expression:

$$I_{corr} \left(\frac{\mu A}{cm^2} \right) = \frac{26}{\rho (K\Omega \cdot cm)} \quad (4)$$

If the I_{corr} is given as V_{corr} in mm/year this expression 3 results in expression 4:

$$V_{corr} = \frac{0.0116 \cdot 26000}{\rho} = \frac{301.6}{\rho} \quad (5)$$

Where V_{corr} = (mm/year), 0.0116 = conversion factor between V_{corr} and I_{corr} and ρ = concrete resistivity (ohm-cm).

This relation has opened the door to derive the corrosion rate from resistivity providing the corrosion is in active state, because when the steel is passive the resistivity cannot be used to forecast corrosion rates.

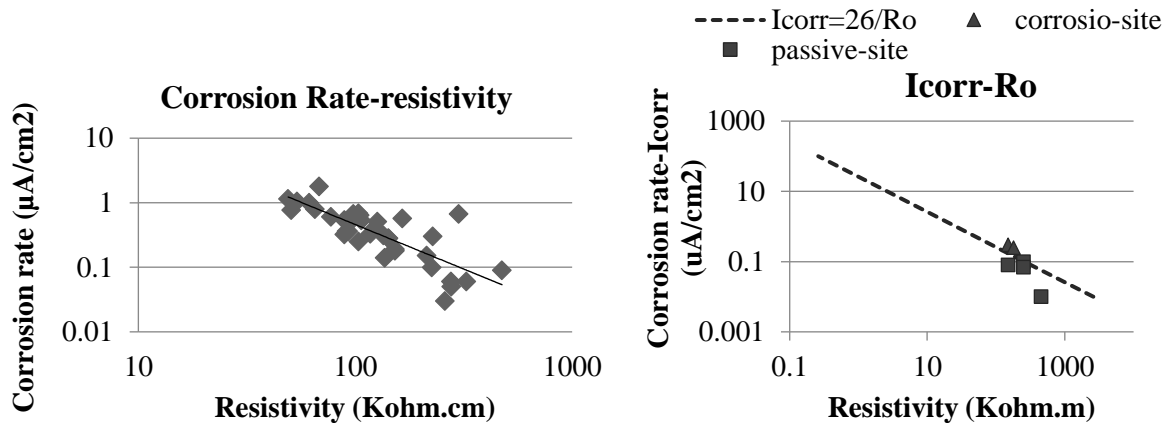


Figure 6. Two examples of the Graph I_{corr} - ρ_{ef} which indicates the relation between the I_{corr} and the degree of concrete saturation.

3.3 Diffusion Coefficient-Corrosion Rate

It is apparent that equation 3 and equation 4 are very similar in spite that one (that of the diffusivity) is based in the well based theory of movement of electrical charges and the other (that of the I_{corr}) is empirical and developed for concrete (perhaps it could be applied to some porous materials as corrosion of metals in soils). What is the physical meaning of that similarity?. The explanation found with respect to the equation of the I_{corr} - ρ was the well-known “resistance control” of the corrosion activity of the micro- and macro-galvanic cells. That is, the resistivity of the electrolyte controls the maximum rate of corrosion (either the movement of the produced iron ions and that of the hydroxides produced in the cathode) while in solution the corrosion activity rate is more controlled by the energy of activation (activation control) or the concentration of the ions oxidized in the anodic areas or reduced in the cathodic ones (concentration control). This resistance control is what expresses the equation 4 of the diffusivity: the ions cannot move faster that the resistivity of the solution allows. Being the movement of electrical charges (ions) involved in the corrosion and in the diffusion, both are controlled by the resistivity of the electrolyte.

Apart from the physical meaning, it has also to be considered the mathematical similarity. This is very interesting from a practical point of view because, in addition to make possible the calculation of the diffusion coefficient and the corrosion rate from the resistivity of the concrete, it also enables the calculation of the maximum corrosion rate to be produced in a concrete if the coefficient of diffusion is known and vice versa, the deduction of the coefficient of diffusion from a measurement of maximum corrosion rate.

Operating mathematically by equalizing both expression 3 and 4 and assuming that for the sake of simplification in equation 4 the value of $k= 2.6 \cdot 10^{-5}$ instead of $k= 2.3 \cdot 10^{-5}$, it can be deduced that:

$$\rho = \frac{26 \cdot 10^{-5}}{D_e} = \frac{26000}{I_{corr}} \quad (6)$$

which aims into:

$$I_{corr} = \frac{26000}{26 \cdot 10^{-5}} \cdot D_e = D_e \cdot 10^8 \quad (7)$$

And

$$D_e = I_{corr} \cdot 10^{-8} \quad (8)$$

Table 1 gives some calculations for different values of I_{corr} and D_{ef} .

Table 1. Equivalence between D_{ef} and I_{corr} for the value of $k=2.6E-5$

D_{ef} (cm²/s)	0.1E-8	1E-8	10E-8
I_{corr} (µm/year)	0.1	1	10

It must be stressed that such relations are based in the so called “effective diffusion coefficient”, D_e which is a steady-state value and not in the Apparent D_{ap} that averages the evolution of the coefficient along the testing time and it is the result of a non-steady-state regime.

3.4 Relation between resistivity and water saturation

Following with analogies, it is possible to calculate the corrosion rate from the water saturation, as this one depends on the resistivity. Substituting equation 2 and 3 in 4 results in equation 6:

$$V_{corr} \left(\frac{mm}{year} \right) = 6 \cdot W^2 \quad (9)$$

Being: $W = S_w \cdot \varepsilon$, S_w = concrete water saturation degree, % and ε = porosity in volume, % This equation enables to deduce the maximum velocity of corrosion in a concrete in function of its volumetric fraction of pores saturated with water. Thus, as an example, for a $W = 0.05$ (50% of saturation degree in a concrete with 10% of porosity in volume), the maximum corrosion rate would be of 15 µm/year.

Then, in figure 7, all the concordances and analogies are summarized.

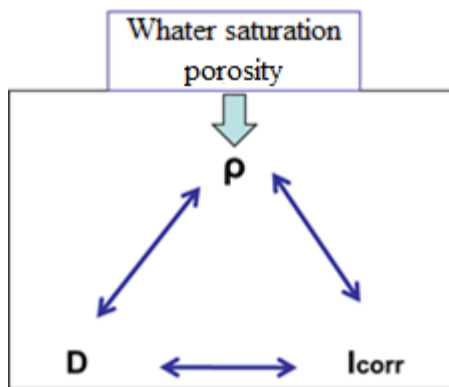


Figure 7. Relations between Resistivity-Diffusivity and Corrosion rate

4. SERVICE LIFE MODEL BASED IN THE RESISTIVITY MEASUREMENTS

Two main aspects must be taken into account when trying to calculate the service life from the resistivity (Andrade, 2004).

- It is necessary to introduce the relation of ρ with time
- The ρ is proportional to the effective diffusion coefficient, that is the reaction of chlorides with the hydrated cement phases has to be incorporated.

4.1 Relation with time

The resistivity can be introduced in a “square root law” enabling the relation between time and the resistivity. Thus, if using the standard square root law:

$$x = V_{CO_2,Cl} \cdot \sqrt{t} = \sqrt{2 \cdot D \cdot t} \quad (10)$$

Where x = depth of carbonation or chloride threshold penetration and t = time life. The model based in the resistivity was proposed (Calleja, 1953) by substituting the value of D by expression 7 which gives:

$$x = \sqrt{2 \cdot \frac{k}{\rho} \cdot t} \quad (11)$$

Based in this relation, a complete model has been developed (Calleja, 1953). For the sake of summarizing it is presented in equation 12 and equation 13:

$$t_l = t_i + t_p = \frac{x_i^2}{V_{CO_2,Cl}} \quad (12)$$

$$t_l = \frac{x^2 \cdot \rho_{ef}}{k_{Cl,CO_2}} \quad (13)$$

Where:

t_i = initiation period

t_p = propagation period

ρ_{ef} = effective resistivity (at 28 days of wet curing)

$k_{CO_2, Cl}$ = environmental factor depending on exposure class

Knowing the value of the resistivity in the same specimen than that used for mechanical strength at 28 days, this model enables the calculation of the time to corrosion and the corrosion propagation period, if some information on the reaction ability of the cement phases and the aging factor are known.

4.2 Consideration of chloride reaction and other factors

As has been mentioned, the ability of resistivity to quantify diffusivity is based in one of the Einstein laws which relates the movement of electrical charges to the conductivity of the medium (Andrade, 1993; Andrade et al, 1993; Andrade, 2004; Garboczi, 1990) (see equation 3). This expression only accounts for the transport of the chloride ions through the pore network which is insufficient to characterize the transport through concrete where reaction of chlorides takes place and this reaction and the hydration make to evolve the porosity. Then some factors have to be applied to equation 3 to account for these effects together with the value of the k factor which takes into account the concentration of the chloride or aggressive substance.

The factors introduced in the equation 3 have been:

- k has been named “environmental factor”. It depends on chloride concentration and in the case of carbonation, on the concrete moisture content (Andrade, 1993; Andrade, 2004)
- r_b “retarder or reaction factor” (Andrade et al, 2014) which multiplies the resistivity to account for the “retarder” effect of chloride binding during penetration of chlorides. It can also be applied to the case of carbonation. This is due to carbonation progresses when the concrete is partially saturated. That is, as higher is the porosity or the empty pores due to dry conditions, higher the carbonation depth will be but a certain moisture level is necessary for the carbonation reaction to proceed.
- Finally, the “aging factor” q (Andrade, Castellote, D’Andrea, 2011) which accounts for the evolution with time of the porous microstructure.

These factors have been quantified to introduce them in an expression linking resistivity with time that will be described later.

Environmental factor F

The environmental factors F_{Cl} and F_{CO_2} depend on the exposure conditions (Andrade, 1993; Andrade, 2004). Table 2 presents values that were calculated by inverse analysis of test results obtained on real structures.

Table 2. Values of environmental factors, k_{Cl} and k_{CO_2} , following the exposure classification of EN206

Exposure class	F (cm ³ Ω/year)
X0,XC1,XC2	200
XC3 moderate humidity	1000
XC4 cycles wet and dry	3000
XS1 (d > 500 m distance to the coast line)	5000
XS1 (d < 500 m distance to the coast line)	10000
XS2 submerged	17000
XS3 tidal	25000

Reaction factor r_b

The reaction factors r_{Cl} and r_{CO_2} (Andrade et al, 2014) depend on the type and amount of cement and therefore on the reaction of the penetrating substance with the cement phases. Equation 3 can be expressed as:

$$D_{CO_2} = \frac{F_{Cl,CO_2}}{\rho_{ef} \cdot r_{Cl,CO_2}} \tag{14}$$

The values can be calculated either by direct measurement, or indirectly by measuring the relation between the effective and apparent diffusion coefficients, or by calculation based on the cement composition. Table 3 presents examples of r_{Cl} values that were calculated based on test results obtained by comparing steady and non-steady diffusion coefficients.

Table 3. Examples of values of the reaction factor of chlorides, r_{Cl} , for 3 types of cement

Cement	r_{Cl}	Standard Deviation
CEM I	1.9	1.3
CEM I + silica fume	1.5	0.5
CEM IIA (with pozzolan and fly ash, in ≤ 20%)	3.0	2.1

Aging Factor q

It accounts for the refinement of the concrete pore system results in an increase of resistivity with time (Andrade, Castellote, D’Andrea, 2011). The resistivity evolves with time due to the progression of hydration, the combination of the cement phases with the chlorides or carbon dioxide which usually decreases the porosity and by the concrete drying out (depending on the environment. It can be calculated through the expression 15.

$$\rho_t = \rho_0 \left(\frac{t}{t_0} \right)^q \tag{15}$$

Where:

ρ_t = resistivity at any age t

ρ_0 = resistivity at the age of the first measurement t_0

Values of q found for different cement types are given in table 4.

Table 4. Values of the ageing factor

Cement	q	Standard Deviation
I	0.22	0.01
II/A -P	0.37	0.06
II/A-V	0.57	0.08

The relation between q and the aging factor n of the diffusion coefficient gives the expression 23:

$$q = 0.8 n \tag{16}$$

4.3 Propagation period

In the case of considering the propagation of corrosion (t_p), considering the loss in rebar diameter, or pit depth, (P_{corr}) as the limit corrosion attack, the service life of structure can be written by the expression 9:

$$I_{corr} \left(\frac{\mu A}{cm^2} \right) = \frac{K_{corr}}{\rho_{ef} (Kohm.cm)} \tag{17}$$

The relation for the service life prediction can be then formulated as follows (16):

$$t_l = \frac{P_{corr} \cdot \left(\rho_{ef} \left(\frac{t}{t_0} \right)^q \cdot W_s \right)}{K_{corr} \cdot 0.00116} \tag{18}$$

Where:

P_{corr} = steel cross section reached at the time t_p

ρ_{ef} = resistivity at 28 days in saturated conditions

q = aging factor of the resistivity (Table 4)

ξ = environmental factor of the corrosion rate (it can be of 10 ± 2 for carbonation and 30 ± 5 for chlorides)

K_{corr} = constant with a value of $26 \mu\text{A}/\text{cm}^2 \cdot \text{k}\Omega \cdot \text{cm} = 26 \text{ mV}/\text{cm}$ relating the resistivity and the corrosion rate I_{corr}

Complete expression of the service life model based in the resistivity.

Then, the final expression of the service life model based on resistivity is:

$$t_l = t_i + t_p = \frac{x_i^2}{V_{CO_2,Cl}} + \frac{P_{corr}}{V_{corr}} \quad (19)$$

$$t_l = \frac{x^2 \cdot \rho_{ef} \left(\frac{t}{t_0}\right)^q}{F_{Cl,CO_2}} \cdot r_{Cl,CO_2} + \frac{P_{corr} \cdot \left(\rho_{ef} \cdot \left(\frac{t}{t_0}\right)^q \cdot W_s\right)}{K_{corr} \cdot 0.00116} \quad (20)$$

Example of application

For the initiation period the application of the above theory can be shown by way of example, assuming a concrete with a cover depth of 4 cm made with cement type I with silica fume (reaction factor = 1.5 and aging factor = 0,22) to be placed in exposure class XS3 (tidal and splash conditions). Considering a service life of 100 years, the values of the reaction, as well as the environmental and aging factors are presented in Table 5. The calculations indicate that the resistivity needed at 28 days of age, measured in saturated conditions, is 215 $\Omega \cdot \text{m}$.

Table 5. Input data for a calculation of the concrete resistivity

Cement type I with silica fume	$r_{Cl} = 1,85$
Exposure class (XS3)	$F (\text{cm}^3\Omega/\text{year}) = 25000$
Service life	$t (\text{years}) = 100$
Cover depth	$X_{Cl} (\text{cm}) = 4$
Ageing factor during 10 years	$q = 0.22$

$$4 = \sqrt{\frac{25000}{\rho_0 \left(\frac{100}{0.0767}\right)^{0.22} \cdot 1.5}} \cdot 100 \} \rho_0 (\Omega \cdot \text{cm}) = 21497 \rightarrow \rho_0 (\Omega \cdot \text{m}) = 215$$

With this resistivity the length of the propagation period following Table 6 is:

Table 6. Input data for the propagation period

Limit Diameter loss, P_{corr}	$100 \mu\text{m} = 0.01 \text{ cm}$
ρ_{ef} at 28 days	21.5 Kohm.cm
q applied during 100 years	0.22
W_s in saturated conditions	1

$$t_l = \frac{0.01 \cdot \left(21.5 \cdot \left(\frac{100}{0.0767} \right)^{0.22} \cdot 1 \right)}{26 \cdot 0.00116} = 34.54 \text{ years}$$

This propagation period may be included in the 100 years or considered apart as an additional safe time until cracking is produced.

5. PRODUCTION OF CONCRETE FOR A SPECIFIED APPARENT RESISTIVITY

Once known the resistivity which is needed to reach a nominal service life, it remains to describe how the concrete producer can design a mix to fulfil the service life specification. This can be done (Andrade and D'Andrade, 2010) by considering a modification of Archie's law linking resistivity and porosity:

$$\rho_{28d} = \rho_o \cdot \varepsilon^{-\tau} \quad (21)$$

where ρ_{28d} is the resistivity of concrete under saturated condition at 28 days, τ is the tortuosity coefficient which is estimated by fit to the experimental data, and ε is the total porosity.

The coefficient τ depends on the concrete composition which is identified to the tortuosity, and could be determined from type or family of cement type by means of measuring the porosity and the resistivity. The values found in present research are. For type I cement $\tau= 1.9$, for type II-AV $\tau= 2.3$ and for type II AP $\tau= 1.6$.

From the specified resistivity the paste porosity can be obtained and through Power's relation on porosity and w/c ratio

$$\varepsilon_p (\% \text{volumen}) \approx \frac{\left(\frac{w}{c}\right) - 0,36\alpha}{\left(\frac{w}{c}\right) + 0,32} \times 100 \quad (22)$$

To use ρ_p in the model based on Archie's law, it must convert the porosity of the paste (ρ_p) to porosity of the concrete (ρ). For this, it is applied a simple method based on multiplying the percentage of capillary porosity of the paste by the volume of paste (γ) in the concrete.

$$\varepsilon = \varepsilon_p \cdot \gamma \quad (23)$$

It is feasible to prepare a mix with the needed effective resistivity at 28 days, providing the consideration of the type of cement and its retarder factor. The concrete producer should verify by testing the reaching of the specified resistivity while the cement producer should give the retarder factor of his cements.

So, the following concrete design methodology based on Archie's law model is proposed to achieve the prescribed value ρ_{28d} :

1. Select a type of cement. It fixes the values of reaction factor (r) and tortuosity (τ) are defined.
2. Select a w/c ratio and calculate porosity of the paste following Powers' model

3. Then calculate the expected resistivity through $\rho = \rho_o \cdot (\varepsilon_p \cdot \gamma)^{-\tau}$.

6. FINAL COMMENTS

Concrete is a very complex material but which is placed on site in many manners by relatively simple practices. It needs to be modelled by sophisticated models, but also by simple ones which could help to improve the quality and spread the tools for it. The electrical resistivity, being a non-destructive method simplifies very much the control of the durability. On the other hand, it enables multiple applications in concrete technology and the quantification of the expected life. It has been summarized some of the possible applications of the concrete electrical resistivity values. Its main advantage is that the measurement is non-destructive and the concrete can be monitored. Concrete resistivity is able to inform on:

- Porosity
- Degree of water saturation
- Degree of curing
- Cement setting time
- Concrete mechanical strength
- Reinforcement corrosion rate
- Gas and water permeability

In present paper is shown the fundamental relations of resistivity with diffusivity and with the reinforcement corrosion rate. Resistivity is the parameter enabling to link microstructure with the macro-performance Also has been summarized the model for service life prediction based in Einstein law relating electrical resistance or conductance with the diffusion coefficient. Making certain assumptions this basic law can be applied to the advance of carbonation front or chloride threshold, and to the representation of steel corrosion propagation. This model can be used for calculating cover thicknesses from actual resistivity values or the minimum resistivity for a certain cover thickness.

7. ACKNOWLEDGEMENTS

The authors would like to acknowledge the financing of the Ministry of Science and Innovation for the INGENIO 2010-CONSOLIDER Project on “Safety and Durability of Structures: SEDUREC”.

8. REFERENCES

- Andrade, C. (1993), *Calculation of chloride diffusion coefficients in concrete from ionic migration measurements*. Cement and Concrete Research, Volume 23, Issue 3, pp. 724-742. [https://doi.org/10.1016/0008-8846\(93\)90023-3](https://doi.org/10.1016/0008-8846(93)90023-3)
- Andrade, C. (2004), “*Calculation of initiation and propagation periods of service-life of reinforcements by using the electrical resistivity*”. International RILEM Symposium on Concrete Science and Engineering: A Tribute to Arnon Bentur, 22-24, RILEM Publications SARL.
- Andrade, C., Bolzoni F., Fullea, J. (2011), *Analysis of the relation between water and resistivity isotherms in concrete*, Materials and Corrosion, 62, no.2 130-138, <https://doi.org/10.1002/maco.201005777>
- Andrade, C., Castellote, M., D’Andrea, R. (2011) *Measurement of ageing effect of chloride diffusion coefficients in cementitious matrices*, Journal of Nuclear Materials, Volume 412, Issue 1, pp 209-216. <https://doi.org/10.1016/j.jnucmat.2010.12.236>

- Andrade C., D'Andréa, R. (2010), *Concrete mix design based on the electrical resistivity- 2nd International Conference on Sustainable Construction Materials and Technologies*. Ancona- Italy June. Ed. Coventry University UK.
- Andrade, C., D'Andrea, R., Rebolledo, N. (2014), “*Chloride ion penetration in concrete: The reaction factor in the electrical resistivity model*”, *Cement and Concrete Composites*, Volume 47, pp 41-46, <https://doi.org/10.1016/j.cemconcomp.2013.09.022>
- Andrade, C., Fullea, J., Alonso, C. (2000), *The use of the graph corrosion rate-resistivity in the measurement of the corrosion current- Proceedings of the International Workshop on “Measurement and interpretation of the on-site corrosion rate*. MESINA- RILEM Proc. No. 18. Ed. C. Andrade, C. Alonso, J. Fullea, J. Polimon and J. Rodriguez. Rilem Publications S.A.R.L. 157-166.
- Andrade C., Fullea J., Alonso C. (2000b), *The use of the graph corrosion rate-resistivity in the measurement of the corrosion current- Proceedings of the International Workshop on “Measurement and interpretation of the on-site corrosion rate*. MESINA- RILEM, Proc. No. 18. Ed. C. Andrade, C. Alonso, J. Fullea, J. Polimon and J. Rodriguez. Rilem Publications S.A.R.L. 157-166.
- Andrade, C. and González, J. A. (1978), *Quantitative measurements of corrosion rate of reinforcing steels embedded in concrete using polarization resistance measurements*, *Materials and Corrosion*, Volume 29, Issue 8, 515. <https://doi.org/10.1002/maco.19780290804>
- Andrade, C., Zuloaga, P., Martinez, I., Castillo, A., Briz, S. (2011), *Effect of temperature on the corrosion parameters and apparent activation energy measured by embedded sensors in a pilot container in “el Cabril” repository*. *Corrosion Engineering, Science and Technology: The International Journal of Corrosion Processes and Corrosion Control*, Vol 46, No 2, pp 182-189. <https://doi.org/10.1179/1743278211Y.0000000007>
- Andrade. C., Alonso, C., Goñi, S. (1993), *Possibilities for electrical resistivity to universally characterize mass transport processes in Concrete*. *Concrete 2000: Economic and Durable Construction Through Excellence*, V. 2, R.K. Dhir and M.R. Jones, eds., E&FN Spon, Cambridge, pp. 1639-1652.
- Archie, G. E. (1942), “*The electrical resistivity log as an aid in determining some reservoir characteristics*” *Transactions of the AIME*. 146, 54. <https://doi.org/10.2118/942054-G>
- Calleja, J. (1953), *Determination of settings and hardening time of high-alumina cements by electrical resistance techniques*. *Journal of ACI*, vol 25, pp. 249
- Dhir, R. K., Jones, M. R. (1999), “*Development of chloride-resisting concrete using fly ash*”, *Fuel*, Volume 78, Issue 2, pp. 137-142
- Garboczi, E. J. (1990), “*Permeability, Diffusivity and Microstructural Parameters: A Critical Review*”, *Cement and Concrete Research*, Volume 20, Issue 4, pp. 591-601. [https://doi.org/10.1016/0008-8846\(90\)90101-3](https://doi.org/10.1016/0008-8846(90)90101-3)
- Gjorv, O. E., Vennesland, O., El-Busaidy, A. H. S. (1986), *Diffusion of Dissolved Oxygen Through Concrete*, *Materials Performance*, Vol. 25, No. 12, December, pp. 39-44
- González, J. A., Algaba, S., Andrade, C. (1980), *Corrosion of reinforcing bars in carbonated concrete*, *British Corrosion Journal*, Volume 15, Issue 3. <https://doi.org/10.1179/bcj.1980.15.3.135>
- Gouda, V. K., Monfore, G. E. (1965), *A rapid method for studying corrosion inhibition on steel in concrete*. *Journal PCA*, vol 7 n. 3, pp. 24.
- Hammond, E., Robson, T. D. (1955), *Comparison of electrical properties of various cements and concretes*. *The Engineer*, vol 199, pp. 78-80 and pp. 114.115.
- McCarter, W. J., Garvin, S., (1989) “*Dependence of Electrical Impedance of Cement-Based Materials on their Moisture Condition*”, *Journal of Physics D Applied Physics*, Vol. 22 (11), pp. 1773 – 1776.
- Monfore, G. E. (1968), *The electrical resistivity of concrete*. *Journal P.C.A. Applied Research Sectlon*. pp. 35.

- Lambert, P., Page, C. L., Vassie, P. R. W. (1991), “*Investigations of reinforcement corrosion, 2: Electrochemical monitoring of steel in chloride-contaminated concrete*”, *Materials and Structures*, 24 (5), pp. 351-358. <https://doi.org/10.1007/BF02472068>
- Page, C. L., Treadaway, K. W. J. (1982), *Aspects of the electrochemistry of steel in concrete*. *Nature* 297, pp. 109-115. <https://doi.org/10.1038/297109a0>
- Tang, L. (1996), *Chloride Transport in Concrete – Measurement and Prediction*, Chalmers University of Technology, Dept. of Building Materials. ISSN: 1104-893X

A holistic conceptual approach to concrete service life: a split into different time-stages

P. Castro-Borges^{1*} , P. Helene² 

*Contact author: pcastro@cinvestav.mx

DOI: <http://dx.doi.org/10.21041/ra.v8i3.324>

Reception: 15/06/2018 | Acceptance: 29/08/2018 | Publication: 31/08/2018

ABSTRACT

The goal of this paper is to analyze and discuss a conceptual approach that considers the holistic character of concrete service life but splits it into seven time-stages that can be compared, for understanding purposes, with those of a human being. The existing concepts about service life may be incomplete regarding those that must consider the whole life of a concrete structure. One of the reasons for this is the lack of certainty of the service life predictions which are based on models that consider a series of non-clearly defined time-stages. The life of a structure has many similarities with that of a human being. In fact, it is no coincidence that engineering has adopted some terms from the medical sciences like “pathology” to refer to structures with problems of “health”. The paper discusses the overlapping of the different time-stages as well as the reasons why the prediction models can fail.

Keywords: service life; durability; structure.

Cite as: P. Castro-Borges, P. Helene (2018), “A holistic conceptual approach to concrete service life: a split into different time-stages”, Revista ALCONPAT, 8 (3), pp. 280-287, DOI: <http://dx.doi.org/10.21041/ra.v8i3.324>

¹ Centro de Investigación y Estudios Avanzados del IPN Unidad Mérida, Carretera Antigua a Progreso, Km 6, 97310, Mérida, Yucatán, México.

² University of Sao Paulo, Escola Politécnica, Av. Prof. Almeida Prado, trav 2, 83 SP 05508-900, Brazil.

Legal Information

Revista ALCONPAT is a quarterly publication by the Asociación Latinoamericana de Control de Calidad, Patología y Recuperación de la Construcción, Internacional, A.C., Km. 6 antigua carretera a Progreso, Mérida, Yucatán, 97310, Tel.5219997385893, alconpat.int@gmail.com, Website: www.alconpat.org

Responsible editor: Pedro Castro Borges, Ph.D. Reservation of rights for exclusive use No.04-2013-011717330300-203, and ISSN 2007-6835, both granted by the Instituto Nacional de Derecho de Autor. Responsible for the last update of this issue, Informatics Unit ALCONPAT, Elizabeth Sabido Maldonado, Km. 6, antigua carretera a Progreso, Mérida, Yucatán, C.P. 97310.

The views of the authors do not necessarily reflect the position of the editor.

The total or partial reproduction of the contents and images of the publication is strictly prohibited without the previous authorization of ALCONPAT Internacional A.C.

Any dispute, including the replies of the authors, will be published in the second issue of 2019 provided that the information is received before the closing of the first issue of 2019.

Un enfoque conceptual holístico para la vida de servicio del concreto: división en diferentes etapas de tiempo

RESUMEN

El objetivo de este documento es analizar y discutir un enfoque conceptual que considera el carácter holístico de la vida de servicio concreta, pero lo divide en siete etapas de tiempo que se pueden comparar, para fines de comprensión, con las de un ser humano. Los conceptos existentes sobre la vida útil pueden ser incompletos con respecto a aquellos que deben considerar toda la vida de una estructura concreta. Una de las razones para esto es la falta de certeza de las predicciones de la vida útil que se basan en modelos que consideran una combinación de etapas de tiempo no claramente definidas. La vida de una estructura tiene muchas similitudes con la de un ser humano. De hecho, no es coincidencia que la ingeniería haya adoptado algunos términos de las ciencias médicas como "patología" para referirse a estructuras con problemas de "salud". El documento analiza la superposición de las diferentes etapas de tiempo, así como las razones por las que los modelos de predicción pueden fallar.

Palabras clave: vida de servicio; durabilidad; estructura.

Uma abordagem conceitual holística para a vida útil das estruturas de concreto: divisão em diferentes estágios de tempo

RESUMO

O objetivo deste artigo é analisar e discutir uma abordagem conceitual que considere o caráter holístico da vida útil das estruturas de concreto, dividida em sete estágios de tempo que podem ser comparados, para fins de compreensão, com os de um ser humano. Os conceitos existentes sobre a vida útil podem estar incompletos em relação àqueles que devem considerar toda a vida de uma estrutura de concreto. Uma das razões para isso é a falta de certeza das previsões de vida útil baseadas em modelos que consideram uma mistura de estágios não claramente definidos. A vida de uma estrutura tem muitas semelhanças com a de um ser humano. De fato, não é coincidência que a engenharia tenha adotado alguns termos das ciências médicas como "patologia" para se referir a estruturas com problemas de "saúde". O artigo discute a sobreposição dos diferentes estágios de tempo, bem como as razões pelas quais os modelos de previsão podem falhar.

Palavras-chave: vida útil; durabilidade; estrutura.

1. INTRODUCTION

The introduction of parameters to define service life of concrete as a holistic concept has been very common during the last thirty years. These parameters are more quantitative today than a few years ago and include concepts which are closely related, like serviceability, functionality, security, reliability and durability. Service life has been defined in codes, standards and articles by many authors. Each author or code has own reasons to propose modifications and inclusions to the definition. Three of the most common definitions of service life, as defined by certain organizations, are given below:

- a) American Concrete Institute: the period of time after installation, during which all the properties exceed the minimum acceptable values when routinely maintained (ACI-365, 200).
- b) DURAR Network: the period of time during which the structure conserves the project requirements in security, functionality and aesthetics, without unexpected maintenance cost (Troconis et al, 1998)

- c) Construction Products Directive (CPD): the period of time during which the performance of the works will be maintained at a level compatible with the fulfillment of the essential requirements (E. Community, 1989).
- d) APROY-NMX-C-530-ONNCCE (2017): Es el tiempo durante el cual el desempeño de un material, elemento o estructura de concreto conserva las características del proyecto en términos de seguridad (resistencia mecánica y estabilidad, seguridad en caso de fuego, seguridad en uso), funcionalidad (higiene, salud y medio ambiente, protección contra el ruido y ahorro energético y confort térmico) y estética (deformaciones, agrietamientos, desprendimientos), con un mínimo de mantenimiento que le permita soportar los efectos ambientales y naturales en su entorno durante su uso.

Although apparently similar, these concepts of service life have differences and do not consider a split into time-stages during which some specific and particular phenomena occur. These particular phenomena like cracking, carbonation, chloride movement, etc., can have different effects according to determined time-stages like beginning or end of service life. Then, modelling and prediction of behaviour must correspond to specific time-stages unless we know exactly how their specific behaviour could be at any time-stage.

This may be the reason why extrapolation of predictions from deterministic, semi-probabilistic or probabilistic models to different time-stages cannot be accurately and completely verified. In other words, the service life of concrete should be divided into different time-stages where the material is exposed to different circumstances besides ageing. Each time-stage is defined as the specific time where the specific materials and environmental effects may be known, without circumstances that could be attributed to other time-stages and then to affectation of predictions from quantitative models.

On the other hand, we still need to understand the concept of service life as a ‘whole life’ concept and as the way we see our own existence as human beings. In fact, we use some concepts in engineering such as “pathology” that are adopted from the medical sciences to refer to problems of “health” of the structure. The objective of this paper is to discuss an approach that considers the holistic character of concrete service life, but splits it into seven time-stages that can be compared, for understanding purposes, with those of a human being. The paper discusses the overlapping of the different time-stages as well as the reasons why the prediction models can fail.

2. SOME ASPECTS ABOUT THE EVOLUTION OF SERVICE LIFE MODELS

Probably one of the most important approaches to service life has been that provided by Tuutti’s model in 1982 (Tuutti, 1982). This model was the first one to propose two stages for the service life: initiation and propagation. Much of the present knowledge to prevent damage and to repair structures is based on this conceptual model. New materials, the aggressiveness of the environment and the new construction techniques have made improvements to Tuutti’s model necessary.

The inclusion of the total amount of damage as well as specific stages like inspection, diagnosis, prognosis, repair and maintenance options were introduced in 1994 by Andrade (Andrade, 1994). In 1996 (Sarja and Vesikari, 1996), several levels of models were proposed to include elements such as materials or complete buildings. The help of deterministic models to predict the programmed service life was discussed together with the importance of stochastic ones. In 1996, two limit states of depassivation and cracking of concrete were taken into account in the conceptual models. A conceptual model showing distributions of degradation, service life and serviceability limits was also presented in that year (Sarja and Vesikari, 1996). Obsolescence of the structures

was taken into account in the conceptual models during 1997 (Somerville, 1997) and the idea of designing for the final life was introduced.

The need to include new concepts in the service life approaches continued in 1998 (Helene, 2003) when the concept of service life was divided into several parts. Helene (2003) presented the service life stage divided into four specific and overlapped parts. All these approaches have helped to improve the predictions of service life through deterministic or probabilistic models. However, the overlapping of their different stages has complicated the precision of the predictions because many chemical, physical or electro-chemical phenomena can have totally different behaviour in different stages of the service life. Therefore, an approach is needed with defined and not overlapped stages that could allow better service life predictions in any of its stages. In other words, we should not make predictions of service life if we do not know the expected behaviour of all the phenomena during the whole service life, which is practically impossible.

In this regard, the literature has provided several other models with interesting concepts and subdivisions of service life in several stages. However, despite these important contributions, little information has been found dealing with the philosophy with which we should analyse the service life of a structure. Since the term “pathology” has been adapted from the medical sciences to the construction field, it is consistent to speak about “construction pathology problems”. This is familiar to us because of the existing analogies between the medical and the constructional sciences; this is between a human being and structures. Therefore, the following approach considers the similarities of the total life between a human being and a structure.

The best known criteria consider the service life of a structure divided into service life and residual life. In recent years and in coincidence with the appearance of durability problems, total service life was divided into more parts like service life, useful life, residual life and others that apply also for a human being, with some obvious exceptions.

3. ANALOGIES BETWEEN THE SERVICE LIFE OF A HUMAN BEING AND A STRUCTURE

Let us consider the following similarities of the service life stages between a human being and a structure.

The first stage is that of the conception. The conception of a human being is given by the relationship between the couple. In the case of a project, the conception is given by the first discussions about the project and its preparation. Depending on the kind of project, the structure can last for many years. This is the stage where the total life is projected. This stage can be called the project planning of the structure’s total life (stage 1) and includes the structural, architectural and durability design (figure 1). The product of this stage or boundary condition, is the executive project.

The second stage is that of the gestation. This is the time in which the mother gestates the new-born. Some professionals like the gynecologist supervise this stage. The analogy with this stage is given by the construction period of the structure. Following the project specifications with adequate supervision will determine the total life period of the structure. This stage can be called the preparation for the service life (stage 2). The product of this stage, or boundary condition, is the final new structure.

The third stage is that of the delivery. A group of professionals like the gynaecologist, paediatrician and the anaesthesiologist are in charge to receive the new-born and assure good conditions during this period. In terms of a structure, this is the day the structure is placed in service, the in-service day. This is the time when the service life starts and constitutes a specific point of time which is the boundary condition. This stage can be called the initiation of the service life (stage 3).

The fourth stage is that from delivery until adulthood (say, 18 years old). This is a critical stage where the parent's supervision is important to prevent, detect and correct any kind of problem related to mental, emotional or physical health, or accidents that would affect the long-time development of the person. The analogy with this stage is that in which the new structure may or may not receive preventive maintenance to avoid future damage. The duration of this stage will depend on the evident needs for corrective maintenance to the structure. A boundary condition for this stage four can be stated as the moment when the aggressive agents reach the reinforcing bar.

In terms of durability, this can be the so-called corrosion initiation stage, or the so-called service life (stage 4). It will be the period from the in-service day until the day in which the aggressiveness of the environment and/or loads result in direct deterioration of the steel/concrete. This stage must consider just the expected behaviour when the structure is healthy and without showing evident deterioration. The boundary condition here is just before the presence of visual evidences of deterioration may be the sign that the behaviour model prediction has to be modified or changed to include different conditions.

The fifth stage includes adulthood until just before the senior citizen age. This is a maturity period where the right development depends on the person and the right habits during previous stages. Certain aspects about health or emotional problems determine the behaviour or boundary condition at the end of this stage. In terms of durability, this stage corresponds to the propagation period. However, as actually defined, the propagation period finishes when the original ability of the structure to support structural and environmental loads cannot be restored to the structure. In reality, this ability has a high probability of being restored if the structure is adequately repaired/rehabilitated at a certain critical time. This is like cancer that can be cured through a correct and in-time diagnosis.

This stage can be called residual service life (stage 5). It is a stage at which the structure will be useful despite its problems, but only if it receives a correct and in-time treatment. The limit or boundary condition between this and the following stage is given by the fact that not every "medicine", or intervention, will have the desired effect.

The sixth stage may be that from the senior citizen to the instant before dying. In this stage, all the functions of the person must be carefully followed because they can fail due to ageing and previous conditions or effects of life. In the case of a structure, it is the time when any preventive or corrective action cannot restore its expected conditions of functionality, serviceability, durability, load carrying ability, etc. It is this period where the inspector and owner must think about a change of use for the structure boundary condition. Some activities like discharging of some zones, evacuation of people, disassembling of some installations, etc, must be planned prior to the 'death' of the structure. This stage finishes just before the death of the structure and can be called just residual life (stage 6). The boundary condition here corresponds to the moment when the structure is not longer useful.

The seventh and final stage is that of death as a result of failures, collapses or prolonged 'pain'. In the case of a structure, this stage corresponds to the beginning of the partial or total collapse. This stage can be called the end of residual life (stage 7).

Every stage of the conceptual model must be accompanied by some specific tests. The results of a kind of test could mean different interpretation if applied in different stages. As an example, we could think about the permeability test (Basheer, 1993). Permeability values could be different in dependence of the aggressive conditions for the structure during certain stages: applying this test in stage 3 may indicate good concrete, but a better one in stage 4 (because of a longer curing period, etc). NMX-C-530 takes this into consideration.

4. THE NEW APPROACH FOR SERVICE LIFE OF CONCRETE

Figure 1 shows an approach for service life of concrete structures which is based on the best characteristics from other approaches as well as on the described analogies between a structure and a human being, given above. This approach is presented with a similar philosophy but with a division of time-stages which is more in accordance with project planning as well as to future predictions.

The optimum performance is obtained during the first three stages and includes the planning, the preparation, and the in-service day of service life. The minimum condition of service will be maintained only during the fourth stage where preventive maintenance against the ingress of aggressive substances is required. In global terms, the stages five, six and seven are those where the structure is no longer capable of exhibiting acceptable performance. These stages include the residual service life, the residual life and the end of residual life.

5. OVERLAPPING AMONG THE DIFFERENT STAGES

Any of the stages from Figure 1, but particularly the last four, must be analyzed individually when performing service life predictions. The literature has given much importance to stages 4 and 5 because it is thought that the information obtained in such stages is enough to predict the future behaviour. The events of each single time-stage must be interpreted and considered for any prediction because of the influence of the phenomena occurring during previous time-stages. The overlapping of phenomena occurring in different stages can result in misleading predictions.

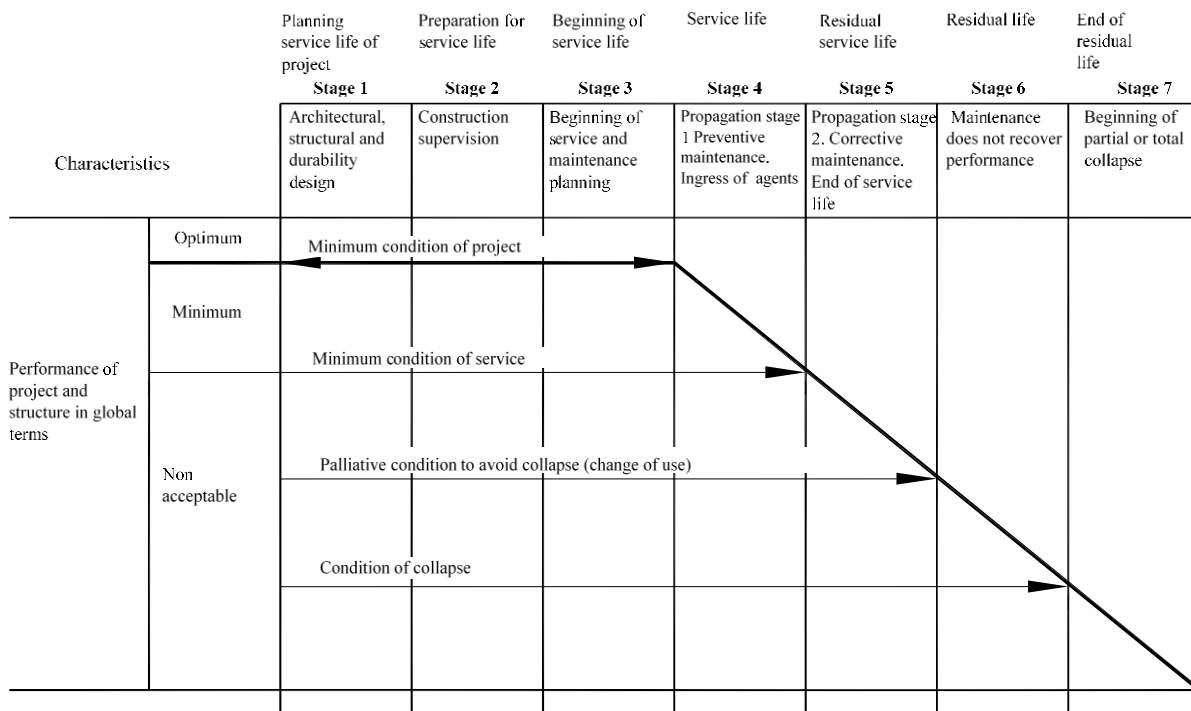


Figure 1. Approach for service life of concrete structures

A simple example is the prediction of the carbonation front or chloride profile adjacent to the reinforcing bar after a few years of exposure to a determined environment. Stage 4, service life, includes the ingress of these agents, but the predictions usually do not take into account stages 5, 6 and 7 where cracking or other phenomena can occur.

This is one of the main reasons why we cannot easily find a valid prediction verification of these phenomena. The best thing in this case is to circumscribe a prediction model to stage 5 and think about modifications or a different one after stage 5. The items included in the seven stages as well as the data needed for predictions will be published elsewhere.

6. EXAMPLE OF APPLICATION OF THE CONCEPTUAL SEVEN STAGE MODEL

The Progreso pier is the oldest reported concrete structure with use of 304 SS. It was designed and constructed by the danish company Christiani and Nielsen. This company thought about a 50 year-service life structure with a minimum of maintenance. Six of the stages of the conceptual model can be easily identified. Several published articles, cited here, can support the use of the conceptual model:

Stage 1.- Planning service life (2 years). The pier was designed to be in service for 50 years. The project preparation lasted about two years.

Stage 2.- Preparation for service life (construction period, 5 years). The structure was constructed between 1936 and 1941.

Stage 3.- Beginning of service life. The structure was inaugurated in 1941

Stage 4.- Service life (60 years). The structure had a satisfactory service from 1941 to 2001, after 60 years in service, when a hurricane (Isidore, 2002) evidenced diverse problems like scour that affected piles, beams and deck.

Stage 5.- Residual service life (15 years). The structure, since then (2002), has been in service thanks to in-time interventions. A new pier was proposed to the ministry of construction, that was finally constructed and inaugurated in 2016. This was the end of stage 5 for the old pier, since most of the strong loads were moved to the new pier.

Stage 6.- Residual life (2 years and counting). Maintenance do not recover original performance and cannot help the pier to sustain the 10 times-increased loads. Then, the use of the pier was modified to allow just part of the original planned loads that are equivalent, nowadays, to touristic cars and trucks, persons and maintenance traffic. In fact, it is having an intervention, to make sure it can sustain a certain percentage of the original loads of design. Under these circumstances, it is expected at least a stage 6 duration of 22 years, that is the complement to have twice the expected initial service life, this means a total of 100 years.

7. CONCLUSION

The contribution of several approaches for service life of concrete structures was discussed. A new approach that takes into account the similarities among the several stages of service life from a human being and concrete structures was proposed. The influence of overlapping service life stages in the predictions of future behaviour was briefly discussed. Based on the new approach, the use of simple prediction models whose results apply to individual stages is recommended.

8. ACKNOWLEDGMENTS

The authors acknowledge their Institutes as well as to CONACYT and CNPq for partial support for this paper and collaboration. The help of M. Balancan with the art work is acknowledged. The opinions expressed here are those of the authors and not necessarily of the supporting organizations.

9. REFERENCES

- American Concrete Institute (2000), “*ACI-365: Service-Life Prediction- State-of-the-Art Report*”.
- Andrade, C. (1994), *Quantification of durability of reinforcing steel, methods and calculation procedures of Concrete technology: New Trends, Industrial Applications*, A. Aguado, R. Gettu and S.P. Shah, Editors. RILEM. Published by E&FN Spon, 2-6 Boundary Row, London SE1 8HN, UK ISBN 0 419 20150 5. pp: 158-175.
- APROY-NMX-C-530-ONNCCE (2017), “*Industria de la construcción – Durabilidad – Norma general de durabilidad de estructuras de concreto reforzado – Criterios y Especificaciones*”.
- Basheer, P. A. M. (1993), *A brief review of methods for measuring the permeation properties of concrete in-situ*, Structures and Buildings, Proceedings of the ICE, vol 99, 74-83. <https://doi.org/10.1680/istbu.1993.22515>
- European Community (1989), “*COUNCIL DIRECTIVE of 21 December 1988 on the approximation of laws, regulations and administrative provisions of the Member States relating to construction products.*”, Off. J. Eur. Communities, vol. 40, no. L, pp. 12–26.
- Helene, P. (2003), *A nova NB 1/2003 (NBR 6118) e a vida útil das estruturas de concreto*, University of Sao Paulo PCC USP.
- Sarja, A., Vesikaeri, E. (1996), *Chapter 7 Durability models*, In *Durability Design of Concrete Structures*. Manuscript of RILEM Report of TC 130-CSL, RILEM Report Series 14. pp: 97-111, E & FN Spon, Chapman and Hall, 165 p.
- Somerville, G. (1997), “*Engineering design and service life: a framework for the future*”, In *Prediction of concrete durability: Proceedings of the STATS 21st anniversary conference /1997*, J. Glanville and A. M. Neville, Editors, pp. 58-76, E & FN Spon, UK.
- Troconis, O., Romero, A., Andrade, C., Helene, P., Díaz, I. (1998), *Manual de inspección, evaluación y diagnóstico de corrosión en estructuras de hormigón armado*, 2nd ed. Red Durar.
- Tuutti, K. (1982), “*Corrosion of steel in concrete*”, Swedish Cement and Concrete Research Institute, Stockholm.

Apparent diffusion coefficient of oxygen and corrosion control of reinforcement rebar coated with primers

E. Pazini Figueiredo^{1*} , C. Andrade² 

*Contact author: epazini@terra.com.br

DOI: <http://dx.doi.org/10.21041/ra.v8i3.336>

Reception: 13/07/2018 | Acceptance: 01/08/2018 | Publication: 31/08/2018

ABSTRACT

The present work evaluates the influence of different primers applied in the reinforcement steel on the apparent diffusion coefficient of oxygen ($D_{ap}(O_2)$) and on the corrosion intensity (I_{corr}), comparing the results with a reference cementitious mortar. Oxygen flow ($J(O_2)$) until the reinforcement steel was measured by potentiostatic method in steady state. The I_{corr} was monitored by the Polarization Resistance technique (R_p). Evaluations related porosity of the primers were made through magnifying glasses, optical microscopy and SEM. Primers that represent barrier protection systems proved to be less permeable to oxygen. The $D_{ap}(O_2)$ values ranged from $2.1 \times 10^{-6} \text{ cm}^2/\text{s}$ to $4 \times 10^{-9} \text{ cm}^2/\text{s}$, causing variation in the I_{corr} due to cathodic control of the corrosion process.

Keywords: reinforced concrete; corrosion control; diffusion of oxygen; primers.

Cite as: Citation: E. Pazini Figueiredo, C. Andrade (2018), " Apparent diffusion coefficient of oxygen and corrosion control of reinforcement rebar coated with primers ", Revista ALCONPAT, 8 (3), pp. 288-300, DOI: <http://dx.doi.org/10.21041/ra.v8i3.336>

¹ Professor Titular da Escola de Engenharia Civil e Ambiental da Universidade Federal de Goiás, Praça Universitária, s/n, Setor Universitário, Goiânia-GO 74.605-220, Brasil.

² International Center for Numerical Methods in Engineering. CIMNE. UPC, Spain.

Legal Information

Revista ALCONPAT is a quarterly publication by the Asociación Latinoamericana de Control de Calidad, Patología y Recuperación de la Construcción, Internacional, A.C., Km. 6 antigua carretera a Progreso, Mérida, Yucatán, 97310, Tel.5219997385893, alconpat.int@gmail.com, Website: www.alconpat.org

Responsible editor: Pedro Castro Borges, Ph.D. Reservation of rights for exclusive use No.04-2013-011717330300-203, and ISSN 2007-6835, both granted by the Instituto Nacional de Derecho de Autor. Responsible for the last update of this issue, Informatics Unit ALCONPAT, Elizabeth Sabido Maldonado, Km. 6, antigua carretera a Progreso, Mérida, Yucatán, C.P. 97310.

The views of the authors do not necessarily reflect the position of the editor.

The total or partial reproduction of the contents and images of the publication is strictly prohibited without the previous authorization of ALCONPAT Internacional A.C.

Any dispute, including the replies of the authors, will be published in the second issue of 2019 provided that the information is received before the closing of the first issue of 2019.

Coeficiente de difusão aparente de oxigênio e o controle da corrosão de armaduras revestidas com primers

RESUMO

O presente trabalho avalia a influência de diferentes revestimentos aplicados nas armaduras sobre o coeficiente de difusão aparente de oxigênio ($D_{ap}(O_2)$) e sobre a intensidade de corrosão (I_{corr}), comparando os resultados com um revestimento de referência (argamassa cimentícia). O fluxo de oxigênio ($J(O_2)$) até a armadura foi medido pelo método potencioestático no estado estacionário. A I_{corr} foi monitorada pela técnica de Resistência de Polarização. Avaliações referentes a porosidade dos revestimentos foram feitas por meio de lupas, microscopia ótica e SEM. Os revestimentos que representam sistemas de proteção por barreira mostraram-se menos permeáveis ao oxigênio. Os valores $D_{ap}(O_2)$ variaram de $2,1 \times 10^{-6} \text{ cm}^2/\text{s}$ até $4 \times 10^{-9} \text{ cm}^2/\text{s}$, ocasionando variações na I_{corr} , devido ao controle catódico do processo de corrosão.

Palavras-chave: concreto armado; controle da corrosão; difusão de oxigênio; primers.

Coeficiente de difusión aparente de oxígeno y el control de la corrosión de armaduras revestidas con primers

RESUMEN

RESUMEN

El presente trabajo evalúa la influencia de diferentes recubrimientos aplicados en la armadura en el coeficiente de difusión aparente de oxígeno ($D_{ap}(O_2)$) y en la intensidad de corrosión (I_{corr}), comparando los resultados con un revestimiento de referencia (mortero cimenticio). El flujo de oxígeno ($J(O_2)$) hasta la armadura se midió por el método potencioestático en estado estacionario. La I_{corr} se controló mediante la técnica de resistencia de polarización. Evaluaciones respecto a la porosidad de los recubrimientos fueron hechas con lupas, microscopio óptico y SEM. Los revestimientos que representan sistemas de protección por barrera han resultado menos permeables al oxígeno. Los valores de $D_{ap}(O_2)$ variaron de $2.1 \times 10^{-6} \text{ cm}^2/\text{s}$ a $4 \times 10^{-9} \text{ cm}^2/\text{s}$, causando variaciones en la I_{corr} debido al control catódico del proceso de corrosión.

Palabras clave: concreto armado; control de la corrosión; difusión de oxígeno; primers.

1. INTRODUCTION

The rebar of the reinforced concrete structures, typically, are protected from corrosion by a passive layer of oxides formed due the high alkalinity of the concrete, which determines the so-called state of passivation of steel reinforcement. This layer protects indefinitely the steel reinforcement of the corrosion, while the concrete preserve your good quality, no cracks and not have physical or mechanical characteristics changed due to the action of aggressive external agents. The passive protection layer is destabilized by the decrease in the pH of the concrete around the reinforcement to values less than 9, due to the carbonation of concrete, or due the penetration of chloride ions through the porosity of concrete, reaching critical limits, leading to despassivation and start corroding. After the passive layer is broken down and triggered the corrosion process, resistivity and temperature of concrete and the flow of oxygen to the surface of the steel rebar are the main controllers factors of the propagation period of corrosion. (Gjorv; Vennesland; El-Busidy, 1986; Andrade et al., 1990; Castelotte et al., 2001; Francinete; Figueiredo, 1997). The reactions of corrosion can be controlled by several factors, according to illustrate the diagrams of Figure 1. These factors change the polarization characteristics of the reinforcement steel.

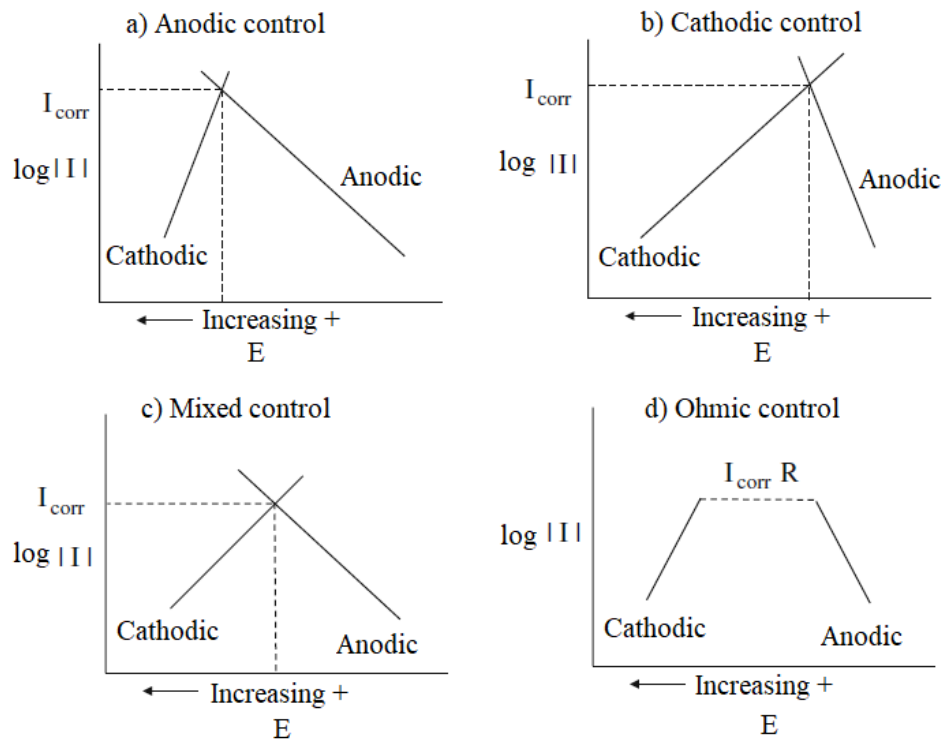


Figure 1. Evans diagram, showing the influence of process of controls anodic, cathodic, mixed and by ohmic resistance about the intensity of corrosion (McCafferty, 2009).

When the polarization occurs mainly at the anode, the corrosion reaction is controlled anodically and the reaction of metal dissolution is diminished. When the resistivity of electrolyte (concrete) is very high, to the point of preventing ion movement, the resulting current is insufficient to polarize the anode and the cathode. In this case, the corrosion reactions are under ohmic resistance control. In practice, the reactions occur in the same intensity at the anode and the cathode and thus has a mixed control. The cathodic control occurs when the oxygen reduction reaction (Equation 1) is constrained by the reduction in oxygen access to the cathodic region, limiting the consumption of electrons from the anode region and, consequently, controlling the kinetics of corrosion.



The presence of oxygen on the surface of the reinforcement steel is essential for reduction reactions occur in the cathodic areas. The oxygen diffusion coefficient in concrete is a concrete property very important and determinant on durability of reinforced concrete structures (Page; Lambert, 1987; Helene, 1993; Hansson, 1993). In some study, the measured oxygen flow is used to predict the durability of the steel reinforcement, based on the relationship between the anodic dissolution, or corrosion, and the amount of oxygen that can be reduced in cathodic areas (Andrade et al., 1990). Kobayashi e Shutton (1991) e Tuutti (1982) studied the influence of the water/cement ratio, the thickness of the covering, the air humidity and the saturation degree of the concrete pores, the presence of mineral additions to cement and concrete curing conditions on the diffusion of oxygen through the concrete.

Restricting the access of oxygen to the steel reinforcement is one of the performance requirements that the coatings applied to the steel reinforcement, or even repair mortars and paints of surface protection, must meet in order to fulfill with efficiency the functions of preservation and restoration of protection and control of reinforcement corrosion.

The measurement of the apparent diffusion coefficient of oxygen ($D_{ap}(O_2)$) through of the concrete covering or through the coatings applied to the steel reinforcement, show the conditions of oxygen supply to the cathodic regions that regulate corrosion kinetics in the anodic regions. Currently, to compose a repair system of concrete structures attacked by corrosion, the technical means has an ample variety of coatings (primers) that are applied on the steel reinforcement. The mechanisms of protection exercised by these coatings can be for barrier, repassivation, inhibition and cathodic protection. In practice usually occurs the joint action of two or more protection mechanisms (Figueiredo, 1994).

The knowledge of the composition and properties of primers (coatings) that are directly related to the ability of protection and control of corrosion is important to the overall assessment of the performance of the primers. Such information is also important for the designers of repairing can choose the products most appropriate for a given situation. Therefore, the present study aims to assess the influence of five different types of coatings, specified for protection of steel reinforcement, on the apparent diffusion coefficient of oxygen ($D_{ap}(O_2)$) and on the intensity of corrosion (I_{corr}), in comparison to a reference coating composed of a cement-sand mortar.

2. EXPERIMENTAL PROGRAM

2.1 Materials and specimens

For the realization of the experiment were casting prismatic mortar specimens in the dimensions 20 mm x 55 mm x 80 mm. The reference mortar was produced with cement/sand ratio of 1/3 and water/cement ratio of 0.50, both in mass. In the mixing water was mixed 3% $CaCl_2$, in relation to the cement mass, to promote the despassivation of steel reinforcement. The cement used was a high early strength. Table 1 shows the chemical and mineralogical composition and physical and mechanical characteristics of Portland cement used to produce the specimens.

Table 1. Mineralogical and chemical composition and physical and mechanical characteristics of employee cement in experiments.

Chemical Composition	Results (%)
CaO	61,34
SiO ₂	18,32
Al ₂ O ₃	5,43
Fe ₂ O ₃	3,28
SO ₃	3,04
MgO	1,51
K ₂ O	1,04
Na ₂ O	0,15
Cl ⁻	0,02
P.F.	3.13
R.I.	1,92
Mineralogical Composition	Results (%)
C ₃ S	60,54
C ₂ S	6,85
C ₄ AF	9,98
C ₃ A	8,84
Mechanical Characteristics	Results (MPa)
Compressive Strength (3 days)	27,8
Compressive Strength (28 days)	59,1

Table 3. Characteristics of the primers (coatings) studied provided by manufacturers.

Primer	Composition	Number of Components	Wet thickness (μm)	Density δ (kg/l)	pH
1	Cement + thermoplastic polymer + special loads	2	1000 a 2000 (applied in 2 coats)	1,90	> 10
2	Cement + thermosetting polymer + inhibitor ($\text{Ca}(\text{NO}_2)_2$)	3	1000 a 2000 (applied in 2 coats)	2,00	N.E.
3	Epoxy + zinc	1	135 μm /demão (applied in 2 coats)	2,00	N.E.
4	Epoxy	2	N.E.	N.E.	N.E.
5	Polymer + lead	1	300 μm (applied in 3 coats)	1,36 \pm 0,05	9,4 \pm 0,2

N.E. (Not specified)

After casting, the specimens was stored in chamber of 100% relative humidity, remaining in this condition for more than 100 days. In the second stage, until the time of the implementation of the measures, the specimens were provided partially submerged, in order to promote the reinforcement corrosion. The measures of oxygen flow (J (O₂)) were made when the specimens completed 1 year.

2.2 Experimental methodologies and evaluations

The oxygen flow through a material is influenced by your thick and interconnectivity of your porous network. In this sense, were made measurements of the thickness of each coat and the total thickness of the wet applied coatings (fresh state), employing a fresh film thickness gauge on a glass plate, as shown in Figure 3. The dry thickness of the primers, the estimate of the size of the pores and your interconnectivity were evaluated by means of magnifying glass, optical microscopy and scanning electron microscopy (SEM). The magnifying glass with increased 4 times was employed to identify surface defects of dry films. These evaluations were also important to detect by comparing possible changes existing surface after the end of the tests and rupture of the specimens. When on the surface were detected imperfections, with suspicion that could have continuity and reach the steel reinforcement, made use of the stereomicroscopic to observe and photograph the defects with more details. At various times, to enter through the defect or surface porosity of the second coat, it was possible to identify the presence of primer from the first coat, reaching the conclusion that the pore no continuity. In this sense it is evident the importance of number of coats to the coating adhere your barrier function. Microscopy allowed estimating pore size and the thickness of hardened coatings, identify elements and semi quantitative composition and observe the presence of resin within the porosity, in order to interrupt the continuity of the pores. While the thickness and porosity of coatings are associated with barrier protection mechanism of the steel rebar, the high pH value of coatings is key to activate the repassivation protection mechanism (FIGUEIREDO, 1994). The pH of the coatings was measured with equipment having glass and calomel electrodes combined with pH range 0 to 14. Ph measurements were obtained 15 minutes after mixing of components of coatings.

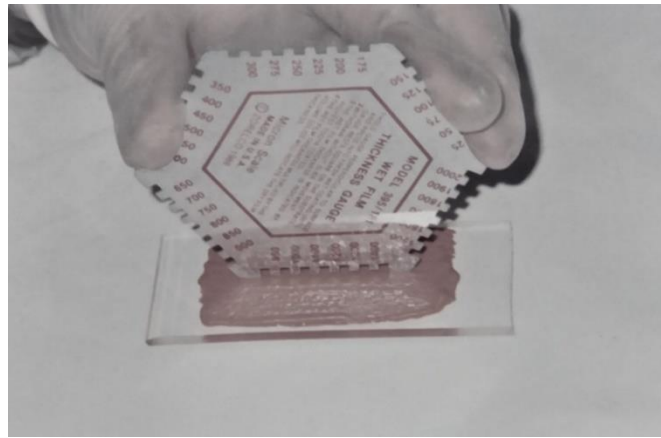


Figure 3. Measurement of thickness of the primer 1 newly applied (wet thickness).

The corrosion intensity (I_{corr}) was measured by Polarization Resistance technique, where a polarization of ± 10 mV around of the corrosion potential (E_{corr}) was applied and the ohmic drop of the covering was compensated by means of the positive feedback of the potentiostat between the working electrode (reinforcement steel) and the reference electrode (calomel electrode saturated). Intensity changes resulting from the application of potential difference were determined with at a sweep rate of 10mV/min. Corrosion intensity (I_{corr}) was calculated using the equation of STERN and GEARY (1957).

To determine the oxygen flow to the surface of the steel rebar inside of the specimen, was measured the cathodic current (I_{cat}) at a constant potential-750 mV relative to the saturated calomel electrode (ECS). At this level of potential the only reaction possible is the cathodic reduction of oxygen (GJORV et al., 1986; ANDRADE et al., 1990). Cathodic intensity (I_{cat}) was measured when the cathodic current versus time curve reached the so-called steady state. After 24 hours of test it was possible to verify that all the reinforcement coated found their stationary states, as shown in Figure 4.

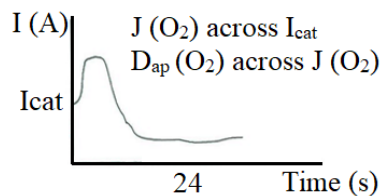


Figure 4. Typical curve of the cathodic current versus Time obtained in the tests carried out.

With the value of the I_{cat} as steady-state applied to Faraday's law to get the oxygen flow $J(O_2)$ until the reinforcement steel.

$$J(O_2) = \frac{I_{cat}}{n \cdot F} \quad \text{(Equation 2) (GJORV et al, 1986)}$$

onde,

$J(O_2)$ → oxygen flow in mol/second;

I_{cat} → cathodic current intensity in the steady-state in amper (A);

n → number of electrons consumed (4);

F → Faraday constant (96500 coulomb/mol).

From the oxygen flow ($J(O_2)$), and using the first Fick's law, it has been calculated the apparent diffusion coefficient of oxygen ($D_{ap}(O_2)$).

$$D_{ap}(O_2) = \frac{J(O_2) \cdot e}{S \cdot C_0} \quad (\text{Equation 3}) \quad (\text{PAGE; LAMBERT, 1987})$$

Onde:

- $D_{ap}(O_2)$ → apparent diffusion coefficient of oxygen in cm^2/s ;
- $J(O_2)$ → oxygen flow in mol/s ;
- e → thickness of the covering in cm (0,7 cm);
- S → study area in cm^2 (5,6 cm^2);
- C_0 → oxygen concentration in a saturated solution of $\text{Ca}(\text{OH})_2$ in mol/cm^3 (1,06 x 10⁻⁶ mol/cm^3 , in accordance with PAGE, LAMBERT, 1987).

3. RESULTS AND DISCUSSION

Figure 5 shows examples of images obtained by optical and scanning electron microscopy (SEM). During the attainments and evaluations of the images was possible to estimate the thickness and pore size of dry coatings applied on the reinforcement steel, as well as assess the interconnectivity of the pores. The results are in Table 4. In Table 4 are also the thicknesses of the fresh film applied on each coat, total fresh film thickness and the pH of the coatings (primers).

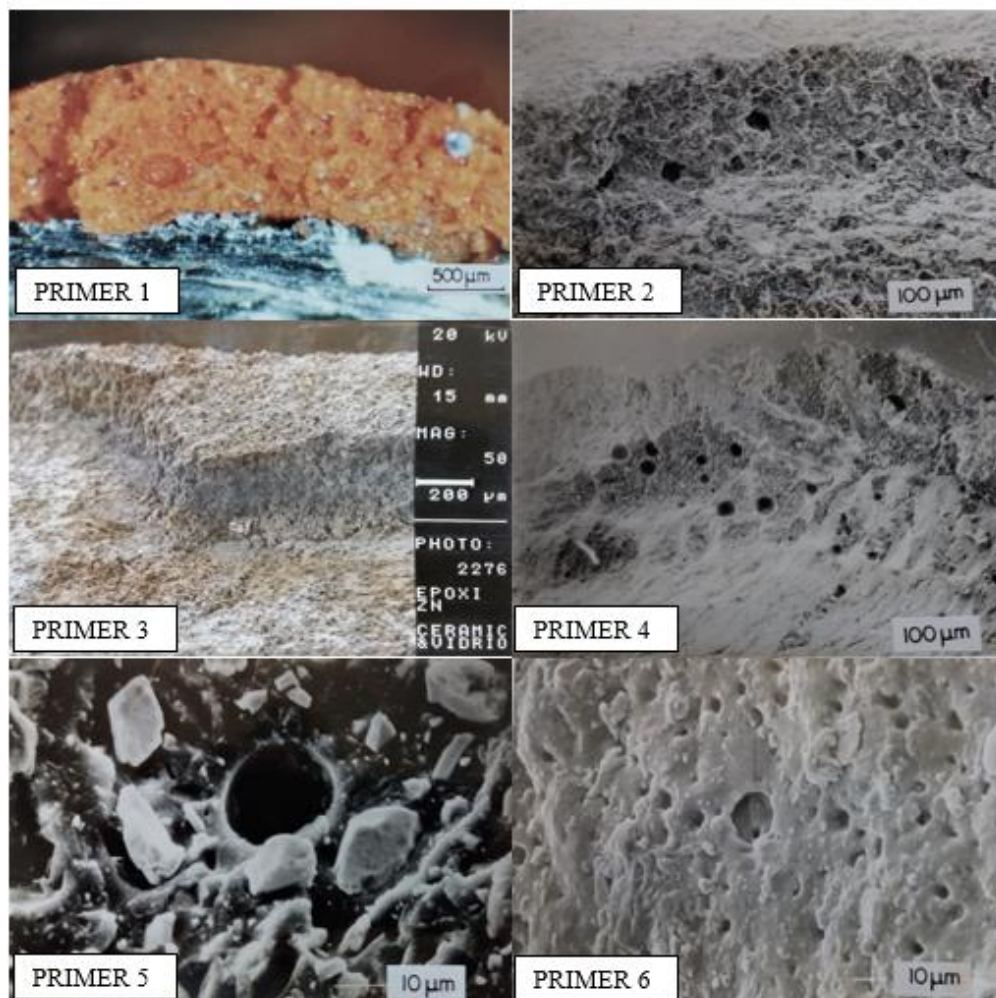


Figure 5. Microphotographs obtained by optical microscopy and scanning electron microscopy (SEM).

Table 4. Results of evaluations with fresh thickness gauge, magnifying glass, optical microscopy, SEM and pH.

Primer	Wet thickness (μm)				Dry thickness (μm)	Estimated pore size (μm)	Pore connectivity	pH
	1 ^a coat	2 ^a coat	3 ^a coat	Total				
Refer	-	-	-	-	7000 (*)	1000 (***)	Existence of connectivity	13,15
1	550	550	-	1100	1000	≤ 250	Frequently interrupted by the presence of resin and overlapping of coats	12,53
2	700	650	-	1350	800	≤ 100	Frequently interrupted by the overlapping of coats	11,47
3	175	175	-	350	330	≤ 50	Despite the low porosity, low presence of resin and high zinc allow a lot of connectivity between the pores	8,48
4	350	-	-	350	500 (**)	≤ 40	Without connectivity	10,91
5	100	100	100	300	250	≤ 20	High presence of small pores with possibility of connections	8,31

* The reference mortar was also on the primers

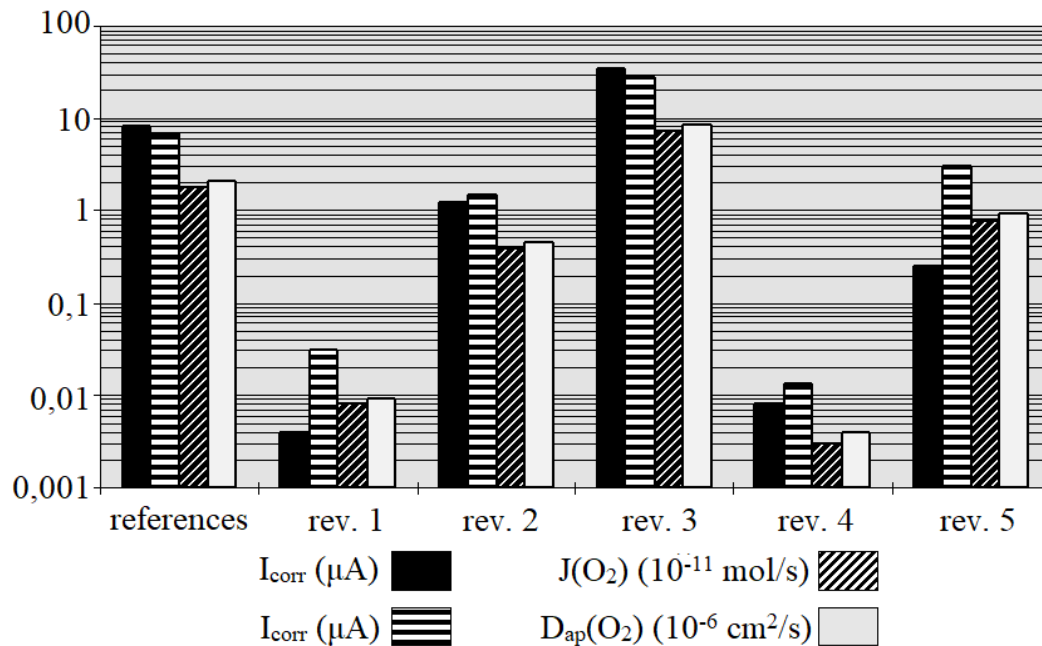
** Greater than the newly applied thickness because the observed area was situated between two ribs, where there is an accumulation of epoxy resin.

*** Air pores

The values of cathodic current (I_{cat}), corrosion intensity (I_{corr}), oxygen flow ($J(\text{O}_2)$) and apparent diffusion coefficient of oxygen ($D_{\text{ap}}(\text{O}_2)$) obtained in experimental evaluation, are presented in Table 5 and Figure 6.

Table 5. Results of I_{corr} , I_{cat} , $J(O_2)$ e $D_{ap}(O_2)$.

Primer	I_{corr} (μA)	I_{cat} (μA)	$J(O_2)$ (mol/s)	$D_{ap}(O_2)$ (cm^2/s)
Refer.	8,000	6,800	$1,76 \times 10^{-11}$	$2,07 \times 10^{-6}$
1	0,004	0,030	$8,00 \times 10^{-13}$	$9,00 \times 10^{-9}$
2	1,200	1,500	$3,90 \times 10^{-12}$	$4,60 \times 10^{-7}$
3	35,000	27,990	$7,25 \times 10^{-11}$	$8,55 \times 10^{-6}$
4	0,008	0,013	$3,00 \times 10^{-13}$	$4,00 \times 10^{-9}$
5	0,250	3,010	$7,80 \times 10^{-12}$	$9,20 \times 10^{-7}$


 Figure 6. Comparison between values of I_{corr} , I_{cat} , $J(O_2)$ e $D_{ap}(O_2)$.

Observing Figure 6 it is possible to note that the less-active rebar, protected with primers 1, 2, 4 and 5, the I_{cat} proved greater than the I_{corr} . This means that in the reinforcement coated with primers of largest barrier effect the anodic dissolution reactions are controlled, while in the cathodic regions of these rebars, due to introduction of a potential-750 mV (ECS) and the presence of some dissolved oxygen in the vicinity of the rebars, the oxygen reduction reactions end up happening. The reinforcement steel protected with the reference mortar and primer 3, after one year of exposure to chlorides, recorded I_{corr} values indicative of that were in the process of corrosion. In this case, the high values of I_{cat} registered may indicate that was taking place, also, the reduction of iron oxides presents on the surface of these reinforcements. Figure 6 shows that there are still major differences between the primers studied with regard to its characteristics of permeability to oxygen. The primers 1, 2 and represent barrier protection systems and showed less permeable to oxygen than others under the conditions tested. The assessments regarding the porosity and pore connectivity shown in Table 4 support and help in the understanding of the smallest values of $D_{ap}(O_2)$, especially with regard to the primer 4 based in epoxy resin.

The values found for the flow and diffusion coefficient, relative to the reference (cement mortar and sand), were of the same order of magnitude of the found by other authors, as can be seen in Table 6.

Table 6. $D_{ap}(O_2)$ values for cement mortar obtained by various authors.

Author	$D_{ap}(O_2)$ (cm ² /s)
Gjorv et al (1986)	$1,3 \times 10^{-6}$ a $3,4 \times 10^{-6}$ *
Andrade et al (1990)	$2,44 \times 10^{-6}$ **
Kobayashi et al (1991)	084×10^{-6}
Hansson (1993)	$2,36 \times 10^{-6}$ **
Figueiredo (1994)	$2,07 \times 10^{-6}$

* variation in function of thickness of the covering

** calculated from data from the authors

The area used for the calculation of the $D_{ap}(O_2)$, presented in Table 5, was 5.6 cm², so the total area under study. It is important to note, however, that this may not be correct, since the barrier effect exercised by certain coatings reduces the area that effectively is in contact with the electrolyte, reducing, thus, the area where it would be possible take place the oxygen reduction reaction on the rebar. When there are identical situations (same metal type, same polarization imposed (-750 mV, ECS), same environment (reference cement mortar) and same ambient conditions) for all specimens, it is expected that the oxygen diffusion coefficient calculated is always the same. The differences found, therefore, are probably due to differences in areas where oxygen reduction takes place, which, for your time, depend on the greater or lesser barrier effect exerted by each primer. Based on the above, it is possible deduce the equations 4, 5 and 6 that can be applied to calculate the effective oxygen reduction areas of each case and to compare with the reference.

$$D_{refer} = D_{primer \ x}(O_2) \quad (\text{Equation 4})$$

$$\frac{D_{refer}(O_2)}{A_{refer} \cdot C_o} = \frac{J_{primer \ x}(O_2)}{A_{primer \ x} \cdot C_o} \quad (\text{Equation 5})$$

$$\frac{J_{refer}(O_2)}{A_{refer}} = \frac{J_{primer \ x}(O_2)}{A_{primer \ x}} \quad (\text{Equation 6})$$

where:

$D_{refer}(O_2)$ → is the diffusion coefficient of oxygen of the reference mortar;

A_{refer} → is the reference area of the study (5,6 cm²);

$D_{primer \ x}(O_2)$ → is the oxygen diffusion coefficient of primer studied.;

$A_{primer \ x}$ → is the effective area of oxygen reduction related to the primer studied in cm²;

J_{refer} → is the oxygen flow of the reference cement mortar, in mol/s;

$J_{primer \ x}$ → is the oxygen flow of the studied primer, in mol/s.

Table 7 presents the effective area values ($A_{primer \ x}$) for each primer studied by using the values of $J(O_2)$ presented in Table 6 and applying Equation 6.

Table 7. Effective area values calculated.

Primer	Refer.	Primer 1	Primer 2	Primer 3	Primer 4	Primer 5
$A_{\text{primer } x}$ (cm^2)	5,6	0,03	1,24	23,13	0,01	2,49

The values shown in Table 7 indicate that, with the exception of primer 3, all other exercised at the time of measurement of I_{cat} , barrier effect superior to the reference mortar. The value obtained for the effective area of the primer 3 probably is due to the registration of the reduction of oxygen on the surface of the zinc particles present in this primer.

Due to corrosion of zinc, both I_{corr} and I_{cat} show higher values than reference because the reactions of anodic oxidation and cathodic reduction get along on the surface of the reinforcement steel and the zinc particles. In this case, the primer 3 would be exercising a cathodic protection mechanism and not by barrier.

The values of $J(\text{O}_2)$ and $D_{\text{ap}}(\text{O}_2)$ presented in Figure 6, as well as the values of $A_{\text{primer } x}$, shown in Table 7 indicate that the primer 4 (epoxy-based polymer coating) represented the largest barrier to the oxygen diffusion.

As time goes by test, primer can deteriorate. Thus, the calculation of the effective area of contact between the electrolyte and the reinforcement steel ($A_{\text{primer } x}$) can be used as a parameter to track the evolution of primer deterioration over time, if the area obtained to increase each test.

4. FINAL CONSIDERATIONS

The primers can protect the reinforcement for passivation, inhibition, cathodic protection and barrier. However, hardly a primer protects the reinforcement steel, along all the time, through a single mechanism. In this study it was found that the majority of primers studied was exercising barrier effect more than reference mortar. The results obtained with the technique employed in this work, show that there are significant differences between the primers with regard to its characteristics of oxygen permeability, and those who represent barrier protection system are less permeable to oxygen under the conditions tested. The value of the oxygen diffusion coefficient obtained in this paper for reference cement mortar are in accordance with the results of other researchers, demonstrating the feasibility of the methodology used to measure the diffusion of oxygen. The electrochemical technique employed in this work allows to track the performance of the primer with the time, watching if there is damage to the primer or not through the monitoring of the effective area of oxygen reduction ($A_{\text{primer } x}$) on the reinforcement steel.

5. REFERENCES

- ASTM International. (1999). *ASTM G1-90(1999), Standard Practice for Preparing, Cleaning, and Evaluating Corrosion Test Specimens*. Retrieved from <https://doi.org/10.1520/G0001-90R99E01>
- Andrade, C.; Alonso, C.; Garcia, M. (1990), *Oxygen Availability in the Corrosion of Reinforcements*. *Advances in Cement Research*, v. 3, n. 11, pp. 127-132. <https://doi.org/10.1680/adcr.1990.3.11.127>
- Andrade, C.; Gonzalez, J. A. (1978), *Quantitative measurements of corrosion rate of reinforcing steels embedded in concrete using polarization resistance measurements*. *Werkstoffe und Korrosion*. V. 29, p. 515-519. <https://doi.org/10.1002/maco.19780290804>
- Castellote, M.; Alonso, C.; Andrade, C.; Chadbourn, G. A.; Page, C. L. (2001), *Oxygen and chloride diffusion in cement pastes as a validation of chloride diffusion coefficients obtained by steady-state*

- migration tests*. Elsevier, Cement and Concrete Research. Volume 31, Issue 4, April 2001, Pages 621-625. [https://doi.org/10.1016/S0008-8846\(01\)00469-0](https://doi.org/10.1016/S0008-8846(01)00469-0)
- Figueiredo, E. J. P. (1994) *Avaliação do Desempenho de Revestimentos para Proteção da Armadura Contra a Corrosão Através de Técnicas Eletroquímicas: Contribuição ao Estudo de Reparo de Estruturas de Concreto Armado*. São Paulo, EPUSP, \Tese de Doutorado\, 423p.
- Francinete, P. J.; Figueiredo, E. J. P. (1999), *Estudo da Difusão de Oxigênio no Concreto*. São Paulo. EPUSP, BT/PCC/238, ISSN 0103-9830, 22p.
- Gjørsv, O.; Vennesland, O.; El-Basaidy, A. H. S. (1986), *Diffusion of Dissolved Oxygen through Concrete*. Materials Performance, v. 25, pp. 39-44.
- Hansson, C. M. (1993), *Oxygen Diffusion Through Portland Cement Mortars*, Corrosion Science, vol. 35, n. 5-8, pp. 1551 – 1556. [https://doi.org/10.1016/0010-938X\(93\)90383-R](https://doi.org/10.1016/0010-938X(93)90383-R)
- Helene, P. R. L. (1993), *Contribuição ao Estudo da Corrosão em Armaduras de Concreto Armado*. São Paulo, CPGECC/EPUSP, \Tese de Livre Docência\.
- Kobayashi, K.; Shutton, K. (1991), *Oxygen Diffusivity of Various Materials*. Cement and Concrete Research, vol. 21, n° 2-3, pp. 273 – 284. [https://doi.org/10.1016/0008-8846\(91\)90009-7](https://doi.org/10.1016/0008-8846(91)90009-7)
- McCafferty, E. (2010), *Kinetics of Corrosion*. In: Introduction to Corrosion Science. Springer, New York, NY. <https://doi.org/10.1007/978-1-4419-0455-3>
- Page, C.; Lambert, P. (1987), *Kinetics of Oxygen Diffusion in Hardened Cement Pastes*. Journal of Materials Science, v. 22, pp. 942-946.
- Stern, M.; Geary, A. L. (1957), *Electrochemical Polarization. A theoretical Analysis of the Sharp of Polarization Curves*. Journal Electrochemical Society, Vol. 104, n° 1, pp 56-63.
- Tuutti, K. (1982), *Corrosion of steel in concrete*. Sweden: CBI, 468 p.

Limitations of sorptivity and water permeability for the estimation of the chloride penetration rate in concrete regarding the accomplishment of prescriptive design for durability in the marine environment

Y. A. Villagrán Zaccardi^{1, 2} * , M. E. Sosa¹ , Á. A. Di Maio¹ 

*Contact author: yuryvillagran@gmail.com

DOI: <http://dx.doi.org/10.21041/ra.v8i3.302>

Reception: 13/03/2018 | Acceptance: 18/07/2018 | Publication: 31/08/2018

ABSTRACT

This paper presents an analysis of experimental data from conventional concrete regarding sorptivity and penetrability under pressure comparing these parameters to chloride diffusion rate determined in the laboratory and in actual marine environment. Prescriptions for durability assurance of reinforced concrete structures is based on the qualitative characterization of transport properties. For the specific case of the marine environment, it is required to assess the resistance of concrete to chloride ingress. The results show the limitations of both parameters as prescriptive indexes, with capillary absorption rate showing some advantages over water penetration under pressure.

Keywords: capillary absorption; water penetration; chloride; durability; prescriptive design.

Cite as: Y. A. Villagrán Zaccardi, M. E. Sosa, Á. A. Di Maio (2018), “*Limitations of sorptivity and water permeability for the estimation of the chloride penetration rate in concrete regarding the accomplishment of prescriptive design for durability*”, Revista ALCONPAT, 8 (3), pp. 301-316, DOI: <http://dx.doi.org/10.21041/ra.v8i3.302>

¹ LEMIT - Laboratorio de Entrenamiento Multidisciplinario para la Investigación Tecnológica - 52 entre 121 y 122 - 1900 - La Plata - Provincia de Buenos Aires

² CONICET - Consejo Nacional de Investigaciones Científicas y Técnicas, Godoy Cruz 2290, Buenos Aires.

Legal Information

Revista ALCONPAT is a quarterly publication by the Asociación Latinoamericana de Control de Calidad, Patología y Recuperación de la Construcción, Internacional, A.C., Km. 6 antigua carretera a Progreso, Mérida, Yucatán, 97310, Tel.5219997385893, alconpat.int@gmail.com, Website: www.alconpat.org

Responsible editor: Pedro Castro Borges, Ph.D. Reservation of rights for exclusive use No.04-2013-011717330300-203, and ISSN 2007-6835, both granted by the Instituto Nacional de Derecho de Autor. Responsible for the last update of this issue, Informatics Unit ALCONPAT, Elizabeth Sabido Maldonado, Km. 6, antigua carretera a Progreso, Mérida, Yucatán, C.P. 97310.

The views of the authors do not necessarily reflect the position of the editor.

The total or partial reproduction of the contents and images of the publication is strictly prohibited without the previous authorization of ALCONPAT Internacional A.C.

Any dispute, including the replies of the authors, will be published in the second issue of 2019 provided that the information is received before the closing of the first issue of 2019.

Limitaciones de la velocidad de absorción capilar y la permeabilidad al agua para la estimación de la velocidad de penetración de cloruro en hormigón respecto a la consecución del diseño prescriptivo para durabilidad en ambiente marino

RESUMEN

Este artículo presenta un análisis de datos experimentales de hormigón convencional respecto a la velocidad de absorción capilar y la penetración de agua a presión comparando estos parámetros con la velocidad de difusión de cloruro determinada en el laboratorio y en ambiente marino real. Las prescripciones para el aseguramiento de la durabilidad de estructuras de hormigón armado están basadas en la caracterización cualitativa de las propiedades de transporte. Para el caso específico del ambiente marino, se requiere evaluar la resistencia del hormigón al ingreso de cloruro. Los resultados muestran las limitaciones de ambos parámetros como índices prescriptivos, con la velocidad de absorción capilar mostrando algunas ventajas sobre la penetración del agua bajo presión.

Palabras clave: absorción capilar; penetración de agua; cloruro; durabilidad; diseño prescriptivo.

Limitações da taxa de absorção capilar e da permeabilidade água para a estimativa da taxa de penetração de cloreto em concreto em relação à realização do design prescritivo para durabilidade em ambiente marinho

RESUMO

Este artigo apresenta uma análise de dados experimentais de concreto convencional em relação à velocidade de absorção capilar e à penetração de água sob pressão para comparar estes parâmetros com a velocidade de difusão de cloretos determinada no laboratório e no ambiente marinho real. Os requisitos para a garantia da durabilidade das estruturas de concreto armado baseiam-se na caracterização qualitativa das propriedades de transporte. Para o caso específico do meio marinho, é necessário avaliar a resistência do concreto à ingestão de cloreto. Os resultados mostram as limitações de ambos parâmetros como índices prescriptivos, com a velocidade de absorção capilar apresentando algumas vantagens sobre a penetração de água sob pressão.

Palavras chave: absorção capilar; penetração de água; cloreto; durabilidade; desenho prescritivo

1. INTRODUCTION

Most of the concrete deterioration mechanisms are related to the performance of cover concrete. This concrete layer is responsible for the durability of the structure to the degree that it provides physical and chemical protection to reinforcement against external aggressive substances. Design methods for durability look into the characteristics of this cover concrete for assessing a certain lifespan.

The service life of a structure regarding the degradation of constituents can be explained by applying the model proposed by Tuutti (Tuutti, 1982). The stipulated service life is the period during which the service requirements must be met, with a level over the acceptable minimum regarding safety, comfort and aesthetics. For this, the exposure conditions to which the structure will be exposed must be considered.

In general, the regulation considers periods of stipulated service life of 50 or 100 years, provided that cracking is controlled, and concrete is properly placed, compacted and cured. Minimum requisites for the properties and depth of cover concrete are defined. This prescriptive approach is widely accepted, but it is limited regarding the accuracy of the projected service life (Rostam, 2000). The general classification of environments and target parameters impedes to consider all the intervening factors. These parameters are often qualitatively restricted, or an indeterminate quantification is established for them (Anoop et al., 2002), and the actual service lifespan cannot be accurately estimated. Reinforcement corrosion is one of the most investigated deterioration processes design for durability of reinforced concrete structures.

Tuutti's model divides the corrosion process into two development periods covering the service lifespan (Tuutti, 1982): initiation and propagation. During the initiation period, the incubation of the conditions necessary for the beginning of the degradation develops. During the propagation period, the situation progressively worsens with lower and lower performance level to the moment in which the deterioration degree of the structure is such that it does not comply with the minimum service conditions required. In general, the time required for reinforcement depassivation is conceived as the initiation period, while cracking and spalling are conceived within the propagation period (Tuutti, 1982; DURAR, 1997; Rostam, 2000).

The influencing factors for the initiation period in the marine environment are classified in internal and external. Internal factors are mainly related to the characteristics of cover concrete. Among these factors the most important are those that determine the material resistance to chloride ingress: porosity of the matrix (Collepari et al. 1970; Monosi et al. 1989) (determined by the w/b ratio, compaction degree, curing), content and type of cement (Collepari et al., 1970; Glass and Buenfeld, 2000), porosity of the interfacial transition zone (Delagrave et al., 1997a), and porosity of aggregate (Fernández Luco, 2001). The aggressiveness of the environment defines external factors (Sandberg et al., 1998; Traversa, 2001; Andrade et al., 2002; Traversa and Di Maio, 2002; Di Maio et al. 2004), characterized by the average temperature and relative humidity, incidence of winds, rain, distance and height with respect to sea level. Finally, the presence of protective surface layers on the structure (paint or finishing) must be considered as these reduce the exposure level (Di Maio et al., 2000). All these factors determine the time required to chlorides to reach reinforcement.

Chloride ingress into reinforced concrete leads to reinforcement pitting. When the chloride threshold content on reinforcement surface is achieved, steel depassivates and starts corroding if oxygen and moisture are available. Therefore, cover concrete must prevent this situation as long as possible. Its transport properties define the time required for corrosion to start. Lower transport rate of chlorides through cover concrete will allow a longer service life of the structure.

The resistance of cover concrete to chloride ingress is usually defined by the apparent diffusion coefficient (Collepari et al., 1970), D_{ap} , which establishes the greater or lesser rate at which ions enter into concrete. The performance-based design applies this coefficient to compute a certain service life of the structure for a certain cover depth. However, D_{ap} is generally not explicitly included in construction regulation as a design parameter for concrete, as its measurement is very time-consuming. Some uncertainties remain regarding the application of diffusion coefficients for service life prediction, as real conditions of exposure are very difficult to simulate in short-term tests, particularly to consider the dependence of the apparent diffusivity on the chloride surface concentration (Andrade et al., 2000). In consequence, design engineers show reluctance to use complex models for the prediction of chloride ingress into concrete, and they are little prone to introduce them into Codes or Standards (Andrade et al., 2013). Instead, the correlation between chloride diffusivity with other properties of concrete is frequently considered for the design. This approach is the basis for the prescriptive design.

Prescriptive criteria are basically maximum or minimum values for different concrete properties to satisfy. These properties may include concrete strength, water/binder ratio, water absorption, capillary absorption rate, water penetration under pressure, cement content and type. All these factors are reported as the main controlling parameters for durability, and on this basis, limits are established from reference values that have proved to provide long-term durability of reinforced concrete exposed to chlorides in the laboratory or in service.

Because of practical reasons, prescriptive criteria is widely included in regulations for durable reinforced concrete structures. Guidelines regarding the durability of reinforced concrete in the marine environment are included in regulations (BS EN 206, 2013; ACI 201.2R, 2016; CIRSOC 201, 2005), where prescriptive criteria are generally established to ensure a service life of 50 years. First, the type of chloride exposure must be defined and rated according to the aggressiveness level. Then, corresponding characteristics for cover concrete are required. These types of limits are easy and reliable when examined. However, prescriptive design for durability does not allow inferring the actual service lifespan. Modern regulations are progressively including performance-based design criteria, but great effort is required in this sense due to extensive experimental work required for the validation of models.

This paper reports comparisons between the chloride diffusion coefficient in saturated and unsaturated conditions and technological properties such as w/b ratio, compressive strength, sorptivity and water penetration under pressure. The main connecting and disconnecting aspects regarding these comparisons are analyzed on the basis of the experimental results.

2. PRESCRIPTIVE DESIGN FOR DURABILITY IN THE MARINE ENVIRONMENT

2.1. Water/binder ratio

The capillary porosity of the cementitious matrix is a function of the w/b, given certain hydration and compaction degrees. During the initiation period, the availability of connected porosity that allows moisture and ion transport is essential for the development of the deterioration process. The limitation to a maximum w/b ratio leads to a decrease in the volume of capillary porosity in concrete. This reduced w/b ratio must be complemented with proper curing treatment that allows sufficient progress of cement hydration, as well as efficient consolidation that eliminates macropores.

The influence of w/b on chloride diffusivity of concrete has been widely investigated (ACI 222, 2003). However, its utility as a prescription parameter cannot be only sustained by the confirmation of incidence. JSCE proposes a potential relationship between w/b and diffusivity through concrete (Song et al., 2008), but, as said, other interrelated affecting parameters cause significant deviation from this relationship. Therefore, concrete properties significantly related to the w/b ratio are generally prescribed. This is also due to the difficulties in controlling the w/b ratio in the field, as no reliable experimental method is available.

Regarding active corrosion of reinforcement, the flux of oxygen through concrete is also a function of the reduction of w/b (ACI 222, 2003). Both chloride and oxygen diffusion are connected with the relationship between permeability and w/b.

2.2. Cement content

Cement content is determining of the durability in the marine environment in several aspects. First, for a certain w/b, more cement means larger volume of paste in concrete. The use of water reducing admixtures may contribute to reducing the cement content in concrete. The reduction of paste content in concrete is potentially a beneficial effect, as aggregates are usually less porous than the

matrix and increasing their contents helps in reducing transport properties of concrete provided that proper compaction is applied.

Conversely, C_3A contained in cement is the largest contributor to the chloride binding capacity in concrete, and this feature is dependent on the type and content of cement (Andrade, 1993; Delagrave et al., 1997b). Chloride binding is a delaying process of chloride ingress, and service life increases when chloride binding is enhanced. Then, increasing cement content in concrete means increasing chloride binding capacity.

Supplementary cementitious materials contained in cement affect durability in the marine environment by two opposite effects, dilution and pozzolanic action. These effects are not so marked in the results of accelerated test methods, but they are verified more extensively with time. For this reason, some procedures make attempts to consider the late reactivity of supplementary cementitious materials. In any case, significant changes with time are caused depending on the cement type.

2.3. Compressive strength

As said, the w/b ratio is the most important parameter regarding transport properties of concrete. This design tool is difficult to be controlled in the field. Then, its relationship with compressive strength, which has been extensively proved and explained on the basis of the conformation of the pore structure, is used for design. This direct relationship is the most developed in the field of concrete technology. Therefore, a strong basis for the use of the compressive strength as an evaluation parameter for virtually any other property of concrete, including chloride diffusivity, is available. As expected, diffusivity in saturated state decreases consistently with increasing compressive strength, and simple empirical relationships between compressive strength at 28 days and chloride diffusivity of concrete have been determined (Frederiksen et al., 1997). These relationships are probably affected by entrained air. Differences caused by the cement type and practices for accelerating strength gain (curing treatment, additives) are also to be expected.

However, the determining factor for the use of compressive strength as a control parameter is its practicality, cost and universality. Then, it is very easily implemented and interpreted. The application of this control parameter has shown a very variable degree of success, and this is the reason for the application of more comprehensive control parameters for durability in the marine environment.

2.4. Sorptivity

The water capillary absorption rate is one of the transport mechanisms through which chloride can penetrate into concrete in the marine environment. This property is an effective descriptor of the pore structure of concrete. Capillary absorption develops in unsaturated concrete, and it can transport chloride into concrete as the wet front progresses. However, pure diffusion takes place only when no liquid flux is produced, and in this sense, it is different from capillary absorption. The pore size ranges participating in both processes and the processes themselves are different. In spite of this, fair correlations between sorptivity and chloride diffusion are presented in the literature (Basheer, 2001; Kropp and Basheer, 2000). These relationships depend on the applied test methods for the determination of each property, which are very sensitive to preconditioning. In this sense, a high sensitivity of the value obtained for sorptivity to test conditions and proportions of constituents of concrete has been documented (Taus, 2010; Bjevović et al., 2015). Moreover, particular consideration must be made for its contrast with chloride diffusion in unsaturated conditions, as in this case only part of the pore structure intervenes in the transport process. The direct correlation between chloride diffusivity and sorptivity may be therefore affected by the saturation degree of concrete.

2.4. Permeability

In the case of structures subjected to a hydrostatic pressure difference, permeability is the parameter that best represents penetration of aggressive substances from the external environment, e.g. transport of chloride in seawater structures. Furthermore, high resistance to chloride penetration for low permeability concrete has been obtained in connection with the limited connectivity of the pore structure (CCAA, 2009). Again, the processes of water penetration under pressure and chloride diffusion are different, especially considering their correspondence with the saturation degree of concrete.

3. MATERIALS AND METHODOLOGY

The studied concrete mixes were 28 in total with multiple batches for most of them, making a total of 73 batches. Proportions of studied concretes correspond to w/b between 0.39 and 0.61, with cement contents between 425 and 250 kg/m³. Three types of portland cement used were: Ordinary (OPC), Limestone (LPC, incorporating 17% limestone), and Composite (CPC, 17% and 12% incorporation of limestone and slag, respectively). Crushed granite aggregates with maximum sizes of 19 and 25 mm were used as coarse aggregate. Fine aggregate was siliceous river sand. Materials with negligible chloride contents were used. Chloride content of concrete coming from constituents (IRAM 1857, 2000) was in all cases lower than 0.03%. For more details on the proportions of these concretes please refer to (Violini et al., 2006; Taus et al., 2008; Villagrán Zaccardi, 2012).

Tests were conducted to determine compliance of concrete mixes to prescriptive parameters. These include compressive strength, measured on cylindrical specimens of 15x30cm in diameter and height, compacted and tested according to IRAM 1524, 1546 and 1553, capillary absorption rate, determined according to IRAM 1871 (IRAM 1871, 2004), and water penetration under pressure according to IRAM 1554 (IRAM 1554, 1983). All specimens were compacted manually, demolded after 24 hours of casting, and cured in a humid chamber (Temp: 23 ± 2 °C; RH > 95%) until the age of 28 days.

Chloride transport rate was evaluated in prismatic specimens 7.5x15x25 cm³. After the curing treatment, these specimens were waterproofed with chlorinated rubber paint on all sides excepting the molding surface, from which unidirectional chloride ingress was allowed. Specimens were exposed in a natural marine environment and immersed in sodium chloride solution, with the ingressing face set as the horizontal upper side. Thus, they were exposed with the same position they were molded.

The natural marine environment exposure was in the city of Mar del Plata, Argentina, approximately 50 meters from the shoreline and 5 m above mean sea level. Direct contact between samples and seawater did not occur at any time during exposure, and the only source of chlorides was the sea spray.

Specimens exposed in immersion were first saturated for 24h in saturated lime water, and then submerged in 30 g/l NaCl solution maintained at 23 ± 5 °C until profiling.

Chloride ingress profiles were analyzed after 12 months of exposure for specimens in the marine environment and after 6 months for specimens in immersion. First, painted sides were discarded in approximate thickness of 1 cm. Then, cuts parallel to the ingress face were made, obtaining progressive slices of about 5 mm. Average depths from the ingress surface were measured for each slice. All cuts were made in dry condition with a diamond disc. Afterwards, the slices were pulverized, and acid-soluble chloride contents were determined in accordance with IRAM 1857, method C (IRAM 1857, 2000).

Data regressions to the most common solution of the Fick's second law, Equation (1) were performed, and values for D_{ap} were determined. In the cases in which non-Fickian behaviour was detected, the procedure indicated in (Andrade et al., 2015) was followed.

$$C_{(x,t)} = C_s \left(1 - \operatorname{erf} \left(\frac{x}{2\sqrt{D_{ap} \cdot t}} \right) \right) \quad (1)$$

where $C_{(x,t)}$ is the chloride content at depth x , in time t , erf is the error function, C_s is the apparent surface chloride content at time t , and D_{ap} is the apparent non-stationary diffusivity.

4. RESULTS AND DISCUSSION

Chloride penetration is driven by the concentration gradient between the surface and the interior of concrete. In consequence, chloride contents that penetrated into concrete in immersion were up to three times higher than those determined in concrete in atmospheric marine exposure. Moreover, unlike during penetration under atmospheric exposure, in saturated concrete, the entire porosity is occupied by pore solution, which constitutes the medium through which chloride enters. Then, faster penetration in saturated than in unsaturated concrete is obvious. The content of pore solution will mainly define the correlation between penetration rates in submerged specimens and exposed to marine environment. This content does not remain constant in specimens under atmospheric exposure, as it is influenced by weather conditions, especially in the more external zone. Therefore, the comparison should take note that both ingress mechanisms are not fully equivalent, and the contrast is merely empirical. Moreover, in a marine environment with different climatic conditions from the one considered in this study, different hygroscopic equilibrium with the environment of concrete will result in a different content of pore solution, and different cycles of wetting and drying.

From the penetration profiles, the direct comparison between the computed values for diffusivity in specimens exposed in the natural marine environment (D_{atm}) and immersed (D_{imm}), is shown in Figure 1. A remarkable trend with little impact of the cement type is noticed. For low penetration rates, greater increments for D_{atm} than for D_{imm} are revealed. This ratio seems to reverse over a certain value, and for high penetration rates, smaller increments for D_{atm} than for D_{imm} are noticed. This may be explained by the concept previously mentioned. Pore size distribution and total porosity are connected. Low diffusivities correspond to concrete mixes with low porosity. In this case, pore liquid remains in a relatively greater volume of small pores of concrete under atmospheric exposure. As porosity increases, larger pores contribute to the penetration of chloride when concrete is in immersion, but they do not remain saturated in concrete under atmospheric conditions.

This is, changes in diffusivity relate more directly to the change in the total pore volume when concrete is saturated, as all porosity contributes to the transport mechanism. On the contrary, only finer pores contribute to transport in unsaturated concrete, and D_{atm} does not continue increasing at the same rate with increasing volume of macropores (Saetta et al., 1993; Climent et al., 2002; Nielsen and Geiker, 2003; Zhang and Zhang, 2014).

Figure 2 shows D_{atm} and D_{imm} compared with w/b. Despite the potentially different chloride binding capacity, no statistically significant differences can be established among the different cement types. The influence of w/b very much hides any difference.

As expected, increasing diffusivity values are obtained with increasing w/b. However, significant variations within each w/b were obtained. The influence of the other variables (hydration degree, maximum aggregate size and cement content) is the primary reason for this. It is particularly important to note that the sum of these influences may result in a similar degree of impact to the variation of the ratio w/b, especially for diffusivities determined in the unsaturated condition.

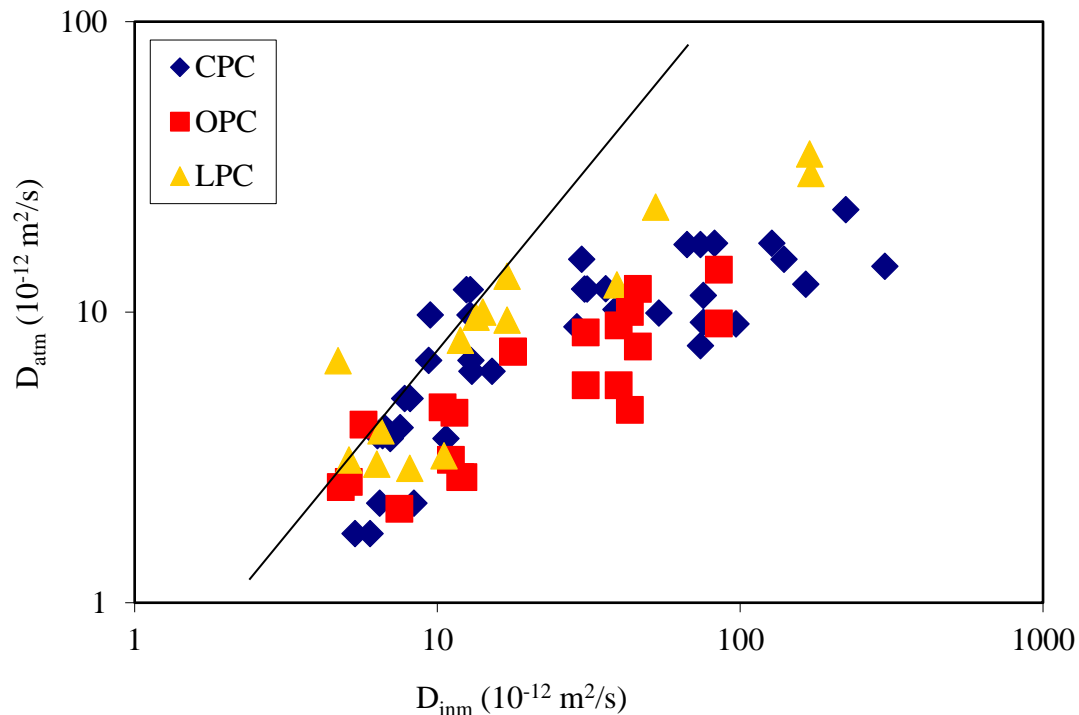


Figure 1. D_{imm} versus D_{atm} .

The differentiation between diffusivity values when in immersion or atmospheric is more pronounced with higher w/b (D_{imm} increases much more than D_{atm} with increasing w/b). Concrete porosity increases with w/b, but this increased porosity results in more content of pore liquid only in the saturated state. Macropores do not affect in the same way to samples exposed to the atmosphere. At unsaturated conditions, the volume of pore liquid is defined by the fine capillary pores, where more or less condensation will occur depending on the relative humidity. In this range of pore sizes, w/b has less significance regarding the volume fraction of pores participating in the transport process.

In this sense, engineering transport parameters, such as sorptivity and penetrability under pressure, are related to pore structure volume and connectivity. They are therefore indirectly connected to chloride diffusivity in saturated concrete (as shown later in Figures 3, 5 and 6).

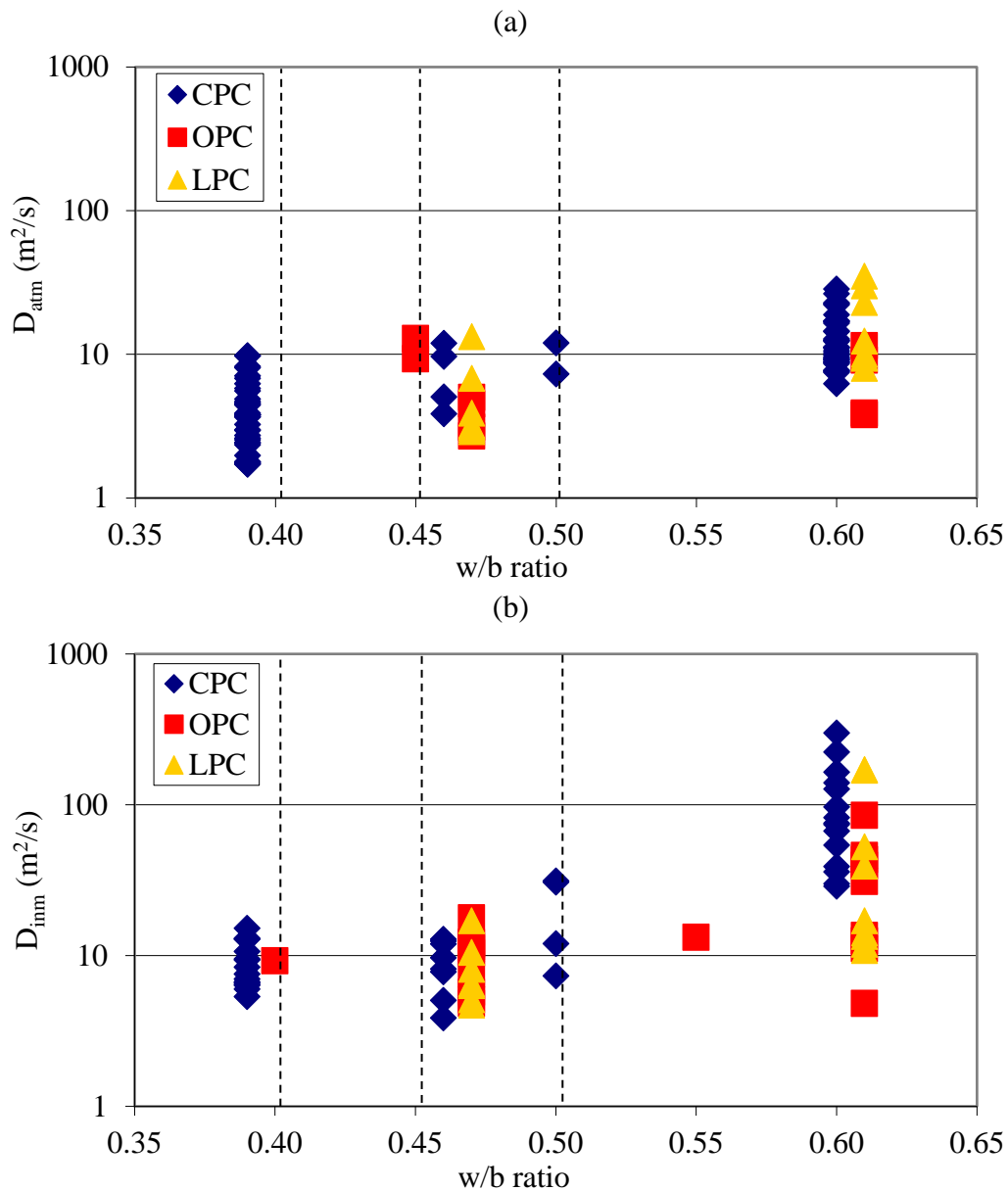


Figure 2. (a) D_{atm} and (b) D_{inm} , versus w/b.

Figure 3 shows the comparisons between sorptivity and diffusivity. Again, the variation in sorptivity is higher than the variation in D_{atm} . The variation in capillary absorption rate is more directly connected with D_{inm} . The variability of sorptivity is greater than the corresponding to the w/b. This indicates how unsuitable is the w/b for defining the transport rate in concrete. As in the case of diffusivity, other factors different from the w/b are also affecting the transport rate, and these are taken into account only when the transport property itself is measured. Fig. 2 shows a significant number of conformity values by w/b (values of 0.40, 0.45 and 0.50 are generally accepted depending on the environment and the consideration of reinforced or prestressed concrete). This number is certainly reduced when limits are based on a tolerable limit for sorptivity. It should be mentioned that the correspondence between w/b ratio and capillary absorption rate will certainly be different in concrete made with water-reducing admixtures, which allow lower mixing water (and in consequence also paste volume) for the same consistency level. In that case, it is estimated that the capillary absorption rate may decrease for the same w/b.

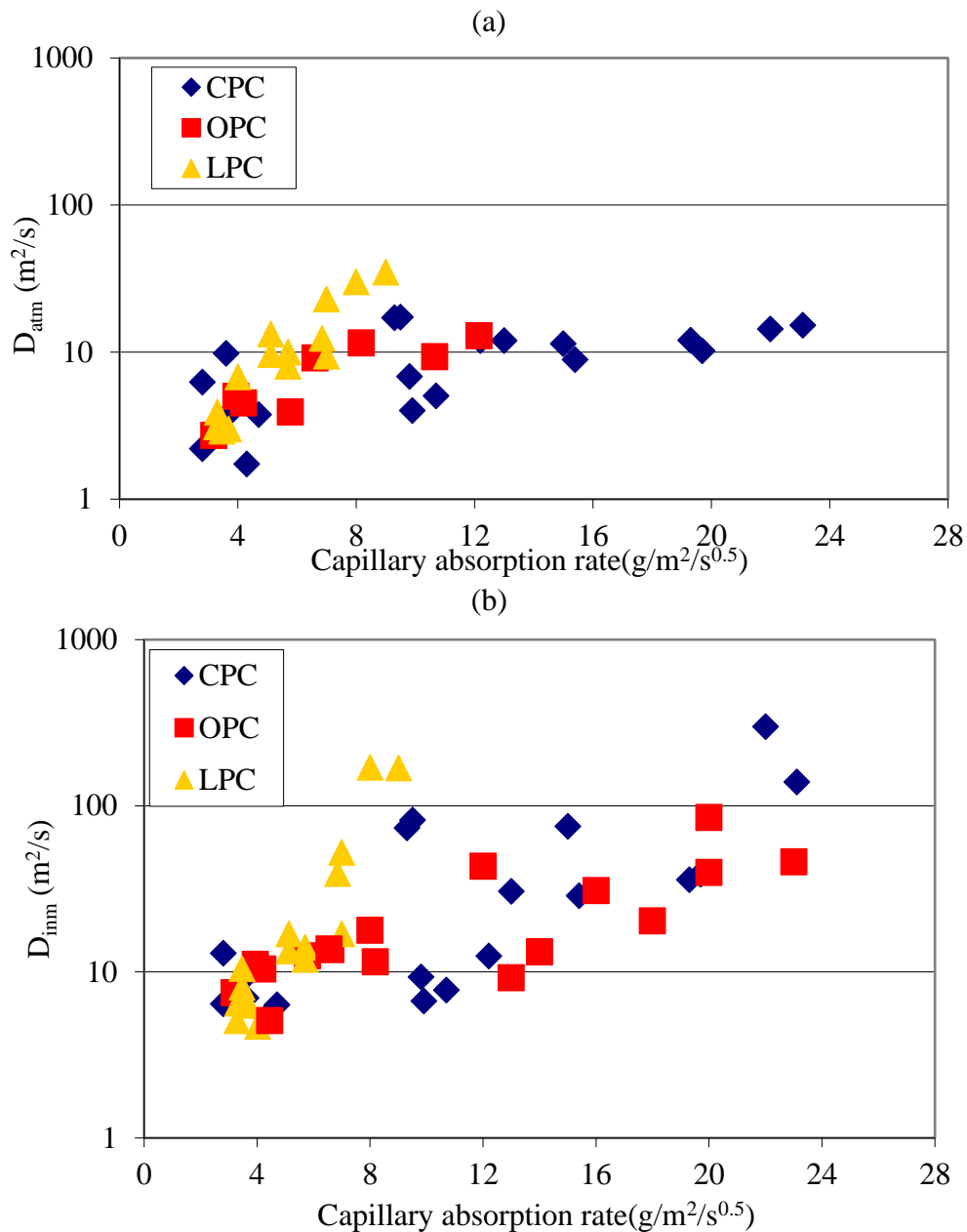


Figure 3. (a) D_{atm} and (b) D_{inm} versus sorptivity.

In Figure 4, the comparisons between diffusivities and compressive strength are presented. An inverse evolution is obtained as a consequence of the opposite relationships of both properties with porosity. A greater dispersion is noted for D_{inm} than for D_{atm} . The number of conformity values according to strength is similar to that according to w/b. Thus, the direct relation between strength and w/b allows a reliable control procedure by the first, in order to assure compliance of the second. This is an aspect of practical necessity due to the lack of reliable methods for experimentally controlling the w/b in fresh concrete. On the other hand, it should be mentioned that strength of cover concrete in the structure will be greatly affected by the consolidation degree, which is in turn highly dependent on the field practices.

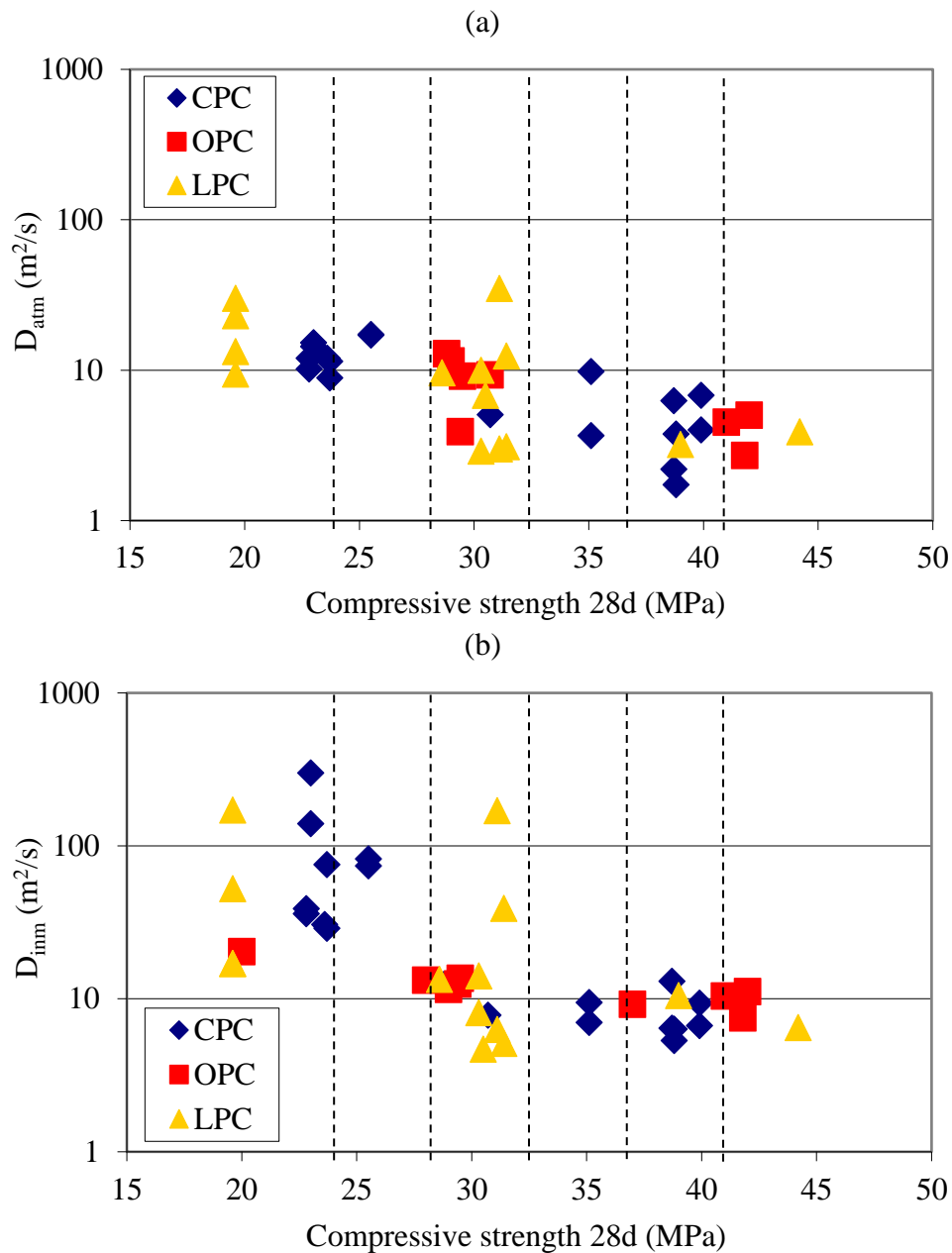


Figure 4. (a) D_{atm} and (b) D_{imm} versus compressive strength.

The experimental determination of the compaction index of fresh concrete is then advisable to define the sensitivity of concrete to compaction and establishing an indicative relative risk for the required level of control during placement of fresh concrete. In practice, the lack of this consideration commonly leads to bad results regarding the durability of the structure.

In Figures 5 and 6, the comparisons between diffusivities and water penetration under pressure, mean and maximum, respectively, are presented. The proportion of conformity values shows water penetration under pressure as a less challenging property than sorptivity.

The compliance of both mean and maximum water penetration depths is equivalent. Compaction defects in the specimen are required for obtaining a significant difference between these two parameters. The good correspondence of values shows that this was not the case for any of the tested specimens. With this in mind, it should be remarked the very limited use of the maximum penetration of water under pressure regarding chloride penetration and other transport properties of concrete.

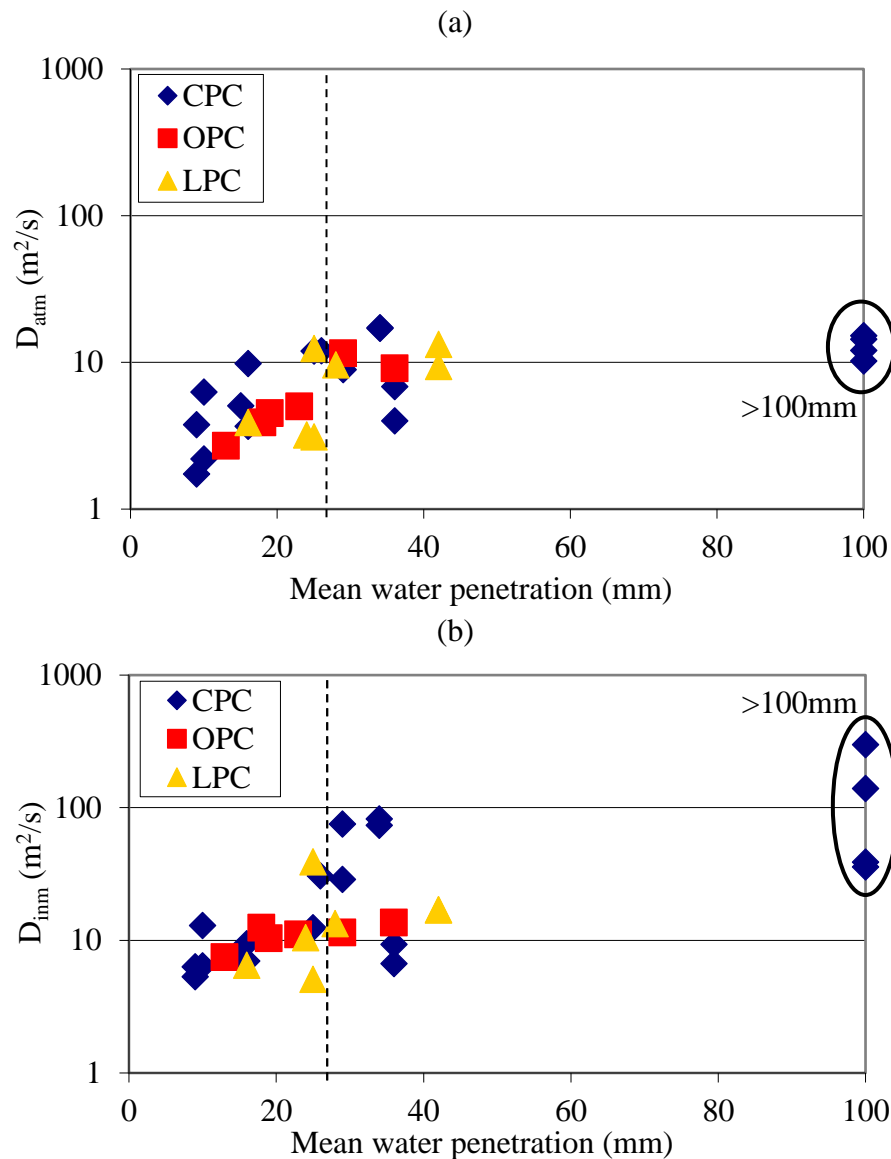


Figure 5. (a) D_{atm} and (b) D_{inm} vs. mean penetration of water under pressure.

Among the analyzed parameters, sorptivity was the one showing the best correlation with chloride diffusivity. Compressive strength, w/b , and water penetration under pressure followed in that order. This is remarkable in the sense that water penetration under pressure may be wrongly recommended over compressive strength for the estimation of chloride penetration in concrete when only considering that transport properties should be better connected to each other. However, all examined properties showed a better correlation with chloride diffusivity in the saturated condition. For unsaturated concrete, macropores are not participating in the process of chloride ingress, but they do in other processes such as water absorption and penetration. Therefore, unsaturated concrete with high w/b tends to be classified as less durable in the marine environment when tested for sorptivity or water penetration under pressure than for chloride ingress rate itself. The saturation degree of concrete is an important aspect that should always be considered in this regard.

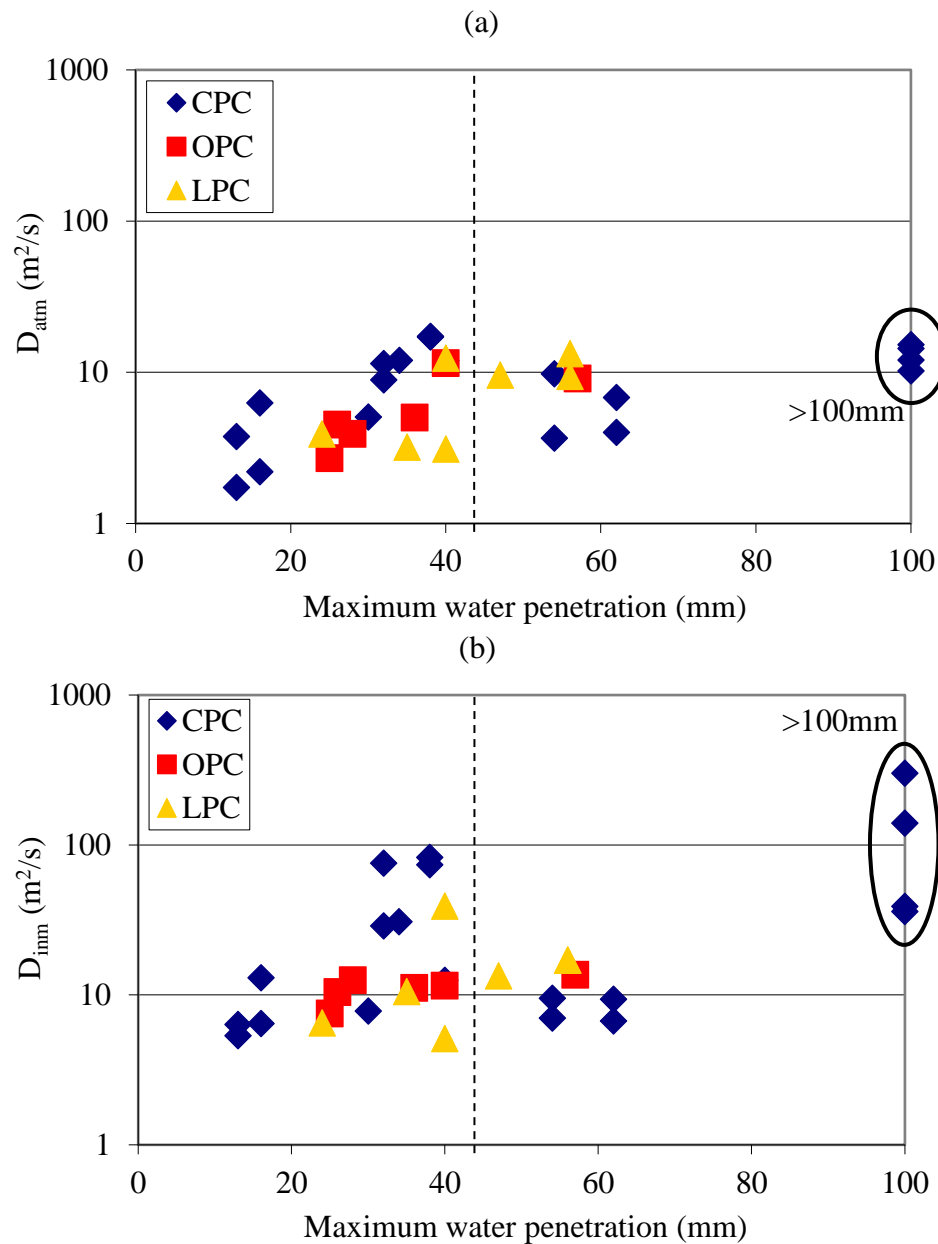


Figure 6. (a) D_{atm} and (b) D_{imm} vs maximum penetration of water under pressure.

5. CONCLUSIONS

The w/b ratio is the technological parameter determining the chloride ingress rate into concrete. However, other parameters also affect this transport property, such as hydration degree, maximum aggregate size, compaction degree, and cement content, and in combination, their effect may exceed the one from the w/b. Therefore, the w/b ratio as a design parameter for durability in the marine environment requires the assistance of complementary prescriptions for transport properties.

The capillary absorption rate demonstrated a consistent correlation with the chloride diffusion rate in the saturated condition. It is convenient to expand the database for this correlation in order to make reliable predictions on this basis with applications in prescriptive design. However, the

connection between sorptivity and chloride diffusion in unsaturated concrete is less consistent, as the pore size range participating in each transport mechanism is different.

Water penetration under pressure showed little application for the design for durability regarding chloride penetration into concrete. In this sense, compressive strength is considered more practical and reliable for estimating the performance of concrete in the marine environment. Therefore, no added value of water penetration under pressure over compression strength is anticipated. An exception could be made for chloride penetration in saturated concrete, where the chloride penetration rate can be better anticipated by the maximum water penetration under pressure than for the case of unsaturated concrete.

As a result, combined data of capillary absorption rate and compressive strength seem to work well as prescriptive parameters for durability in the marine environment. In many cases, the determination of the capillary absorption rate faces some practical inconveniences for its application in the field, mostly due to its sensitivity to testing variables and the required testing time. The values for prescriptive limits for sorptivity are still a matter of study.

6. ACKNOWLEDGEMENT

Prof. Carmen Andrade is a great inspirer for scientists and engineers working on reinforced concrete durability all over the world. She has permanently searched for simple methods which are practical and precise for engineers, and accurate and comprehensive for scientists. We really appreciate the advice and support we have received from her over the years.

7. REFERENCES

- America Concrete Institute (2016), *"ACI 201.2R-16 Guide to Durable Concrete"*, Farmington Hills, USA, p. 84.
- America Concrete Institute (2003), *"ACI 222.3R-03 Design and Construction Practices to Mitigate Corrosion of Reinforcement in Concrete Structures"*, Farmington Hills, USA, 29p.
- Andrade, C. (1993), *"Calculation of chloride diffusion coefficients in concrete from ionic migration measurements"*, Cement and Concrete Research, Vol. 23, pp. 724-742. [https://doi.org/10.1016/0008-8846\(93\)90023-3](https://doi.org/10.1016/0008-8846(93)90023-3)
- Andrade, C., Castellote, M., Alonso, C., González, C. (2000), *"Non-steady-state chloride diffusion coefficients obtained from migration and natural diffusion tests. Part I: Comparison between several methods of calculation"*, Materials and Structures, Vol. 33, pp. 21-28. <https://doi.org/10.1007/BF02481692>
- Andrade, C., Alonso, C., Sarria, J. (2002), *"Corrosion rate evolution in concrete structures exposed to the atmosphere"*, Cement & Concrete Composites, Vol. 24, pp. 55-64. [https://doi.org/10.1016/S0958-9465\(01\)00026-9](https://doi.org/10.1016/S0958-9465(01)00026-9)
- Andrade C., Prieto, M., Tanner, P., Tavares, F., d'Andrea, R. (2013), *"Testing and modelling chloride penetration into concrete"*, Construction and Building Materials, Vol. 39, pp. 9–18. <https://doi.org/10.1016/j.conbuildmat.2012.08.012>
- Andrade, C., Climent, M. A., de Vera, G. (2015), *"Procedure for calculating the chloride diffusion coefficient and surface concentration from a profile having a maximum beyond the concrete surface"*, Materials and Structures, Vol. 48, pp. 863-869. <https://doi.org/10.1617/s11527-015-0543-4>
- Anoop, M. B., Rao, K. B., Rao, T. V. S. R. A. (2002), *"Application of fuzzy sets for estimating service life of reinforced concrete structural members in corrosive environments"*, Engineering Structures, Vol. 24, pp. 1229-1242. [https://doi.org/10.1016/S0141-0296\(02\)00060-3](https://doi.org/10.1016/S0141-0296(02)00060-3)

- Basheer, P. A. M. (2001), "*Permeation Analysis*", in: Ramachandran, V. S., Beaudoin, J. J. (Eds.), *Handbook of analytical techniques in concrete science and technology. Principles, Techniques and Applications*, Noyes Publications, New Jersey (USA), pp. 658-737.
- Bjegović, D., Serdar, M., Oslaković, I. S., Jacobs, F., Beushausen, H., Andrade, C., Monteiro, A. V., Paulini, P., Nanukuttan S. (2015), "*Test Methods for Concrete Durability Indicators*", in: Beushausen, H., Fernández Luco, L. (Eds.), *Performance Based Specifications and Control of Concrete Durability*. State-of-the-Art Report RILEM TC 230-PSC, Springer, New York (USA), pp. 51-105. https://doi.org/10.1007/978-94-017-7309-6_4
- British Standards Institution (2013), "*BS EN-206: Concrete. Specification, performance, production and conformity*", (London, UK: CEN), p. 106.
- CCAA (2009), "*Chloride Resistance of Concrete*", (Sydney, Australia: Cement Concrete & Aggregates Australia), p. 37.
- CIRSOC 201-2005 (2005), "*Proyecto de Reglamento Argentino de Estructuras de Hormigón*", (Buenos Aires, Argentina: INTI), p. 452.
- Climent, M. A., de Vera, G., López, J. F., Viqueira, E., Andrade, C. (2002), "*A test method for measuring chloride diffusion coefficients through non-saturated concrete. Part I: the instantaneous plane source diffusion case*", *Cement and Concrete Research*, Vol. 32, p. 1113–1123. [https://doi.org/10.1016/S0008-8846\(02\)00750-0](https://doi.org/10.1016/S0008-8846(02)00750-0)
- Colleparidi, L., Marcialis, A., Turriziani, R. (1970), "*La cinetica di penetrazione degli ioni cloruro nel calcestruzzo*", *Il Cemento*, N°67, pp. 157-164.
- Delagrave, A., Bigas, J. P., Ollivier, J. P., Marchand, J., Pigeon, M. (1997a), "*Influence of the interfacial zone chloride diffusivity of mortars*", *Advanced Cement Based Materials*, Vol. 5, pp. 86-92. [https://doi.org/10.1016/S1065-7355\(96\)00008-9](https://doi.org/10.1016/S1065-7355(96)00008-9)
- Delagrave, A., Marchand, J., Ollivier, J. O., Juliens, S., Hazrati, K. (1997b), "*Chloride binding capacity of various hydrated cement paste systems*", *Advanced Cement Based Materials*, Vol. 6, pp. 28-35. [https://doi.org/10.1016/S1065-7355\(97\)90003-1](https://doi.org/10.1016/S1065-7355(97)90003-1)
- Di Maio, A. A., Eperjesi, L., Gassa, L., Traversa, L. P., Zerbino, R. L., (2000), "*Exposed reinforcement: Assessment of corrosion activity*", *Concrete International*, Vol. 22, N°3, pp. 47-51.
- Di Maio, A. A., Lima, L. J., Traversa, L. P. (2004), "*Chloride profiles and diffusion coefficients in structures located in marine environments*", *Structural Concrete*, Vol. 5, N°1, pp. 1-4. <https://doi.org/10.1680/stco.2004.5.1.1>
- DURAR (1997), "*DURAR - Manual de inspección, evaluación y diagnóstico de corrosión en estructuras de hormigón armado*", (Maracaibo, Venezuela: CYTED), p. 205.
- Fernández Luco, L. (2001), "*La durabilidad del Hormigón: su relación con la estructura de poros y los mecanismos de transporte de fluidos*", in: E. F. Irassar (Ed.), *Durabilidad del Hormigón Estructural*, AATH, Buenos Aires (Argentina), pp. 1-45.
- Frederiksen, J. M., Sørensen, H. E., Andersen, A., Klinghoffer, O. (1997), "*HETEK, The effect of the w/c ratio on chloride transport into concrete - Immersion, migration and resistivity tests*", (Copenhagen, Denmark: The Road Directorate), 35 p. <https://doi.org/10.13140/2.1.3735.3600>
- Glass, G. K., Buenfeld, N. R. (2000), "*The influence of chloride binding on the chloride induced corrosion risk in reinforced concrete*", *Corrosion Science*, Vol. 42, pp. 329-344. [https://doi.org/10.1016/S0010-938X\(99\)00083-9](https://doi.org/10.1016/S0010-938X(99)00083-9)
- IRAM 1554 (1983), "*Hormigón de Cemento Pórtland. Método de determinación de la penetración de agua a presión en el hormigón endurecido*", (Buenos Aires, Argentina: IRAM), p. 13.
- IRAM 1857 (2000), "*Determinación del contenido de ión cloruro en el hormigón*". (Buenos Aires, Argentina: IRAM), p. 19.
- IRAM 1871 (2004), "*Hormigón. Método para la determinación de la capacidad y velocidad de succión capilar de agua para hormigón endurecido*", (Buenos Aires, Argentina: IRAM), p. 12.

- Kropp, J., Basheer, L. (2000), "Assessment of the durability of concrete from its permeation properties: A Review", in: Basheer, P.A.M. (Ed.), V CANMET/ACI International Conference on Durability of Concrete, Barcelona (Spain).
- Monosi, S., Moriconi, G., Alverá, I. (1989), "Effect of water/cement ratio and curing time on chloride penetration into concrete", *Materials Engineering*, Vol. 1, pp. 483-489.
- Neville, A. M. (1977), "Concrete Technology, Volume 1", (Mexico D.F., Mexico: IMCyC), p. 383.
- Nielsen, E. P., Geiker, M. R. (2003), "Chloride diffusion in partially saturated cementitious material", *Cement and Concrete Research*, Vol. 33, p. 133-138. [https://doi.org/10.1016/S0008-8846\(02\)00939-0](https://doi.org/10.1016/S0008-8846(02)00939-0)
- Rostam, S. (2000), "Vida útil de las estructuras de hormigón. Cómo satisfacer los requerimientos del nuevo milenio", *Hormigón*, N°36, pp. 11-44.
- Saetta, A. V., Scotta, R. V., Vitaliani, R. V. (1993), "Analysis of chloride diffusion into partially saturated concrete", *ACI Materials Journal*, Vol. 90, p. 441-451.
- Sandberg, P., Tang, L., Andersen, A. (1998), "Recurrent studies of chloride ingress in uncracked marine concrete at various exposure times and elevations", *Cement and Concrete Research*, Vol. 28, pp. 1489-1503. [https://doi.org/10.1016/S0008-8846\(98\)00124-0](https://doi.org/10.1016/S0008-8846(98)00124-0)
- Song, H. -W., Lee, C. -H., Ann, K. Y., (2008), "Factors influencing chloride transport in concrete structures exposed to marine environments", *Cement & concrete Composites*, Vol. 30, pp. 113-121. <https://doi.org/10.1016/j.cemconcomp.2007.09.005>
- Taus, V. L. (2010), "Análisis de la Succión Capilar en Hormigones: Influencia de distintos Parámetros de Ensayo", MSc Thesis, UNCPBA, p. 170.
- Taus, V. L., Villagrán, Y. A., Di Maio, A. A. (2008), "Influence of curing conditions on transport properties of blended cement concrete", in: Pazzini et al. (Eds.), Fifth ACI/CANMET International Conference on High-Performance Concrete Structures and Materials, Manaus (Brazil).
- Traversa, L. P. (2001), "Corrosión de armaduras en atmósferas rurales, urbanas, marinas e industriales", in: E.F. Irassar (Ed.), Durabilidad del Hormigón Estructural, AATH, Buenos Aires (Argentina), (2001), pp 217-257.
- Traversa, L. P., Di Maio, A. A. (2002), "Difusión de cloruros en el hormigón", in: L. P. Traversa, A. A. Di Maio (Eds.), Memoria Jornadas Tecnológicas sobre Corrosión de Armaduras en Estructuras de Hormigón: Evaluación, Diagnóstico y Reparación, AATH, Mar del Plata (Argentina), pp. 87-95.
- Tuutti, K. (1982), "Corrosion of steel in concrete", PhD Thesis, SCCI, CIB, Research Report No. 4, p. 468.
- Villagrán Zaccardi, Y. A. (2012), "Estimaciones del ingreso de cloruro en hormigón y de la despasivación localizada de armaduras", PhD Thesis, UNLP, p. 226.
- Violini, D., Giaccio, G., Milanese, C. A., Zerbino, R. (2006), "Efecto del contenido de caliza, en las propiedades del hormigón. Parte 3: Evaluación de la durabilidad", in: Sota et al. (Eds.), 16ª Reunión Técnica de la Asociación Argentina de Tecnología del Hormigón, Córdoba (Argentina).
- Zhang, Y., Zhang, M. (2014), "Transport properties in unsaturated cement-based materials – A review", *Construction and Building Materials*, Vol. 72, p. 367-379. <https://doi.org/10.1016/j.conbuildmat.2014.09.037>

Cracks width-corrosion rate correlation on the durability of reinforced concrete in a very high aggressiveness tropical marine environment

O. Troconis de Rincón^{1*} , V. Milano¹ , A. A. Torres-Acosta² , Y. Hernández-López¹ 

*Contact author: oladistr@gmail.com

DOI: <http://dx.doi.org/10.21041/ra.v8i3.321>

Reception: 12/06/2018 | Acceptance: 02/08/2018 | Publication: 31/08/2018

ABSTRACT

The aim of this investigation was to evaluate the correlation between crack width and apparent corrosion rate in reinforced concrete specimens exposed for more than six years to a tropical marine environment, at the natural test site La Voz, Venezuela. Six specimens from DURACON Project (prismatic 15x15x60 cm, with 0.65 w/c ratio) were monitored; each specimen having six reinforcing steel bars placed at three different depths (two each at 15, 20, and 30 mm) for electrochemical tests (corrosion potential and corrosion rate). An empirical correlation between surface crack propagation rate and i_{CORR} was established, which may help i_{CORR} estimation indirectly if values of maximum surface crack widths due to reinforcement corrosion are obtained in at least one-year period of monitoring.

Keywords: reinforced concrete; marine environment; corrosion rate; cracks width.

Cite as: O. Troconis de Rincón, V. Milano, A. A. Torres-Acosta, Y. Hernández-López (2018), “Cracks width-corrosion rate correlation on the durability of reinforced concrete in a very high aggressiveness tropical marine environment”, Revista ALCONPAT, 8 (3), pp. 317-332, DOI: <http://dx.doi.org/10.21041/ra.v8i3.321>

¹ Centro de Estudios de Corrosión (CEC), Facultad de Ingeniería, Universidad del Zulia, Maracaibo, Venezuela.

² Universidad Marista de Querétaro (UMQ), Facultad de Ingeniería, Laboratorio de Materiales de Construcción; Instituto Mexicano del Transporte (IMT), Coordinación de Ingeniería Vehicular e Integridad Estructural, Sanfandila, Querétaro, México.

Legal Information

Revista ALCONPAT is a quarterly publication by the Asociación Latinoamericana de Control de Calidad, Patología y Recuperación de la Construcción, Internacional, A.C., Km. 6 antigua carretera a Progreso, Mérida, Yucatán, 97310, Tel.5219997385893, alconpat.int@gmail.com, Website: www.alconpat.org

Responsible editor: Pedro Castro Borges, Ph.D. Reservation of rights for exclusive use No.04-2013-011717330300-203, and ISSN 2007-6835, both granted by the Instituto Nacional de Derecho de Autor. Responsible for the last update of this issue, Informatics Unit ALCONPAT, Elizabeth Sabido Maldonado, Km. 6, antigua carretera a Progreso, Mérida, Yucatán, C.P. 97310.

The views of the authors do not necessarily reflect the position of the editor.

The total or partial reproduction of the contents and images of the publication is strictly prohibited without the previous authorization of ALCONPAT Internacional A.C.

Any dispute, including the replies of the authors, will be published in the second issue of 2019 provided that the information is received before the closing of the first issue of 2019.

Correlación entre ancho de grietas y velocidad de corrosión en la durabilidad de concreto reforzado en un ambiente marino tropical altamente agresivo

RESUMEN

El objetivo de esta investigación fue evaluar la correlación entre ancho de grieta producido por corrosión y la velocidad de corrosión aparente (i_{CORR}) de especímenes de concreto reforzado, expuestos por más de 6 años a un ambiente marino tropical en la estación La Voz, Venezuela. Seis especímenes del Proyecto DURACON (prismas de 15x15x60 cm, y concreto con relación a/c de 0.65) fueron monitoreados; los cuales tienen 6 varillas de refuerzo a diferentes profundidades (dos a 15, 20 y 30 mm), para las pruebas electroquímicas. Se estableció una correlación empírica entre la velocidad de propagación de la grieta superficial e i_{CORR} , que podría ayudar a estimar el valor de i_{CORR} , si se dispone de valores promedio de ancho máximo de grieta del elemento corroyéndose durante un periodo de monitoreo por lo menos de un año.

Palabras clave: concreto reforzado; ambiente marino; velocidad de corrosión; ancho de grieta.

Correlação entre a largura da fissura e a taxa de corrosão na durabilidade do concreto armado em um ambiente marinho tropical altamente agressivo.

RESUMO

O objetivo desta investigação foi avaliar a correlação entre largura de fissura e taxa de corrosão aparente em espécimes de concreto armado expostos há mais de seis anos a um ambiente marinho tropical, no local de teste natural La Voz, Venezuela. Seis espécimes do Projeto DURACON (15x15x60 cm prismáticos, com relação 0,65 w / c) foram monitorados; cada espécime possui seis barras de aço de reforço colocadas em três profundidades diferentes (duas de 15, 20 e 30 mm cada) para testes eletroquímicos (potencial de corrosão e taxa de corrosão). Uma correlação empírica entre taxa de propagação de trincas superficiais e i_{CORR} foi estabelecida, o que pode ajudar a estimar a i_{CORR} indiretamente se valores de largura máxima de trincas superficiais devido à corrosão de reforço forem obtidos em pelo menos um ano de monitoramento.

Palavras-chave: concreto reforçado; ambiente marino; velocidade de corrosão; ancho de grieta.

1. INTRODUCTION

During the last 20 years, the term concrete durability has been used more frequently among members of the scientific society worldwide. In some developed countries as the United States of America, Spain, France, United Kingdom, and Japan, durability has been addressed as a very important subject, attracting seven figures investment for research in this area. Reinforced concrete structure deterioration due to rebar corrosion has increased as consequence of cracks on the concrete cover surface. Many investigations so far, have been performed based on the study of durability during the initiation period. However, very few have been focused toward its performance during its residual life.

Some studies related to the residual life stage of concrete structures, have been made where accelerated corrosion was performed by applying a constant anodic current to the rebars (Tachibana, et.al., 1990; Huang and Yang, 1997; Rodriguez et.al., 1997; Almusallam, et.al., (1997); Cabrera, 1996). After applying such anodic currents to the rebar in a short period of time, reduction of the structural capacity was correlated with corrosion parameters such as gravimetric metal loss and corrosion-induced concrete cracking (Almusallam, 1997; Mangat and Elgarf, 1999; Torres-Acosta, 1999). Torres-Acosta, 1999; Torres-Acosta and Martínez-Madrid, 2003, have conducted several studies related to

this subject, but also under natural conditions (Torres-Acosta and Castro-Borges, 2013; Cabrera-Madrid et al, 2014). In a previous investigation (Torres-Acosta and Martínez-Madrid, 2003), they reported results on residual life degradation parameters, using reinforced concrete slabs (0.42 w/c ratio, chloride contamination during mixing to accelerate rebar corrosion) and no anodic current application. At the end of the experimentation, corrosion-induced crack position, width, and length were measured and correlations with the cross-section mass loss were also performed. Based in their experimental results, empirical relationships between average rebar radius loss (x_{AVG}) divided by the original rebar radius (r_0) and load capacity were established. As an example, 10% radius loss might result in a 50% load capacity loss in reinforced concrete beam elements. They also developed an empirical relationship between crack width, WC, and the relation x_{AVG}/r_0 . Apparently, when corrosion rate is small ($12\text{-}60 \mu\text{m y}^{-1}$) cracks appear and grow in length and width faster than in accelerated corrosion tests. Finally, the last empirical correlation obtained included x_{AVG} and maximum pit depth (PIT_{MAX}), giving a factor of seven times: $PIT_{MAX} \sim 7 \cdot x_{AVG}$ (Torres-Acosta and Martínez-Madrid, 2003).

Subsequently, in 2003, Vidal et.al. studied crack width and rebar diameter loss due to corrosion in reinforced concrete beams (0.5 w/c, 35 g l^{-1} NaCl contamination). They discussed that reinforcement corrosion obtained in this investigation is closer to what is observed in natural conditions (with respect to the distribution of corrosion, types of corrosion, and oxides produced) than the obtained by impressed current or addition of calcium chloride in concrete. They developed a new model relating crack width vs. rebar cross section loss and observed that the rebar cross section loss seems to be independent of their diameter and the concrete cover/rebar diameter ratio, except when evaluated in the period of crack initiation.

In 2007, Torres-Acosta et.al. reported an empirical correlation between rebar corrosion rate and crack width, using reinforced concrete beams (0.6 w/c, contaminated with NaCl: 1 wt% Cl^- on cement basis), and subjected to a bending stress. The beams were sprayed in a central area of 25 cm long twice a week, with saline solution (3.5 wt% Cl^-) in order to accelerate rebar corrosion in this area. They concluded that in a process of natural corrosion, cracks generated by the corrosion products expansion develop more slowly (width and length) than those generated by accelerated corrosion. The results obtained, showed that for a corrosion radius loss (x_{AVG}/r_0) from 4% to 10%, cracks were produced with a maximum width (CW_{MAX}) of 0.1 mm and 1 mm, respectively. The trend obtained in this study was similar to that obtained in previous research with natural corrosion (Torres-Acosta and Castro-Borges, 2013; Cabrera-Madrid et al, 2014).

The present work show the results of one of DURACON project test natural exposure sites (La Voz, Venezuela). It was located in a coastal marine environment of high aggressiveness, where some of the reinforced concrete prisms (0.65 w/c ratio concrete) in this project presented surface corrosion-induced cracks, and an empirical correlation was obtained between maximum cracks width and corrosion rate (i_{CORR}) expressed as average rebar radius loss (x_{AVG}/r_0) from natural corrosion data.

2. EXPERIMENTAL PROCEDURE

2.1 Prismatic specimens

In this investigation, reinforced concrete prismatic specimens from DURACON project (Troconis de Rincón et.al., 2007) were used. These were installed in a project's natural exposure sites called La Voz (in Venezuela), classified as marine environment of very high aggressiveness (>C5 according to ISO⁽¹⁾ 9223: 2012. Figure 1 shows a schematic diagram of the prismatic specimens under evaluation. Concrete prisms of 15x15x30 cm (0.65 w/c ratio) and reinforced with six rebars

⁽¹⁾ISO, 1, Ch. de la Voie-Creuse, Case postale 56, CH-1211 Geneva 20, Switzerland.

(9.5 mm in diameter), placed at different concrete depths (two each at 15, 20 and 30 mm). Three of them were placed at the windward face and the other three on the leeward face. The ends of each bar were protected with epoxy coating to avoid oxygen differential and crevice corrosion, leaving a central portion of 15 cm length uncovered. Figure 2 shows the specimen supports installed at La Voz test station.

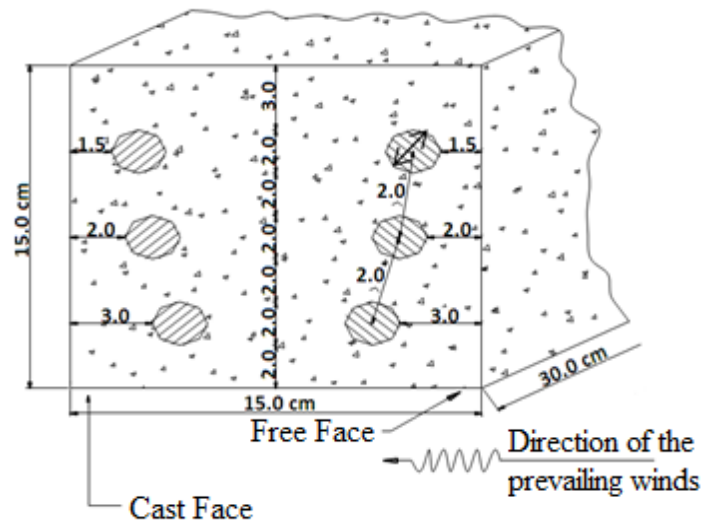


Figure 1. Schematic diagram of the rebar configuration in the concrete specimen



Figure 2. Test Station in Marine Environment (La Voz)

2.2 Environmental assessment

Climatic and environmental parameters were assessed according to the methodology established by ISO 9223 standard determining environmental aggressivity in the test station. Parameters as relative humidity (RH), time of wetness (TOW/ τ), wind speed and direction, rainfall amount, daily temperature, chloride concentration, CO₂ concentration and sulfur compounds concentration, were measured during the experimental period. It is important to mention that there are currently no regulations to identify the aggressiveness of the environment for reinforced concrete structures; therefore, ISO standard for metallic materials was used as a first approach.

2.3 Electrochemical evaluation

For electrochemical monitoring, a GECOR 6^(†2) field corrosimeter instrument was used, which measured corrosion potential (E_{CORR} , vs. Cu/CuSO₄ reference electrode), and corrosion rate (i_{CORR}) of the reinforcement, by the linear polarization technique (Feliú et.al., 1993).

2.4 Cracks survey

Rebar corrosion-induced concrete surface cracks, both in the windward face as well as in the leeward face were monitored by a careful visual examination using a (nonstandard) 15cm x 30cm grid to report the length and location of each corrosion crack. Cracks widths were measured using a crack comparator card. Thereby, an overview crack map was recorded, showing the length, location, and width of all cracks in all specimens. Experimental data were fitted linearly and compared with data obtained by other authors with natural and accelerated corrosion techniques. In order to assess the rebar cross section loss, an estimate was made using the area under i_{CORR} vs. time plot. This value was then correlated with maximum crack width (MCW), corresponding to each of the rebars of the specimens tested. Rebar mass loss estimates were calculated using Faraday law (Equation [1]):

$$\Delta W_f = \frac{55.5}{n \times F} \left(\int I dt \right) \quad (1)$$

Where: ΔW_f is faradaic mass loss (g); 55.85 g/mol is the atomic weight of Fe; $\int I dt$ is the area under the curve i_{CORR} vs. time; n is the valence number for iron (+2), and F is Faraday's constant (96,500 C/mol). This value is then used to estimate the average radius loss due to corrosion (X_{AVG}), in mm, which is calculated using Equation (2):

$$X_{avg} = \frac{\Delta W_f \times 1000}{\rho \times \pi \times D \times l} \quad (2)$$

Where: ρ , iron density (gr/cm³); D , rebar diameter (mm) and l , length of the rebar (mm). At the end of the experimentation, concrete specimens were demolished and the steel rebars were retrieved to determine the real cross section loss based on average pit depth estimates.

3. RESULTS AND DISCUSSION

3.1 Environmental assessment

Figure 3 shows the weather parameters results of the natural test site monitored during the exposure time. It is clear to observe the rain-drought periods, typical of tropical environments. There was only one short period of high rain precipitation and was at the end of year 2006, as a result of the weather phenomenon caused by hurricane Ivan, which passed through the Lesser Antilles and the Caribbean Sea.

Regarding monthly average temperature, it varied only 3 °C during the entire evaluation period (six years). The minimum value was 26.7 °C (March 2003 and February 2009), while the maximum value was about 30 °C (October 2004 and September 2008). The small variations observed for this parameter, shows a climatic stability in this test station and the geographic region itself.

^(†2) Trade name

The highest monthly average relative humidity (RH) value from the whole evaluation period was observed in August 2004, which was 84%. This coincides with the highest rain precipitation value for the year.

For wind speed data, in general it can be seen that it vary in a range between 17 and 24 km/h, with large variations when sudden changes occur in the microclimate, as the phenomena that have been explained above where the wind speed was substantially increased. Chloride and sulfate estimates present in this atmosphere and the time of wetness during the 6-year exposure time are shown in Table 1. A very high corrosive ambient, according to ISO 9223, for the first three years of this test station, was corroborated based on the monitoring of parameters in Table 1. For the 4th and 5th year, a decrease in corrosivity was noticed, possibly due to high rainfall from storms and hurricanes occurred in those years; however, remains highly corrosive. The time of wetness (TOW) was also estimated with the weather parameters such as temperature and RH using ISO procedure (see Table 1).

Table 1. Aggressive agents and time of wetness (TOW) at the test station La Voz

Evaluation Time (y)	Chlorides (mg m ⁻² d ⁻¹) /S		Sulfates (mg m ⁻² d ⁻¹) /P		TOW (hy ⁻¹) /τ		ISO 9223 Corrosivity class
1	683.907	S3	22.645	P1	4818	τ4	C5
2	382.561	S3	27.800	P1	4818	τ4	C5
3	128.898	S2	19.726	P1	6132	τ5	C5
4	154.159	S2	13.111	P1	3451	τ4	C4
5	165.691	S2	5.616	P0	2823	τ4	C4
6	183.682	S2	-		-		-

Corrosion induced by chloride ions attack was favored because high relative humidity facilitates the transport of aggressive agents in the atmosphere enhanced by the high temperature, which accelerates localized corrosion of the bars.

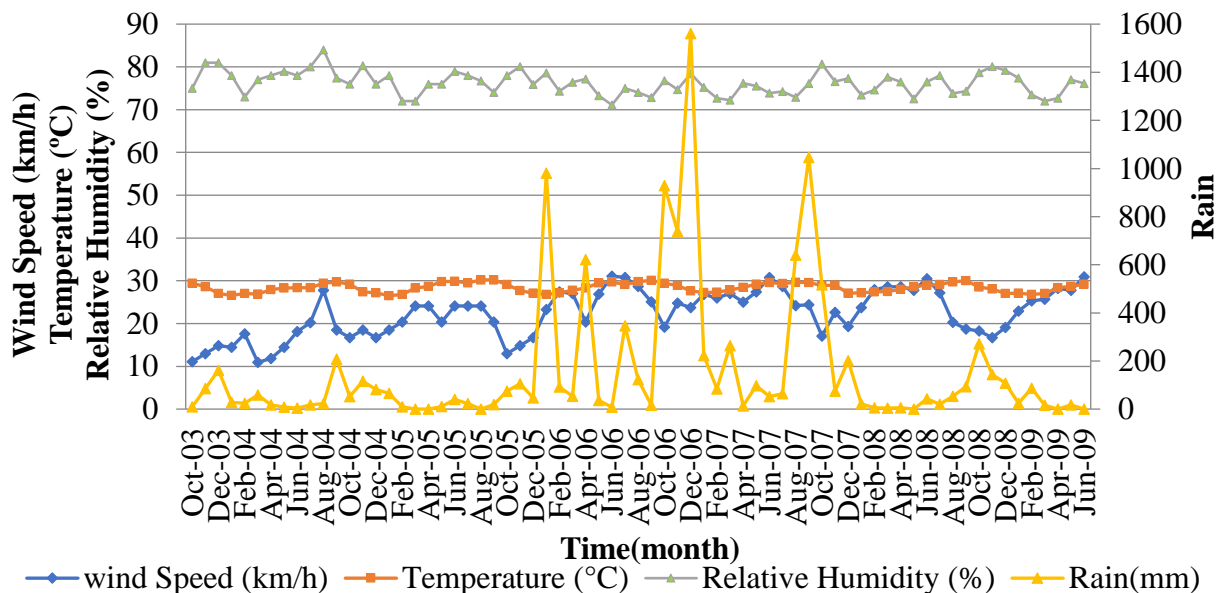


Figure 3. Behavior of meteorological parameters at test station La Voz.

3.2 Electrochemical parameters

Figures 4 and 5 show the results obtained from the electrochemical monitoring: corrosion potential and corrosion rate vs. time for 15-mm and 30-mm concrete depth rebar, respectively. These figures clearly show the time in which the bars began to depassivate (E_{CORR} and i_{CORR} more negative than -250 mV vs. Cu/CuSO₄ and greater than 0.1 $\mu\text{A}/\text{cm}^2$, respectively); coinciding with the first change in slope of the accumulated corrosion rate vs. time curve. In addition, these figures show 30-mm depth rebars stayed passive for longer time than the 15-mm depth rebars, but the propagation rate for the first set were higher than the second set. This might be due to the winds at the La Voz natural test site did not show a preferential trade wind direction (North-East in this case), but rather slashing winds which also allows the ingress and diffusion of chloride ions through the prism's bottom face. This was the top cast face and the most porous one, which was the closer to the deeper bars (30-mm depth rebars), thus giving this unusual performance.

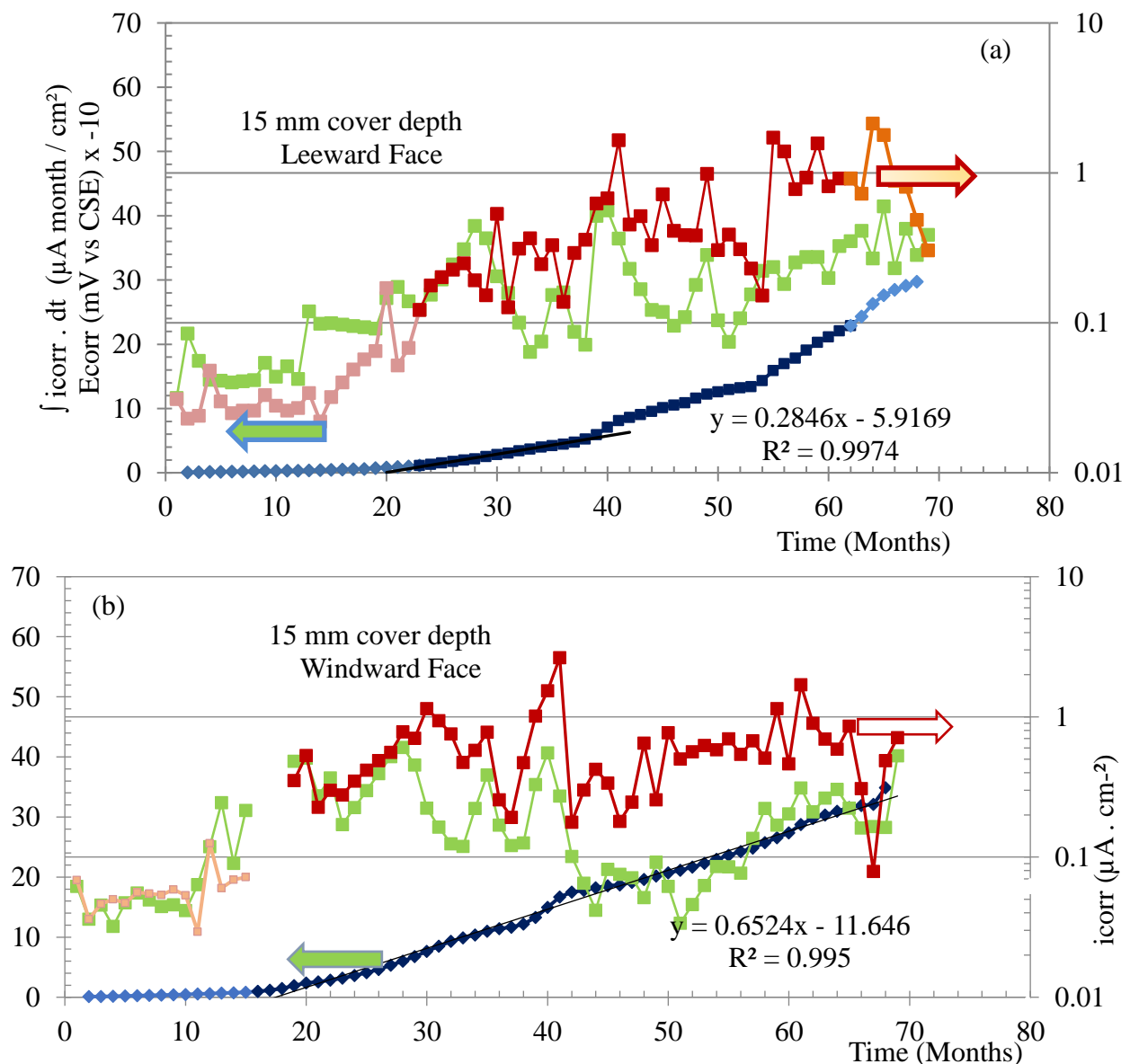


Figure 4. Electrochemical parameter monitoring (E_{CORR} ; i_{CORR} and cumulative i_{CORR} values) vs. time for 15-mm concrete depth rebar, leeward (a) and windward (b) faces.

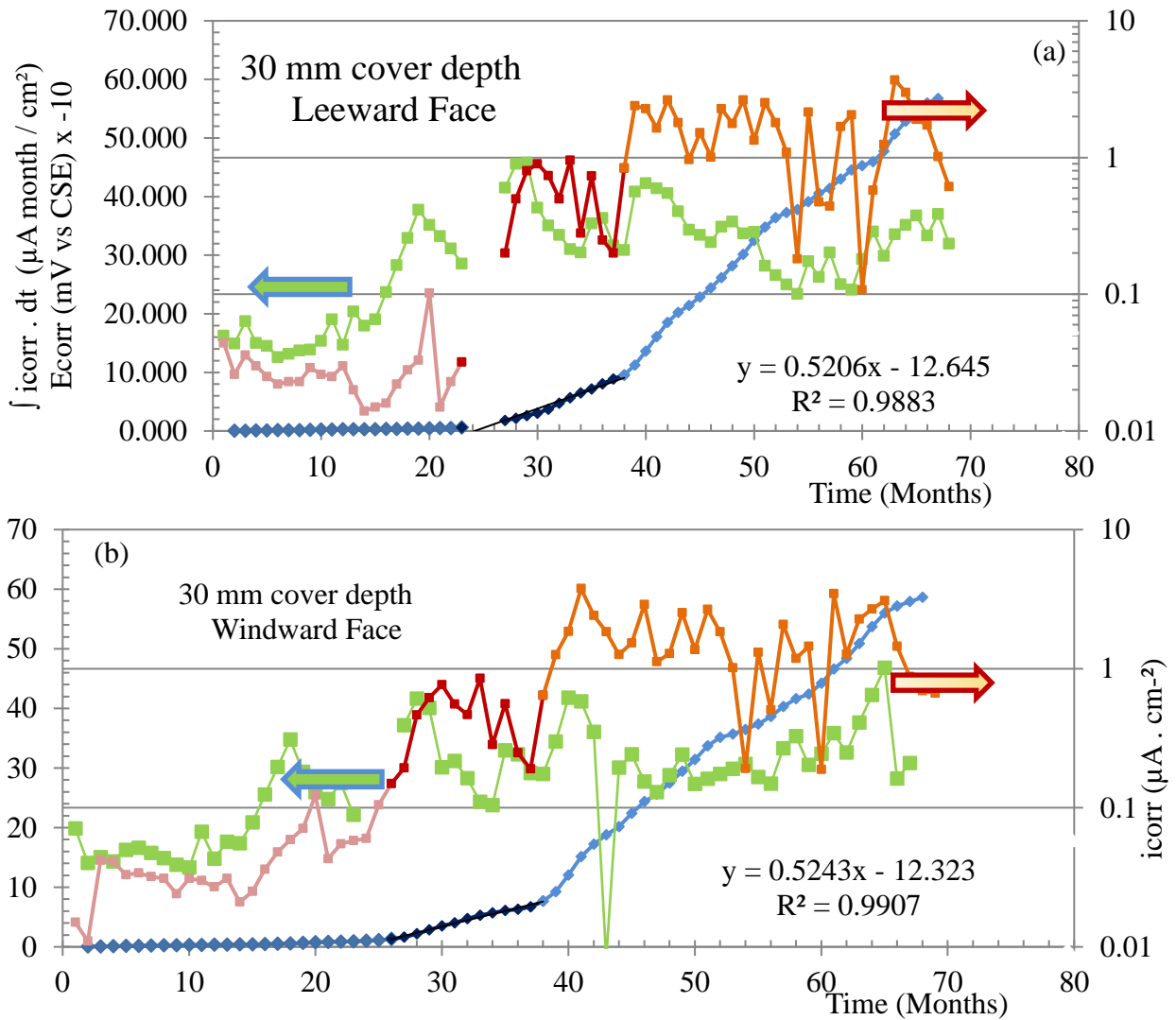


Figure 5. Electrochemical parameter monitoring (E_{CORR} ; i_{CORR} and cumulative i_{CORR} values) vs. time for 30-mm concrete depth rebar, leeward (a) and windward (b) faces.

3.3 Crack width and corrosion rate correlation

Figure 6 shows the state in which one of the three representative specimens were found after a 6 year exposure period in La Voz natural test site. This figure also shows a photograph of the specimen's windward face and a schematic representation of the surface fissures/cracks survey that presented such specimen.

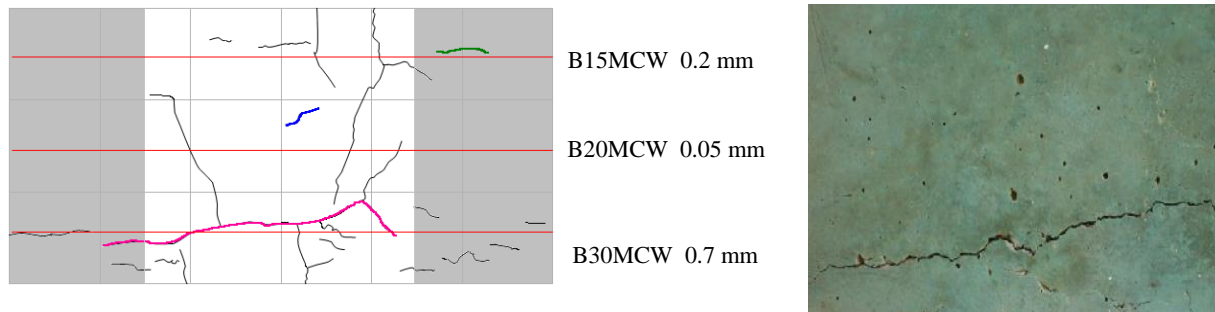


Figure 6. Specimen 6 (w/c ratio 0.65, and windward face) surface crack survey (left) and photographic evidence of such distress (right)

Figure 7 shows that with increasing loss of cross section area of the rebars (estimated from $\int i_{CORR}dt$ data and equations 1 and 2), the surface MCW also increases (at the specimen's windward face). The effect of the concrete cover on crack initiation and propagation (on the windward face) was also demonstrated in Figure 7: crack widths were bigger at rebars with smaller concrete cover having the same rebar cross section loss. This might be due to the concurrent effect of high relative humidity prevailing in the area (> 80%) together with a high chloride ions content, which maintains moisture inside the bulk concrete, such that the chloride ions (129-684 mg m⁻²d) can diffuse easily, promoting reinforcement corrosion.

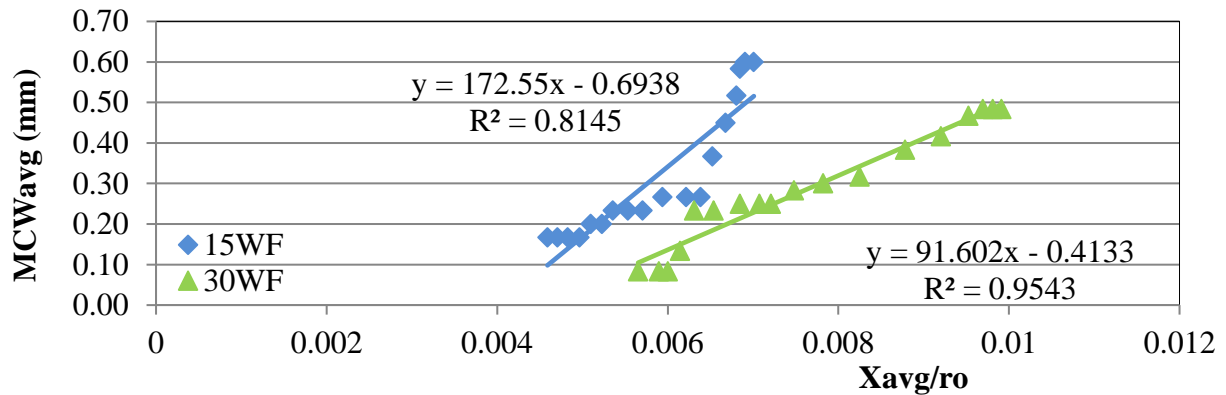


Figure 7. Average maximum crack width of concrete in relation to the rebar cross section loss, at the natural test site La Voz, w/c ratio 0.65, windward face

It is also important to mention that there is a direct relationship between the MCW and rebar's x_{AVG}/r_0 . The goodness of the correlation is high for the first years of exposure (MCW < 0.3 mm), while for MCW's wider than 0.3 mm the data was disperse, causing the correlation to decrease. Additionally, the mean MCW increases with very little loss of material due to corrosion. Also when MCW's are too wide, voids were created, which interfered with the i_{CORR} measurement using the described corrosimeter field instrument. This raises some doubts over the last year's i_{CORR} data, which was used to obtain x_{AVG}/r_0 . Thus, it was necessary to discard the latest i_{CORR} measurements and determine the correlation between MCW and x_{AVG}/r_0 using first year data.

A more representative correlation between MCW and x_{AVG}/r_0 are presented in Figure 8, where the last years i_{CORR} bias measurements of both bars were removed, thus better correlations were obtained ($R^2 \sim 0.9722$ and 0.9038 for 15-mm and 30-mm depth rebar, respectively).

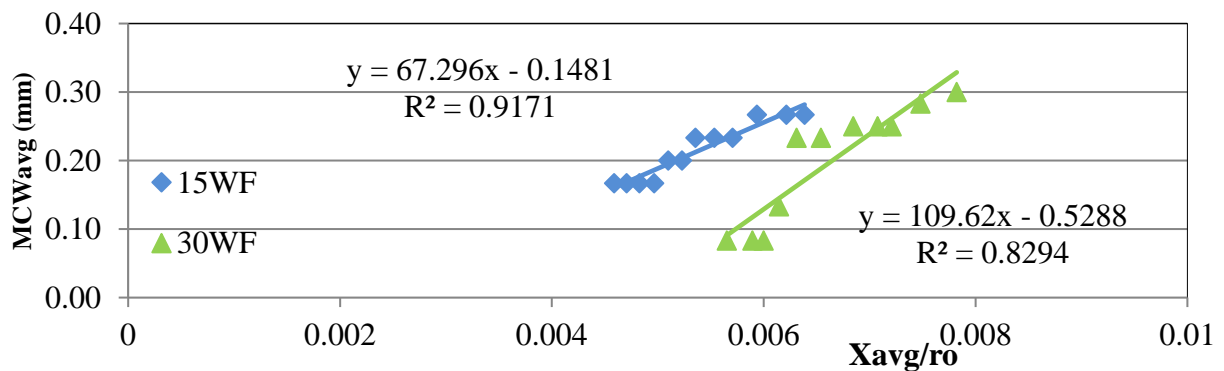


Figure 8. Representative behavior (last year's data removed) of the average maximum crack width of concrete in relation to the rebar cross section loss, at the natural test site La Voz, w/c ratio 0.65, windward face

Figure 9 shows a typical crack surveys and photograph of one of the specimen's leeward face from a representative 0.65 w/c concrete specimen after 6 years of exposure. As observed from these results, wider cracks were observed than at the windward face. This performance might be due because it remains wet for longer periods of time, which favors the transport of characteristic environment's aggressive agents, and spread into the bulk concrete as compared to the windward face, which was in continuous contact with hot/high speed wind that could dry out the concrete's internal moisture. This performance is observed also in Figures 4 and 5, where the corrosion rates of leeward face rebars show small increments at the end of the exposure period.

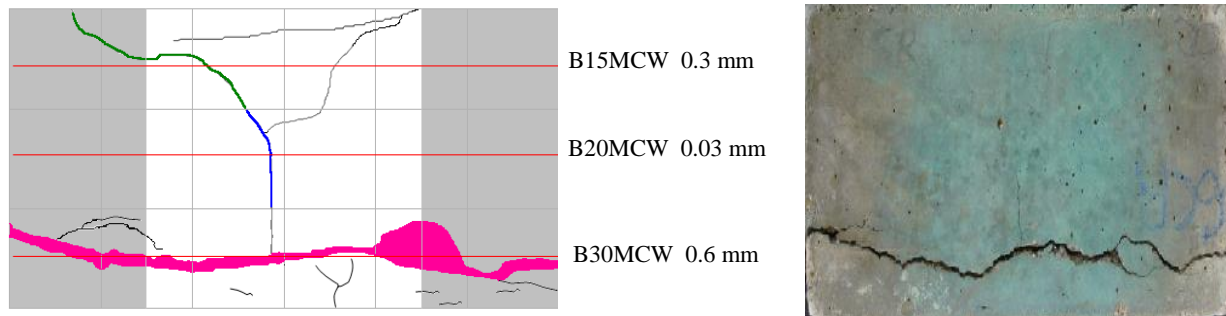


Figure 9. Left, General map of cracks and right, photo of the specimen 6, w/c ratio 0.65, leeward face

Similarly to the windward face data, the leeward face data did not have good correlation between the MCW and rebar's x_{AVG}/r_0 when cracks were wider than 0.5 mm, and the last year data points were also bias. Thus in Figure 10, the more representative relationship between MCW and x_{AVG}/r_0 was obtained by removing last year's data of the two rebars, which significantly improves the correlation ($R^2 \sim 0.9397$ and 0.9843 for the 15-mm and 30-mm depth rebar, respectively).

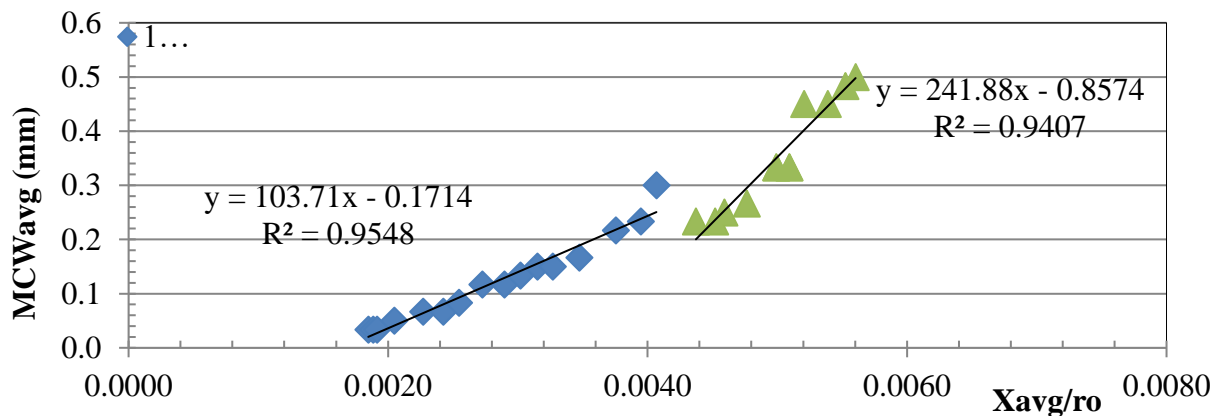


Figure 10. Representative behavior (last year's data removed) of the average maximum crack width in relation to the loss cross section area of the bar at the test station La Voz, w/c ratio 0.65, leeward face

On the other hand, the effect of concrete cover on crack propagation unexpectedly was the opposite than the windward performance: the largest crack widths were found for the 30-mm depth rebar. This might be due to (as explained in Section 3.2) the winds at the La Voz natural test site did not show a preferential trade wind direction (North-East in this case), but rather slashing winds which also allows the ingress and diffusion of chloride ions through the prism's bottom face. This was the top cast face and the most porous one and the closer to the deeper bars (30-mm depth rebar), thus giving this unusual performance.

Figure 11 shows as a comparison, a compilation of the MCW_{avr} (average MCW) and x_{avr}/r_0 data obtained in this investigation together with data from a previous investigation (Torres-Acosta and Martínez-Madrid, 2003) with natural and accelerated corrosion conditions. Accelerated corrosion data was plotted in Figure 11 using symbols without any filling color, as compared the natural corrosion data symbols, which all are either black filled for previous investigations data or blue-pink-orange for this investigation data.

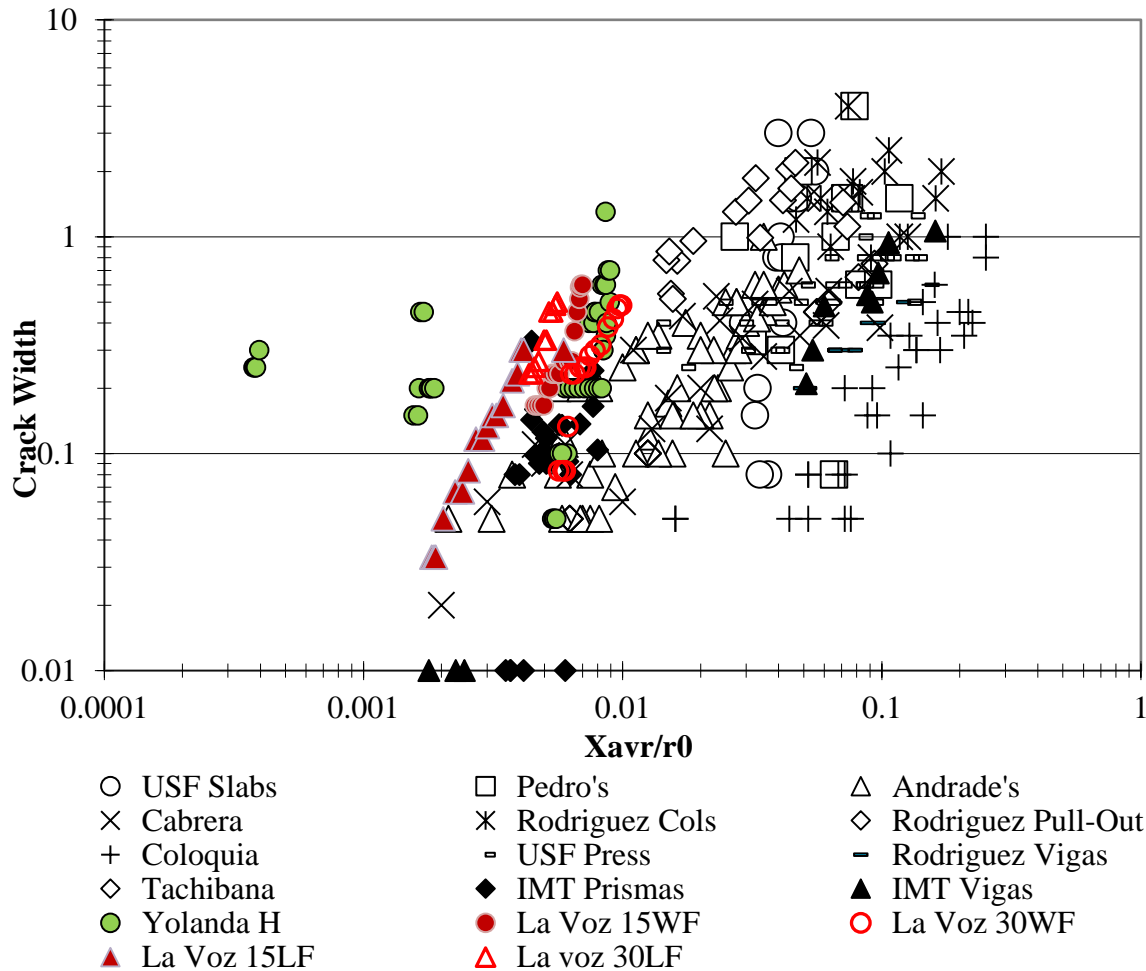


Figure 11. Data compilation of average maximum crack width in relation to the loss cross section area of the bar for different authors and test conditions (Torres-Acosta and Martínez-Madrid, 2003)

It is observed that in the case of accelerated corrosion methods, data follow a good trend and are close from each other (Torres-Acosta and Martínez-Madrid, 2003). There is also a difference between accelerated corrosion data from reinforced concrete (Δ , \times , \diamond , \circ , \ast , \square symbols) vs prestressed concrete (+ symbol) elements when general corrosion was obtained: wider cracks were observed from reinforced concrete elements than from prestressed concrete elements. If the corrosion is localized in a small area of the strand (- symbol) in prestressed concrete elements instead of general corrosion (+ symbol), the crack widths trend was similar than the obtained in reinforced concrete elements. Therefore, if the entire prestressed strand (or wire) is corroded, the crack propagation apparently was mitigated by the compressive state of stresses in the concrete, but if the prestressed strand (or wire) corrodes only in a short portion of the entire length, the crack propagation follows reinforced concrete elements trend.

On the other hand, natural corrosion data presented a more disperse performance than accelerated corrosion, as seen from the colored symbols. In general, the natural corrosion data follows similar trend than accelerated corrosion data, but with higher crack widening (higher Crack Width vs x/r_0 slope). The higher crack propagation rate in natural corrosion tests may indicate that crack repair might be done earlier than the obtained from accelerated corrosion tests. This performance must be checked with collection of a larger data from the literature and data in the remaining DURACON project outcomes.

Data from this investigation follows a well-defined trend: less corrosion-induced material loss is required for cracks to appear at the concrete element surface. In natural conditions, like the present investigation's specimens, the concrete is affected by the ingress of aggressive agents such as chlorides ions, which produce a localized rupture of the passive film until corrosion products are formed in sufficient amount to crack the concrete, which depends on concrete quality (internal porosity).

This cracking process on low quality concrete, may requires a smaller amount of corrosion products for crack formation and propagation (Torres-Acosta and Castro-Borges, 2013; Torres-Acosta et al., 2007). But compared with previous investigations with natural corrosion specimens exposed during a period between 3 and 6 years (■, ●, ◆ symbols), there is a difference of, approximately, 10 times the amount of mass needed to produce the same crack wideness.

It is important to remind that data from this investigation were obtained from electrochemical mass loss determinations, mainly linear polarization resistance (or also known as R_p). If corrosion were uniform, the faradaic metal loss might be twice as much as the estimated gravimetric metal loss, but if rebar corrosion is localized (i.e. pitting corrosion), the faradaic metal loss could be estimated even up to ten times the gravimetric metal loss (González et.al., 1995). All rebar radius loss data in Figure 11 was estimated from gravimetric procedure, except data from Hernández et.al.2016 (green color points) and the present investigation. Actual rebar loss estimates in these two investigations also have the particularity of being performed in highly porous concrete (with w/c ratio > 0.65), therefore, lower mechanical strength and easier crack formation is also expected.

Similar concrete type was used by Hernández et.al., 2016, to fabricate beams that were some of them loaded at the same time they were exposed to chloride rinse at the center of the beam elements to produce corrosion without using anodic currents. As seen in Figure 11, data from loaded beams (Hernández et.al., 2016) separate from all the natural and accelerated data to lower radius loss for same MCW_{avr} opening. This performance might be due to not only the possible differences between gravimetric and the faradaic mass loss, but also from the applied tensile stresses from flexure loading application, that may increase the crack opening propagation rate. In same reference some other beams were unloaded, thus the MCW_{avr} vs x/r_0 data follows similar trend than the present investigation where concrete prism tested maintained unloaded during experimentation.

3.4 Empirical correlation between reinforcement corrosion rate and surface crack propagation rate

Figure 12 shows the crack width propagation vs. time of exposure. As observed in this figure, there is no correlation between rebar depth and crack propagation for these specimens located at La Voz, Venezuela, test site. Two of the cracks on each rebar depth behaved in the same range of maximum crack widths (between 0.05 and 0.3 mm), and only one of such cracks showed wider maximum crack (about 0.4 mm and above). The regression lines for each crack propagation are also shown in Figure 12, showing goodness fitness above 0.8. The slope of such regression lines are considered in this investigation as the surface crack propagation rate (SCPR in mm/month).

Based on the available data up to date, an empirical correlation between SCPR and i_{CORR} results was performed and shown in Figure 13. As observed from this figure, there is not an apparent difference between the correlation for 15 mm and 30 mm. Upon further experimental data from the other w/c ratio concrete prisms in La Voz, Venezuela, test site and the other active corrosion prisms, when surface cracks appeared at the concrete element, the rate of widening is directly proportional to the i_{CORR} of the rebar, which in turns is the expansive oxides to produce such cracks.

This empirical correlation will help to establish an indirect estimate of the corrosion rate of the reinforcing steel if the people in charge of the maintenance of the corroded structure is not able to have test equipment to determine such electrochemical values, and only a crack width survey is performed in a period of time for at least one year (12 months).

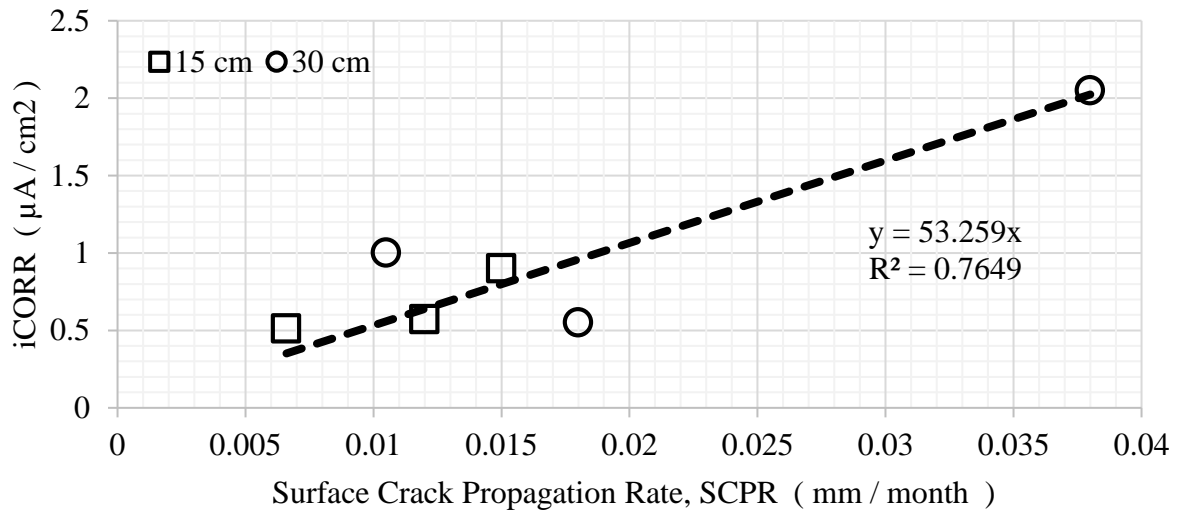


Figure 13. Empirical correlation between SCPR and i_{CORR} , 0.65 w/c ratio concrete prisms, La Voz, Venezuela, natural test site

4. CONCLUSIONS

1. An excellent correlation between average maximum crack width (MCW_{AVER}) and corrosion-induced radius loss (x_{AVG}/r_0) (rebar with 15 mm and 30 mm concrete cover, at windward and leeward faces, for 0.65 w/c ratio specimens) was found, which can be used to predict the rebar section loss for a given crack width.
2. MCW_{AVG} vs x/r_0 trend slope for natural corrosion data was higher than the obtained from accelerated corrosion data. This might reduce time for rehabilitation of corroded concrete elements in naturally exposed structures in marine environment.
3. An empirical correlation between surface crack propagation rate (SCPR) and i_{CORR} was established for 0.65 w/c ratio prisms exposed to La Voz, Venezuela, test site, which can help to estimate i_{CORR} indirectly if values of MCW_{AVR} of corroding element are obtained in a period of time of at least one year.

5. ACKNOWLEDGMENTS

The authors would like to thanks CYTED and the Universidad del Zulia for funding this research, and all people whom help with the corrosion and crack survey monitoring for such a long period of time, this would not have being possible without them; also to Dr. Douglas Linares to help in the translation of the paper.

6. REFERENCES

- Almusallam, A. A., Al-Gahtani, A. S., Maslehuddin, M., Khan, M. M., Aziz, A. R. (1997), *Evaluation of Repair Materials for Functional Improvement of Slabs and Beams with Corroded Reinforcement*. Proc. ICE-Struct. Build 122 (1): 27-34.
- Cabrera, J.G. (1996), *Deterioration of concrete due to reinforcement steel corrosion*, Cement and Concrete Composites, 18 (1), pp. 47-59. [https://doi.org/10.1016/0958-9465\(95\)00043-7](https://doi.org/10.1016/0958-9465(95)00043-7)
- Cabrera-Madrid, J. A., Balancán-Zapata, M., Torres-Acosta, A. A., Castro-Borges, P. (2014) “*Effect of tropical marine microclimates on depassivation and corrosion-induced cracking of reinforced concrete*,” International Journal of Electrochemical Science, vol. 9, pp. 8211 – 8225, ISSN: 1452-3981.
- Feliú, S., González, J. A., Feliú, V., Feliú, S. Jr., Escudero, M. L., Rodríguez Maribona, I. A., Ausin, V., Andrade, M. C., Bolano, J. A., Jimenez, F. (1933), *Corrosion detecting probes for use with a corrosion-rate meter for electrochemically determining the corrosion rate of reinforced concrete structures*, U.S., Patent 5259944 A.
- González, J. A., Andrade, C., Alonso, C., Feliú, S. (1995), *Comparison of rates of general corrosion and maximum pitting penetration on concrete embedded Steel reinforcement*. Cement and Concrete Research, 25 (2), pp. 257-264. [https://doi.org/10.1016/0008-8846\(95\)00006-2](https://doi.org/10.1016/0008-8846(95)00006-2)
- Hernández, Y., de Rincón, O., Torres, A., Delgado, S., Rodríguez, J. (2016), “*Relación entre la Velocidad de Corrosión de la Armadura y el Ancho de Fisuras en Vigas de Concreto Armado Expuestas a Ambientes que Simulan el Medio Marino*”. Revista ALCONPAT, 6 (3), pp. 272-283. DOI: <http://dx.doi.org/10.21041/ra.v6i3.152>.
- Huang, R., Yang, C. C. (1997), *Condition Assessment of Reinforced Concrete Beams Relative to Reinforcement Corrosion*. Cement and Concrete Composites, 19 (2), pp. 131-137. [https://doi.org/10.1016/S0958-9465\(96\)00050-9](https://doi.org/10.1016/S0958-9465(96)00050-9)
- ISO 9223:2012 (latest revision), “*Corrosion of metals and alloys -- Corrosivity of atmospheres -- Classification, determination and estimation*”, (Geneva, Switzerland: ISO).
- Mangat, P. S., Elgarf, M. S. (1999), “*Strength and serviceability of repaired reinforced concrete beams undergoing reinforcement corrosion*”. Magazine of Concrete Research, 51 (2), pp. 97-112. <https://doi.org/10.1680/mac.1999.51.2.97>
- Rodríguez, J., Ortega, L. M., Casal, J. (1997), *Load carrying capacity of concrete structures with corroded reinforcement*, Construction and Building Materials, 11 (4), pp. 239-248. [https://doi.org/10.1016/S0950-0618\(97\)00043-3](https://doi.org/10.1016/S0950-0618(97)00043-3)
- Tachibana, Y., Maeda, K. I., Kajikawa, Y., Kawamura, M. (1990). “*Mechanical behaviour of RC beams damaged by corrosion of reinforcement*. *Corrosion of Reinforcement in Concrete*” in Third International Symposium on Corrosion of Reinforcement in Concrete Construction, paper no. 00606810: Elsevier Science Publishers/CICC Publications, ISBN: 1-85166-487-4, May 21-24, p. 178-187.
- Torres Acosta, A.A. (1999) “*Cracking induced by localized corrosion of reinforcement in chloride contaminated concrete*”, Ph.D. Thesis, University of South Florida, Tampa, FL.
- Torres Acosta, A. A., Martínez Madrid, M. (2003), *Residual Life of Corroding Reinforced Concrete Structures in Marine Environment*. Journal of Materials in Civil Engineering, 15 (4), pp. 344-353. [https://doi.org/10.1061/\(ASCE\)0899-1561\(2003\)15:4\(344\)](https://doi.org/10.1061/(ASCE)0899-1561(2003)15:4(344))
- Torres Acosta, A. A., Hernández, Y., Troconis de Rincón, O., Delgado, S., Rodríguez, J. (2007). “*Agrietamiento de vigas de concreto por corrosión del acero de refuerzo cuando se les aplica una carga externa permanente*,” Boletín del Instituto Mexicano del Transporte (IMT), Notas 109, N°2, <http://ww.imt.mx/SitioIMT/Boletines/resumen-boletines.aspx?IdArticulo=314&IdBoletin=110> (Aug. 05, 2014).

- Torres-Acosta, A. A. and Castro-Borges, P. (2013). “*Corrosion-Induced Cracking of Concrete Elements Exposed to a Natural Marine Environment for Five Years*”, Corrosion, v. 69, No. 11, November, pp. 1122-1131, ISSN: 0010-9312.
- Troconis de Rincón, O., et al. (2007), “*Effect of the marine environment on reinforced concrete durability in Iberoamerican countries: DURACON project/CYTED*”. Corrosion Science, 49 (7), pp. 2832-2843, <https://doi.org/10.1016/j.corsci.2007.02.009>
- Vidal, T., Castel, A., Françoise, R. (2004), “*Analyzing crack width to predict corrosion in reinforced concrete*”, Cement and Concrete Research, 34 (1), pp. 165-174. [https://doi.org/10.1016/S0008-8846\(03\)00246-1](https://doi.org/10.1016/S0008-8846(03)00246-1)

Concrete strength control: ABNT, ACI and EN comparative procedures. Site study case

R. Boni¹, C. Britez¹, P. Helene^{1*} 

*Contact author: paulo.helene@concretophd.com.br

DOI: <http://dx.doi.org/10.21041/ra.v8i3.303>

Reception: 16/03/2018 | Acceptance: 19/07/2018 | Publication: 31/08/2018

ABSTRACT

This paper presents an approach regarding the control of compressive strength of concrete performed by Brazilian standard, additionally was proceeded with an analysis, from the same data, performed by ACI 318-14 and EN 206. In Brazil, the control of the axial compressive strength of concrete proceeds by following ABNT NBR 12655:2015. However, when this control is proceeded by other standards criteria, the results are not coincident. The ACI 318 procedures of sampling and the acceptance criteria are different from the model adopted by Brazilian standard. For this paper, a real case study was carried out, where a $f_{ck}=40\text{MPa}$, (SCC) has been produced, during 2 years and 9 months and poured on the building structure located in the city of São Paulo.

Keywords: strength control of concrete; variability of concrete compressive strength; comparison standard ABNT NBR 12655 with ACI 318 and EN 206.

Cite as: R. Boni, C. Britez, P. Helene (2018), "Concrete strength control: ABNT, ACI and EN comparative procedures. Site study case.", Revista ALCONPAT, 8 (3), pp. 333-346, DOI: <http://dx.doi.org/10.21041/ra.v8i3.303>

¹ Universidade de Sao Paulo y PhD Engenharia, Brasil.

Legal Information

Revista ALCONPAT is a quarterly publication by the Asociación Latinoamericana de Control de Calidad, Patología y Recuperación de la Construcción, Internacional, A.C., Km. 6 antigua carretera a Progreso, Mérida, Yucatán, 97310, Tel.5219997385893, alconpat.int@gmail.com, Website: www.alconpat.org

Responsible editor: Pedro Castro Borges, Ph.D. Reservation of rights for exclusive use No.04-2013-011717330300-203, and ISSN 2007-6835, both granted by the Instituto Nacional de Derecho de Autor. Responsible for the last update of this issue, Informatics Unit ALCONPAT, Elizabeth Sabido Maldonado, Km. 6, antigua carretera a Progreso, Mérida, Yucatán, C.P. 97310.

The views of the authors do not necessarily reflect the position of the editor.

The total or partial reproduction of the contents and images of the publication is strictly prohibited without the previous authorization of ALCONPAT Internacional A.C.

Any dispute, including the replies of the authors, will be published in the second issue of 2019 provided that the information is received before the closing of the first issue of 2019.

Control de la resistencia a la compresión del concreto: análisis comparativo entre los procedimientos propuestos por la ABNT, ACI y EN. Estudio de caso

RESUMEN

Se presentan resultados del control de resistencia a compresión del concreto con la normalización brasileña, así como comparaciones con los controles propuestos por ACI 318-14 y EN 206. En Brasil, el control de resistencia a compresión del concreto es conforme la ABNT NBR 12655:2015. Sin embargo, cuando este control se realiza bajo otras normas, los resultados finales no coinciden, debido a que el procedimiento de muestreo y los criterios de aceptación son distintos. Para este artículo se realizó un estudio de caso real, donde se empleó una dosificación de concreto con $f_{ck}=40\text{MPa}$, auto consolidable, producido durante 2 años y 9 meses y aplicado en la estructura de un emprendimiento en la ciudad de São Paulo.

Palabras clave: control de la resistencia del concreto; variabilidad de la resistencia a la compresión del hormigón; comparación normas ABNT NBR 12655: 2015 con ACI 318-14 y EN 206

Controle da resistência à compressão do concreto: análise comparativa entre os procedimentos propostos pela ABNT, ACI e EN. Estudo de Caso

RESUMO

Neste artigo estão apresentados os resultados obtidos no controle de resistência à compressão do concreto realizado conforme normalização brasileira, bem como análises comparativas com os controles propostos pelo ACI 318-14 e EN 206. No Brasil, atualmente, o controle da resistência à compressão do concreto é realizado conforme a ABNT NBR 12655:2015. Entretanto, quando este controle é realizado à luz de outras normas, os resultados obtidos não coincidem, devido ao fato dos procedimentos de amostragem e critérios de aceitação serem distintos. Este artigo apresenta um estudo de caso real, onde foi empregado um traço de concreto $f_{ck}=40\text{MPa}$, autoadensável, produzido durante 2 anos e 9 meses e aplicado na estrutura de um empreendimento localizado na cidade de São Paulo.

Palavras-chave: controle da resistência do concreto; variabilidade da resistência à compressão do concreto; comparação normas ABNT NBR 12655:2015 com ACI 318-14 e EN 206

1. INTRODUCTION

Currently in Brazil, the control of the compressive strength of the concrete is carried out according to the requirements of ABNT NBR 12655:2015 "*Portland cement concrete - Preparation, control, and acceptance - Procedure*", which presents, in section 6.2 "*Compressive strength tests*", maximum limits for the formation of concrete lots, sampling criteria and the two types of technological control considered: statistical control by partial sampling and control by total sampling, 100% of concrete production.

In the control by partial sampling the samples are randomly collected from different concretes, regarding the minimum number of specimens for subsequent determination of $f_{ck,est}$ (f_c) by mathematical expressions (with statistical basis) denominated estimators. These expressions consider a number of samples between $6 \leq n < 20$. For samples with twenty or more units ($n \geq 20$), the determination of $f_{ck,est}$ uses the mean resistance (f_{cm}) and the deviation production standard, denominated as s_d , by $f_{ck,est} = f_{cm} - 1,65*s_d$.

In partial sample control, the value of $f_{ck,est}$ is obtained and must be compared with the minimum values allowed. Some exceptional cases are also considered: concretes produced by small volume concretes and samples composed of a number of specimens between $2 \leq n \leq 5$.

It should be noted that in Brazil, partial sample control is commonly employed in concrete precasting plants, mainly due to the dynamics of production. For concreting in site, the total sampling (100%) is used in buildings, bridges and all the others concrete uses.

As for the control by total sampling (100%), all concretes are sampled and the characteristic compressive strength of the estimated concrete ($f_{ck, est}$) is given by the value of the compressive strength of the specimen of each concrete, in this case of 100%, the sample is equivalent with the population. It is a control widely used in Brazil in commercial and residential buildings of multiple floors from the validation of ABNT NB-1 in 1978.

As established in section 6.2.2 "Sampling" of the standard ABNT NBR 12655: 2015, each sample must consist of two specimens of the same concrete portion and molded in the same act. The strength of the specimen, for a given rupture age, is the highest of the two values obtained in the compressive strength test, while in general, in others codes the representative value is the mean and not de highest.

The control of the compressive strength of concrete in building structures and infrastructures is an integral part of the introduction of safety in structural design, and its permanent verification throughout the execution of the structure is indispensable (Pacheco & Helene, 2013a), as well as their respective traceability through the appropriate mapping of the concrete launch.

In this paper the results obtained during the control of compressive strength of the concrete realized by total sampling according of ABNT NBR 12655 are presented, as well as comparative analyzes with the control proposed by the American standard ACI 318-14 "*Building Code Requirements for Structural Concrete*" and European standard EN-206:2013 "*Concrete - Specification, performance, production and conformity*". To do so, a $f_{ck} = 40\text{MPa}$, self-compacting concrete SF 2 spreading class (*slump-flow* from 660mm to 750mm) was analyzed, according to ABNT NBR 15823:2010 "*Self-consolidating concrete. Part 1: Classification, control and acceptance in the fresh state*", produced in a single central weighing and mixed in trucks during a period of 2 years and 9 months and applied to the reinforced concrete structures of one commercial tower and two corporates, with 24 to 36 floors, of a large enterprise located in the city of São Paulo.

2. CONTEXTUALIZATION AND PREMISES

2.1 Concrete characteristics and particularities of production

Based on the guidelines of the IBRACON mix design method (Tutikian & Helene, 2011), in the project specifications, available materials and conditions and particularities of the construction an extensive rational and experimental mix design study was carried out to elaborate a self-compacting concrete with $f_{ck} = 40\text{MPa}$. This study was developed in accordance with the standards ABNT NBR 12655 and ABNT NBR 15823.

Considering all the mentioned aspects, the concrete detailed in Table 1 was obtained.

Table 1. Concrete $f_{ck} = 40\text{MPa}$, by mass, dry materials, for 1m^3 .

Materials	$f_{ck} 40\text{MPa}$
cement (CP III-40-RS)	380kg
active silica	20kg
water	180kg
thin sand	364kg
sandstone	546kg
gravel (dimension: 4.5mm – 9.5mm)	279kg
gravel (dimension: 9.5mm - 19mm)	651kg
polyfunctional additive, 0.6% in mass of cement	2,3kg
superplasticizer additive, 1.2% in mass of cement	4,6kg
density of concrete (kg/m^3)	2420
slump flow (ABNT NBR 15823)	SF2
air entrained content (%)	0,8

Previously to the use of the concrete, a prototype concreting event was carried out to evaluate the behavior of the concrete studied in the laboratory, under the construction conditions. At the opportunity, it was observed in the field that the amount of superplasticizer additive could be reduced by up to 30%, due to the greater mixing power of the concrete mixer truck and the favorable climatic conditions. Figure 1 shows the visual appearance of the concrete in question, in its fresh state, observed during the execution of the *slump flow* test carried out during the prototype concreting event.

Figure 1. Visual aspect of the self-compacting concrete observed during the *slumpflow* test.

Considering the satisfactory results obtained in the laboratory and in the prototype event in the field, this concrete was adopted for regular production and was adequate throughout the almost 3-year period considered in this case.

The concrete production was carried out in a ready-mixed concrete equipped with an automated loading system, covered bays and loading point, scales and hydrometers calibrated monthly and availability of six concrete mixer trucks. The ready-mixed concrete was located inside the construction site and produced concrete only and exclusively for the project in question, with a production capacity of up to $70\text{m}^3 / \text{hour}$.

As for loading procedures, the brittle, sand, cement, water and polyfunctional additives were added at the loading point of the Plant and the active silica was placed on the conveyor directly on the aggregates to ensure a better homogenization of the final mixture, which was carried out in the truck mixer.

The humidity of the fine aggregates was determined at least 3 times daily using the Chapman vessel (ABNT NBR 9775: 2011 "*Fine aggregate - Determination of the superficial humidity by Chapman vessel - Test method*"). The humidity obtained was sent to the balance system software of the ready-mixed concrete, which automatically performed the necessary corrections.

After loading the concrete, the superplasticizer additive was added. This addition was carried out in volume, by a professional trained through the use of graduated buckets. On some occasions, 100% ice was used instead of the kneading water (in the case of concretions of large-volume foundation elements). In addition to the ice, as superplasticizer additive and active silica, the control of the added amounts was monitored by extra professionals contracted with the Laboratory responsible for the control of the compressive strength of the concrete (counting of ice bags, silica bags and verification of the volume of additive).

It is important to note that, once outside the ready-mixed concrete, it was not allowed to add water to the concrete, in any case. If there was a need for scattering correction, the superplasticizer additive was added (possibly added to a construction site by a trained professional after authorization by the supervisor and only to correct the fluidity of the fresh concrete).

In this context, the concrete was always supplied with the same mix proportions, by the same ready-mixed concrete plant during a period of 2 years and 9 months. In total, approximately 1,600 concrete mixer trucks were produced, with a maximum of 8m³ each, totaling around 12,000m³ of concrete, or 360m³ / month on average.

2.2 Resistance control plan

The control of the compressive strength of the concrete was performed by total sampling regarding the requirements of the standard ABNT NBR 12655 by a Laboratory accredited by INMETRO belonging to the Brazilian Network of Laboratory of Tests, which used qualified laboratories and certified by IBRACON through its Nucleus of Qualification and Certification of Personnel.

The concrete resistance control plan adopted during the entire production process consisted of the molding of four cylindrical specimens with a diameter of 10 cm and a height of 20 cm for each of the concrete mixer trucks being one for compression test at 7 days, two for 28 days and one for 63 days of age.

The specimens were molded in metallic form in a flat place, protected from the weather and later (after a dismantling between 24 h and 36 h), transported in boxes of dry sand to the center of the Laboratory of technological control located at approximately 15 km of the construction site, for seasoning and testing. These were stored in a humid chamber, had their tops prepared by means of grinding, and were tested on periodically calibrated presses in accordance with ABNT NBR 5738: 2015 "*Concrete - Procedure for molding and curing concrete test specimens*" and ABNT NBR 5739: 2007 "*Concrete - Compression test of cylindric specimens – Method of test*".

3. RESULTS

3.1 Results of compressive strength according of ABNT

The compressive strength of each specimen was determined after rupture of the specimens, according to the requirements of ABNT NBR 5739.

Figure 2 shows the chart of individual compressive strength values of concrete at 28 days of age, histogram and corresponding normal distribution. The axis of the abscissae presents the copies in chronological order and, the axis of the ordinates, the values of resistance to compression of each of the copies (the greater resistance obtained in the rupture of two test specimens, according to established in ABNT NBR 12655).

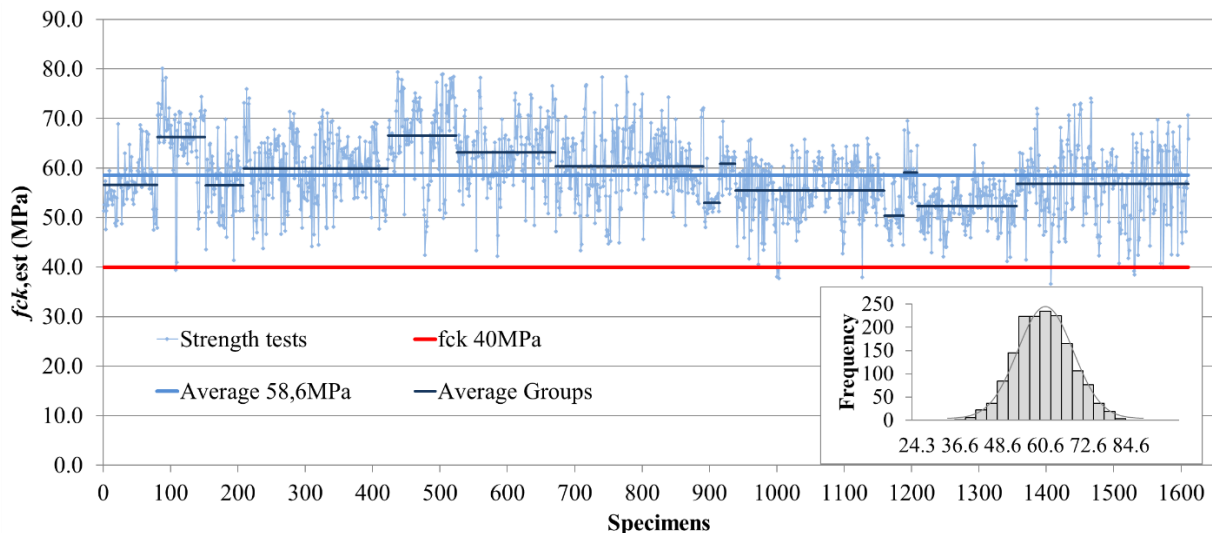


Figure 2. Chart of individual values based on the results of compressive strength of concrete at 28 days of age and corresponding histogram.

The chart features about 1,600 compressive strength results obtained over 2 years and 9 months. These results ranged from 36.6 MPa to 80.1 MPa, with a mean of 58.6 MPa, the lowest value being equivalent to $0.91 * f_{ck}$. Eleven results were found below the specified design strength ($f_{ck} = 40\text{MPa}$), or about 0.7% of the total truck load. In a normal distribution (Gaussian curve) the defective quantile would correspond to a coefficient of 2.46.

The variability of the compressive strength of the same concrete mix proportion can oscillate around different values, because in the course of the production process changes of centering take place, mainly due to different sets of cement and aggregates.

Considering the concept of characteristic strength of the concrete described in section 12.2 “Characteristic values” of ABNT NBR 6118: 2014 “Design of structural concrete – Procedure”, the value of the compressive strength of this concrete, obtained directly from the population, would be $f_{ck,5\%} = 46.5\text{MPa}$. The standard deviation of the production and test operations obtained was $s_c = 6.6\text{MPa}$ and the coefficient of variation $V_c = 11.2\%$.

The characteristic strength of this concrete adapted from the ABNT NBR 12655 partial sampling criterion would be $f_{ck,est} = f_{cm} - 1.65 * s_c = 47.7\text{MPa}$, although in this case it is only a mathematical speculation, since the effective criterion to be used should be 100% total sampling.

3.2 Evaluation of the control of the production process

According to section 7 “Process analysis” of ABNT NBR 7212: 2012 “Ready-mixed concrete – Procedure” the evaluation of process control should be performed based on the standard deviation, as presented in Table 2.

Table 2. Standard deviation of the process, ABNT NBR 7212: 2012.

Place of production	Standard deviation (MPa)			
	Level 1	Level 2	Level 3	Level 4
Plant	$s < 3,0$	$3,0 < s < 4,0$	$4,0 < s < 5,0$	$s > 5,0$

Thus, through the analysis of the standard deviation and the criteria recommended by ABNT NBR 7212: 2012, it is a Level 4 Plant.

According to the parameters currently established by ABNT NBR 12655, this standard deviation of the production is high and not compatible with production of concrete in plant, class A. On the other hand, the standard ABNT NB-1 of 1960, considered that production of concrete with a standard deviation equal to or lower than 15% should be classified as strict production, that is, it would correspond to the best classification at the time.

According to ACI 214 section 4.5 “Standards of control”, for concrete of $f_{ck} \geq 35\text{MPa}$ (case in question), the coefficient of variation (V_c) is the parameter that must be used to qualify or classify the concrete production presented in Table 3, in which case the production can be classified with good / reasonable accuracy.

Table 3. Coefficient of variation of production and test operations (V_c), ACI 214.

Production	Coefficient of variation				
	Excellent	Very good	Good	Fair	Faulty
Construction site	< 7,0%	7,0% a 9,0%	9,0% a 11,0%	11,0% a 14,0%	> 14,0%
Laboratory	< 3,5%	3,5% a 4,5%	4,5% a 5,0%	5,0% a 7,0%	> 7,0%

3.3 Influence of testing and control operations

The 28-day compressive strength results were analyzed from the point of view of the influence of the test and control operations according to the criteria recommended by the American Concrete Institute in the ACI-214R-11 “Guide to Evaluation of Strength Test Results of Concrete”.

This methodology consists of the calculation of the standard deviation and the coefficient of variation due to the test and control operations, based on the result of the compressive strength of sibling specimens and later comparison with the control criteria suggested in Chapter 4 “Analysis of Strength Data” which states the following:

a) Calculation of the standard deviation of test and control operations:

$$se = \frac{\sum_{i=1}^n Ai}{n.d2} \quad (3.1)$$

where:

- s_e : the standard deviation of the test operations in MPa;
- n : number of specimens considered to be composed of specimens (not less than 10 specimens);
- A : difference between the largest and smallest result of specimens representing the same specimen;
- d_2 : coefficient depending on the number p of representative specimens of the same specimen, according to Table 4.

Table 4. Coefficients d_2 for calculation of the standard deviation of the test and control operations.

Number p of specimens	d_2
2	1,128
3	1,693
4	2,059

b) Calculation of the coefficient of variation or variability of the test and control operations:

$$V_e = \left(\frac{s_e}{f_{cmj}} \right) \cdot 100 \quad (3.2)$$

where:

- s_e : the standard deviation of the test operations in MPa (value obtained in item a);
- V_e : coefficient of variation due to test and control operations (%);
- f_{cmj} : mean of all results used, j days old, in MPa.

c) Determination of the Control Standard, according to Table 5:

Table 5. Coefficient of variation of test and control operations (V_e), ACI 214.

Production	Coefficient of variation				
	Excellent	Very good	Good	Fair	Faulty
Construction site	< 3,0%	3,0% a 4,0%	4,0% a 5,0%	5,0% a 6,0%	> 6,0%
Laboratory	< 2,0%	2,0% a 3,0%	3,0% a 4,0%	4,0% a 5,0%	> 5,0%

Considering the difference in compressive strength between the two fractured specimens ruptured at 28 days of age, the results obtained throughout the concrete production period indicated a standard deviation of the test and control operations (s_e) varying from 0.6MPa to 1.0MPa and coefficient of variation due to the test and control (V_e) operations between 1.1% and 1.6%. According to the limits recommended by ACI 214, all the results pointed to a standard of control of the operations of test, in construction site, excellent. On the other hand, it is observed that the results obtained are more rigorous than the tests performed in experimental research conducted in the laboratory, which is not common.

3.4 Comparative analysis between the control methods proposed by ABNT and ACI

As previously detailed, the control of the compressive strength of the concrete was performed by total sampling in accordance with the requirements of ABNT NBR 12655. However, when the compressive strength values of the same concrete production are analyzed according of ACI 318 judgment does not match. This is justified because the sampling procedures, as well as the acceptance criteria prescribed by the ACI, are different from the model adopted by the ABNT.

Regarding sampling, ACI 318 in section 26.12 “Concrete evaluation and acceptance” recommends as minimum criteria:

- ✓ one per day of concreting;
- ✓ one for each 115m³ of concrete produced;
- ✓ one per 465m² of surface area for slabs or walls;
- ✓ the control for volumes lower than 38m³ is dispensed, provided that there is an approved concrete.

According to ACI 318, the value of the compressive strength of each of the specimens is determined by the simple arithmetic mean of the results obtained. According to ASTM C39-16b “Standard Test Method for Compressive Strength of Cylindrical Concrete Specimens”, if the individual values of the specimens differ by more than 8%, the results are inadequate, and the test should be repeated. The ACI 318, as well as ABNT NBR 12655 and the European standard EN-206: 2013 “Concrete - Specification, performance, production and conformity” also consider that of each mixed concrete only one compressive strength value is obtained.

ACI 318 prescribes the following acceptance and compliance criteria:

- ✓ for $f_{ck} \leq 35\text{MPa}$, no individual result shall be less than $f_{ck} - 3,5\text{MPa}$;
- ✓ for $f_{ck} > 35\text{MPa}$ (case in question), no individual result can be less than $0,9 * f_{ck}$;
- ✓ the average of any three consecutive results shall be equal to or greater than the characteristic resistance defined in the design (f_{ck}).

Thus, in order to perform a comparative analysis between the controls performed by ABNT and ACI, all values of compressive strength obtained at 28 days of age were also treated and organized according to the sampling and acceptance criteria proposed by ACI 318, as shown below.

Considering the minimum sampling criterion proposed by the ACI of one specimen per 115m³ of concrete (1 molding of specimens for each 14 truck mixer of 8m³), it became possible to analyze numerous combinations of results, since they were molded test bodies for all concrete mixer trucks (population). Thus, to study all possibilities, the envelope of the individual values and the moving average of 3 (three) consecutive results (maximum and minimum values assumed) were determined.

According to the criterion recommended by ACI 318, all individual values must be greater than 36MPa ($0,9 * f_{ck}$). It is observed in Figure 3 (envelope of the individual values) that, before all possibilities, no value is less than 36MPa (it should be noted that the lowest individual mean value recorded was 36.2MPa). Therefore, this criterion of acceptance was always met.

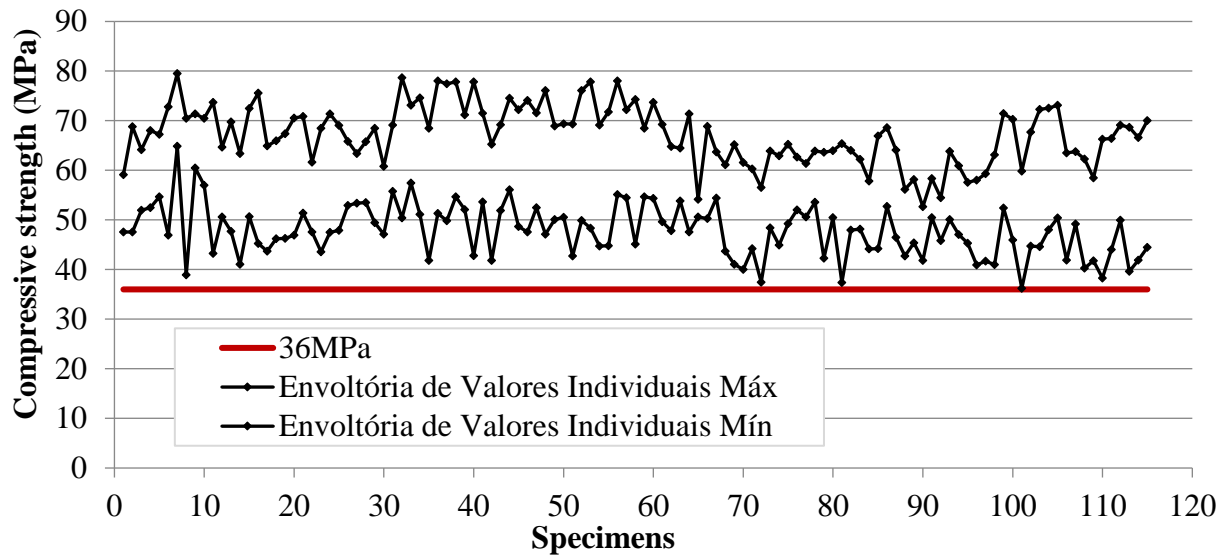


Figure 3. Strength tests of each concrete mixer truck.

According to the ACI, to ensure acceptance of the concrete, another type of analysis must be done. In Figure 4 is presented the envelope of the moving average over the entire production period [maximum and minimum values of any 3 (three) consecutive results]. Note that in no case the moving average was less than the characteristic resistance defined in design (40MPa). The lowest recorded value was 40.1 MPa. Therefore, regardless of the combination of results considered, this criterion of acceptance was also met.

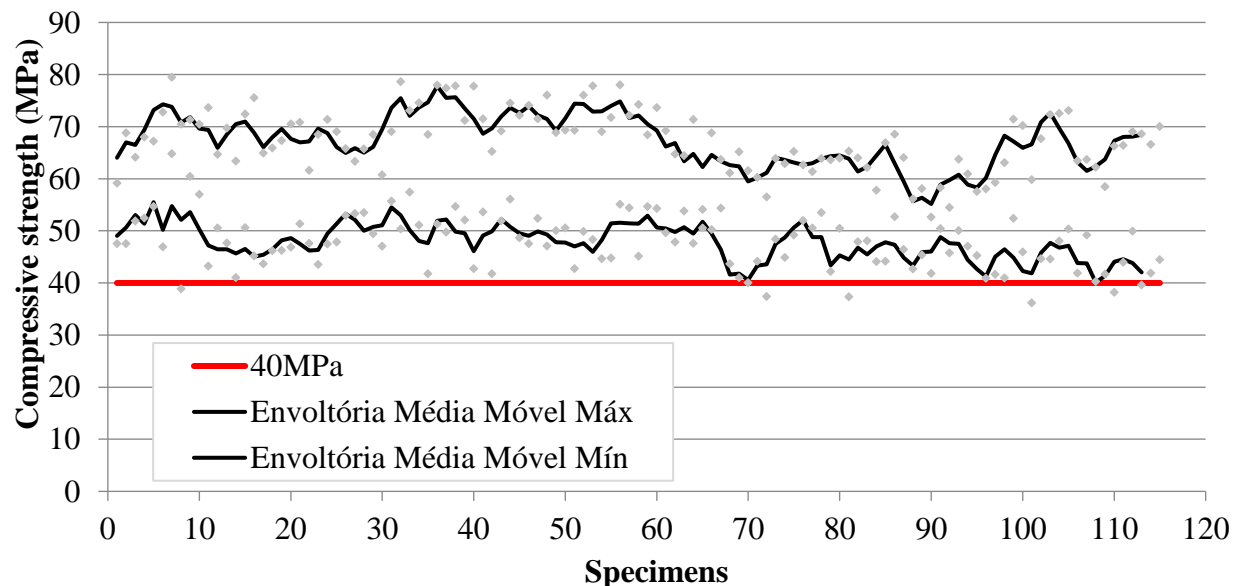


Figure 4. Average of three consecutive strength tests throughout the production period.

Therefore, considering the most unfavorable scenario, if the technological control of the concrete were performed according to ACI 318, there would be no non-conformities since both criteria (individual values and average) were always satisfied simultaneously.

3.5 Comparative analysis between control methods proposed by ABNT and EN

Like the American standard, the European code EN 206 establishes 2 (two) criteria for analysis of the concrete compressive strength conformity: criterion for individual results and criterion for average results.

In the case of analysis by means of the individual criterion, each result must satisfy the following condition: any individual value must be $\geq f_{ck} - 4\text{MPa}$.

As for the criterion for medium strengths, the standard in question allows that the compressive strength be evaluated by one of the following methods:

- ✓ method A or control of the initial production. In this case, the average strength of 3 (three) consecutive results should be $\geq f_{ck} + 4\text{MPa}$, and the compliance criteria were developed based on non-overlapping test results. Therefore, the application of overlapping criteria (consecutive results moving average) increases the risk of rejection;
- ✓ method B or continuous production control. This is an option when continuous production criteria are established, when at least 35 (thirty-five) test results are available within a 3 (three) month period. According to this method, the average of 15 (fifteen) or more consecutive results [made available in a period not exceeding 3 (three) months] should be $\geq f_{ck} + 1.48 * \sigma$ (adopting as σ the standard deviation determined at the end of the start of production control).

The EN 206 still allows the conformity of the compressive strength of the concrete to be evaluated using control charts (method C), provided that the conditions of continuous production are established and that it is certified by third parties, which is not the case.

As for the formation of lots, when continuous production is carried out in concrete plants with production control certification, samples should be taken every 200 m³ (or one every 3 days of production). If concrete production does not have production control certification (case in question), samples should be taken out every 150 m³ (or one per day of production). Important: in the first 50 m³ of production, at least 3 samples must be taken.

It is valid to record that this standard allows a copy of the value obtained from a single specimen or, in case of more breaks, the result is defined as the average value. Individual results that deviate more than 15% from the average value should be disregarded.

Similarly to the case discussed previously (ACI), since molded concrete specimens were used for all concrete mixer trucks, in the case of EN, it was also possible to carry out an analysis considering numerous combinations of results.

According to the minimum sampling criterion proposed by the EN of 3 (three) specimens in the first 50 m³ of production and, subsequently, 1 (one) specimen per 150 m³ of concrete (1 molding of specimens at each 18 concrete mixer trucks of 8 m³), the individual value envelope shown in Figure 5 was obtained.

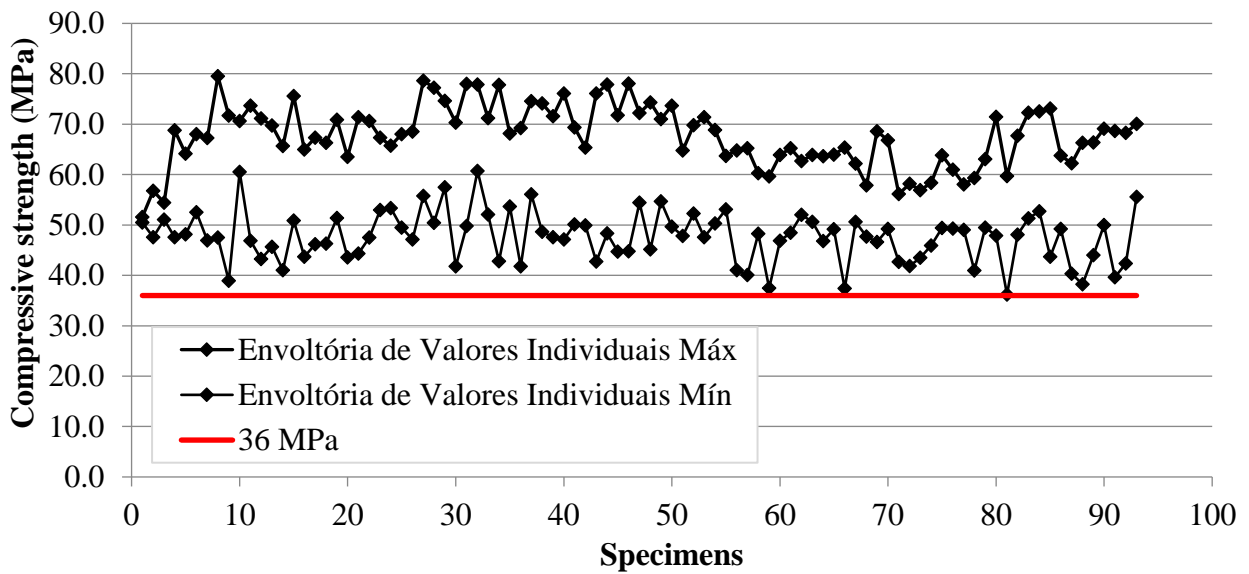


Figure 5. Compressive strength of the individual values.

It is noted that during the production period the criterion of individual values recommended in section 8.2.1.3.1 “Criteria for individual results” of EN 206: 2013 was met in all cases. Again, it is worth remembering that the lowest value of compressive strength obtained in this period was 36.2 MPa, considering the average of two (2) sibling specimens.

As to the analysis of the average results, in order to contemplate all possibilities, we considered the envelope of the mean values of 3 (three) non-overlapping consecutive results, as evidenced in Figure 6.

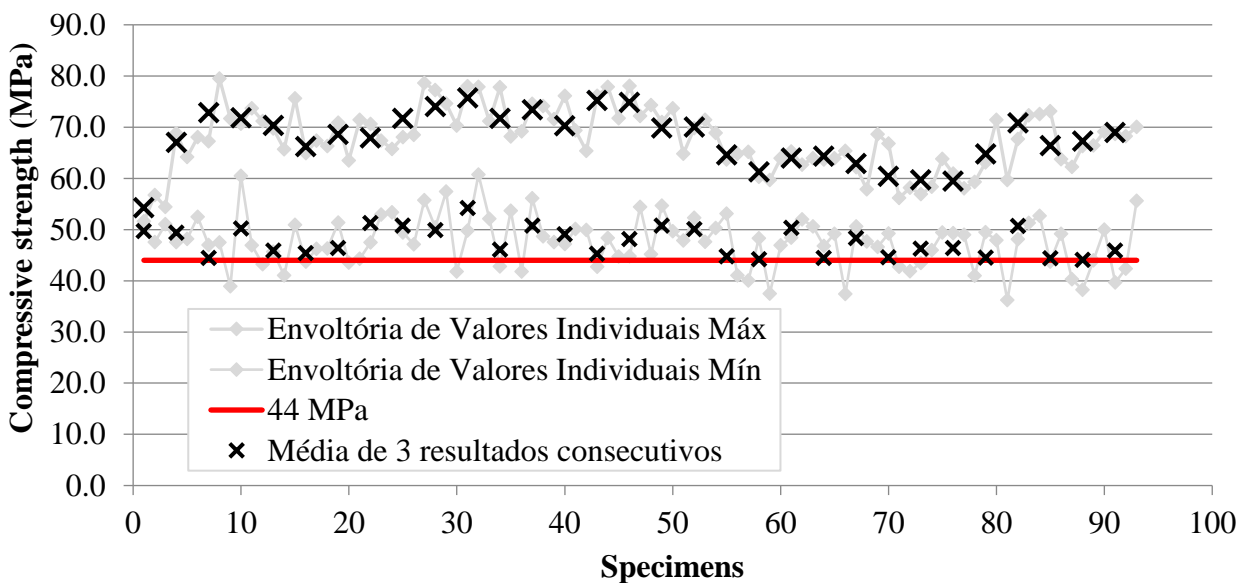


Figure 6. Average envelope of 3 (three) non-overlapping consecutive values over the production period.

It is worth noting that, as in the case of the individual values curve, the mean value curve obtained during the whole production period has always met the requirements established in section 8.2.1.3.2 “Criteria for mean results” of EN 206: 2013. In this case, the lowest value was 44.1 MPa, that is, higher than the criterion $\geq f_{ck} + 4\text{MPa} = 44\text{MPa}$.

The safety criteria of the structures established in the European standard are different from the criteria adopted by the American and Brazilian standards, since they involve probability of rupture, characteristic values of actions and different resistances. Therefore, it is reasonable to expect that the values of compressive strength obtained in this case are somewhat different from the previous cases.

4. CONCLUSIONS

The control of compressive strength of the concrete recommended by the Brazilian standard is very strict and the safest. Sampling is 100% total (population) and the results are analyzed individually, without tolerances. Any resistance value that is lower than the project specification will be considered non-compliant. However, although very safe, it is a costly control because it involves molding, handling, transportation, curing, grinding and breaking of many concrete specimens of all concrete mixer trucks received on site (total sample control).

It is noted that the control methodology prescribed by ACI 318 and EN 206 is much milder when compared to the criteria of the Brazilian standard. In these standards the control is not performed by total sampling, tolerances are established for the individual values of compressive strength and, in addition, the concept of the average of consecutive results is also applied as criterion of acceptance.

In the opinion of the authors of this paper, the acceptance and compliance criteria recommended by ABNT NBR 12655 are demanding and it would be advisable to flex the value of individual results within a margin of up to $0.9 * f_{ck}$. On the other hand, the sampling criterion adopted in Brazil is in favor of safety and in the opinion of these authors, although onerous, it should be maintained as it stands.

In this case, the results obtained through the technological control prescribed by ABNT NBR 12655 pointed to a non-conformity index related to the compressive strength of 11-fold concrete in approximately 1,600 concrete mixer trucks (0.7%). This unimportant nonconformity generated absolutely unnecessary wear and design revisions. On the other hand, the same results, when analyzed in the light of the methodologies prescribed by ACI 318 and EN 206, indicated a zero-non-compliance index.

Adopting flexibilization and accepting a few individual values of up to $0.9 * f_{ck}$ as conforming would certainly impact positively on the production process, minimizing possible costs, rework, project reviews, delays in work schedules and unnecessary wear and tear among stakeholders of the concrete production chain, without compromising the safety, durability and final quality of the concrete structures.

1. REFERENCES

ABNT - Associação Brasileira de Normas Técnicas (2015), *NBR 12655: Concreto de cimento Portland – Preparo, controle, recebimento e aceitação – Procedimento*, Associação Brasileira de Normas Técnicas, p. 23.

ABNT - Associação Brasileira de Normas Técnicas (2014), *NBR 6118: Projeto de estruturas de concreto – Procedimento*, Associação Brasileira de Normas Técnicas, p. 238.

American Concrete Institute (2011), *ACI 214R-11: Guide to Evaluation of Strength Test Results of Concrete*, American Concrete Institute, p. 16.

American Concrete Institute (2014), *ACI 318-14: Building Code Requirements for Structural Concrete*, American Concrete Institute, p. 524.

- ASTM International. (2016). *ASTM C39/C39M-16b Standard Test Method for Compressive Strength of Cylindrical Concrete Specimens*. Retrieved from https://doi.org/10.1520/C0039_C0039M-16B
- EN 206 (2013), *Concrete – Specification, performance, production and conformity*, European Committee for Standardization, p. 93.
- Pacheco J. & Helene P. (2013), *Controle da resistência do concreto - 1ª Parte*, Revista Concreto e Construções n. 69, pp 75 - 81.
- Pacheco J. & Helene, P. (2013), *Controle da resistência do concreto - 2ª Parte*, Revista Concreto e Construções n. 70, pp 90 - 98.
- Tutikian B. & Helene P. (2011), *Dosagem dos Concretos de Cimento Portland*. In: Geraldo C. Isaia (Org). *Concreto: Ciência e Tecnologia*. 1 ed. São Paulo: Ibracon, v. 1, pp 415 - 451.

Load rating assessment of a corroded pier structure in the Gulf of Mexico

M. Martínez-Madrid*¹ , A. A. Torres-Acosta¹ , S. Aschermann², B. Commander², J. Grimson²,
P. Castro-Borges³ 

*Contact author: martinez@imt.mx

DOI: <http://dx.doi.org/10.21041/ra.v8i3.323>

Reception: 15/06/2018 | Acceptance: 16/08/2018 | Publication: 31/08/2018

ABSTRACT

This work assesses the structural integrity of a pier located in the Gulf of Mexico through a live-load testing analysis of a corroded structure that withstands heavy loads. Procedures included instrumentation for load application of four different loads (50, 60, 350, and 700 Ton) to examine its structural performance, then calibrate the resultant finite-element models of the structure, and finally estimate the load rating factors using AASHTO methodology. Results showed that corrosion damages did not appear to represent an extreme structural menace; however, it was found that several piers' structural elements are currently overloaded and need to be externally reinforced. This paper outlines the testing procedures, describing both the followed analysis and the data management criteria.

Keywords: load capacity; structural rate; corrosion-damage.

Cite as: M. Martínez-Madrid, A. A. Torres-Acosta, S. Aschermann, B. Commander, J. Grimson, P. Castro-Borges (2018), "Load rating assessment of a corroded pier structure in the Gulf of Mexico", Revista ALCONPAT, 8 (3), pp. 347-362, DOI: <http://dx.doi.org/10.21041/ra.v8i3.323>

¹ Instituto Mexicano del Transporte (IMT), Km. 12 Carretera Querétaro - Galindo, Sanfandila, Querétaro, México

² Bridge Diagnostic Inc., 1995 57th Court North Suite 100, Boulder CO 80301-2810, Estados Unidos.

³ CINVESTAV, Unidad Mérida, Km 6 Carretera Antigua a Progreso, Cordemex, Mérida, Yucatán, México.

Legal Information

Revista ALCONPAT is a quarterly publication by the Asociación Latinoamericana de Control de Calidad, Patología y Recuperación de la Construcción, Internacional, A.C., Km. 6 antigua carretera a Progreso, Mérida, Yucatán, 97310, Tel.5219997385893, alconpat.int@gmail.com, Website: www.alconpat.org

Responsible editor: Pedro Castro Borges, Ph.D. Reservation of rights for exclusive use No.04-2013-011717330300-203, and ISSN 2007-6835, both granted by the Instituto Nacional de Derecho de Autor. Responsible for the last update of this issue, Informatics Unit ALCONPAT, Elizabeth Sabido Maldonado, Km. 6, antigua carretera a Progreso, Mérida, Yucatán, C.P. 97310.

The views of the authors do not necessarily reflect the position of the editor.

The total or partial reproduction of the contents and images of the publication is strictly prohibited without the previous authorization of ALCONPAT Internacional A.C.

Any dispute, including the replies of the authors, will be published in the second issue of 2019 provided that the information is received before the closing of the first issue of 2019.

Evaluación de la capacidad de carga de la estructura de un muelle corroído en el Golfo de México

RESUMEN

Se realizó una prueba de carga viva y un análisis de calificación en un muelle dañado por la corrosión en el Golfo de México para evaluar su integridad estructural. Los procedimientos incluyeron instrumentación para la aplicación de carga de cuatro cargas diferentes (50, 60, 350 y 700 Toneladas) para examinar su rendimiento estructural, luego calibrar los modelos de elementos finitos resultantes de la estructura y finalmente estimar los factores de clasificación de carga utilizando la metodología AASHTO. Los resultados mostraron que los daños por corrosión no representaron una amenaza estructural extrema; sin embargo, se descubrió que los elementos estructurales de varios pilares actualmente están sobrecargados y necesitan ser reforzados externamente. Se describen los procedimientos de prueba, el análisis y el manejo de datos.

Palabras clave: capacidad de carga; tasa estructural; daño por corrosión.

Avaliação da capacidade de carga da estrutura de um cais corroído no Golfo do México

RESUMO

Uma prova de carga e análise de classificação em um cais danificado pela corrosão no Golfo do México foi realizado para avaliar sua integridade estrutural. Os procedimentos incluíram instrumentação para aplicação de carga de quatro cargas diferentes (50, 60, 350 e 700 t) para examinar seu desempenho estrutural, calibrar os modelos de elementos finitos resultantes da estrutura e, finalmente, estimar os fatores de classificação de carga usando a metodologia AASHTO. Os resultados mostraram que os danos causados pela corrosão não representaram uma ameaça estrutural extrema; no entanto, constatou-se que os elementos estruturais de vários pilares estão atualmente sobrecarregados e precisam ser reforçados externamente. Este documento descreve os procedimentos de ensaio, de análise dos resultados e os critérios de gerenciamento de dados.

Palavras-chave: capacidade de carga; taxa estrutural; dano de corrosão.

1. INTRODUCTION

It is well known that reinforced steel corrosion represents an enormous and expensive problem to solve in marine structures, yet a preventive investment is mandatory to preserve them (Schmitt Günter, 2009), (Hays).

Concrete structures which are exposed to ocean water are commonly susceptible to corrosion. When salts and chemicals diffuse through the concrete, usually promote crack formation due to the reinforcing steel oxide layer expansive forces. Furthermore, the formed cracks along with humidity and salts can permeate towards the reinforcing steel faster and then again, cause premature damage due to corrosion (NASA Kennedy Space Center). Even though cracking is the most visible concrete reaction after corrosion starts, it is related to other damages, such as structural deteriorations, a loss in flexural stiffness as well as loading capacity capability. Also, corrosion products weaken the bonding between the concrete and its reinforcing steel, this further affects the mechanical properties of the damaged structures, resulting in a decrease in its original structural integrity.

Most of the piers in Mexico show a degree of corrosion as stated in a 100% inspection report (Torres Acosta, 2012). Mexico's Institute of Transportation (IMT) together with Bridge Diagnostics, Inc. (BDI) set up an original procedure to make a pier corrosion damaged assessment to establish if the corroded piers are still suitable for use as originally designed. This was meant to be applied as a diagnostics toll to important Mexico's piers.

A primary component in this assessment is a load testing to determine if a pier, exhibiting significant corrosion damages, can still operate risk-free, withstanding all its required service loads, including cranes and container vehicles that are currently present during normal uploading and downloading procedures. This is done by evaluating the structural performance through a series of controlled load tests and then developing the appropriate field verified models from which the pier is load rated using AASHTO LRFD specifications (AASHTO, 2002).

As the term implies, diagnostic load testing in a non-destructive process that can determine a structure's performance under normal load conditions. For bridges and piers, loading is usually accomplished by driving vehicles (trucks or cranes) with measured axle weights along prescribed paths. The location of the vehicle must be monitored along with all the measurements from the various attached sensors.

After the load tests are complete, the measured values are used to verify and calibrate the theoretical responses generated by a representative software model. For the process to work out the model, it must have realistic geometry and stiffness characteristics. This is done by essentially reproducing the entire load test procedure with a finite element analysis (FEA) model; this includes generating a Two-Dimensional or Three-Dimensional model of the structure (depends on complexity of the structure), applying virtual sensors on the model and applying identical load scenarios that were utilized during the field load test procedures. By having accurate geometric representation and reproducing the load test a direct comparison between the field and analytical responses can be made.

Once a representative model is obtained, the required design or rating loads can be applied, and load ratings can be computed for all the components in the model. Because the loads applied to each structural element are generated by a realistic representation of the entire structure, the component loads are much more accurate. Another advantage to diagnostic load testing is to determine whether a section that appears damaged or significantly corroded is causing a redistribution of loading to other structural components. Still, due to corrosion damage, the component's capacity may be significantly impaired, causing a reduced load capacity miscalculation for that particular structural member.

This is an important distinction because the structure may be responding in a perfectly appropriate manner under typical loads as verified by the field tests, but, the load carrying capacity is significantly lower due to diminished structural capacity. Therefore, structural measurements may not indicate that a member is "weak", even if it looks "damaged". This gap between visual inspections and known adequate structural response is what led to the development of the "Integrated Approach" that essentially combines the field measurements, the visual inspection, and the analytical modeling to reduce the uncertainty inherent in all three of these evaluation tools.

With regards to the component load rating, the same equation specified by the AASHTO - Manual for the Condition Evaluation of Bridges is applied in (1). Furthermore, the critical load conditions are likely different than those applied during the load tests. All the required vehicle loadings are applied to the structure model including all necessary multi-presence scenarios and dynamic effects.

$$RF = \frac{C - \gamma_{DC}(DC) - \gamma_{DW}(DW) \pm \gamma_P(P)}{\gamma_L(LL + IM)} \quad (1)$$

Where:

RF = Rating Factor for individual member.

C = Member Capacity.

γ_{DC} = LRFD load factor for structural components and attachments.

DC = Dead-load effect due to structural components.

γ_{DW} = LRFD load factor for wearing surfaces and utilities.

DW = Dead-load effect due to wearing surface and utilities.

γ_P = LRFD load factor for permanent loads other than dead loads = 1.0

P = Permanent loads other than dead loads.

LL = Live-load effect.

IM = Impact effect, either AASHTO or measured

2. METHODOLOGY

2.1 Structural testing procedures

2.1.1 Instrumentation process

The tested pier was a reinforced-concrete (R/C) structure which was designed to carry important loads including a gantry crane, vehicular, and container loads from the loading and unloading of container ships. Its superstructure comprised of 11 longitudinal beams framed into transverse inverted T-beams, and a 5-span continuous concrete deck with no apparent wearing surface indicated in the plans of Figure 1. The pier's overall length is 250m, composed by 25 10m spans, and its width is 20.8m, divided into 7 interior stringers spaced 2m on center, 2 main girders beneath the rails of the gantry cranes, and 2 small exterior fascia stringers.

In general, the pier presented different degrees of structural degradation, showing signs of steel corrosion mainly evidenced by large areas of spalling. There were some visible cracks on the stringers, floor beams, and on the top of the slab. Overloading was evident by the crushing of the stay-in-place precast deck forms adjacent to the stringers. Figure 2 shows the pier damage survey results between floor beams 38 and 47, obtained before the pier was instrumented. Tables 1 and 2 shows some of the typical degradation pathologies observed from the damage survey performed to the pier.

Two areas of the pier (between floor beams 38 and 47 were instrumented and load tested: one area with minimal degradation, defined as "healthy" (between floor beams 38 and 40, Table 1), and another one with large amounts of degradation, defined as "damaged" (between floor beams 45 and 47, Table 2). Both sections were instrumented with 44 strain transducers, 8 displacement transducers, and 7 rotation transducers (Figure 1). There were 61-cm extended gage lengths used on the primary girders and inverted T-beams to provide averaged surface strains on the reinforced concrete.

The strain transducers and tiltmeters were affixed to the structural members by using a fast-setting adhesive and removable mounting tabs, or "feet". The sensors were installed and once the testing was completed, they were removed. Cantilever type displacement sensors were attached to the structure by installing two ¼ in wedge anchors and bolting the sensors to the anchors.

2.1.2 Load testing

The pier went through several types of load tests, which included various transverse truck positions, a gantry crane movement, and a Gottwald crane movement plus a load pick from the crane Figure 3. Fixed markers were placed on the deck in order to determine where the vehicles crossed, so this way future analysis comparisons could be made with the loading vehicle in the same locations as it was in the field. A “zero” or initial reference point was selected so all other measurements on the deck could then be related to it. Once the zero-reference location was known, the lateral load paths for the vehicle were determined. Usually, at least two passes were made at each “Y” position to ensure data reproducibility.

The first was a series of semi-static live-load tests consisting of a loaded container truck rolling across the instrumented spans at 6 different lateral positions. All tests were continuously recorded at a minimum sample rate of 33.33 Hz. Load tests were performed at crawl speed (4-8 km/h) to minimize dynamic effects.

The second set of tests consisted of rolling one of the large rail gantry cranes across the instrumented spans. Like the truck tests, measurements and crane position were recorded continuously at a minimum sample rate of 33.33 Hz. The railed gantry crane for testing weighted 700tons (43.75tons per axel with a support separation of 15.24m).

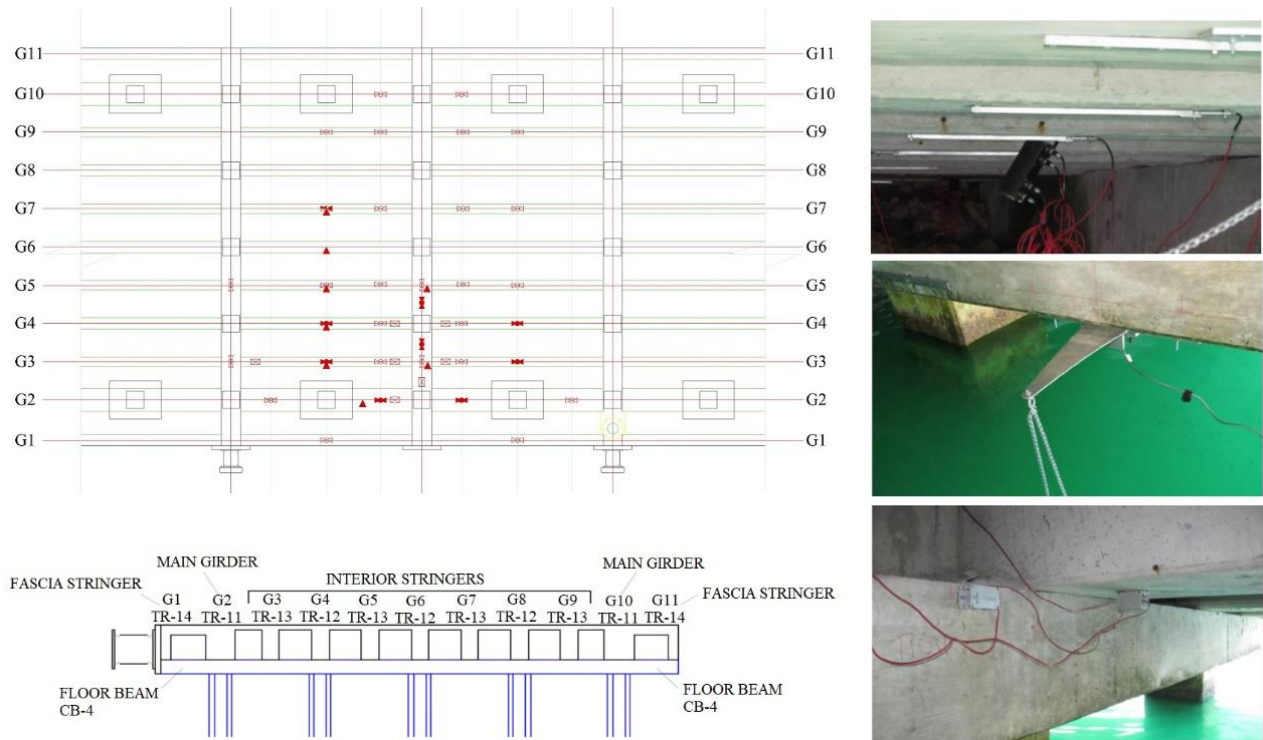


Figure 1. General instrumentation plan with gage locations and cross sections and structural element designation. Top photo: Midspan strain gages; center photo: Deflection sensor; bottom: Tiltmeter rotation sensors

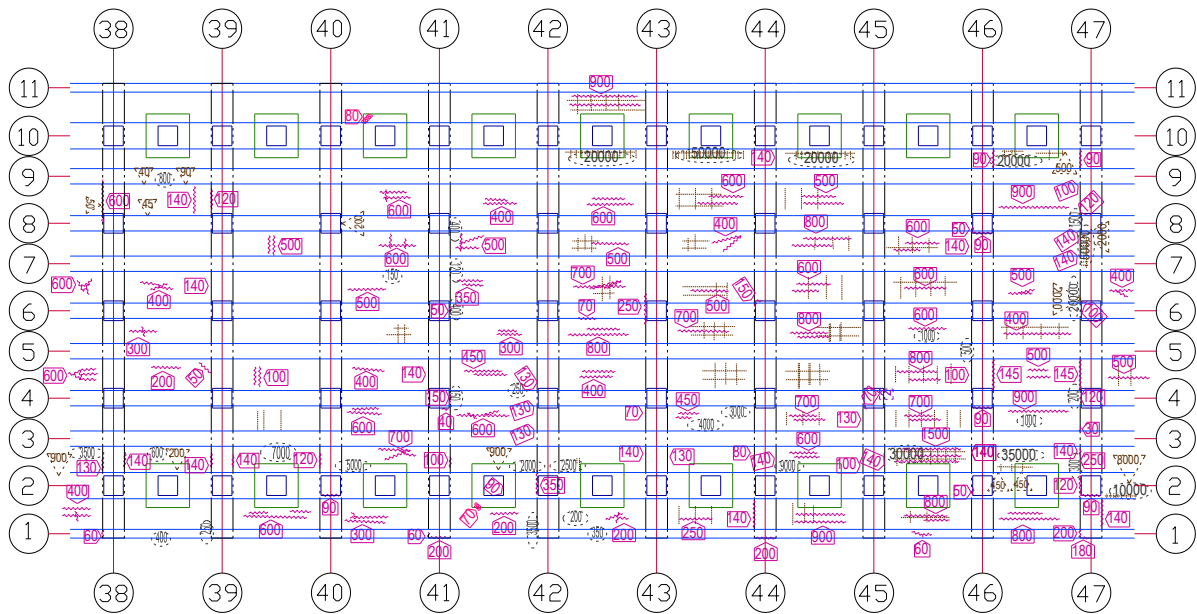


Figure 2. Damage survey of the pier between floor beams 38 and 47. The “healthy” section was defined as the pier area between floor beams 38 and 40. The “damaged” section was defined as the pier area between floor beams 45 and 47.

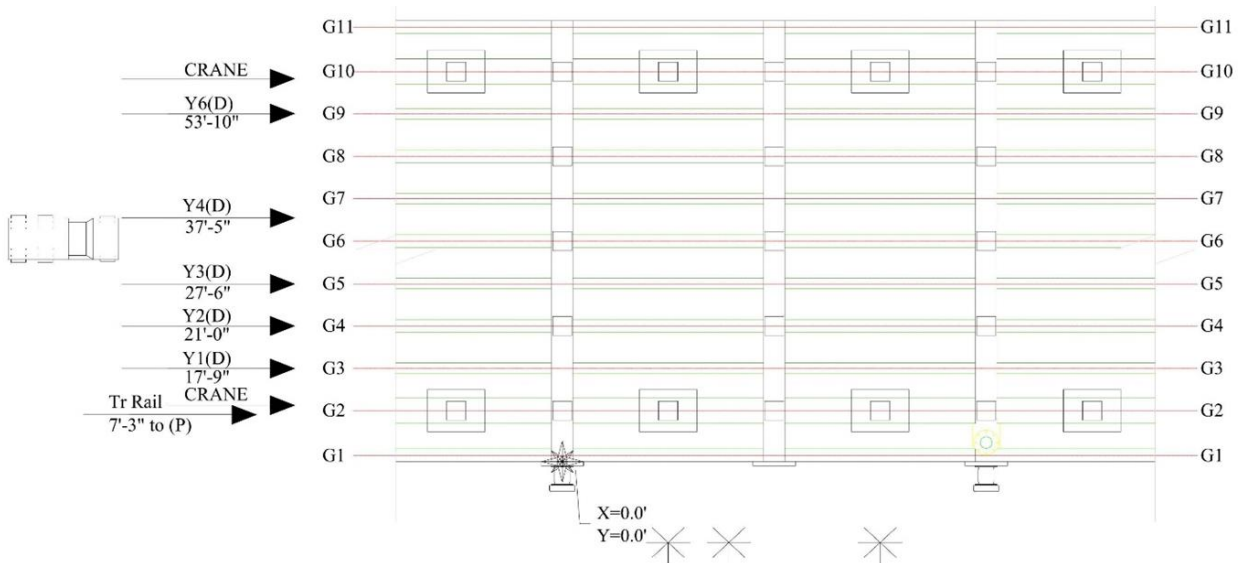


Figure 3. General truckload position plan and load types applied during testing (from left to right, truck, gantry and Gottwald cranes).

On the “healthy” section, the used truck weight was 48.18tons, distributed as 3.01tons on axel 1 (with a wheel separation of 2.03m), 11.67tons on axel 2 and 3 (with a wheel separation of 2.13m), and 10.63tons on axel 4 and 5 (with a wheel separation of 2.13m). The “damaged” section was tested with a truck with 39.70tons weight, distributed as 3.13tons on axel 1 (with a wheel separation of 2.06m), 9.91tons on axel 2 and 3 (with a wheel separation of 2.18m), and 8.13tons on axel 4 and 5 (with a wheel separation of 2.18m). Ideally the same truck and container would have been used for both tests, but this was not feasible due to normal port operations.

The third type of load testing was static tests performed using the gantry crane, but this time without movement. For these tests, the crane was placed so that the center of its west trolley was located at midspan of the first instrumented span (12 & 19 respectively). Data was continuously recorded as the crane performed a series of typical loading/unloading procedures: pick up a fully loaded container, then move the container to the far end of the boom (over the water), then move the container back to the near end of the boom, then lay down the container back over the ground. These static tests were performed to obtain a qualitative understanding of the load transfer characteristics of the crane during the loading and unloading process.

The fourth and final set of load tests was one live-load and one static test performed with the smaller, moveable Gottwald crane. As with the other live-load tests, sensor measurements and longitudinal crane position were recorded continuously at a minimum sample rate of 33.33 Hz as the crane was moved along the instrumented spans at crawl speed. Due to crane malfunctions and limitations, only one test was performed along one path, and only on the “damaged” section of the pier. The static test consisted of recording data as the crane extended its outriggers, lowered the outriggers, raised itself fully off the ground, lowered itself back down, and retracted its outriggers. The Gottwald crane weighted 360tons, distributed equally on its axels with 60tons on each one (with a support separation of 4.65m).

Table 1. Damage survey of pier’s “healthy” section.

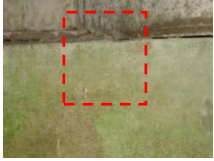
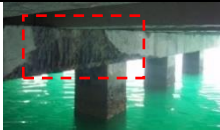
Floor Beams 38-39	
Floor Beam 38 General view, East Face	
Floor Beam 39 General view, West Face	  Small crack between G8-G9.  Small delamination below G1
Pile 1, Floor Beam 38 East Face	 

Table 2. Damage survey of pier’s “damaged” section.

Floor Beam 46-47	
Floor Beam 46 General view, East Face	
Floor Beam 46 General view, West Face	    
	Detail floor beam 47, West face, Between G6-G7.

3. RESULTS

3.1 Preliminary investigation of tests results

All the field data was first examined graphically to provide a *qualitative* assessment of the structure live-load response.

The structural responses as a function of load position were recorded from the wireless truck position indicator, providing a stress data as a function of stress position.

The tests results from identical truck crossings were reproducible, and all strains appeared to be linear with respect to load magnitude (truck position) and the clear majority of responses returned to zero, indicating that the structure was acting in its linear-elastic regime. The truck strain results can be seen in Figure 4, in which linear-elastic behavior and reproducibility of the tests were observed.

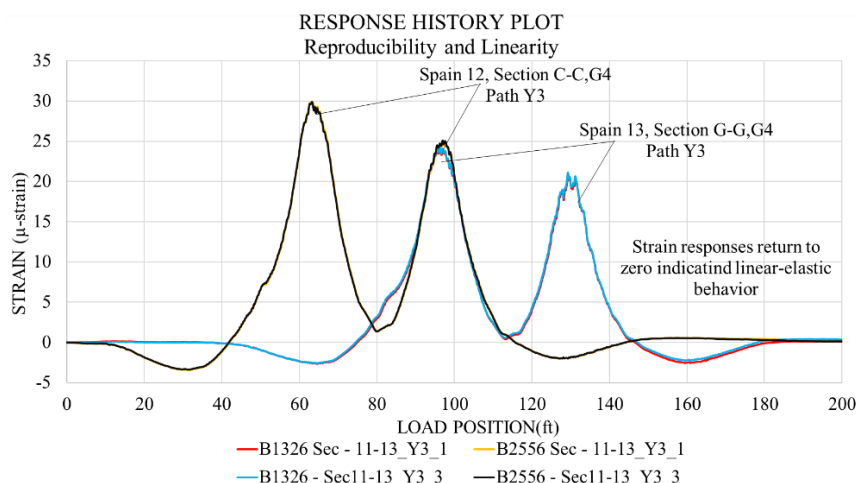


Figure 4. Linear-elastic behavior and reproducibility of test results – strains.

Strain response magnitudes from the midspan gages on the “damaged” section were much less consistent than the strain magnitudes from the “healthy” section. These responses were fairly expected due to the higher level of degradation observed in the “damaged” section versus the “healthy” section of the pier and indicate that lower stiffness values may be confirmed in the FE model of the “damaged” section. Figure 5 illustrates consistent strain magnitudes recorded in the “healthy” section, and Figure 6 does the same for the inconsistent results on the “damaged” section. Maximum deflection measurements were directly compared for the “healthy” section and the “damaged” section. In general, there was an agreement between both regions and often the “healthy” section had slightly greater deflections (because the load applied to the “healthy” section was greater).

A direct comparison of displacement and strain results were made for the Truck and Gottwald Crane responses. The Gottwald crane induced significantly greater responses in the floor beams and stringers compared to the fully loaded truck. This is seen in Figure 7 for stringer displacement values and in Figure 8 for stringer strain values. The lateral load distribution of this structure was examined by looking at bottom flange strain and displacement values for all beams for the truck positions that generated maximum midspan responses. The apparent lateral distribution was very low in both spans.

This could be since the Gottwald structural members are very long and absorb much of the loading, and also the deck was likely to be flexible due to the extremely long point loads being applied by the loaded container trucks and the Gottwald moveable crane. During the load testing process, it was observed that the stay-in-place (SIP) forms were crushed most severely at the inside face of the main girders.

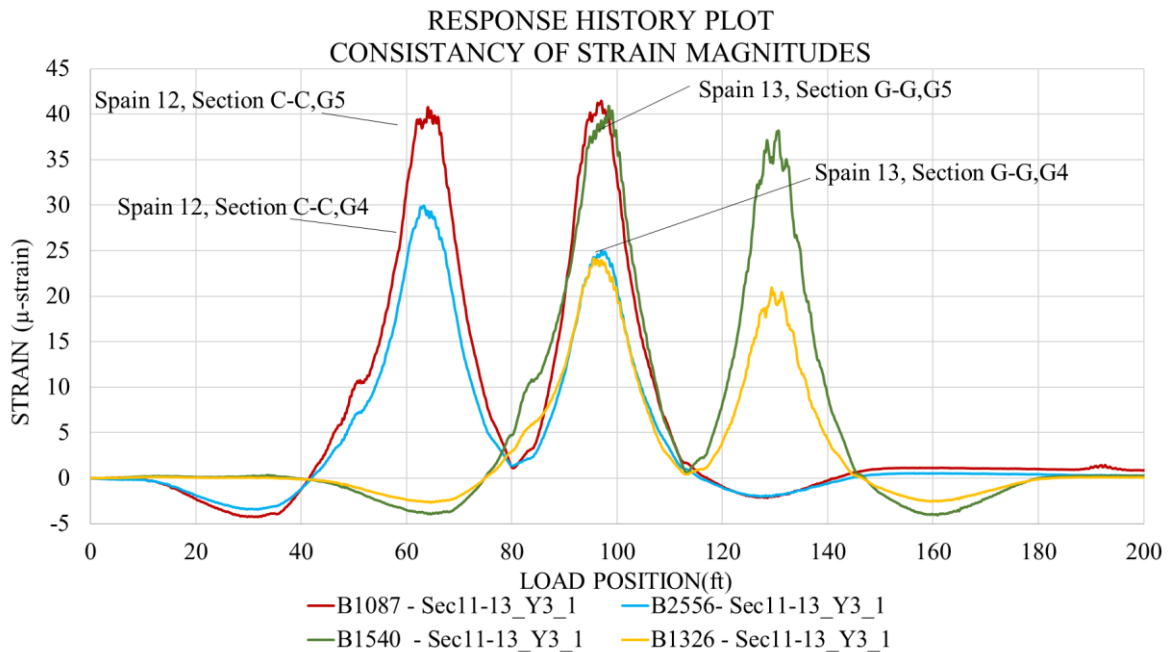


Figure 5. Consistent midspan strain magnitudes recorded on the “healthy” section.

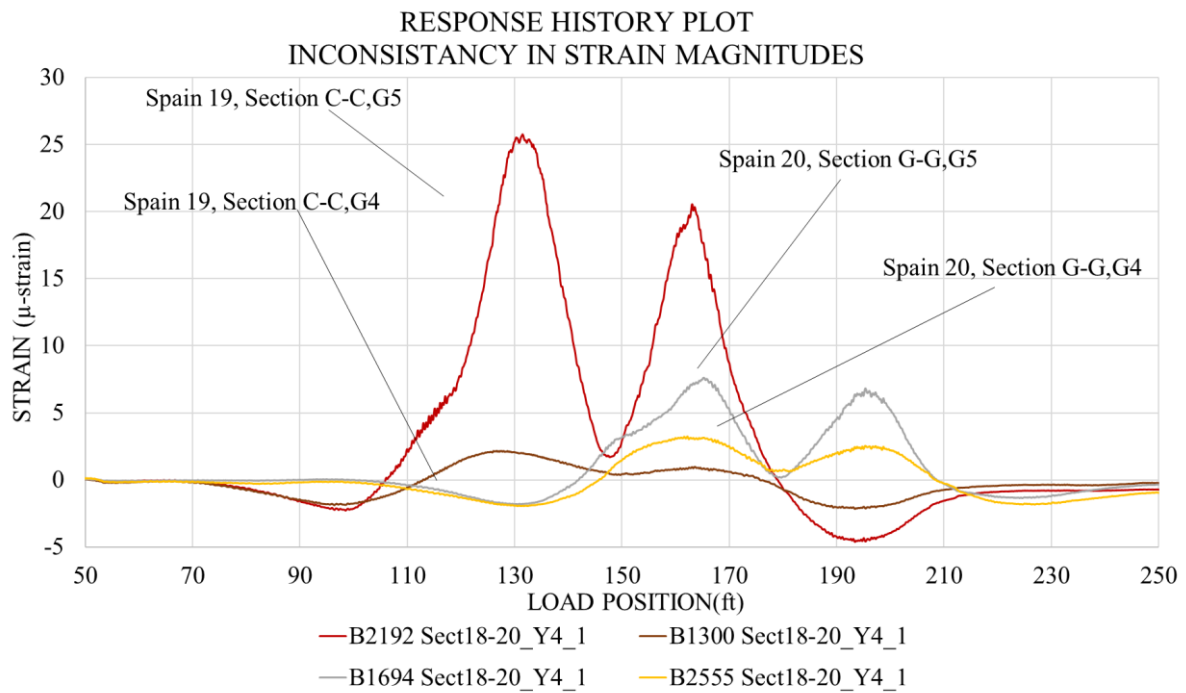


Figure 6. Inconsistent midspan strain magnitudes recorded on the “damaged” section.

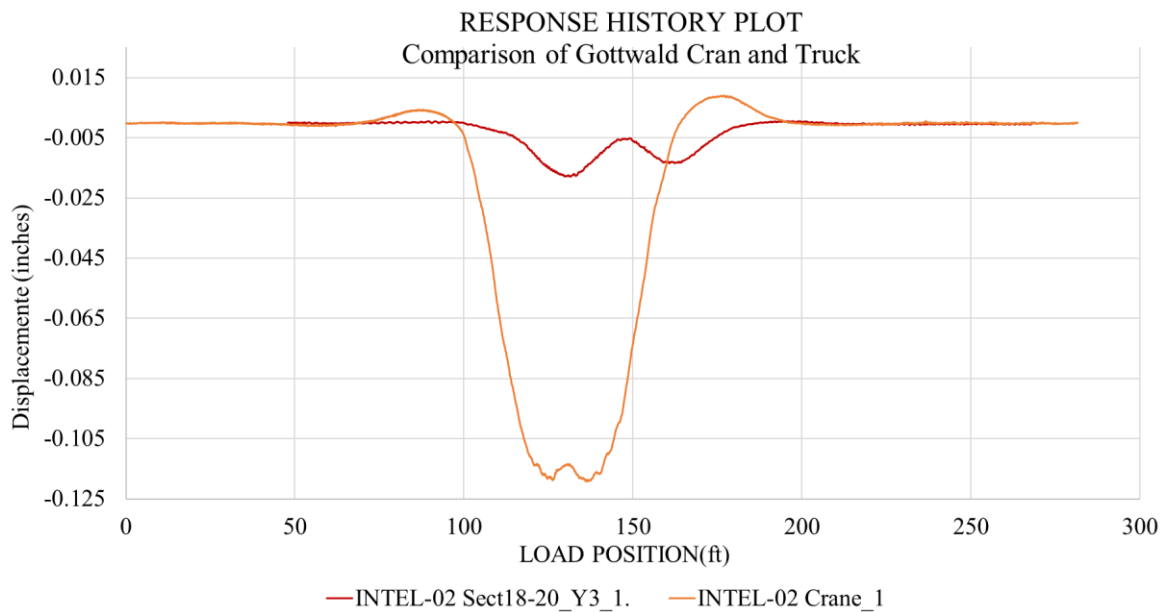


Figure 7. Stringer displacement due to Truck & Gottwald Crane.

This could be due by cause of the gantry crane rails are offset to the inside face of the main girders and the fact that the Gottwald crane outriggers primarily load the deck and stringers immediately adjacent to the main girders. This indicated that the slab in these locations was only transferring load in one direction. It appeared that the truck loading on the interior stringers got transferred to the main girders fairly well, but that the crane loading did not get transferred to the interior stringers as expected. This was an important factor in the model. The distribution of crane load to interior stringers is illustrated in Figure 9.

As previously stated, all test data was initially processed and assessed for quality. Then, one set of test data for each truck path was selected for having the best apparent quality. This selected data was then used to calibrate the finite-element (FE) models of the structure, which were in turn used to produce the load ratings.

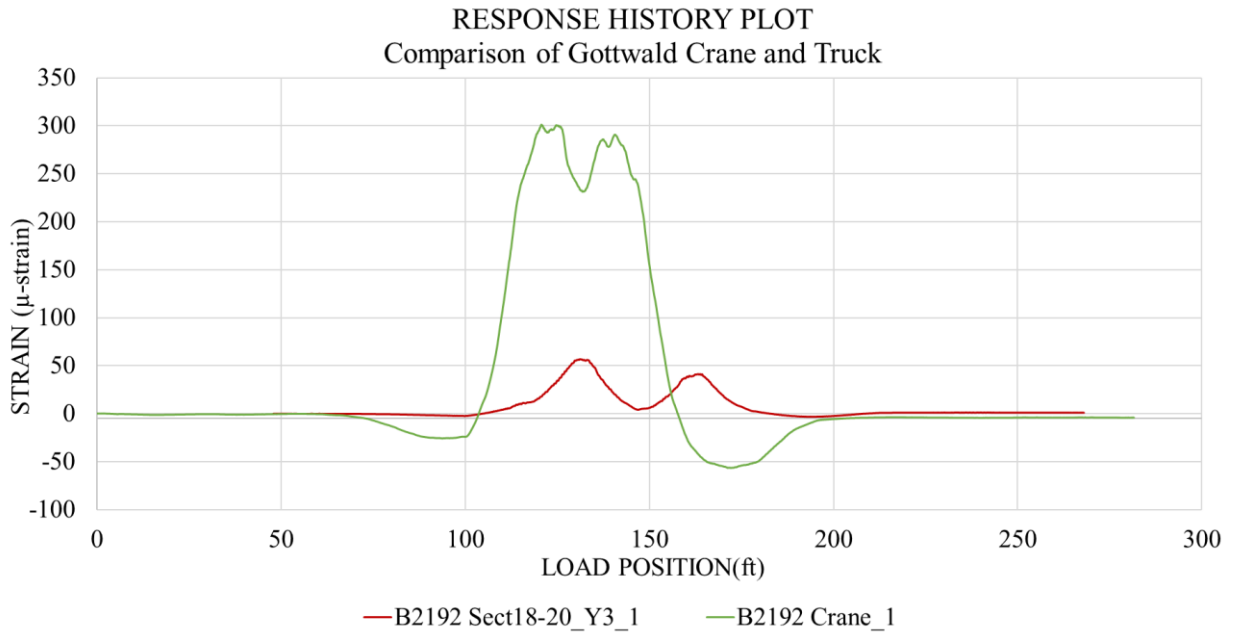


Figure 8. Stringer strain due to Truck & Gottwald Crane.

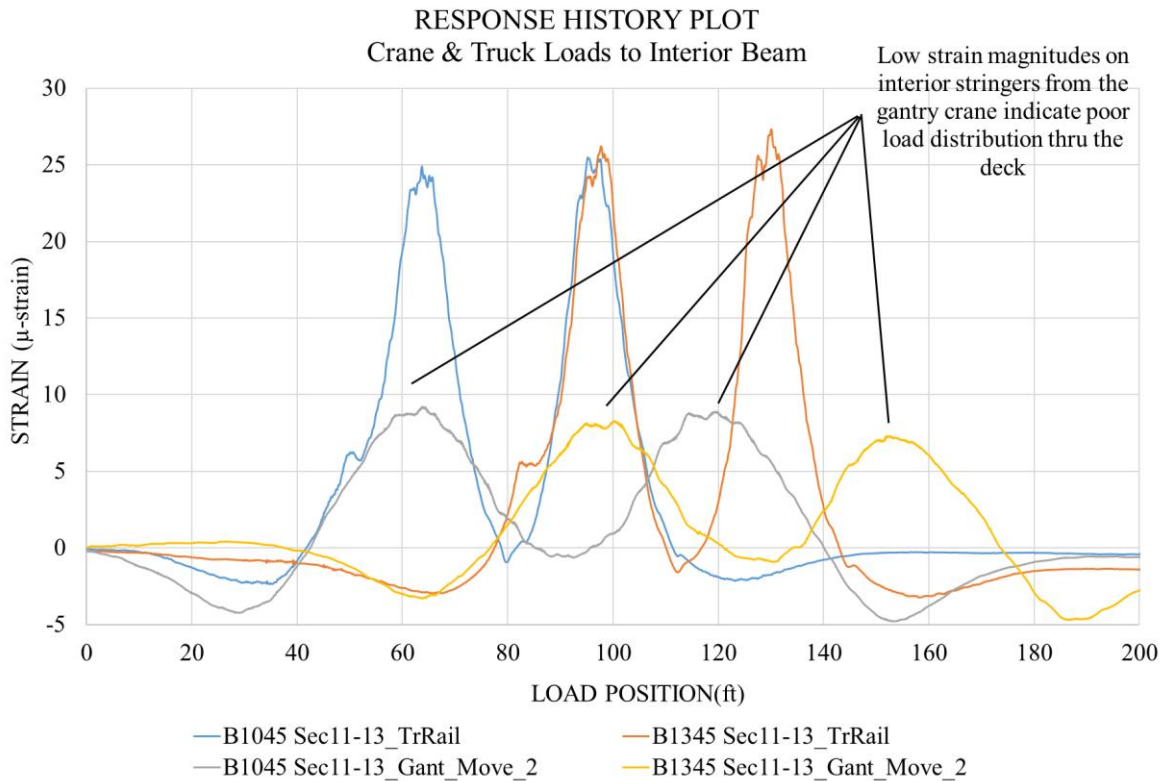


Figure 9. Distribution of crane load to interior stringers.

3.2 Modeling, analysis, and data correlation

The information obtained from the preliminary investigation of these test results was subsequently used to verify the accuracy of a finite element model (Figure 10). The three methods and findings of the Finite Element (FE) modeling procedures were: Finite Element Model Generation; Model Calibration Procedures, and finally Model Calibration Results.

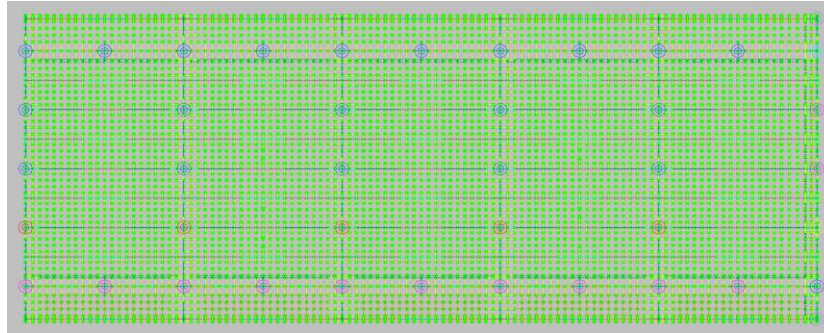


Figure 10. Finite-element model of the pier structure evaluated.

Following the optimization procedures, the “healthy” model produced an average correlation coefficient of 0.9729, while the “damaged” model produced an average correlation of 0.9704. Both of these correlations can be considered as a proper match for an R/C structure of this kind. Table 3 shows the parameter and model accuracy values used in the initial model and obtained for the final models. These values were determined to establish the initial ones as theoretical, and the final ones by adjusting them to the finite model results.

3.3 Load rating results

Once the finite element model was calibrated to field conditions, engineering analysis was followed to address any optimized parameter that could possibly change over time or that could be unreliable with heavy loads or further damage. The Load Rating Factor was determined by a formula based on a certain element capacity, the applied live and dead loads (and their corresponding factors), and a considered impact effect. It is known that a load-rating factor greater than 1.0 indicates a member capacity exceeds the applied loads with the desired factors of safety (AASHTO, 2002). A rating factor less than 1.0 indicates a structural member is deficient such that a specific vehicle or load cannot cross the bridge with the desired factor of safety. A number near 0.0 indicates the structure cannot carry its own dead weight and maintain the desired safety factor. The lowest component rating-factor generally controls the load rating of the entire structure. As mentioned before, the rating equation specified by the AASHTO - Manual for the Condition Evaluation of Bridges was applied (1).

3.3.1 Capacity Calculations

Shear and moment capacities were calculated for the R/C stringers using the AASHTO LRFD Bridge Design Specifications 5th Edition – 2010 and the structural as-built plans provided by IMT. As per the provided plans, the reinforcing bar yield strength was assumed to be 4,200kg/cm². The concrete compressive strength was assumed to be 233 kg/cm² based on cylinder compression tests performed on concrete core samples by IMT.

3.3.2 Load Rating Procedures

Load ratings were performed on the calibrated model according to the AASHTO LRFR method. Load and resistance factors used in the load rating calculations are provided in Table 4. Several combinations of load vehicles were also considered for load rating. Load combinations were based on normal operating procedures and attempted to include other feasible combinations

that may or may not be “typical” operating procedures. There were 6 specific scenarios: one with the gantry crane by itself, one with the Gottwald crane by itself, one with the same Gottwald crane, but static, one with four container trucks, one with the gantry crane and one truck, and the final one with the gantry crane and four trucks.

3.3.3 Load Rating Results

Table 5 shows a summary of the load rating factors and responses for the aforementioned load rating vehicles. Critical positive moment rating factors occurred at the midspan of the inverted T-beams due to an insufficient amount of positive moment reinforcing steel. Negative moment ratings were controlled at the ends of the T-beams but were just barely below 1.0 for all inventory ratings. Critical shear ratings were controlled by the flange bearing capacity of the inverted T-beams for hanger failure. The overall controlling Load Rating Factor for this structure was 0.20 produced at the positive moment with the Gottwald moveable crane.

Table 3. Model accuracy and parameter values.

Modeling parameter	Initial model value	Final model value
Effective Modulus (E [kg/cm ²])		
- Deck	225,000	35,150
- Deck adjacent to T-beams	225,000	17,580
- Deck adjacent to TR-11 beams	225,000	17,580 / 0
- TR-13 beams at midspan	225,000	81,275 / 60,960
- TR-13 beams at ¼ span	225,000	220,400
- TR-13 beams at ends	225,000	43,940
- TR-12 beams at midspan	225,000	142,510 / 106,870
- TR-12 beams at ¼ span	225,000	220,400
- TR-12 beams at ends	225,000	70,300
- TR-11 beams at midspan	225,000	101,900
- TR-11 beams at ends	225,000	109,700
- T-beams at midspan	225,000	89,150
- T-beams at ends	225,000	256,600
Effective Torsional Stiffness (J [cm ⁴])		
- Inverted T-Beam	69,960,000	52,208,000
Vertical Pile Resistance at T-Beam Bearings(Fz [kg/cm])		
- Interior Pile Springs	1,597,000	1,160,800
- Intermediate Pile Springs	1,597,000	803,600
- Exterior Pile Springs	1,196,500	1,303,700
ERROR PARAMETERS	INITIAL MODEL VALUE “HEALTHY”/“DAMAGED”	FINAL MODEL VALUE “HEALTHY”/“DAMAGED”
Absolute Error	95,515 / 35,500	33,000 / 29,600
Percent Error	36.7% / 13.0%	5.6% / 12.1%
Scale Error	2.9% / 4.3%	1.5% / 3.9%
Average Correlation Coefficient	0.8973 / 0.9133	0.9729 / 0.9704

4. DISCUSSION

Analyses were made for critical loads and their response for the positive moment, for the negative moment, and for shear. Most load rating resulting values were below 1.0, meaning that loads exceeded the elements capacities. The critical load rating factor and responses for the positive moment was 0.20 produced by the moving Gottwald crane. For the negative moment, the combination of the gantry crane with four container trucks was critical with a factor of 0.94. The critical load rating factor and responses for shear turned out to be 0.50 with the Gottwald crane, again, but static.

Regarding deflections, overall, there were not many differences between the “healthy” and “damaged” sections. These two sections were instrumented identically and showed slightly different results, having a deflection of -4.55×10^{-02} cm on the “damaged” section.

Table 4. Applied load and resistance factors.

Rating Method	Description	Loading Type	Factor
AASHTO LRFR (Inventory)	Dead Load - Structural	All Vehicles	1.25
	Live Load	Gantry Crane (Design)	1.75
		Gottwald Crane (Legal)	1.40
		Trucks (Design)	1.75
	Impact Factor	Gantry Crane (Design)	5%
		Gottwald Crane (Legal)	5%
Trucks (Design)		33%	
AASHTO LRFR (Operating)	Dead Load - Structural	All Vehicles	1.25
	Live Load	Gantry Crane (Design)	1.35
		Gottwald Crane (Legal)	1.40
		Trucks (Design)	1.35
		Gantry Crane (Design)	5%
		Gottwald Crane (Legal)	5%
Trucks (Design)		33%	
AASHTO Resistance Factors	Moment	N/A	0.90
	Shear	N/A	0.90

Table 5. Critical LRFR load rating factors and weights for five load configurations.

Rating Vehicle	Response, Location	LRFR – Inventory		LRFR – Operating	
		RF	Tons	RF	Tons
Gantry Crane	+ Moment, TR – 11	0.86	399 (one side)	1.11	515 (one side)
Gottwald Crane	+ Moment, T-Beam	0.20	72 (gross)	0.20	72 (gross)
Gottwald Crane Static	Shear, T-Beam Flange	0.50	180 (gross)	0.20	72 (gross)
Container Trucks	+ Moment, T-Beam	0.55	12.8 (dual axle)	0.71	16.6 (dual axle)
Container Trucks + Gantry Cane	+ Moment, T-Beam	0.49	N/A	0.64	N/A

5. CONCLUSIONS

Load test results indicated that the pier was performing in a linear-elastic manner, even though inconsistencies in response magnitudes were observed in the “damaged” section. Many of the structural beams, especially the lateral inverted T-beams, did show signs of fairly severe concrete spalling due to an expansion of the reinforcing steel (corroded). However, this is primarily a serviceability issue and does not have a major effect on the structural capacity of the sections until there is significant steel loss due to corrosion. It could be thus possible that the large applied loads generated strain cracks, which then prompted a higher exposure of the reinforced steel to corrosive ions. A healthy correlation was obtained by the analysis after the calibration process, further indicating that all structural responses were linear.

The critical rating factor for this pier was 0.20 obtained with the Gottwald moveable crane and was controlled by the positive moment in the transverse inverted RC T-beams. It is important to note that the poor load rating was due to insufficient positive moment reinforcing steel in the bottom flange of the inverted T-beams. Non-destructive evaluation (NDE) should be performed on the inverted T-beams to locate and determine the amount of steel remaining present.

Several other structural components also had rating factors less than 1.0 for the Gottwald moveable crane. In fact, the flange bearing capacity of the inverted T-beams produced only slightly better rating factors at 0.50, and the midspan moment capacity of the TR-13 beams rated at only 0.75. Consequently, careful technical considerations are to be followed since these results suggest that the removal of the crane from normal operations should be considered until the deficient or damaged members are sufficiently strengthened (to increase their load capacity). Strengthening all the insufficient members may be a feasible option since the weak components are relatively isolated; it is still recommended however that NDE to be performed first to verify that the capacities used for load rating were indeed correct based on the actual steel present in the members. At a very minimum, steps should be taken so that the Gottwald crane is never placed within a span of the gantry crane.

Future inspections should focus on the escalation of moment cracks in the transverse inverted T-beam and stringers. In addition, careful attention should be paid to the flange bearing areas of the inverted T-beams and the signs of failure associated with beam ledges.

The load rating factors and conclusions presented in this report are provided as recommendations based on the structure response behavior and condition at the time of load testing. Further structural degradation must be considered in future load ratings.

6. ACKNOWLEDGEMENTS

This investigation was funded by the Instituto Mexicano del Transporte (Mexican Transport Research Institute). M. Balancan-Zapata’s help during the damage survey and the load testing in the pier structure is also acknowledged. The findings and opinions in this publication are those of the authors and not necessarily those of the sponsoring organizations.

7. REFERENCES

- Torres Acosta, A. A., Castro Borges, P., Martínez Madrid, M. (2008), “*Reporte final del “Proyecto núm. EE 04/08: Inspección y evaluación por durabilidad de los muelles 6 y 7 de la terminal remota de la API Progreso”*”, Instituto Mexicano del Transporte, Sanfandila, Querétaro, México, diciembre.
- Günter, S., Schütze, M., Hays, G. F., Burns, W., Han, En-H., Pourbaix, A., Jacobson, G. (2009), “*Global Needs for Knowledge Dissemination, Research, and Development in Materials Deterioration and Corrosion Control*,” World Corrosion Organization, Worldwide rights reserved.

Hays, G. F., "Now is the Time," World Corrosion Organization, <http://www.corrosion.org/>
Kennedy Space Center, *Corrosion Technology Laboratory*, NASA Privacy Statement, Disclaimer, and Accessibility Certification, Florida. (<http://corrosion.ksc.nasa.gov/corrincon.htm>)
Broomfield, J. P. (1997). *Corrosion of Steel in Concrete: Understanding, Investigation and Repair*.
Torres Acosta, A. A. (2012). "Project No. EE 05/12 Informe Final: Inspección Preliminar de la Infraestructura del Muelle en 13 Puertos Federales Mexicanos" Instituto Mexicano del Transporte, Sanfandila, Querétaro, México, May.
AASHTO (2002) "AASHTO Manual for the Condition Evaluation of Bridges" American Association of State Highway and Transportation Officials.
Bridge Diagnostics, Inc. (2012). *Integrated approach to Load Testing*, Bridge Diagnostics, Inc.